UNIVERSITÉ DE STRASBOURG

École Doctorale des Sciences Chimiques
Institut Charles Sadron, CNRS

Thèse présentée par :

Dionysia-Nteniz
Saranti-Karamesini

soutenue le :**21Novembre 2018**

pour obtenir le grade de : **Docteur de l'Université de Strasbourg**

Discipline/Spécialité : Chimie des Polymères

Synthesis and utilization of sequence-defined polyurethanes for anti-counterfeit applications

THÈSE dirigée par :
M. Jean-François LUTZ   Directeur de recherche, CNRS, ICS, Strasbourg

RAPPORTEURS :
Mme. Sophie Guillaume   Directeur de recherche au CNRS, ISCR, Rennes
Mme. Anja Palmans   Associate Professor TU/e, Eindhoven

AUTRES MEMBRES DU JURY :
M. Didier Gigmes   Directeur de Recherche CNRS, ICR, Marseille
M. Michel Bouquey   Maître de conférences, ICS, Strasbourg
M. Rémi Perrin   Directeur R&D, Soprema, Strasbourg

To my family!

Dr. Guillaume Fiers my second office mate and lab mate! Thanks for helping me in French bureaucracy, it was so many times! You are always so well-informed that you were every time precious for all of us!

Dr. Evgeniia Konishcheva, we shared the same project! Thanks for the useful information about technical things and your precious help to improve my presentations skills!

I would like to acknowledge Dr. Clotilde Le Guen and Dr. Sofia Telitel, you were always calm and positive energy in our working environment and as office colleagues!

Vincent Greff, my stagier! During your work you were always positive, smiley and willing to work for acquiring nice results. Thanks for your help in our common project!

In the end, I would like to thank some people who were important for conducting my research; Catherine Foussat, Dr. Melanie Legros from the Institut Charles Sadron characterization team, François Courtier and Christophe Lambour from the "Atelier" of the institut who helped me a lot with the wood labeling project.

Last but not least, I would like to say a big thank to my family for supporting me and staying by my side in every new beginning! Without them, my success and career would not have happened. I would also to thank my friends from Greece for keeping me company even by far and being happy with my success!

Thank you very much for being present in my Ph.D. trip!

Denise

TABLE OF CONTENTS

VIII

x

ABBREVIATIONS LIST

A

A: Adenine

ACN: Acetonitrile

ASCII : American Standard Code for Information Interchange

ATRP: Atom-Transfer radical polymerization

B

Bis-A: Bis-Acrylamide (here N,N'-Methylenebis(acrylamide)

Boc: tert-Butyloxycarbonyl protecting group

C

C: Cytosine

CID: Collision-Induced Dissociation

$CHCl_3$: Chloroform

CPG: Controlled pore glass

D

Đ: Polymer dispersity

DCC: N,N'-Dicyclohexyl carbodiimide

DCM: Dichloromethane

DESI-MS: Desorption Electrospray Ionization-Mass spectrometry

DMAP: 4-Dimethylaminopyridine

DMT-Cl: 4,4'-DimethoxytritylChloride

DMSO: Dimethyl Sulfoxide

d_6-DMSO: Deuterated DMSO

DMF: Dimethylformamide

DNA : Deoxyribo Nucleic Acid

DP: Degree of Polymerization

DSC:N,N'-Disuccinimidyl carbonate

E

EEMA: 2-Ethoxyethyl methacrylate

EGDMA: Ethylene glycol dimethylacrylate

ESI-MS: Electrospray Ionization-Mass spectrometry

ESI-HRMS: Electrospray Ionization-High Resolution Mass spectrometry

G

G: Guanine

H

HF: Hydrofluoric acid

HPLC: High Performance Liquid Chromatography

I

ISO: International Organization for Standardization

M

MALDI-TOF: Matrix-Assisted Laser Desorption/Ionization Time-Of-Flight (mass spectroscopy)

MeOH: Methanol

MS: Mass spectrometry

MS/MS: Tandem mass spectrometry

mRna: Messanger RiboNucleic Acid

MD: Molecular dynamics

m/z: Mass-to-charge ratio

MgSO4: Magnesium sulfate anhydrous

N

NaOH: Sodium Hydroxide

NMP: 1-Methyl-2-pyrrolidinone

NMR: Nuclear magnetic resonance

^{1}H-NMR: Nuclear magnetic resonance

^{13}C-NMR: Nuclear magnetic resonance

P

PBS: Phosphate buffer solution

PCR: Polymerase Chain Reaction

PEG: Poly(ethylene glycol)

c-PEEMA: Crosslinked poly(2-ethoxyethyl methacrylate)

PET: Poly(ethylene terephthalate)

PNA(s): Peptide nucleic acid(s)

PNIPAM: Poly(N-isopropylacrylamide)

PU(s): Poly(urethane)(s)

PVA: Poly(vinyl alcohol)

PVC: Poly(vinyl chloride)

PPT: Parts per trillion

PS: Polystyrene

Q

QDs: Quantum dots

R

RFID : Radio Frequency Identification

RNA: RiboNucleic Acid

rRNA: Ribosomic RiboNucleic Acid

RT: Room temperature

S

SCPs: Sequence-Controlled Polymers

SEC : Size Exclusion Chromatography

T

T: Thymine

TFA : Trifluoroacetic acid

THF : Tetrahydrofuran

d_8-THF: deuterated THF

3D: Three dimensional

2D: Two dimensional

tRNA: Transfer RiboNucleic Acid

U

U: Uracil

UPLC-MS: Ultra performance liquid chromatography-Mass spectrometry

USD: United States Dollars

Introduction Générale

Au cours des dernières décennies, le commerce illicite a fortement augmenté en raison du développement d'Internet, provoquant un phénomène inquiétant pour l'économie. Personne ne peut vraiment contrôler l'authenticité de la totalité des produits qui y sont vendus, causant ainsi de nombreuses victimes de fraudes.

Jusqu'à aujourd'hui de nombreux efforts ont été faits pour créer des codes-barres efficaces pour restreindre les contrefaçons. Tels que des codes-barres qui basent leur fonctionnalité sur un modèle ou uniforme spéciale pour encoder les particules, d'autres sont basées sur leurs propriétés optiques intéressantes et on peut aussi penser aux stratégies mettant en place de l'encodage chimique et qui vont donc jouer sur la composition chimique ou sur la séquence de la particule codante. Cette dernière option semble dominer dans ce domaine[1]. Mais la contrefaçon est toujours d'actualité et les crimes associés aux droits de propriété intellectuelle ont atteint une perte de 461 million USD par an à travers le monde, touchant pratiquement tous les types de produits et toutes les régions du monde[2]. Les technologies d'anti-contrefaçon requièrent des stratégies inédites pour tracer les produits. Il faut qu'elles soient difficiles à copier mais efficace pour différencier les produits originaux des produits contrefaits[3]. C'est en suivant cette idée que les codes-barres moléculaires ont été proposés comme une alternative intéressante. Des polymères avec une séquence définie de monomères peuvent constituer une signature unique pour les matériaux destinés à être marqué avec ce genre de technologie. Récemment, des biopolymères comme les polypeptides[4,5] et les acides nucléiques[6-9] ont été utilisés comme des codes-barres moléculaires. Néanmoins, leur faible résistance[10] aux certain paramètres ne permet pas de les utiliser avec des procédés plus élaborés et dans de plus nombreuses applications.

L'avantage d'utiliser des polymères synthétiques est la possibilité de créer un polymère avec les caractéristiques désirées (stabilité thermique, résistance chimique…). Encore plus d'avantages sont reliés à la variété quasi infinie de structures chimiques théoriques possibles et leurs méthodes de lecture. Les polymères synthétiques à séquences contrôlées peuvent être préparés en utilisant les méthodes de polymérisations classiques telles que les polymérisations en chaîne ou par étapes. Ils peuvent également être synthétisés via une synthèse sur support solide couramment utilisé lors de la synthèse de biopolymères et de machines moléculaires[11].

Pour le moment, la synthèse sur support solide est la façon la plus facile et la plus simple pour préparer un polymère à séquence contrôlé, surtout lorsqu'il n'est pas nécessaire d'utiliser des groupements protecteurs qui entraînent de la perte de temps lors des étapes de protections et de déprotections[12]. En effet, en utilisant la synthèse itérative sur support solide, il est possible de préparer des séquences contrôlées de poly(uréthane)s très facilement et très rapidement. Ce type de polymère est une classe de matière plastique très populaire, souvent utilisé dans les revêtements, les adhésifs,

l'isolation, la construction, l'industrie automobile et pour des applications biomédicales. D'ordinaire ils sont synthétisés via une polymérisation par étape d'isocyanates et de diols formant une structure non-uniforme et demandant une procédure spéciale vis-à-vis de la toxicité des isocyanates. Dans un cadre plus large de ce travail, une approche avec une multi-étape chimio-sélective a été développée[13]. Cette stratégie se base sur deux étapes consécutives qui se répètent autant de fois que nécessaire durant la synthèse du polymère ayant ainsi la longueur et la séquence désirée. En suivant ce protocole, un contrôle total de la structure primaire de ces poly(uréthane)s peut être atteint et ainsi de l'information peut être stockée dans la chaîne de polymère. Pour cette raison, les deux co-monomères utilisés ont été arbitrairement définis comme 0 et 1 bit. En alternant et en combinant correctement ces deux bits, il faut possible d'encoder dans les PUs préparés, des messages en utilisant le code ASCII. De plus, il a été prouvé que les séquences contrôlées de PUs sont très faciles à analysés par spectrométrie de masse en tandem. L'utilisation de deux monomères de masses différentes était adéquate pour écrire un code séquentiel qui en mode négatif de MS/MS peut être facilement déchiffré grâce à la liaison carbamate C-O qui est facilement clivable. En combinant tous ces avantages les séquences contrôlées de PUs peuvent constituer un recours dynamique pour la contrefaçon. En effet, en encodant un numéro de lot et d'autres informations nécessaires dans les chaînes de polymères de PUs et ensuite en introduisant ces polymères dans le matériau, celui-ci devient codé et difficile à contrefaire.
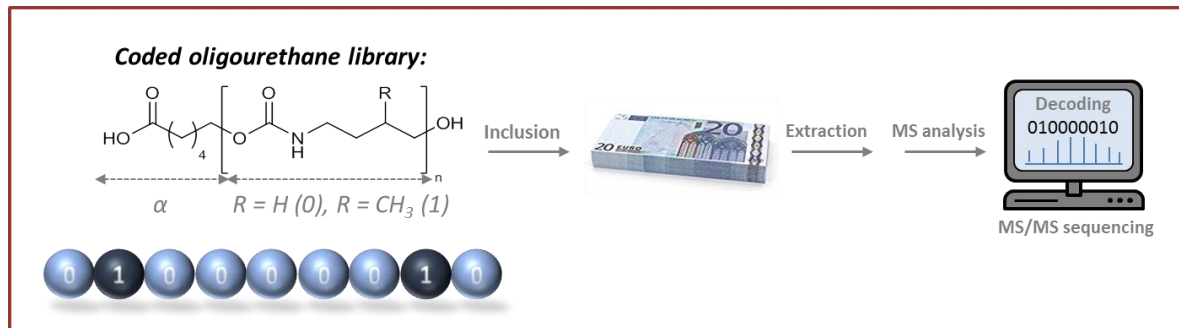
Figure 1: Concept général de l'utilisation des oligouréthanes à séquence définie comme codes à barres moléculaires

Ce manuscrit contient les articles publiés sur le sujet pendant les trois années de mon doctorat et des données non publiées incluses dans les chapitres IV et VI. Six chapitres au total vont expliquer en détail toutes les réalisations importantes dans le domaine de la lutte contre la contrefaçon et les vastes possibilités d'applications futures.

Dans le **Chapitre II**, les polyuréthanes à codage numérique ont d'abord été testés comme marquage anti-contrefaçon pour l'étiquetage de lentilles intraoculaires à base de méthacrylate. Les oligomères à séquence définie ont été préparées comme décrit ci-dessus par synthèse itérative en phase solide. La première étape de la synthèse itérative été basée sur la réaction du groupe hydroxyle de la résine

fonctionnalisée et du carbonate de N, N 'dissuccinimidyle résultant en un carbonate activé. Dans un second temps, on a fait réagir le produit précédent avec le monomère amino-alcool (amino-1-butanol (0 bit), amino-2-méthyl-1-butanol (1 bit) pour obtenir le carbamate substitué avec un hydroxyle. L'alternance contrôlée de la séquence binaire 0/1 a permis le codage du message sur les chaînes de polymères. Comme représenté dans le tableau 1, des marquages avec différentes longueurs de chaîne et séquences de monomères ont été préparés et utilisés pour cette application.

L'insertion de code-barres dans les implants a été réalisée par deux approches différentes : la première était leur inclusion in situ au cours de la copolymérisation radicalaire du méthacrylate de 2-éthoxyéthyle et du diméthacrylate d'éthylène glycol. La seconde était le gonflement des lentilles commerciales dans une solution d'oligomère suivi d'un séchage. Les deux approches ont permis le marquage des lentilles avec l'étiquette en polyuréthane. Il a fallu ensuite extraire les étiquettes de l'implant afin de les analyser. Une solution de méthanol a été utilisée pour extraire l'oligomère et l'analyser par spectrométrie de masse à électrospray. Dans tous les cas, les étiquettes ont été extraites du matériel marqué et leur séquence codée a bien été identifiée par le séquençage MS/MS, validant le concept d'étiquetage et prouvant que cette méthode est une candidate intéressante pour l'utiliser comme marquage anti-contrefaçon dans les implants. De plus, leurs effets sur les propriétés de biocompatibilité et de transparence des lentilles ont été testés, donnant aucuns résultats décourageants.

Table 1 : Liste des oligomères codant de l'information

	Sequence	m/z_{th}[a]	m/z_{exp}[a]
PU1	α-0-0-0-1	605.3403	605.3403
PU2	α-0-0-1-0	605.3403	605.3399
PU3	α-1-0-0-0-1	734.4193	734.4191
PU4	α-1-1-0-1-1-1	891.5296	891.5286
PU5	α-0-0-1-1-1-1-1-0	1121.6562	1121.6557

Pour éviter l'augmentation des scandales médicaux provoqués par l'utilisation de faux implants ou implants dégradés, les codes-barres moléculaires en PU ont été testés pour la première fois en tant que marqueurs in vivo pour l'identification des implants au **Chapitre III**. Préparés manuellement mais également via des protocoles automatisés pour simplifier leur utilisation, les oligomères ont été testés en premier lieu en termes de toxicité, indiquant une excellente cyto-compatibilité. Après, ils ont été inclus en petite quantité (1% en poids) dans des films modèles en poly(alcool vinylique) réticulés. Les membranes préparées ont été implantés dans l'abdomen de rats, par voie intramusculaire et sous-cutanée. Après trois différentes périodes d'implantation, les implants marqués ont été retirés du corps

du rat et le processus d'identification a eu lieu. Les tissus de rats exposés aux implants ne présentaient aucun effet indésirable, suggérant ainsi que les marqueurs ne sont pas nocifs et qu'il n'y a probablement aucune fuite. De plus, dans tous les cas, le message binaire crypté a été lu avec succès grâce à l'analyse de spectrométrie de masse en tandem.

Pour aller encore plus loin que l'étiquetage des matrices plastiques, l'étiquetage du bois a également été tenté sur **le Chapitre IV**. Des meubles en bois de grande valeur, des instruments musicaux ou des cadres en bois décorant des tableaux célèbres pourraient être étiquetés avec des codes-barres moléculaires pour lutter contre la menace de la contrefaçon. Il a été prouvé que les poly(uréthane)s codés numériquement ont réussi à étiqueter différents types de bois par une technique facile, celle de gonflement par immersion. Des séquences de polymères codant pour des messages binaires de plusieurs longueurs ont été utilisées pour marquer le bois. Dans tous les cas, le code-barres moléculaire a pu être détecté et lu par spectrométrie de masse, ce qui prouve son efficacité pour un large éventail de matériaux, y compris le plastique et le bois, et promet beaucoup pour l'avenir.

Afin de fournir des codes-barres moléculaires sécurisés supplémentaires, nous avons développé des codes-barres en deux dimensions dans le **Chapitre V**. Grâce à la 2D il y aura une plus grande intégration d'informations ainsi qu'une empreinte plus complexe. Pour ce faire, des mélanges d'oligo(uréthane)s à séquence uniforme ont été testés en tant que codes-barres moléculaires 2D pour le marquage de matières plastiques de base, telles que le polystyrène, le chlorure de polyvinyle et le polyéthylène téréphtalate. Une fois que chacun des oligomères définis par la séquence a été synthétisés par le protocole en phase solide chimio-sélective et caractérisés en termes de dispersité et de séquence, ils ont pu être utilisés dans les mélanges. Plus particulièrement, une bibliothèque de trois et une autre de quatre oligomères codant pour un message en code ASCII de deux octets ont été incorporés dans les matrices plastiques par un procédé simple de coulée de solvant. Les films plastiques marqués ont ensuite été découpés dans différentes régions pour étudier la dispersion homogène du marqueur par spectrométrie ^{1}H-RMN. Le marqueur multi-composants a ensuite été extrait et identifié par spectrométrie de masse. Le spectre de masse polydispersé obtenu a ensuite été analysé pic par pic pour confirmer la séquence de chaque oligomère de la banque. L'extraction des oligomères et le déchiffrage des messages réalisés à partir de tous les polymères hôtes ont ouvert la voie à des applications sécurisées de lutte contre la contrefaçon et de traçabilité.

La dernière partie de cette thèse, le **Chapitre VI**, porte sur l'attachement covalent d'un code-barrre en PU à un réseau de polymères. Pour ce faire, les PU à séquences définies ont été synthétisés par le protocole itératif de deux étapes déjà développé pour la synthèse en phase solide. Toujours ancrés sur le support solide, les séquences ont été spécifiquement modifiées par leur groupe terminal par un segment de liaison méthacrylamide contenant une liaison disulfidique. Une fois clivées de la résine, les séquences fonctionnelles étaient prêtes à être incorporées dans le réseau de polymères par une
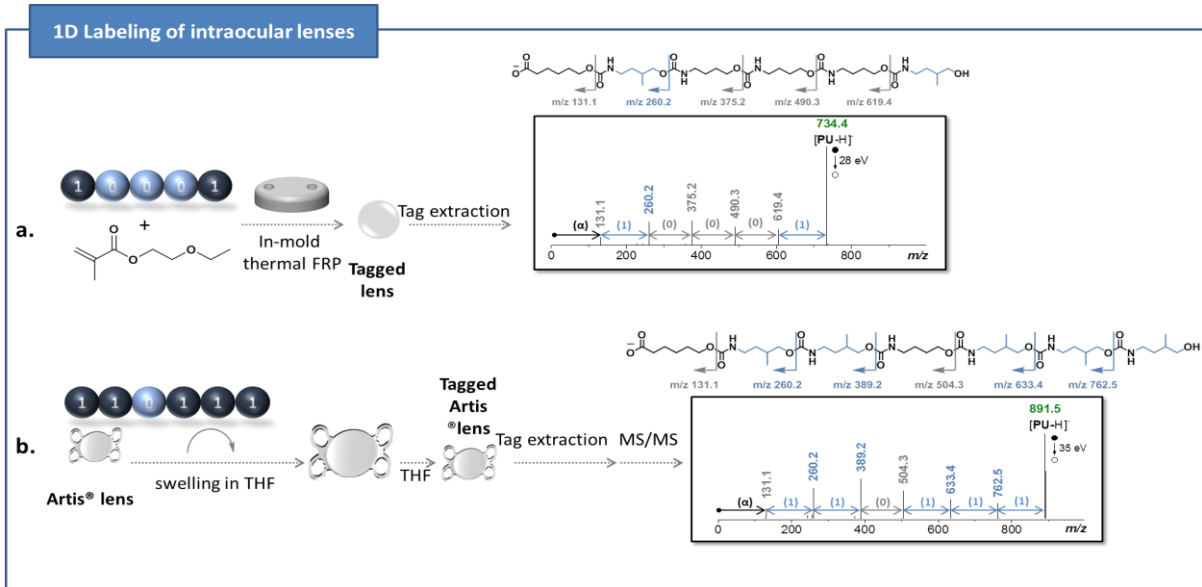
Figure 2 : Représentation des deux approches utilisées pour l'étiquetage des lentilles intraoculaires avec les codes-barres en PU et leur lecture par analyse MS. (a): l'étiquetage des lentilles à base de méthacrylate par polymérisation par contrôle radicalaire in situ (b): marquage des lentilles Artis préfabriquées par voie de gonflement / déshumidification.
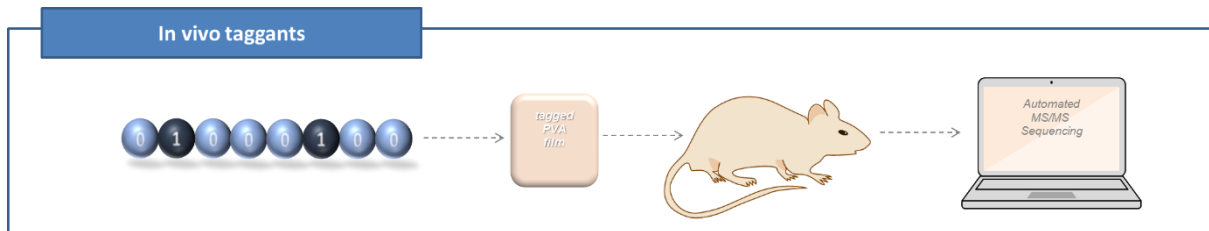
Figure 3 : Incorporation de code-barres 1D de PU dans le film de poly(alcool vinylique) et son implantation ultérieure chez des rats vivants. Explantation de l'implant de marquage – Identification par MS/MS.
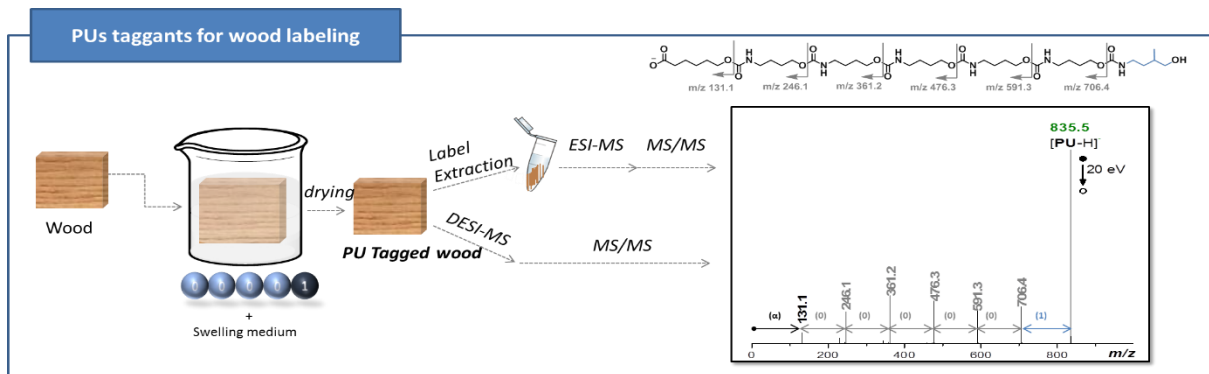
Figure 4 : Les codes-barres 1D en poly(uréthane) ont été utilisés pour l'étiquetage du bois par immersion dans une solution de polyuréthane. La lecture a été réalisée par une approche non destructive pour le bois, DESI-MS, ou par le procédé d'extraction déjà utilisé en broyant le bois et en le plongeant dans une solution de méthanol. La confirmation de la séquence de marquage a été effectuée par spectrométrie MS / MS dans les deux cas.
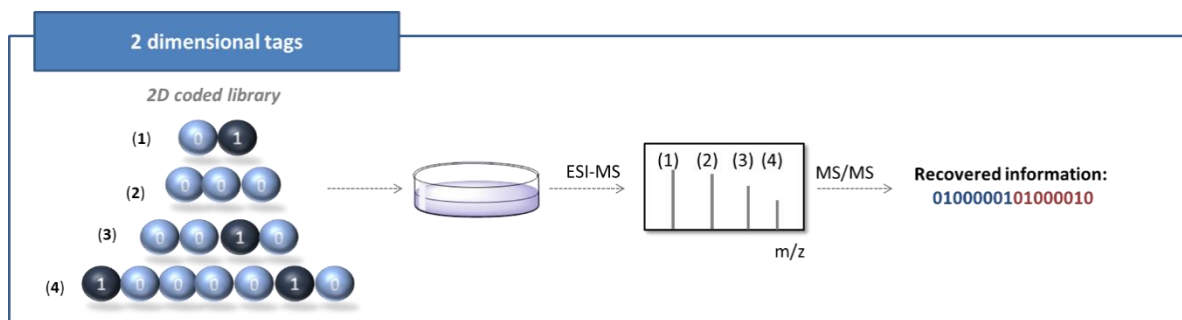
Figure 5 : Représentation des codes-barres 2D en PU, leur inclusion dans les films plastiques, leur empreinte de masse et la récupération finale des informations chiffrées par analyse MS/MS
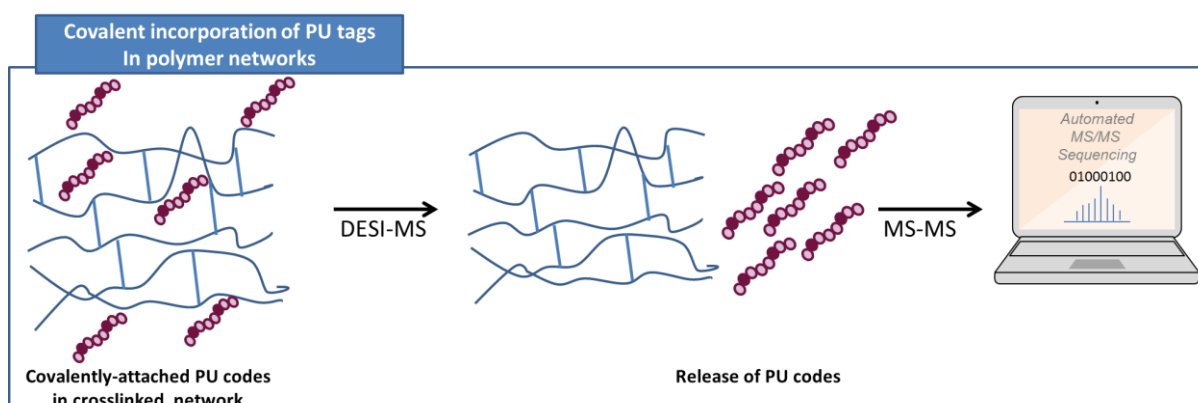
Figure 6 : Les codes-barres en PU étaient attachés de manière covalente sur les réseaux de polymères pour améliorer le niveau de sécurité. Leur lecture a été effectuée via DESI-MS pour libérer les séquences PU, puis par MS/MS pour identifier le message exact.

polymérisation radicalaire. La présence de la liaison disulfidique à la fin de la séquence polymérique permet d'isoler facilement le message codé par coupure en DESI-MS et ensuite son séquençage par MS/MS. Ce travail conduit ainsi nos systèmes de marquage à des solutions encore plus sécurisées, applicables pour une grande variété de matériaux avec des besoins différents.

En conclusion, le domaine des polymères à séquence définie est déjà bien implanté dans la communauté scientifique et bien introduit dans de nombreuses applications. Mais il semble qu'il ait encore plus à offrir. Les technologies anti-contrefaçon manquent de nouveauté et de solutions révolutionnaires pour lutter contre les falsifications.

C'est donc le bon moment pour combiner ces deux domaines et développer une nouvelle technologie. Dans le cadre de cette thèse des oligo(uréthane)s à séquences définis ont été utilisés comme codes-barres moléculaires. Leur synthèse a également été automatisée pour faciliter leur utilisation notamment par les industries. Les codes-barres moléculaires ont été testés pour l'étiquetage d'une large gamme de matrices polymères utilisées pour la majorité comme produits commerciaux en plastique. L'incorporation covalente et non covalente dans les réseaux de polymères, l'utilisation in vitro et in vivo des marqueurs, ont été des réalisations importantes. L'étiquetage des produits non

plastiques mais ceux fabriqués avec du bois, a permis de traité le sujet de façon plus large et a ouvert de nouveaux horizons à l'activité anti-contrefaçon dans les applications industrielles réelles.

References

1   Paunescu, D., Stark, W. J. & Grass, R. N. Particles with an identity: Tracking and tracing in commodity products. *Powder Technology* **291**, 344-350, doi:https://doi.org/10.1016/j.powtec.2015.12.035 (2016).

2   OCDE & Office, E. U. I. P. *Trade in Counterfeit and Pirated Goods*. (2016).

3   Bansal, D., Malla, S., Gudala, K. & Tiwari, P. Anti-Counterfeit Technologies: A Pharmaceutical Industry Perspective. *Scientia Pharmaceutica* **81**, 1-13, doi:10.3797/scipharm.1202-03 (2013).

4   Kydd, P. H. Polypeptides as chemical tagging materials *Google Patents* (1982).

5   Nikolaiev, V., Stierandová, A., Krchnák, V., Seligmann, B., Lam, K. S., Salmon, S. E. & Lebl, M. Peptide-encoding for structure determination of nonsequenceable polymers within libraries synthesized and tested on solid-phase supports. *Peptide Research* **6**, 161-170 (1993).

6   Jung, L., Hayward, J. A., Liang, M. B. & Berrada, A. DNA marking of previously undistinguished items for traceability, Google Patents (2014).

7   Puddu, M., Paunescu, D., Stark, W. J. & Grass, R. N. Magnetically Recoverable, Thermostable, Hydrophobic DNA/Silica Encapsulates and Their Application as Invisible Oil Tags. *ACS Nano* **8**, 2677-2685, doi:10.1021/nn4063853 (2014).

8   Bloch, M. S., Paunescu, D., Stoessel, P. R., Mora, C. A., Stark, W. J. & Grass, R. N. Labeling Milk along Its Production Chain with DNA Encapsulated in Silica. *Journal of Agricultural and Food Chemistry* **62**, 10615-10620, doi:10.1021/jf503413f (2014).

9   Paunescu, D., Fuhrer, R. & Grass, R. N. Protection and Deprotection of DNA—High-Temperature Stability of Nucleic Acid Barcodes for Polymer Labeling. *Angewandte Chemie International Edition* **52**, 4269-4272, doi:doi:10.1002/anie.201208135 (2013).

10   Lindahl, T. Instability and decay of the primary structure of DNA. *Nature* **362**, 709, doi:10.1038/362709a0 (1993).

11   Lewandowski, B., De Bo, G., Ward, J. W., Papmeyer, M., Kuschel, S., Aldegunde, M. J., Gramlich, P. M. E., Heckmann, D., Goldup, S. M., D'Souza, D. M., Fernandes, A. E. & Leigh, D. A. Sequence-Specific Peptide Synthesis by an Artificial Small-Molecule Machine. *Science* **339**, 189-193, doi:10.1126/science.1229753 (2013).

12   Lutz, J.-F. Defining the Field of Sequence-Controlled Polymers. *Macromolecular Rapid Communications* **38**, 1700582, doi:doi:10.1002/marc.201700582 (2017).

13   Gunay, U. S., Petit, B. E., Karamessini, D., Al Ouahabi, A., Amalian, J.-A., Chendo, C., Bouquey, M., Gigmes, D., Charles, L. & Lutz, J.-F. Chemoselective Synthesis of Uniform Sequence-

Coded Polyurethanes and Their Use as Molecular Tags. *Chem* **1**, 114-126, doi:10.1016/j.chempr.2016.06.006 (2016).

General Introduction

This thesis is dealing with the synthesis of sequence-defined poly(urethane)s and their use in anti-counterfeit technologies. Indeed, the amount of forgeries has significantly grown during the last decades leading to major economic consequences and even in some extreme cases, endangering the health and life of customers. For instance, Intellectual Property Rights crimes reported recently that the losses caused by counterfeiting reach up to USD 461 billion annually worldwide, touching almost all types of products and all geographical areas[1].

Therefore, the need for creating new anti-counterfeiting solutions and providing secure alternatives available in the market is growing importantly[2]. Domains like pharmaceuticals, food industry, currencies, electronics, luxury products and high-value artworks are threatened continuously by counterfeiters. In this context, a wide variety of anti-counterfeiting solutions have been developed and are currently used for products' identification[3,4]. These solutions are extremely diverse and can be macroscopic (e.g. standard barcodes or QR codes), nanoscale (e.g. nanoparticles or nano-assemblies) or molecular markers. The generic word for denoting such identification markers is "taggant". A taggant is a specific fingerprint that can be added to a product and detected by an analytical method. Various chemical and physical properties have been exploited for preparing taggants. For instance, optical properties[5-7], fluorescence[5,7], nanoscale patterns and shapes[8,9] as well as chemical composition[10] are used as taggants. In the case of molecular taggants, detection methods are usually based on the determination of the chemical composition of mixtures. For example, combinatorial libraries, such as haloaryls[10] and lanthanides[11] have proposed for anti-counterfeiting applications. However, these methods give access to a limited number of codes[3] and are therefore not very broad in scope.

A new appealing solution to protect genuine products is the utilization of sequence-defined polymers[12], i.e. uniform macromolecules that contain a perfectly controlled sequence of functional comonomers as shown in **Fig. 7**. Indeed, in such polymers, the sequence of monomers can be used as a unique identification sequence. For example, using two functional comonomers (i.e. a binary language) more than a million of different sequences can be written on a polymer chain of 20 residues. Using three comonomers, this number is increased to several billions of potential identification sequences. Therefore, the information about a product of interest (batch number, production date, producer, etc.) can be written at the molecular scale in a sequence-defined polymer. The coded polymers can be deposited on the surface of a product or blended into it. Afterwards, the sequence can be identified using a sequencing technique, which is an analytical method that permits to decipher the sequence of the copolymer.[13] Hence, the detection or reading out of the code sequence allows to distinguish between counterfeit and genuine products.

Sequence-defined biopolymers such as polypeptides[14,15] and nucleic acids[16-19] have been already studied as taggants. For instance, several companies commercialize DNA sequences for anti-counterfeiting applications. Since DNA can be amplified by the polymerase chain reaction, these nucleic acids taggants can be deposited in trace amounts (sometimes at the ppt level) on a host material. However, this approach suffers from several drawbacks. First, DNA taggants can be contaminated by external genetic traces. Furthermore, like all polymers, DNA[20,21] is prone to chemical, photo-oxidative and heat degradation and is not optimal for all materials processing conditions. To overcome these problems, it was recently proposed that non-natural information-containing macromolecules can be used as molecular taggants[22].

Figure 7: Schematic representation of the use of sequence-defined polymers as anti-counterfeiting taggants for materials labeling

In 2014[23], it has been proposed that, similarly to DNA, abiotic macromolecules may contain monomer-based molecular information. These information-containing macromolecules cannot be prepared by standard polymerization methods such as chain-growth[24,25] and step-growth[26-28] polymerizations because these methods lead to polydisperse polymers containing sequence defects. Thus, they are usually synthesized by solid-phase syntheses, in which monomers are attached one-by-one to a support. Various types of non-natural information-containing macromolecules such as oligo(triazole amide)s[29,30], poly(phosphodiester)s[31], poly(alkoxyamine amide)s[32], poly(thiolactone)s[33,34], poly(alkoxyamine phosphodiester)s[35] or multi-components sequence-defined macromolecules[36],[37] have been reported in the literature.

Among all reported information-containing macromolecules, sequence-coded polyurethanes are promising candidates for anti-counterfeit technologies. PUs are widely used polymers in various industrial applications like coatings, biomedical, construction and automotive purposes due to their high stability. In general, poly(urethane)s are prepared via step-growth polymerization using isocyanate and diols precursors. However, these precursors are toxic[38], and the resulting polymers are non-uniform. The use of solid-phase iterative synthesis results in absolute control over the sequence and dispersity of poly(urethane)s[39]. Moreover, sequence-defined PUs can be easily decrypted by tandem mass spectrometry (MS/MS) [40]. It should be noted that in the entire thesis a binary code is used to encrypt messages in the sequence-defined PUs. Although, this binary alphabet was chosen as a model, more complex monomer codes can be used for real anti-counterfeit applications.

14

Early, in the spectrum of this work, I focus on the labeling of two model plastic materials, a polymer film and a 3D printed sculpture. By demonstrating that in both cases, the incorporation of the PU barcode, the preservation of the PUs structure and the MS detection were efficient for such applications; sequence-defined PUs were further used as molecular taggants for various materials. Investigation of the labeling and reading-out procedure, as well as the improvement of their security level were carried out in the herein Ph.D. thesis. This manuscript contains the published articles on the topic during the three years of my doctoral research and some unpublished data included in the chapters IV and VI. Six chapters, in total, are going to explain in depth all the important achievements on the domain of anti-counterfeiting and the broad possibilities for future applications.

The **Chapter I** of the thesis constitutes a bibliographic research on the topics and methods which were useful for the work carried out in the rest chapters. It is divided in three parts. The first focuses on sequence-controlled polymers from their discovery until the latest achievements, methods of preparation and characterization. Thereinafter, a very interesting aspect of them was analyzed, their use as information-containing polymers. In the last part, anti-counterfeit technologies are presented. To this context, information-containing polymers are proposed as an appealing solution to struggle forgeries.

Thus, they are used in the **Chapter II** as anti-counterfeiting taggants in ophthalmic implants. More particularly, sequence-coded polyurethanes were tested as anti-counterfeit tags for the labeling of intraocular lenses. ASCII-Coded messages stored in the molecular level in sequence-defined oligomers. The ophthalmic lenses were labeled via two different approaches: a) inclusion during the in situ free radical polymerization of methacrylate mixture and b) inclusion during swelling/deswelling of pre-made commercial lenses in PUs' solution. Important issues of the tags used, related with such biomedical applications like biocompatibility and transparency properties, were also tested.

As an evolution of the molecular taggants application, the barcodes were tested *In vivo* **in the Chapter III**. Due to the fact that fake medical implants for instance spinal, vascular, breast implants have been found counterfeited and have provoked health issues from simple allergies till uncontrolled bleeding even possible death, it is important to track and trace the medical devices that are included in our body. Thus, we proposed labeling of a model plastic implant with PUs molecular barcodes to distinguish genuine implants from implants made of low-grade materials that don't meet with the European safety requirements. Following the toxicity test of the poly(urethane)s, the labeled implants
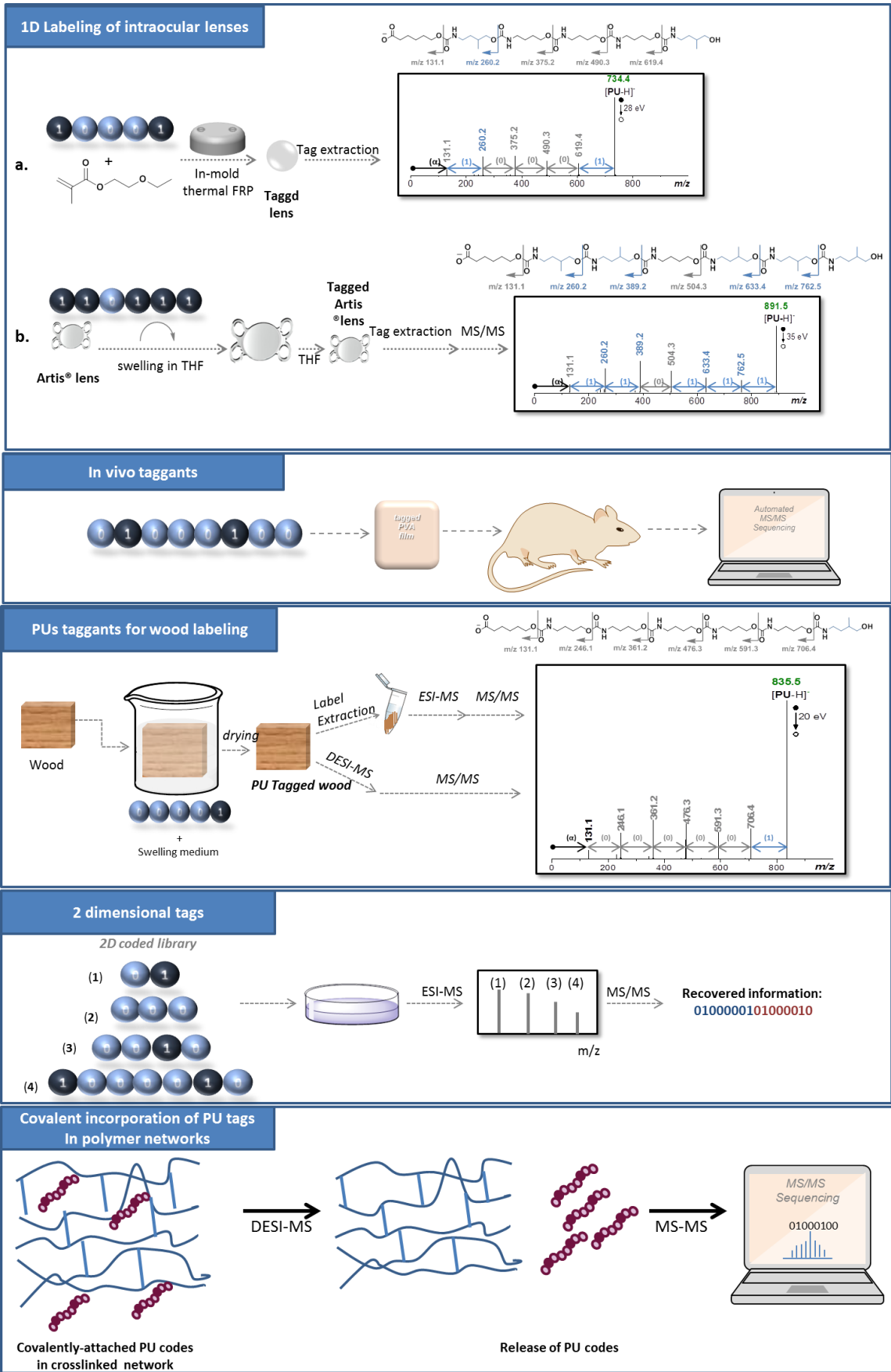
Figure 8: Representation of the research chapters and the general strategy for the labeling and the reading – out of the sequence-defined oligourethane taggant.

were introduced to live rats. After three different implantation periods, the labeled implants were explanted and the decryption of the barcode procedure took place.

One step further from the labeling of plastic matrices, labeling of wood is described on this **Chapter IV**. Wooden high-value furniture, musical instruments or wooden canvas decorating famous paintings could be potentially tagged with molecular barcodes since the threat of counterfeiting lurks. Digitally-encoded oligo(urethane)s were used to label different types of wood through immersion of the later in the solution of the taggant. The investigation of the labeling was carried out through two strategies, by DESI-MS on the massive wood and by ESI-MS on the extracted taggant in solution. MS/MS was used in both cases to sequence the oligourethane. These results are unpublished.

A need for providing extra secure molecular barcodes led us to the development of a 2-dimensional barcode design in the **Chapter V**. The idea of incorporating higher amount of information resulting in a more complex mass fingerprint could facilitate this purpose. The increase of information capacity was achieved by mixing distinct information chains. The only limitation of this concept is to merge sequences of different length and different molar mass in order to avoid reading-out problems by mass spectrometry. The 2-D barcodes were synthesized by iterative solid-phase synthesis and then they were applied on three different polymer films to test their effectiveness. Intentionally-formed polydispersed mass spectra were analyzed further by MS/MS to decrypt the complex message and to recover the encoded information.

Finally, in the **Chapter VI** it is described the attempt of covalently attach the PUs taggants into polymeric matrices on the direction of increasing the security and broaden the applicability field of the molecular taggants. Special modification of the oligourethane sequences was performed in order to incorporate them in a model p(NIPAM) gel through radical polymerization. A second modification was necessary in order to recover the coded oligourethane from the polymer network. Thus, the insertion of a disulfide DESI-MS cleavable bond on the oligomer enabled the release of the coded-message through reactive DESI-MS to be available for sequencing by DESI-MS/MS.

Chapter I:

Sequence-Controlled polymers &Anti-counterfeit technologies

1. Introduction

The objective of this first chapter is to describe prior-art and the broad scientific context of this thesis. In particular, three main topics are discussed within the next pages. In a first section, the important emerging field of sequence-controlled polymers is described. This first part is not meant to be fully comprehensive but shall give the readers an idea about the main methods that are used for the preparation and characterization of sequence-controlled polymers. In particular, some details are provided about solid-phase synthesis, which is the method that has been used in this work for the preparation of sequence-coded oligourethanes. In a second section, emphasis is put on information-containing macromolecules, which is an interesting sub-class of sequence-controlled polymers. In these polymers, a defined sequence of co-monomers is used to store information. Some details about the synthesis and decoding of these functional macromolecules are provided in this second section. The relevance of these polymers for anti-counterfeiting applications is also discussed. Finally, in the third and last section of this chapter, some anti-counterfeiting technologies are discussed. This field is particularly broad and therefore only some selected aspects are discussed herein. Yet, it shall give the readers a general overview about this important technological area.

2. Sequence-controlled Polymers

2.1 Terminology

Since the field of sequence-controlled polymers is relatively new, a brief reference to useful terms is included in this paragraph to introduce the reader to the context. The following terms are the most recent results found in the literature according to a latest review[41], however they are not yet official and some changes can still be made.

The term **sequence-controlled polymer** refers to a macromolecule in which monomer sequences are controlled to some degree. This control can be absolute but not necessarily. For example, an alternating copolymer prepared by radical chain-growth polymerization is a sequence-controlled polymer, although it is also a non-uniform polymer in which chains have different lengths and slightly different compositions.

Sequence-defined polymers: or sequence-specific polymers or sequence-ordered polymers constitute a subclass of sequence-controlled polymers. A sequence-defined polymer is a

uniform macromolecule with an exact chain-length and a perfectly defined sequence of monomers. In other words, each monomer unit is at a defined position in the chain.

Primary structure: *Syn. Microstructure [IUPAC official term].*In the context of macromolecules such as proteins, constitutional formula, usually abbreviated to a statement of the sequence and if appropriate cross-linking of chains[42]. According to the review even though the above term belongs to

the glossary of biology can be adopted by non-natural sequence-defined polymers to characterize their sequence distribution.

Sequencing: An analytical technique that allows to decipher comprehensively the monomer sequences of a sequence-defined polymer[13]. Sequencing methods are restricted to the analysis of uniform sequence-defined polymers.

2.2 Sequence control in biological polymers

Sequence control plays the key role in biology. The biopolymers, polymers synthesized by living organisms like polynucleotides, polypeptides or polysaccharides consist of long chains made of repeating and covalently bonded units arranged in an ordered manner[43,44].

It has been known for over 50 years that nucleic acids, DNA and RNA have the ability to store hereditary information in biological organisms thanks to their four-monomer nucleotide code (A, T, C, G for DNA and A, U, C, G for RNA). The well-defined sequence of nitrogenous bases along the DNA chain is responsible for the information storage which then passes from generation to generation. Moreover, the properties of the protein-based biomaterials owe their complexity and precision to their primary structure, in other words to their defined peptide sequences[45,46]. A short description of the sequence-controlled biopolymers and important facts in the evolution of the sequence definition are pointed out in the following paragraphs.

2.2.1 Nucleic Acids

DNA is a biomolecule responsible for the storage of genetic information in all the cellular organisms. The importance of the role of DNA was discovered first in bacterials in 1940s[47,48]. DNA is a linear polymer composed of four different monomers. The main backbone is built from sugar (deoxyribose)-phosphate units from where other substituents protrude the four nitrogenous bases. DNA was found to be in a double-helix form composed of two complementary strands [49]arranged in such way where the sugar-phosphates are in the outer side and the bases in the inner. This structure is owed to the specific bond pairs of the bases, named base-pairing rule. Adenine interacts with double hydrogen bonds with thymine and cytosine with triple hydrogen bonds with guanine **(Fig. I.1)**. So, one DNA strand with its defined nucleotide sequence can completely control the sequence of the bases on its complementary strand (during DNA replication)[50] as well as the sequence of the transcribed RNA (through transcription) and of the expressed proteins[44]. All the important genetic information required to "build" a new organism or maintain a living organism is stored in our DNA, into genes. Family medical history, heredity clues, everything that establishes our "identity" in its integrity is coded in sequences of the four bases of nucleic acid. And this information can be really long. For example, the E. Coli bacterium carries its genetic instructions in a DNA molecule of five million nucleotides. More interestingly, every cell in the human body carries in its nucleus, DNA of three billion nucleotides divided in 23 paired DNA molecules, the chromosomes
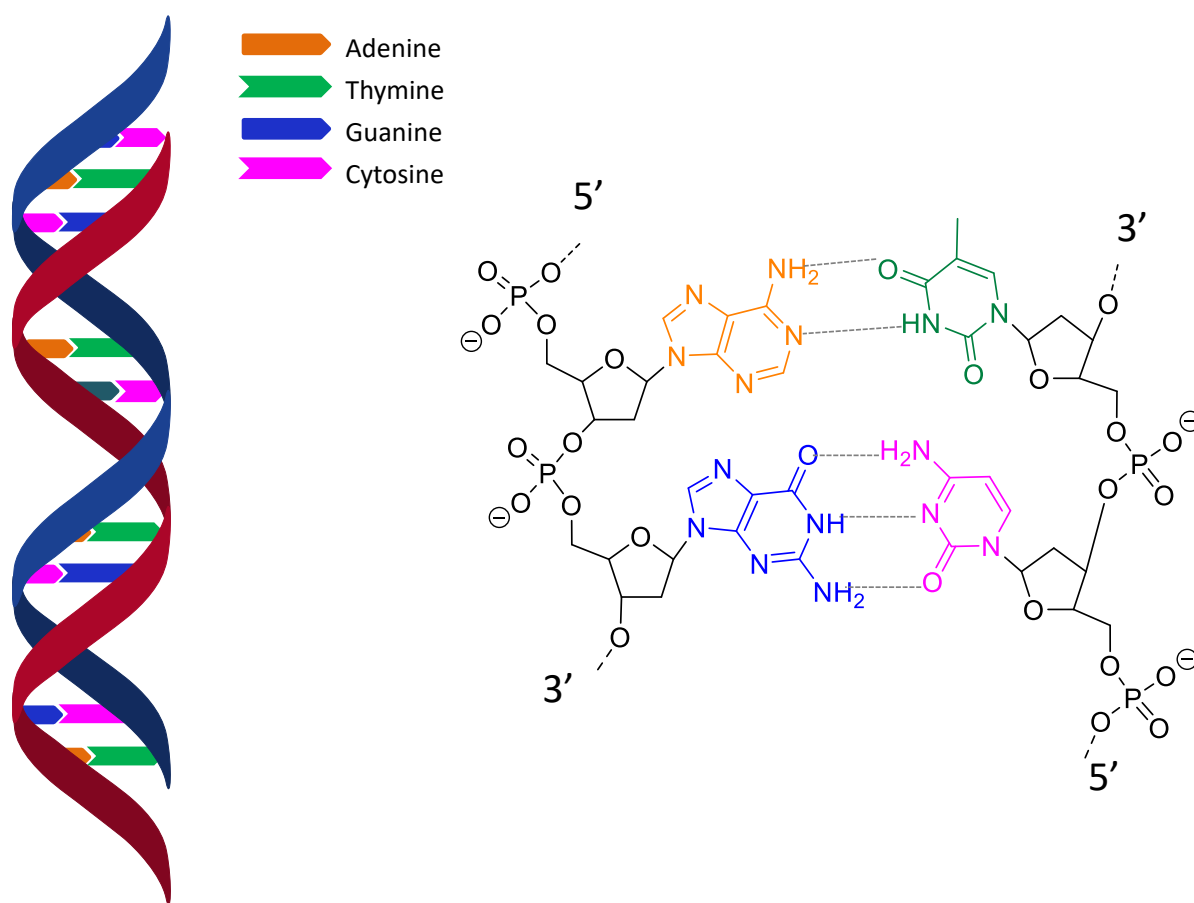
Figure I. 1: Representation of DNA double helix, its chemical structure and nitrogenous bases' bonding.

2.2.2 Proteins

Proteins were first described in the late 1830s from a Dutch chemist Mulder[51] and their secondary structure was discovered almost hundred years later by Pauling[52]. Proteins are biological macromolecules which are involved in many biological processes. They play the role of catalysts, they can transport or store other molecules like oxygen, they control growth and differentiation or they provide mechanical support and immune protection.[53] They are constructed by the ordered arrangement of 20 different α-amino acid monomers. They are synthesized from mRNA through the translation process where the nucleotide sequences are transcribed into amino acid sequences. Ribosomes of ~2.6-MD (bacterial) to ~4.3-MD (eukaryotic) size carry out the peptide synthesis by assembling amino acids from tRNA building blocks into peptidic chains following an ordered arrangement indicated by the sequence of mRNA strand that it moves along. With this very dynamic process the information "changes hands" moving from poly (phosphodiester)s to polyamides structure. Proteins start to fold in three dimensions structures directly after their translation. This folding of the protein chains into defined secondary, tertiary and quaternary structures relies on the sequence of the amino acids and determines importantly their functions[54]. In order to understand

better the correlation between the structure and the function of a protein the following example of the enzyme rearrangement is given. Enzymes, proteins who act as catalyst, fold in such way that distant amino acids of the primary structure come closer in order to compose the active site. The active site is the site in their structure which catalyzes an enzymatic reaction. After the protein folding the formed active site is ready to bind selectively to the substrate molecule called ligand initializing the reaction[55].
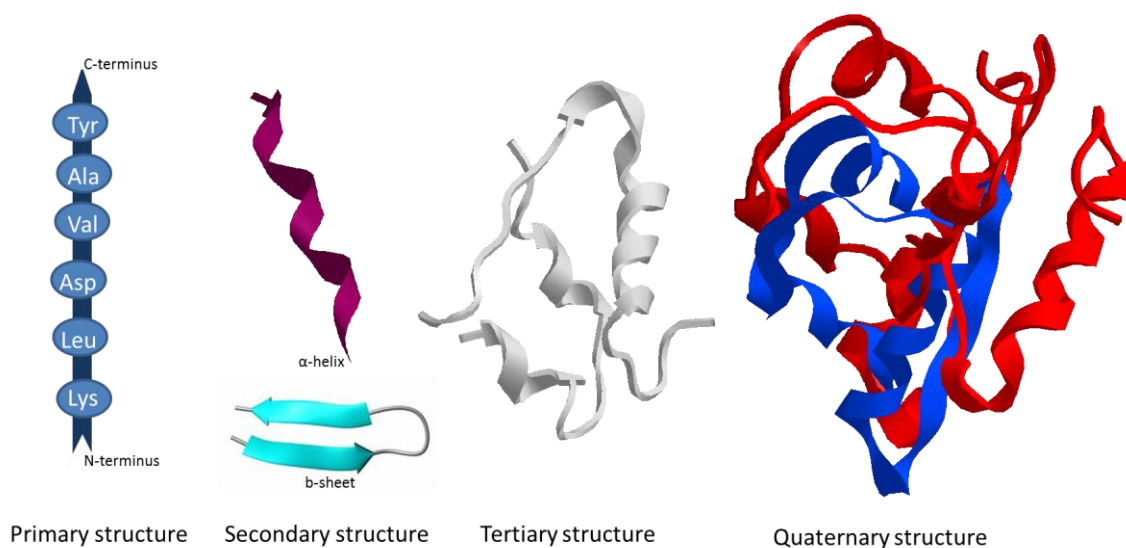
Figure I. 2: The four structures of proteins

Local regular structures such as α-helices or β-sheets are stabilized by hydrogen bonding of the amide backbone and are called secondary structure. The packing of such structure elements in domains localizes all atoms of the sequence and defines the tertiary structure whereas the quaternary structure is the eventual local arrangement with other proteins **(Fig.I.3)**. It is noteworthy that the primary structure of a protein inherently contains all information for its three-dimensional structure and complex interaction, yet, *in silico* prediction of folding is to-date unaccomplished.

2.2.3   Sequence-defined Oligosaccharides

Oligosaccharides are defined small molecules made typically of 2 to 10 monosaccharide residues linked with glycosides bonds. They have many important functions due to their defined structure. They are responsible for cell-cell interaction, communication between cells and extracellular surroundings, cell migration, immune response, blood clotting and other biological processes[56-58]. Monosaccharides (simple sugars) are the building blocks of oligo- or poly-saccharides. They are linked by O-glycosidic bonds between the hydroxyl groups, for example in a trisaccharide maltotriose **(Fig.I. 4)** the three D- glucose residues are joined by a glycosidic linkage between the a -anomeric form of C-1 on one sugar and the hydroxyl oxygen atom on C-4 of the adjacent sugar. This bond is called α-1,4-glycosidic bond. Like the proteins have directionality defined by the amino and the carboxyl end groups so do oligosaccharides, defined by reducing or non-reducing ends. The

carbohydrate unit at the reducing end has a free anomeric carbon atom that has reducing activity because it can form the open-chain form. By convention, this end of the oligosaccharide is still called the reducing end. The fact that monosaccharides have multiple hydroxyl groups means that many different glycosidic linkages are possible.
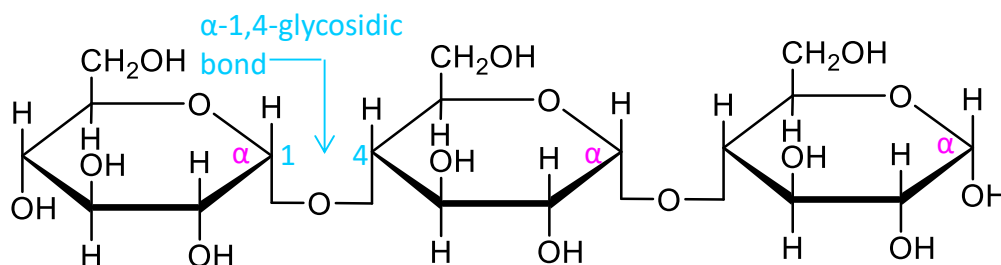
Figure I. 3: The chemical structure of a trisaccharidemaltitriose composed of three D-glucose monomer units

Oligosaccharides are more structurally complex than other biologically important molecules such as proteins and nucleic acids due to the fact that they are often highly branched and have several different linkage types between their fundamental monosaccharide units. The numerous structural possibilities make characterization of oligosaccharides a challenging but vital task because of their important biological role[59].

2.3 Sequence-control in synthetic polymers

As mentioned in the introduction of this chapter, the field of sequence-controlled polymers is a relatively new discipline. Most of the important discoveries in this field have been made during the last ten years. The main routes for synthesizing sequence-controlled polymers are briefly described within the next paragraphs. Since many of these approaches cannot be used for the synthesis of information-containing macromolecules, they are only succinctly described. The reader is guided to several recent reviews for additional information.

2.3.1 Bio-inspired methods

A logical transition from biological sequence-controlled polymers to artificial ones, was the adaptation of biological mechanisms for the synthesis of non-biological polymers. For example ribosomal synthesis constituted the inspirational tool for the preparation of synthetic SCPs. Like ribosomes have the role to bring together amino acids and arrange them in an ordered way determined by the RNA, molecular machines invented by D. Leigh[60,61] undertake the job of peptide synthesis imitating ribosomes. Artificial automatic molecular machines in the chemical form of a rotaxane are
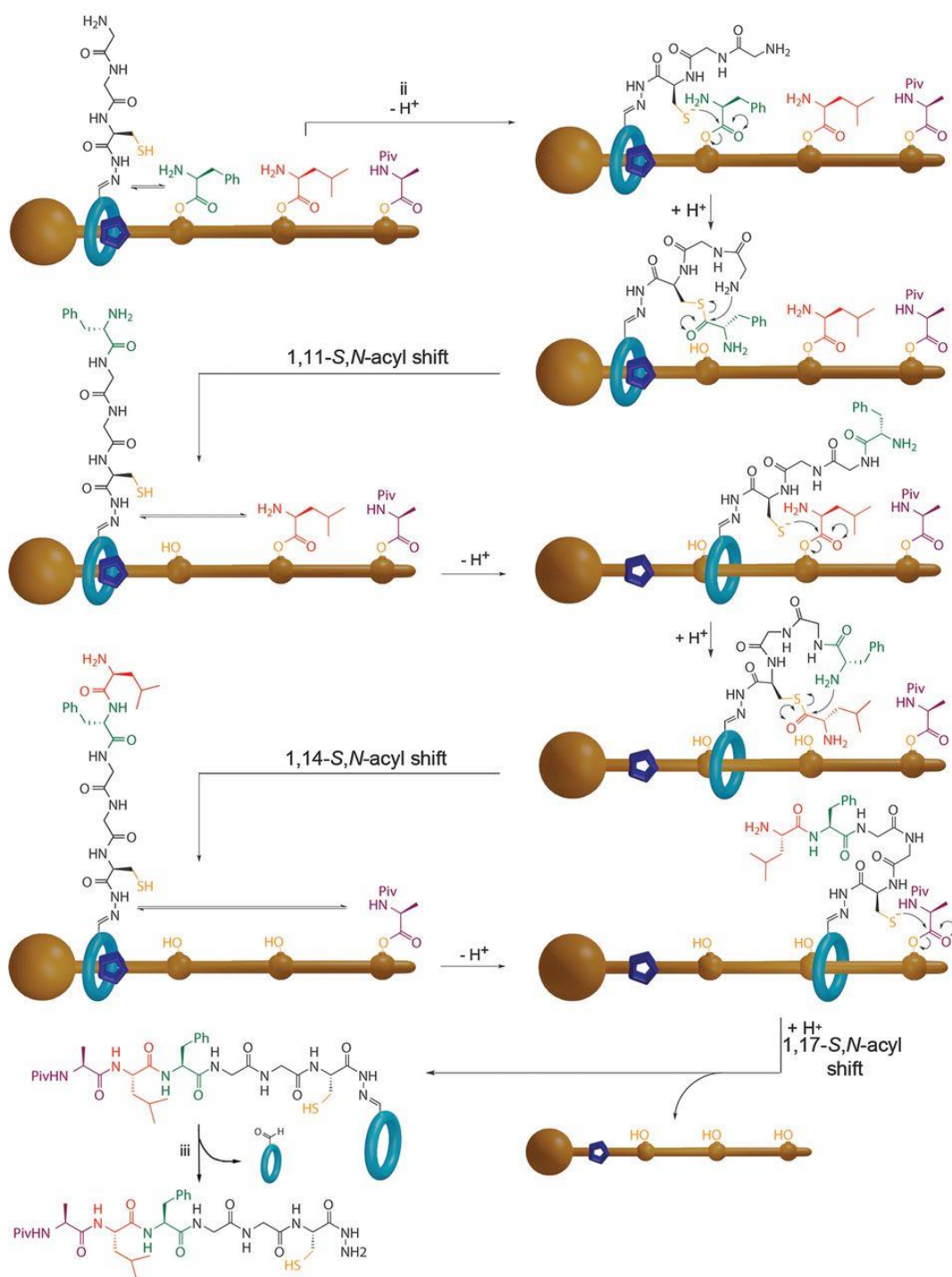
Figure I. 4: Proposed mechanism for sequence-specific peptide synthesis by molecular machine. After activation of the machine by acidic cleavage of the Boc and Trt protecting groups (not shown here), under basic conditions successive native chemical ligation reactions transfer the amino acid building blocks to the peptide-elongation site on the macrocycle in the order they appear on the thread. Once the final amino acid is cleaved, the macrocycle bearing the synthesized oligopeptide threads from the strand. The hydrazide peptide is subsequently released from the macrocycle by hydrolysis. Reaction conditions: (i) 20% CF₃CO₂H in dichloromethane, room temperature, 2 hours, 100%. (ii) ((CH₃)₂CH)₂NEt, (HO₂CCH₂CH₂)₃P in 3:1 acetonitrile: dimethylformamide, 60°C, 36 hours. Et, ethyl. (iii) 30% CF₃CO₂H in 3:1 dichloromethane: water, room temperature, 18 hours.

moving along a molecular strand picking up amino acids that block their movement to synthesize a peptide. The final peptides, their chemical structure and their amino acids sequence is confirmed by mass spectrometry.

The peptide synthesis after the activation of the molecular machine is shown in details on the **Figure I.4**. The stand on which the rotaxane is moving is composed of three different amino acids separated with a spacer in order to avoid reaction of the macrocycle with an amino acid out of the determined sequence. The molecular machine is operated at 60°C under microwave heating in presence of a non-nucleophilic base N,N- diisoproylethylamine and a reducing agent that cleaves possible disulfide bridges formed during thiol oxidation. Once the thiolate residue is deprotected, it is ready to react with the first amino acid phenolic ester found in the strand. There is afterwards a subsequently S-N acyl transfer according to which the amino acid is transferred to the end of the growing peptide. The generated thiolate group is again free to add new amino acids that will block the way of the rotaxane to the growing peptide. Once the peptide is formed and the rotaxane reaches the end of the strand is detached from it, bearing the newly formed peptide.

2.3.2 Sequence-regulation in polymerizations

As recently proposed[62], synthetic polymers can be prepared by three main mechanisms: *(i)* step-growth polymerization, *(ii)* chain-growth polymerization and *(iii)* multi-step growth synthesis. In general, comonomer sequences are poorly controlled in the former two approaches, while the later strategy is more suitable for the synthesis of sequence-defined polymers. Nevertheless, some examples of sequence-regulation in chain-growth and step-growth polymerizations have been reported.

a. Step-growth polymerization

Step-growth polymerizations lead to polymers with poor control of the chain length and the molecular weight distribution. Monomers containing multiple reactive functions react to give linear in the case of AB monomers or more complex architectures (like cyclic or cross-linked).
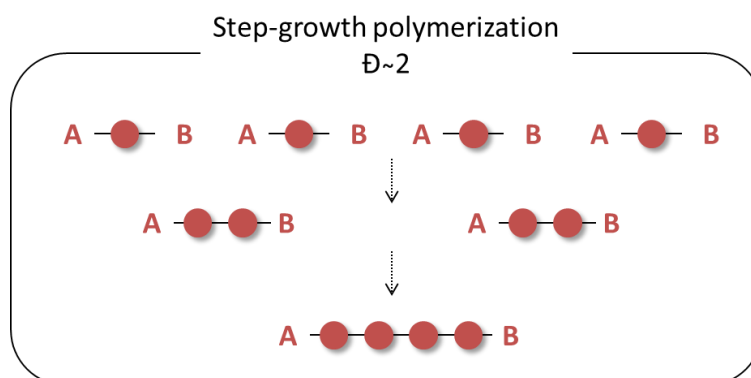
Figure I. 5: Schematic representation of the step-growth polymerization

In these cases, the resulting polymers are not characterized by regulated monomer sequences unless between the two reactive functions of the monomer is included a wide spacer made of prelinked monomers placed in certain position[65]. The monomers with the reactive, unconjugated C=C and C–Cl bonds, react through copper-catalyzed step-growth radical polymerization to give long sequence-regulated polymers. [63,64]
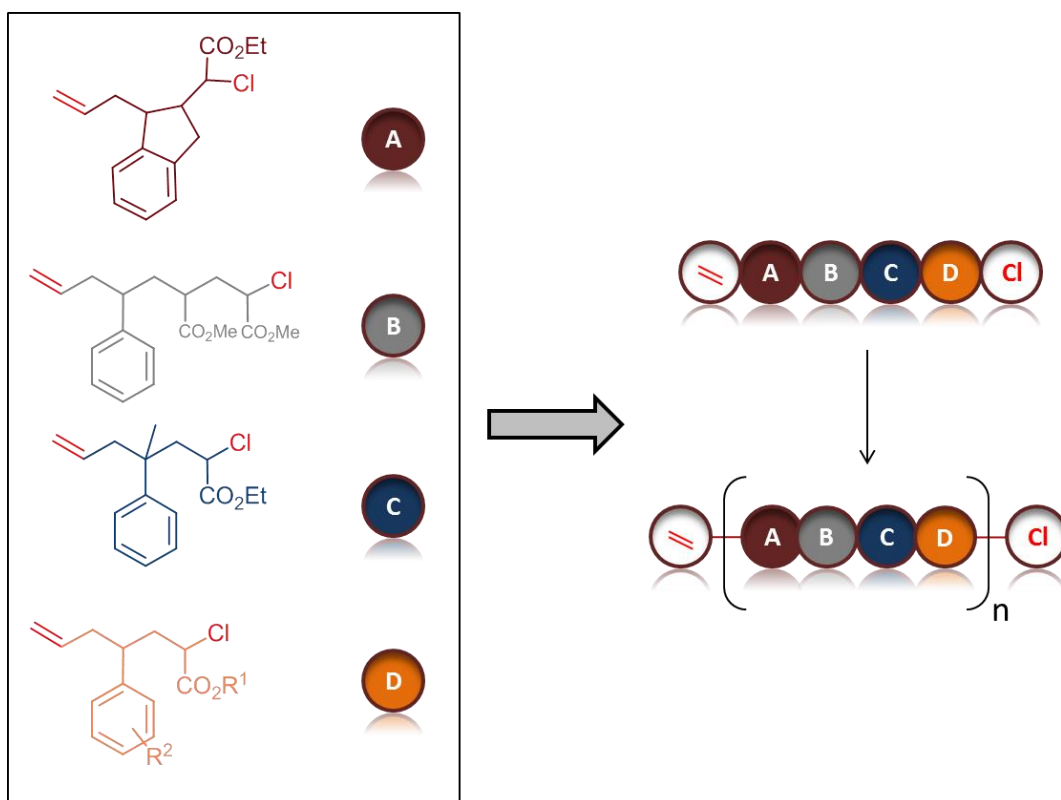
Figure I. 6: Strategy for the synthesis of sequence-regulated polymers made from prelinked monomers with reactive end groups: double bonds and –Cl[63].

b. Chain-growth polymerization

Generally, in chain-growth polymerization, the growing polymer chain contains at least one active center which each monomer can react with and be added to the polymer chain. The active center is transferred each time to the new monomer added until the termination stops the polymer growth through disproportionation or combination of two active centers. However, generally conventional chain-growth polymerizations lead to polydisperse polymers. Optimized chain-growth polymerization can be achieved via anionic, cationic, radical and ring-opening mechanisms. In all the above cases, the resulting polymer chains are uniform due to slower propagation step comparing to the initiation and chain transfer or termination are suppressed. Among the others, radical controlled polymerization with its subclasses (ATRP[65,66], NMP[67] and RAFT[68]) are the most used technique due to a wider variety of monomers and easy reaction procedures. [69]
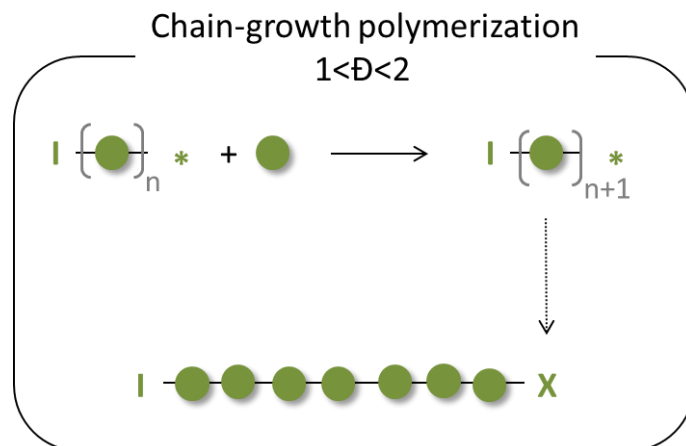
Figure I. 7: Schematic representation of the chain-growth polymerization

For instance, an interesting approach for the control of monomer sequence distribution through radical polymerization is depicted on the **Figure I.8**. According to an earlier work[70], it was showed that maleic anhydrides and N-substituted maleimides differ from styrene in terms of reactivity ratios leading to the copolymerization of the first with styrene more favorably than their homopolymerization. Based on this, a protocol for precise insertion of different N-substitute maleimides in the polystyrene chain via atom ATRP was developed[71]. The results showed that the formed copolymer might not be perfectly sequence-defined but it is still possible to acquire a sequence of functional side groups of the N-substitute maleimides through ATRP.
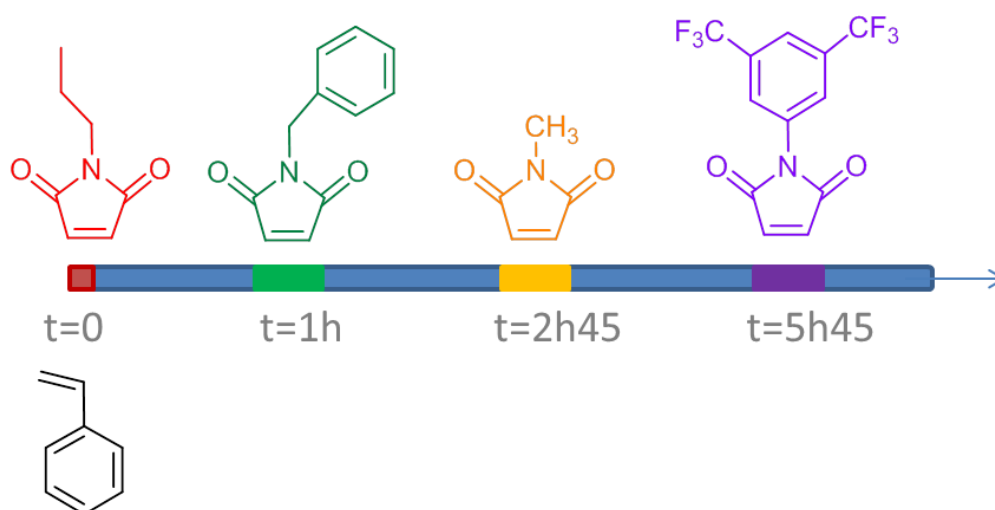
Figure I. 8: Sequential Atom Transfer Radical Copolymerization of Styrene and Various N-substituted maleimides

c. Multistep-growth polymerization

In multistep-growth polymerization, uniform polymers are prepared by stepwise chemical reactions. The polymerization technique is based on the use of bifunctional monomers XY[12]. A protection of one

of the two reactive functions is preceded in order to achieve uniform polymer chains (Đ≈1). The iterative reaction of the XY monomers is a very useful multi-step growth approach because a wide variety of chemical structures and sequences can be attained. The X function reacts with the Y function of the second bifunctional, which has the X function protected. Deprotection of the previously protected X function will allow to the next monomer attachment. Multiple iterative steps of reaction/deprotection /reaction can achieve long uniform polymer sequences. When performed in solution, such a stepwise approach is time-consuming and requires purification at each step. However, such process can be significantly simplified by the use of a solid-support. This aspect is described in details in the following section. For instance, phosphoramidite chemistry for the preparation of non-natural sequence regulated polymers demands reaction/deprotection/reaction steps as demonstrated by our group[72] and by Sleiman[73].
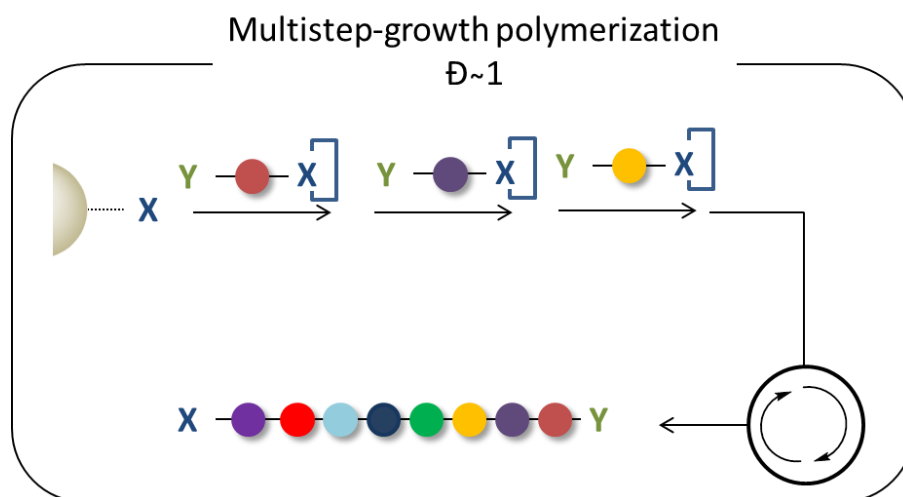
Figure I. 9: Schematic representation of a multistep-growth polymerization

Sleiman and coworkers attempted to enrich their molecules with molecular recognition. For this purpose they created DNA-polymer conjugates consisting of a DNA portion functionalized at its 5' terminus with a series of hexaethylene or hexaethylene glycol units punctuated by phosphate moieties. DNA was synthesized on CPG solid-support and the oligomers were appended on DNA strand using the same phosphoramidite chemistry. Thus, coupling efficiency was monitored after removal of the dimethoxytrityl (DMT) of the DNA block as well as of the monomer units DMT-hexaethyloxy glycol and DMT-dodecane-diolphosphoramidites. In the end, the synthesized block copolymers were cleaved from the solid support and deprotected from the protecting groups under basic conditions. (**Figure I.10**)
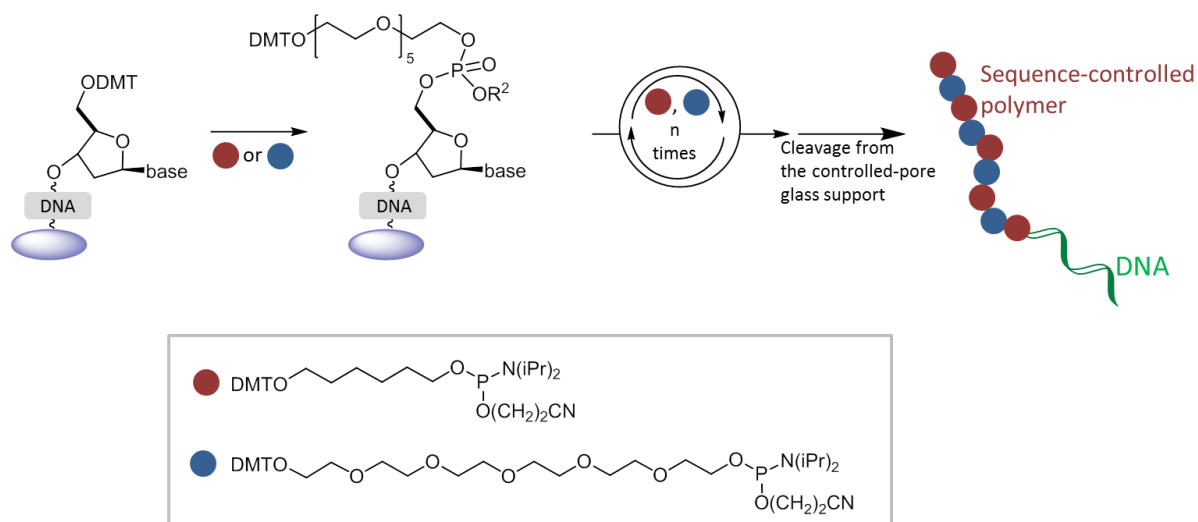
Alternative strategies for the stepwise synthesis of sequence-defined polymers without the need of protecting units were developed. Interesting examples are the submonomer solid phase synthesis for the peptoids preparation[74], poly(alkoxyamine amides)[75] and the Passerini three-component reaction[76]

2.4 Solid Phase Synthesis

2.4.1 General concept

As described in the previous paragraph, iterative synthesis on solid support constitutes one of the most convenient ways for monomer sequence regulation. The procedure requires special solid phase synthesizers made of glass or plastic equipped with frit (**Figure I.11**). Insoluble supports (e.g. cross-linked resin) are placed on the frit of the synthesizer vessel and reagents and solvents are added in excess. The key to this approach is the use of resin beads to anchor the growing polymer chain via a cleavable bond. After the reaction finishes, washing steps follow in order to remove the non-reacted monomers in excess or coupling agents and addition of the next monomer is taking place. After repeating this procedure several times the monomers are attached one-by-one on the resin manually or in novel developed automated synthesizers. In the end and once the desired sequence and length is achieved, the sequence-defined polymers are cleaved from the solid support and can be isolated. Although performing the synthesis on solid support can prevent the fast access of reactants to all the beads of the resin, the addition of reagents in large excess can compromise this disadvantage by increasing the rate and driving the reaction to completion. The positive point about this synthetic path is the rapid purification and thus the short assembly times.
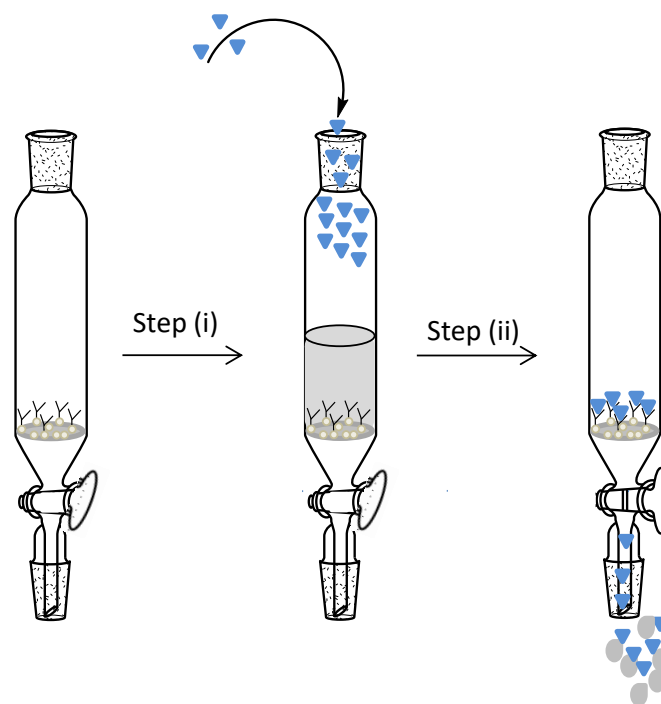
Figure I. 11: Representation of the solid-phase synthesis principle.

Solid phase synthesis was first developed for peptide synthesis by Merrifield[77]. Merrifield was awarded with the Nobel Prize after this development[78]. The series of heterogeneous reactions between the growing peptide anchored on the solid support (solid phase) and all the reagents which were in solution form, leading him to name the procedure "solid phase synthesis". All the intermediate formed peptides were purified very easily by a simple filtration through the frit of the synthesizer. The technique is easy and present several advantages such as the acceleration of the multistep synthesis avoiding losing material during transfers and complicated purification steps, the acquisition of high yields by simple use of reagent excess and the increased solvation and decreased aggregation of the intermediate products. Although solid-phase synthesis was initially developed for peptide synthesis, the concept was afterwards applied the synthesis of polynucleotides[79] and polysaccharides.[80] Still today, this approach is the most commonly used strategy for the preparation of sequence-defined oligomers and polymers.
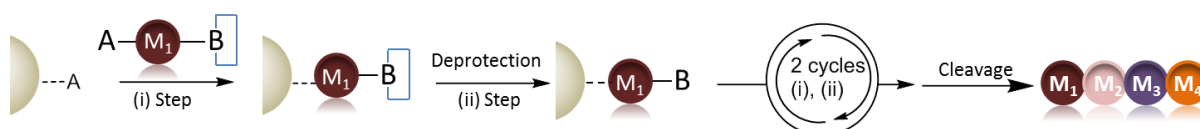
Figure I. 12: General approach of solid-phase synthesis with protecting groups

As described in section **2.3.2.c**, solid-phase synthesis approaches usually require protection of one of the two functions of a bifunctional monomer AB type. The protection is demanded in order to avoid undesired polycondensation reactions which will lead to uncontrolled sequences[81,82]. However, as shown in **Figure I.13**, some protecting-group-free approaches have been also been reported.[83,84]
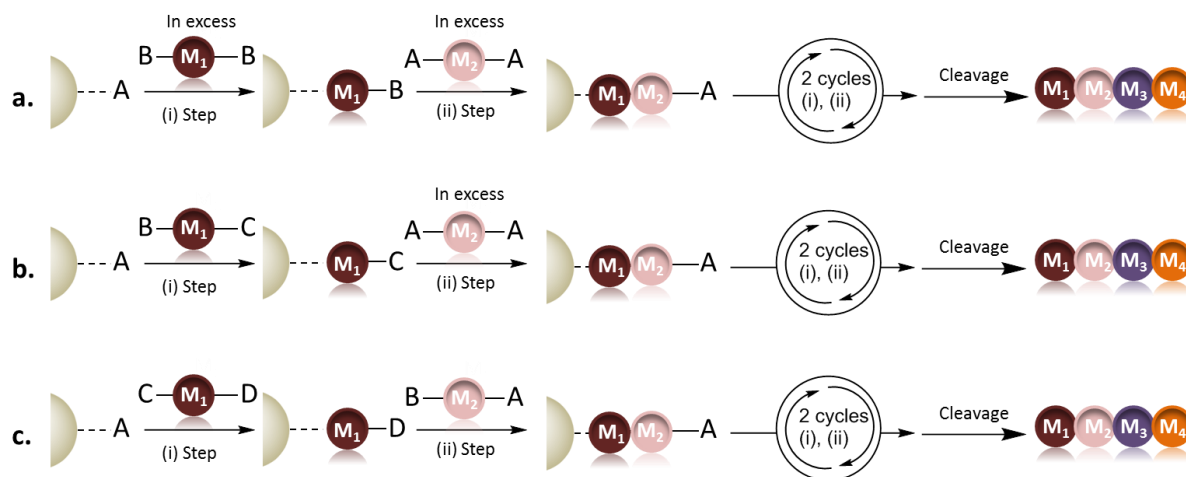
Figure I. 13: Three different approaches for protecting groups-free solid phase synthesis. a) AA+BB approach where the function A reacts with the function B of the other monomer. The two bifunctional monomers are used in excess in both steps (i) and (ii); b) AA+BC approach where the function A reacts selectively with function B of the next added monomer BC during the reaction step (i). Function C reacts selectively with function A during the step (ii). The monomer AA is added in excess during the same step; c) AB+CD approach where function A reacts selectively with function C and B with D on the coupling steps (i) and (ii) respectively.

2.4.2   Solid Support

One important parameter that should be considered in the solid phase synthesis is the nature of the solid support. The selection of the appropriate solid support is made according to the mode of attachment and cleavage conditions needed (linker), the nature of chemistry planned for the library synthesis, the amount of the material desired (loading rate) and the size of beads (affects efficiency of diffusion within the polymer and reaction times).The characteristics that a solid support should bear are: good swelling ability for efficient accessibility to all the reactive groups of the resin, mechanical and thermal stability to be flexible in the reaction conditions[85]. Some mainly described solid supports are the following: polystyrene resins, polyamide resins, polyethylene glycol containing resins, hybrid resin like Tentagel (PEG [<70%]-*g*-PS),including cross-linked ethoxyacrylate (CLEAR) resins and H-Rink Amide (ChemMatrix), cellulose (spot synthesis on paper), inorganic (controlled-pore glass for oligonucleotide synthesis or controlled pore ceramics offering high thermal stability). The resins can be modified with a huge range of cleavable linkers.
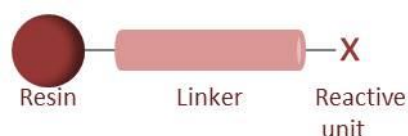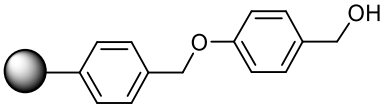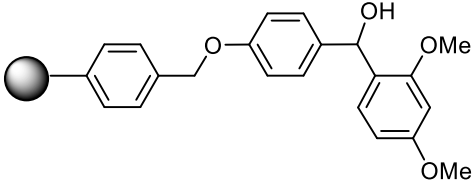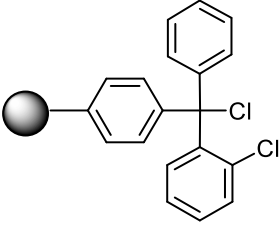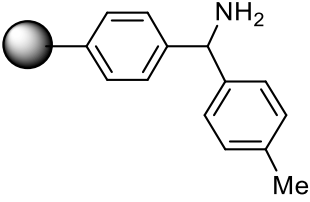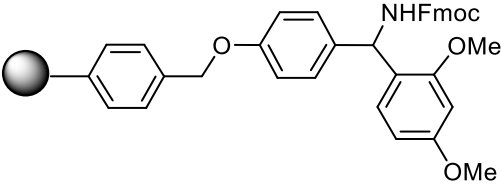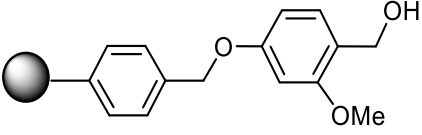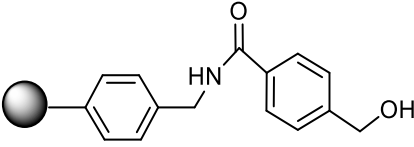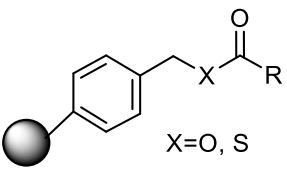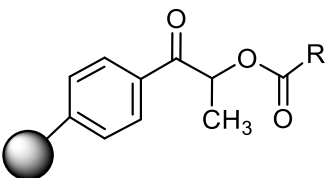
Figure I. 14: Representation of structural units of one resin bead

A linker is a molecule covalently attached to the solid support as it is shown in the **Fig. I. 13** and determines the chemical attachment of the first monomer to the support and the final cleavage conditions of the synthesized oligomer from the resin (cleaved under acidic or basic conditions or photo-cleavable). The linker is attached to the resin with a labile bond to be cleaved afterwards easily and it is attached to the solid phase polymer with a more stable bond. Although, the resins can be purchased with built-in linkers, it is important to note that the linker is independent of the resin type. There are several interesting reviews which deal with the linkers used in peptide solid phase and synthetic molecules solid phase synthesis[86-89]. The linkers can be categorized in three main types: i) acid labile: strong volatile acids like HF and mostly TFA are used to cleave the polymer from the resin in the linker position. The more stable cation formed, the more labile is the linker to acid. ii) base labile. Under basic conditions and usually through reactions involving nucleophilic addition/elimination or base catalyzed reactions such as elimination or cyclization the basic labile linker is cleaved off the resin. iii) photolabile linkers, cleaved after photo-irradiation.

The table below contains the most popular linkers described in bibliography.

Table I. 1: Resin Linkers[90]

Linker Type	Linker	Resin name	Resin Structure	Cleavage conditions	Product
Acid labile	Hydroxymethyl	Wang resin		90–95% TFA in CH2Cl2 (1–2 h)	acid
Acid labile	Benzylic	Rink acid resin		1–5% TFA in CH2Cl2 (5–15 min) or 10% AcOH in CH2Cl2 (2h)	acid

Acid labile	Benzylic	2-Chlorotrityl chloride resin		1–5% TFA in CH_2Cl_2 (1 min)	acid
Acid labile	Amide	MBHA		HF 0ºC (1 h)	amide
Acid labile	Amide	Rink amide		50% TFA in CH2Cl2 (1 h)	amide
Acid labile	benzyl alcohol	Sasrin resin		1% TFA in CH2Cl2 (5–10 min)	acid
Base labile	HMBA	HMBA resin		NaOH, N2H4, NH3 In MeOH(24 h), ROH LiBH4	Acid Hydrazine, amide Ester Alcohol
Base labile	Merrifield	Merrifield resin	X=O, S	ROH, base LAH	ester
Photo labile		α-Methylphenacyl ester resin		hv	acid

35

2.4.3 Automation

The solid phase synthesis was automated almost directly after the manual solid phase synthesis development[77]. For first time a special apparatus[91] was constructed for performing automated peptide synthesis. It was equipped with a pumping system of proper solvents and reagents connected with the reaction vessel made of glass and two motor-driven circular selector valves. Solvents and reagents were stored in reservoirs and transferred through a glass-Teflon system to the vessel.

(Semi)automated protocols were then developed with the intention to accelerate and facilitate the iterative solid phase procedure of oligonucleotides[92] and oligopeptides[93] to lead afterwards to the automated synthesis of other chemical structures of non-natural sequence-controlled polymers[72,94-96].

2.4.5 Solid-phase synthesis of bio-oligomers

The chemical synthesis of peptides was described by Fischer with the glycine-glycine dipeptide in 1901.[97] Sixty years later, after achievements of Curtius, Bergmann and Zervas, Akabori and Du Vigneaud[98], Merrifield[99] carried out the peptide synthesis on solid support as presented on the **Figure I. 15.** He developed a functionalized resin to which an amino acid could be anchored and the synthesis of uniform long polypeptides could be achieved avoiding difficult intermediate purification steps. The protocol starts with the attachment of the first amino acid which as ω-terminus has a carboxyl group. The amino- group was protected earlier and the linkage takes place through a stable covalent bond. The N-protected amino-group is then deprotected with minimal loss of the anchoring bond or of the other protecting groups, constituting a new active site where the next N-protected amino acid will be attached. The deprotection and the coupling steps are repeated until the desired peptide is synthesized. In the end of the synthesis the polypeptide is cleaved from the solid support. The carbobenzyl protecting groups (Cbz) used in the first protocol of 1963 were replaced in the automated protocol by Boc[77] making the polypeptide synthesis more efficient.
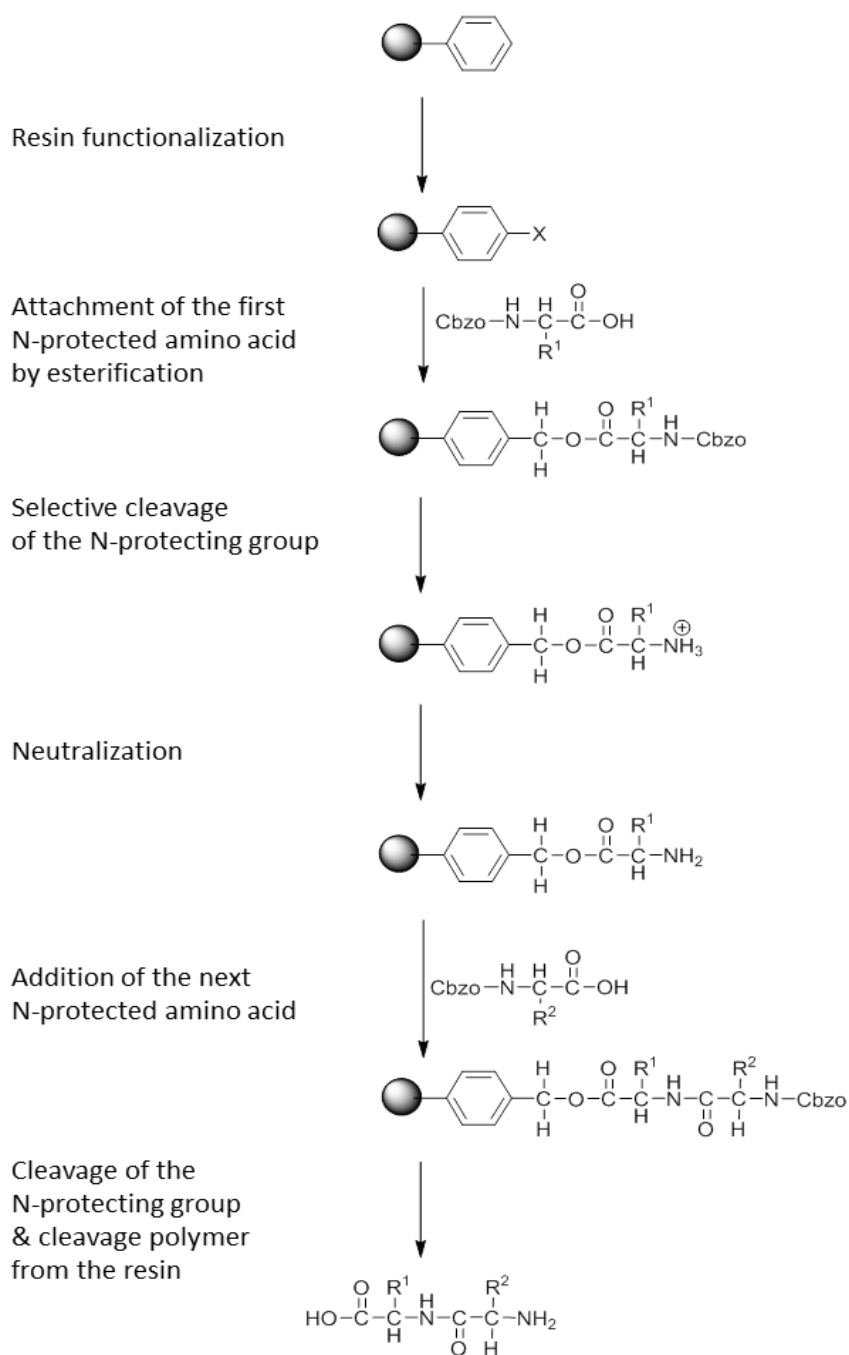
Figure I. 15: Diagram of the Merrifield synthetic protocol for the proteins' preparation

2.4 Solid phase synthesis of non-natural oligomers

Although widely used for the synthesis of bio-oligomers, solid-phase synthesis is also a powerful tool for the synthesis of abiotic sequence-defined polymers. In this section, some selected examples are described. This part is not exhaustive and several additional examples can be found in recent reviews.

The Lutz group developed many different synthetic paths for sequence-defined polymers with polydispersity close to 1 with and without protective groups. These syntheses will be analyzed in details in the digital polymers section (Ch. 1 Section: 3.4)

Du Prez and coworkers made extensive research on the thiolactone chemistry -based sequence-defined polymers.[34,84] Firstly, a carboxyl-functional thiolactone linker was coupled to a 2-chlorotrityl resin using standard conditions to start the synthesis with an immobilized thiolactone on the solid support. Then, ring opening of the thiolactone ring took place by their reaction with primary amines. During the protecting-group free aminolysis, several functionalized amines could serve for different coded units to the polymers[34]. Chain extension was achieved after on-resin aminolysis by using a thiolactone building block to reestablish the thiolactone functionality by a bromo-substituted thiolactone or an N- acryloyl-thiolactone suspected to thiol-bromo substitution and thiol-Michael addition, respectively. After cleaving the synthesized oligomers through their acid-labile linkage from the solid support, they were fully characterized by NMR spectroscopy and HRMS (High Resolution Mass Spectrometry)
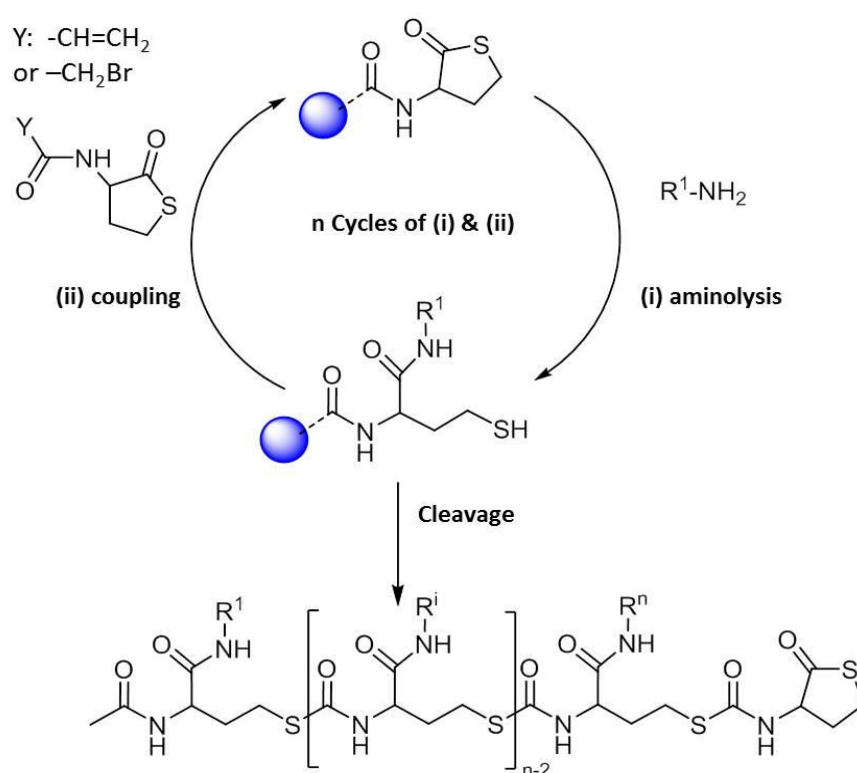
Figure I. 16: Two-step iterative method for the synthesis of functionalized oligomers on solid support: aminolysis of the resin-bound thiolactone followed by coupling of a thiolactone-containing building block that selectively reacts with the generated thiol

Using solid phase synthesis, Hartmann and coworkers[95,100,101] prepared monodisperse, sequence specific polymers. The strategy is based directly on the classical Merrifield peptide synthesis but instead of using *N*-protected *α*-amino acid derivatives which are coupled sequentially, here, alternating condensation of dicarboxylate and diamine monomers is performed. The resulted polymers bear polyamide segments with additional functionalities within the chain or in the side chains depending on the structure of the building blocks. Different combinations of monomer diacid/diamine sets or anhydride/diamine can be established in order to create a particular polyamide sequence structure permitting the introduction of desired functionalities such as cationic groups (tertiary,

secondary or primary amines) or different spacers (ethyl, ethylene glycol). The conjugated monodispersed segments with either poly(ethylene glycol) (PEG) or oligopeptides or oligonucleotides allow the fine-tuned interactions with biological systems for example the plasmid DNA.

The formation of the desired product and the absence of possible side products was confirmed at different steps of the synthesis by electron spray ionization mass spectrometry (ESI-MS) and NMR analysis.
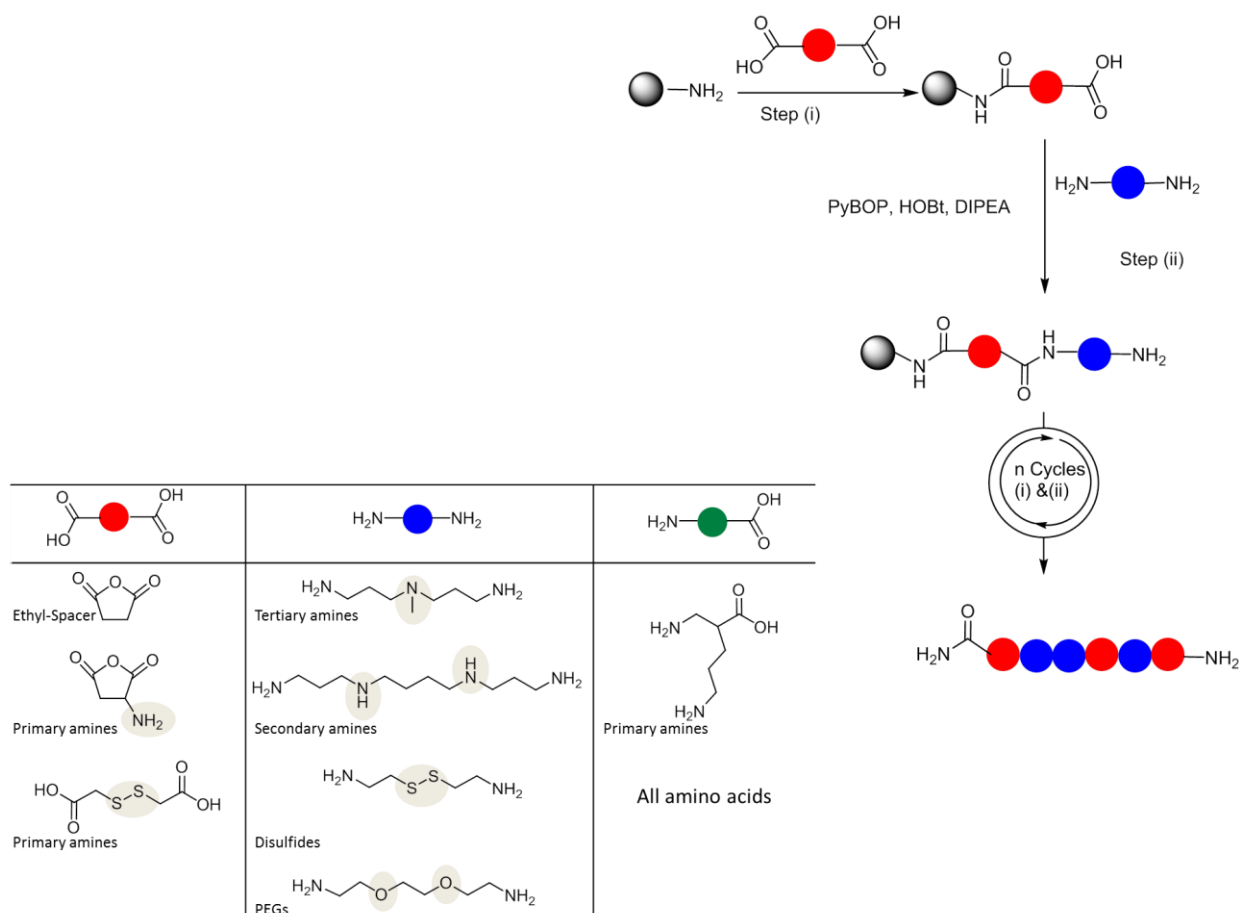
Figure I. 17: Two step synthesis of sequence-defined poly(amido amine)s[101] a) Step (i) addition of diacid building block b) addition of diamine building block facilitated by benzotriazol-1-yl-oxytripyrrolidinophosphonium hexafluorophosphate (PyBOP), Hydroxybenzotriazole (HOBt) and *N,N*-diisopropylethylamine (DIPEA)

Another solid support synthesis was reported by Grate and co-workers for the synthesis of sequence-defined triazine-based macromolecules with side-chain diversity and backbone-backbone interactions[102]. The synthesis is based on the nucleophilic aromatic substitution of cyanuric chloride. Sequence-defined hexamers bearing neutral and ionizable side-chains were prepared through this approach. In brief, each reaction of the cyanuric chloride compound deactivates the substrate and then it demands elevated temperatures in order to react further. This cyanuric chloride deactivation helps conducting the synthesis without any protecting group. The use of different mono-substituted cyanuric chloride sub-monomers allows the insertion of the term sequence in these polymers as they act as building blocks and they lead to specific non-covalent backbone interactions. By molecular dynamics

simulations, it could be shown that triazine-based sequence-defined polymers exhibit backbone interactions, such as π–π-interactions or hydrogen bonding. These properties might be interesting in terms of intermolecular self-assembly and the formation of three-dimensional structures.
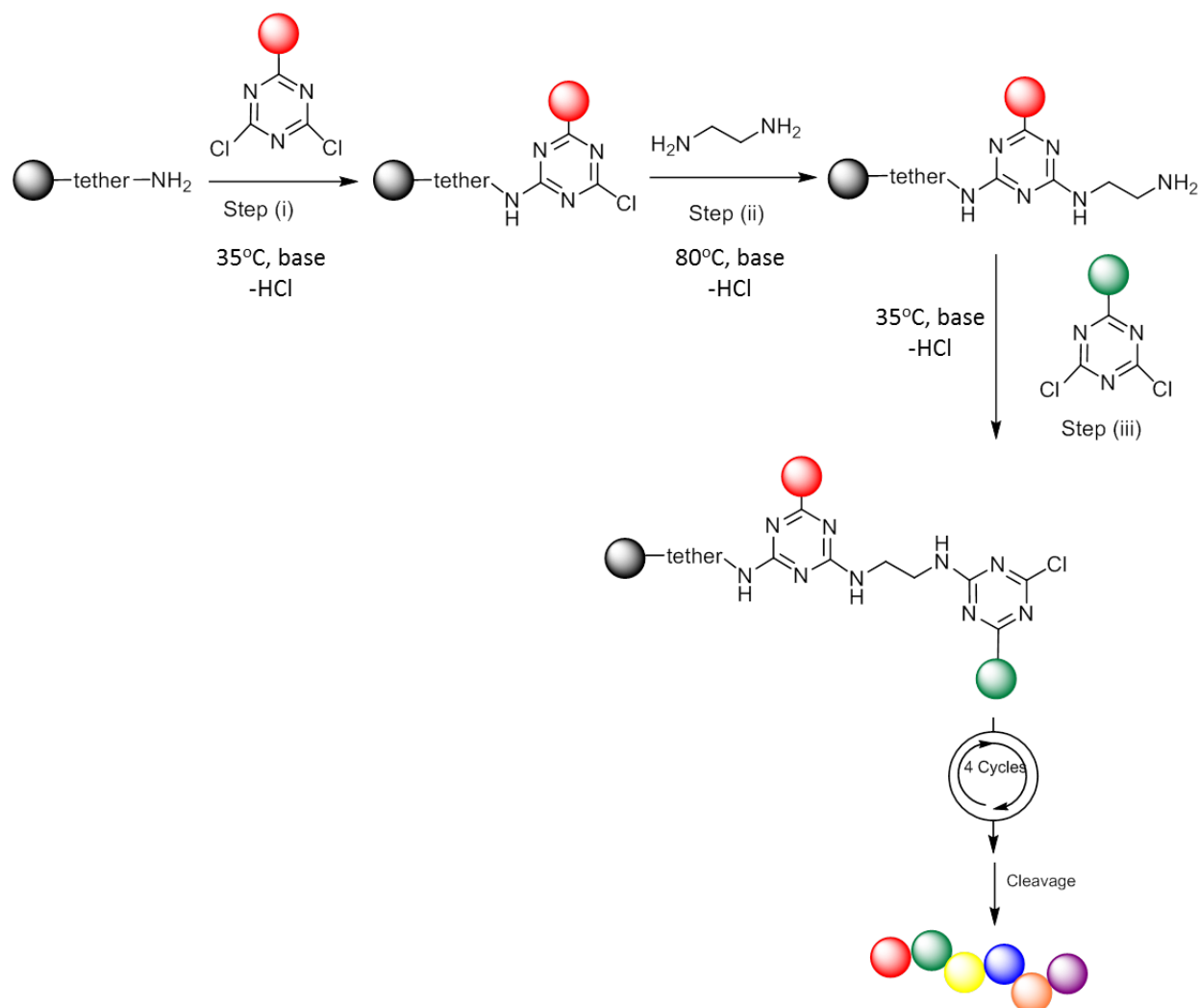
Figure I. 18: Representation of the solid-phase synthesis of triazine-based sequence-defined polymers.

Of course there are sequence-defined polymers that are synthesized successfully on other kinds of supports such as soluble[76,103,104] supports and a combination of the aforementioned supports, the fluorous support[105-107]. In the case of fluorous liquid-phase synthesis, monodispersed macromolecules are obtained by adding in the reaction solution fluorous soluble tags. By assembling the fluorous tags with the prolonging macromolecule it is easy to add the monomers in solution and to get rid of possible impurities and reactants excess through fluorous solid phase extraction.

2.5 Sequencing and characterization

2.5.1 Sequencing methods for biopolymers

Sequencing of biopolymers (see definition page 14) is one of the greatest achievements of biology in the 20th century because it contributed to the understanding of the code of life. Its use is now extended in analyzing non-natural macromolecules for the identification of their monomer sequences. The tools for the sequencing of synthetic polymers are not only based on biology but rather on chemistry and particularly polymer chemistry. This paragraph is focused on the breakthroughs until the development of the sequencing methods as we know them today.

Peptide sequencing was first invented in 1950 by Edman whose method was based on the determination of the amino acids sequence in a peptide by cleaving each time the N-terminal amino acid residue to identify it later on by chromatography or other possible methods[108-110]. DNA sequencing methods were discovered two decades later by Sanger[111-113]. He first introduced the concept of DNA polymerase use for DNA sequencing. The work was completed in 1975 with the named "plus and minus" method[111] for the determination of the nucleotide base sequence of bacteriophage φX174. This method proved later to be not so trustful and rapid, leading to a new sequencing technique with chain-terminating inhibitors[112]. This method is faster and more accurate than the previous one and needs 2', 3' dideoxy and arabinonucleoside analogues of the normal deoxynucleoside triphosphates, which act as specific chain-terminating inhibitors of DNA polymerase. Once the mixture of fragments is ready then it's fractioned by electrophoresis on denaturing acrylamide gels and the pattern of the bands of all the different fragment mixtures shows the sequence of the nucleotides. Maxam and Gilbert in 1976-1977 discovered a method of DNA sequencing by its chemical modification and subsequent cleavage in the position of specific bases[114]. The discovery of polymerase chain reaction (PCR) amplification by Mullis[115] evolved much the field. Among the others the DNA cloning resulted by PCR amplification is used afterwards for the determination of DNA sequence. Except for these first breakthroughs in the DNA sequencing domain, a plethora of other next-generation sequencing (NGS) methods have been found and are described in the review of Metzker and Mardis[116,117]. NGS are the newest DNA sequencing technology for parallel deciphering of millions of DNA molecules at once. Among other techniques mass spectrometry is used for DNA sequencing and is considered as a more accurate technology[118] than other state-of-art methods like sequencing by fluorescence detection of fragments[119]. Electrospray Ionization (ESI)[120], matrix assisted laser desorption ionization (MALDI)[121] and MALDI time-of-flight (MALDI-TOF)[118] mass spectrometry (MS) has been widely explored for nucleic acids detection with more efficient the last mentioned. The most advanced achievements of the last decade on the DNA field was the fully mapping of the human genome[122,123] and more recently the creation of an Encyclopedia Of DNA

Elements (ENCODE)[124] which is filled systematically with regions of transcription, transcription factor association, chromatin structure and histone modification.
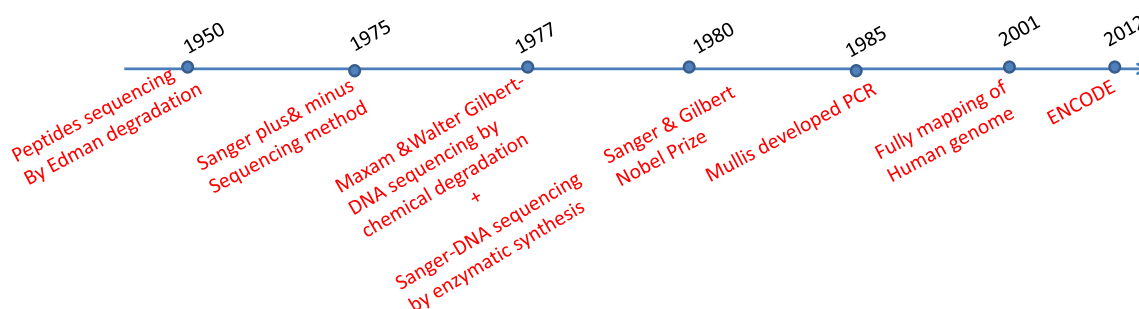
Figure I. 19: Map of Breakthroughs in biomolecules sequencing

2.5.2 Sequencing methods for synthetic polymers

It is proved that common characterization methods for the analysis of simple polymers are not sufficient for the characterization of sequence-defined polymers. Although some well-established methods can be used, they meet some limitations. The methods which follow are the existing analytical techniques for the determination of the monomer sequence of the synthetic sequence-controlled polymers.[125].

a. <u>NMR</u> constitutes of course one of the potential analysis for sequence-controlled polymers. ^{1}H-NMR, ^{13}C-NMR, two dimensional NMR can give us information about the monomer sequence in synthetic polymers.[124,125] But there are some limits in terms of the length of the polymer. It has been showed that this method is efficient for short sequences up to 8 units[125]. NMR resonance of a specific monomer unit in a polymer chain depends on its close neighbors so of the previous and the following monomer unit.

Colquhoun and his coworkers had showed an interesting path to determine the sequence through NMR spectrometry by the use of a molecular tweezer.[126] Indeed, electron-rich molecules play the role of a molecular tweezer and bind selectively with a particular chain part containing 13 aromatic rings which corresponds to a specific monomer sequence. So, aromatic co-polyimides are recognized through their π-stacking and hydrogen-bonding interactions with a sterically and electronically complementary molecular tweezer through the sensitivity of imide ^{1}H NMR resonances to multiple adjacent binding of tweezer molecule (absence of binding: the imide groups lead to a unique NMR signal, presence of binding: imide NMR signal split off from the main peak).

b. <u>Cleavage/Depolymerization.</u> Inspired by Edman protein degradation[108], this cleavage method was developed also for synthetic polymers. Chemical, enzymatic-induced or thermal degradation can occur and cut the long sequence in smaller of lower molecular weight which then are easier to be characterized by NMR and MS to define finally the entire sequence of the polymer chain. Until now,

several examples have been reported for the study of chemical composition or comonomer sequences of copolymers but not for sequence-defined polymers[127], although this is not far to happen.

c. <u>Nanopore Analysis.</u> Another approach that could be potentially used to sequence synthetic sequence-defined polymers is through nanopore analysis, It's a technique that was developed for the determination of biopolymers' sequence through a biological or synthetic pore. A recent publication showed some preliminary results towards this purpose by detecting the different polymer length via this strategy[128]..

d. <u>Mass spectrometry.</u> The most widespread technology for proving the monomer sequence in a polymer chain is focusing on the different mass values of the monomers which constitute the polymer chain[125]. Tandem mass spectrometry is a technique that provides structural information about the ionized molecules based on the way they fragment once they excited.

The most powerful technique to investigate the primary structure of any copolymer is tandem mass spectrometry (MS/MS). Two conditions should be fulfilled for the efficient reading out of information encrypted in a macromolecule due to its monomers' sequence i) the building units of the polymeric chains to be of different mass ii) the energy fragmentations not to result in rearrangements of the original co-monomers' order. The only restriction of mass sequencing abiotic polymers is that the fragmentation strategies are not universal so each molecule once is excited, new fragmentation rules should be established. Before MS/MS spectrometry, MS is performed first in order to determine the mass-to-charge (m/z) values for the ions which will be subsequently fragmented by MS/MS by collision-induced dissociation. In addition, the monodispersity of the sample is proved through the same process (single MS stage) in case of sequence-defined polymers or the wider mass distribution of oligomer chains in sequence-controlled polymers. When we have all the produced ions resulted from the ionization source, some of them depending on their *m/z* ratio can be selected and subjected to higher energy in order to acquire the molecular dissociations. These dissociations give to the analyst the desired fragments to precise the monomer sequence in the polymer chain[129].

In order to have easy-to-read message, deciphered from the MS/MS spectrum, the molecule has to be chemically designed in the appropriate way. As long as the MS/MS dissociations depend on the chemistry of the polymer backbone, the latter should carry selectively cleavable bonds in low energy. For example the labile alkoxyamine C-ON bond in sequence-defined poly(alkoxyamine amide)s which is cleaved in low energy before any other fragmentation occurs, helps extremely to the sequence-reading.
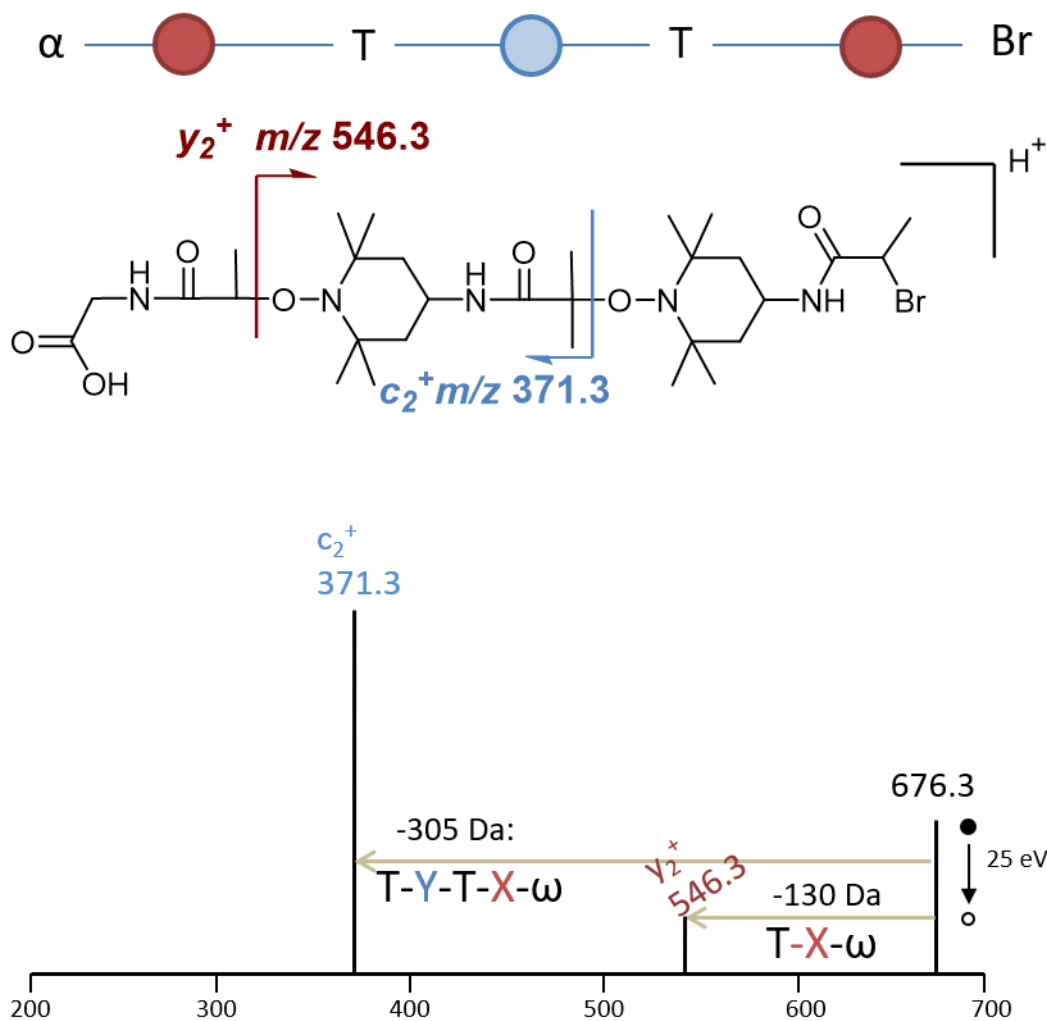
Figure I. 20: MS/MS sequencing in positive mode of poly(alkoxy amine amide)s via the labile C-ON bonds

As it is depicted on the **Figure I. 20**, the fragmentation of the oligo(alkoxyamine amide) occurs only to the C-ON bond between the monomer-coding unit and the spacer- TEMPO moiety, leading to two series of ions, having either the α-terminus or the Br-terminus. The one series holding the α terminus is named on the figure **c** and the other holding the Br (ωterminus) is named **y.** The distance between the m/z peaks in MS/MS spectrum corresponds to smaller fragments of the sequence and they are differing depending on the different monomer used in the sequence. Here the two monomers used have different mass thus different mass fragments. For example, C_2^+ is attributed to α-X-T-X where X: 71.0 Da for one monomer or 85.1 Da for other. So in the case of Figure I.20 the ion $C_2^{+:}$ 371.3 correspond to α-X-T-Y or α-Y-T-X. Once the other fragment y_2^+will attributed to a monomer sequence, then the entire oligomer sequence can be read.

Consequently, it is very easy in some minutes to read-out the monomer sequence of a polymer by measuring the distance between the fragment peaks[130]. Though, it is even faster to attribute all the produced fragments automatically by a computer program which brings the revolution in the message decoding from a polymer and in the future writing of messages in chemical structures[131]!

3. Information-containing polymers

Among the broad family of sequence-controlled polymers discussed in the previous section, information-containing macromolecules constitute an appealing new class of functional polymers. In such polymers, a defined monomer sequence is used to store a message, which can be genetic, digital, alphabetical or alphanumerical. Such polymers are therefore strictly sequence-defined (see 2.1 for definition). DNA is the archetypal example of information-containing polymers. Indeed, it was designed by Nature to store and transmit monomer-encrypted genetic information (see 2.2.1 for details). Yet, it was also demonstrated in recent years that intentional digital message can be stored in DNA. Alternatively, it has been proposed[23] that digital information can be stored in the comonomer sequences of abiotic macromolecules. These polymers are usually synthesized by solid-phase synthesis (see **§2.4**) and decrypted by a sequencing technique (see **§2.5**). These new polymers open up very interesting opportunities for data storage, cryptography, traceability and anti-counterfeiting applications; the latter being the core application studied in this thesis. In this section, some general information about biological and non-biological information-containing macromolecules are provided.

3.1 Artificial information storage in DNA

DNA stores and processes our genetic information but not only[132]! As genetics have shown, the message served in DNA sequenced chains can be preserved for thousands of years if the degradation of the nucleic acids is prevented. Recently scientists proposed the storing of a book[133] or even a movie[134] in DNA sequences. DNA is indeed a very interesting biopolymer to be used as an initial information-storage method[135] as it has been under investigation for already many years and its synthesizing, copying and reading procedures are accessible to everyone. The process to store digital data in DNA sequences can be characterized as DNA digital data storage and DNA sequencing techniques can be used for the information retrieval.

The first storage of extra-biological information to DNA codes was demonstrated in 1988 where graphic image was converted to DNA sequences[136]. The two dimensional graphic image was first translated into seven series of 5-bits each one (five by-seven bit-mapped Microvenus). The linear thirty five bit binary sequence of these seven series: 10101011100010000100001000010000100 was then ready to be translated into DNA language and be replaced by the four nucleotides letters A, C, T, G. The attribution relied on the size or the molecular weight of the bases(C> T> A> G) for the creation of an incremental reference, but it was based also on the phase-change coding method. Once the binary information was converted in a DNA form and was chemically synthesized then it could be inserted in a carrier, a plasmid to be saved for years and replicate many copies.

Later in 1999 a 23 characters' message was encoded in DNA microdots and recovered after amplifying and sequencing[137]. A key code was designed for the 24 letters of alphabet and 9 numbers and some punctuation marks.

Then, Church[133] and his group achieved in writing book of 53,426 words and 11 images and one JavaScript program into a 5.27-megabit bit stream by ink-jet printing in a form a oligonucleotide library. By attributing each bit to a single DNA base, where adenine or cytosine represented for zeroes and guanine or thymine represented for ones(A or C to 0 bit, G or T to 1 bit) they build the coding system. The synthesized library was composed of 54,898 159-nt oligonucleotides each one containing 96 nucleotides coding for information, 19 nucleotides containing indexing information and flanking 22-nucleotides sequence for amplification and sequencing purposes. In order to recover the encrypted information and to read the book, amplification by limited-cycle polymerase chain reaction and sequencing with next-generation sequencing methods should take place first. Small tips were used in order to avoid sequencing errors, cloning and stability issues resulting in 10 bit errors in total out of 5.27 million.

Figure I. 21: Depiction of strategy followed for storing digital information in DNA form and each sequential retrieval by sequencing techniques.

Afterwards, Goldman[138] and his coworkers from European Bioinformatics Institute in UK, achieved to encode in DNA five files, including 154 Shakespeare's sonnets, an audio clip, a scientific article, a medium-resolution photo and a file describing the process of the files conversion/ Huffman[139] code. The encoding of 757,051 bytes of information into DNA was done by a more complex method, where each byte corresponds to a word of five letters whose letters are the four DNA bases, A, C, T, G. To limit the errors they broke the DNA sequences in sets of 100 bases-long strings, each overlapping the previous by 75 bases and including indexing information for the identification of the string. The overlapping strings provide to the system fourfold redundancy and have the ability of cross-check potential errors in one string comparing with the other three strings.
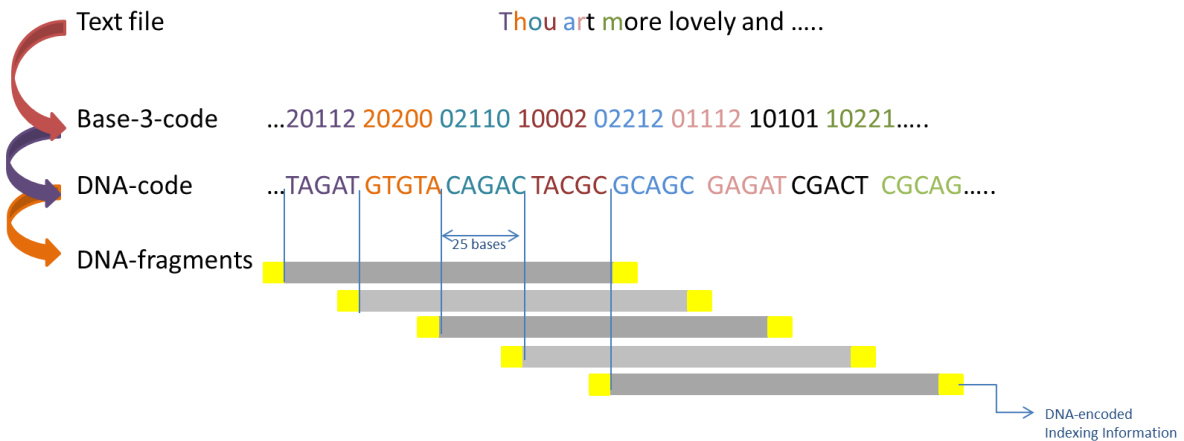
Figure I. 22: Digital information coding in DNA bases sequences. The method of converting the text into DNA bases sequences following three consecutively steps is illustrated.

But, despite the fact that the issue of space in storing information by using the DNA is solved, the second part concerning the durability should still worry scientists. It is known that nucleic acids cannot survive under harsh environmental conditions[20,21], they need cool and dry environment in order to preserve their chemical structure. The highly charged and water soluble chains of DNA make the processing of nucleic acid difficult, outside of their biological environment as long as any exposure to light, oxygen, humidity, temperature can accelerate DNA degradation.

Grass et al.[140,141] suggested a way to physically keep DNA stable over the years so that information storage in DNA sequences can be accomplished. They showed how to encapsulate DNA in silica particles simulating the preservation of DNA in seeds and spores.

Silica particles have been chosen because of their chemical and thermal stability to act as a protective layer for the DNA. The process starts with the absorption of a standard DNA ladder to the surface of submicron-sized silica particles functionalized first with positively-charged aminosilanes. A thin layer of amorphous silica started to grow as a following step on the nucleic acid surface using *N*-trimethoxysilylpropyl-*N,N,N*-trimethylammonium chloride (TMAPS) as co-interacting species and tetraethoxysilane (TEOS) as silicon source. After the slow reaction of several days a dense layer of silica was generated having in its interior as a form of sandwich the DNA helix.

The reverse procedure for the release of the DNA helix performed without destroying the chemical composition of the nucleic acid. So silica was dissolved by an aqueous solution of hydrofluoric acid without being harmful for the nucleic acids.
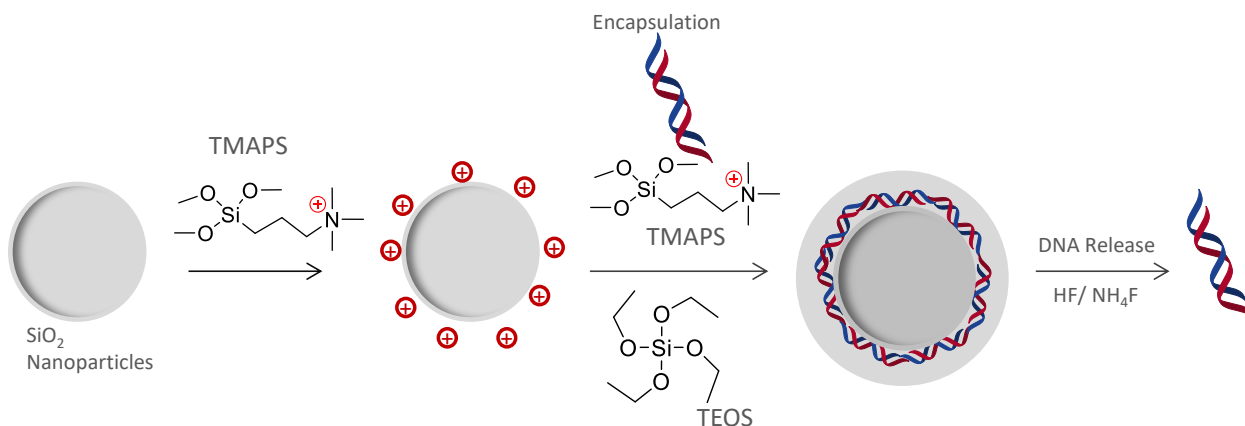
Figure I. 23: Encapsulation of DNA in silica particles for the protection of the stored information against harsh environmental conditions.

Indeed DNA was isolated and analyzed by gel electrophoresis, quantitative PCR (qPCR) and sequencing where no quantitative differences like strand breaks were observed. Overall, this strategy constitutes an interesting alternative for long-term storage of non-biological information in DNA or potential DNA taggants applications but reaches some limits that render it still weak[140].
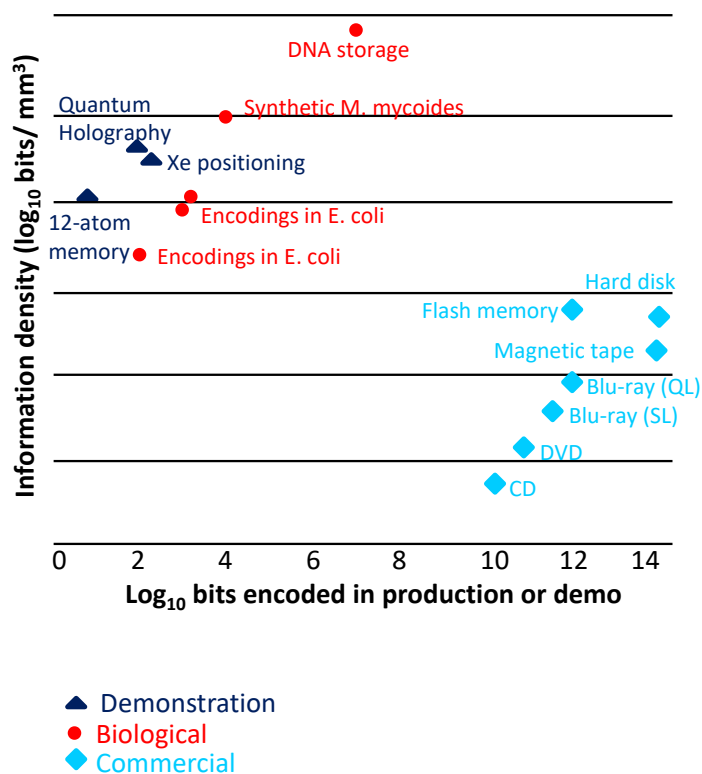
Figure I. 24: Mapping of several existing data storage technologies commercial or academically used. Plot of information density (log$_{10}$ of bits/mm^3) versus current scalability as unit.

According to the **Fig. I. 24** storing information in DNA sequences open the applicability frame since the amount of information that can be stored is really big[133]. The information density of DNA storage dominates over already existing commercial methods, other biological or demonstration based ones.

In the same publication it was proved that 5.27 Mb can be stored in with density of 5.5 petabits/mm^3 (at 100× synthetic coverage) fact which classifies the DNA data storage higher that all the mentioned technologies. It is obvious that these values can be even improved by other polymers or DNA modifications.

Nowadays, plenty of research projects are dealing with DNA data storage and ways to further improve its quality and its capabilities. By combining computers technology and DNA chemistry, it is feasible to access the encoded information without errors[142,143] even other the existing difficulties[144]. Very interestingly it was also managed to retrieve selectively written information either from a small scale stored data[145] or from long DNA sequences[146]. As an evolution of the information storage in DNA, the latter is used for anti-counterfeiting technologies as it can potentially bear in its sequences product information about the manufacturer or production date. This application will be further discussed in the section 4.3.

3.2 Synthetic digital polymers

Facing all these issues with DNA data storage scientists[147] assumed that DNA is not the only sequence-controlled polymer that can be used for encoding information at the molecular level. Information can be encrypted in any polymer chain that contains more than one monomers arranged in an ordered way[23]. Simply, binary information could be contained in a polymer string of two different co-monomers named arbitrarily as zero and one bit. This concept is adjusted to encode digital information in synthetic sequence-controlled polymers. Digital non-natural polymers can bear all the characteristics that sequence-controlled biopolymers are missing in order to make their field of applicability really broad. The only two important conditions that should be fulfilled in order to have data storage at the level of a polymer chain are a) a precise writing mechanism, a mechanism where the co-monomers are placed in a strict ordered way b) a reliable reading mechanism, where the information can be deciphered and read out at the level of a single macromolecule[23].

From the synthetic/writing point of view the last decades, a big variety of simpler and more complicated structures of synthetic monodispersed polymers have been designed. Distinguished scientific polymer groups such as Church[133] and Goldman[138] and Lutz group can save digital information in either chemically synthesized biopolymers or synthetic polymer. The latter group has been working on the creation of new information-containing polymers by exploiting the chemical possibilities and not sticking on biopolymers structures. Their methodology is based on the use of two mainly monomers defined arbitrarily as 0-bit and 1-bit as the digits of the ASCII computer language uses to represent text. The two monomers slightly differ in chemical structure as a consequence they have slightly different mass enough to distinguish their different fragments in mass spectrometry. Correlating the ASCII code and its binary sequences with the sequence-defined polymers synthesis it

is possible to synthesize alternating polymers of monomers corresponding to 0 and 1- bit and encrypt binary messages. The only requirement of the monomer selection except for satisfying the chemistry protocol is the different mass to make attainable the determination of the chain sequence through mass fragmentation as it will be explained further in the following text.

But also from the reading-out side(see **§2.5.2**) a great progress has been achieved to make feasible the excellent performance of all the application of digital polymers[125].

3.2.1   Oligo(triazole amide)s

For this type of synthetic digital polymers the AB+CD approach (**Figure I. 12c**) was followed. Monomers with alkynes as terminal groups (A) could react selectively with azides (D) terminal groups of the other monomer and carboxylic acids (B) react with primary amines terminal groups (C). These two reactions were performed selectively without any need of protecting group. On an unmodified Wang resin used as solid support or on soluble polystyrene support[104] and through repeating cycles of amidification and copper-assisted alkyne-azide cycloaddition, the oligomers were synthesized. In order to prove the concept, two different monomers of AB form were utilized. The 6-heptynoic acid defined as 0 bit and its methylated analogue defined as 1-bit. The work was extended basing on the type of the alkynoic acid. 4-pentynoic acid was used as 0-bit and 2-methyl-4-pentynoic acid as 1-bit. Another monomer, the 1-amino-11-azido-3,6,9-trioxaundecanein CD type was used as a spacer in both cases. Monodispersed pentamers of different monomer combinations were synthesized containing three AB building blocks and two CD spacers[148]. 2^3 different monomer sequences could be prepared by using the two monomers coding for 0 and 1-bit. This protocol was further optimized for the synthesis of longer sequences and for decreasing reaction time purposes. A ligation approach of dyad-encoded building blocks was used[149]. For this purpose prepared dyads made of the two monomer units 0 and 1 and coding for 00, 01 10 and 11 and by bearing the functions AB could be combined in order to synthesize a long monomer sequence in less time than by adding one by one the two monomers.

All the sequences were characterized by NMR and SEC following their cleavage from the support under acidic conditions. But the real confirmation of the monodisperse oligo(triazole amide) sequences came by mass spectrometry analysis. MALDI-TOF and electrospray ionization mass spectrometry (ESI-MS) can be conducted in order to confirm the mass of the synthesized sequence. Later on tandem mass spectrometry (MS/MS) was evaluated as a very efficient and reliable method for sequencing oligo(triazole amide)s and deciphering the encoded message[150,151].
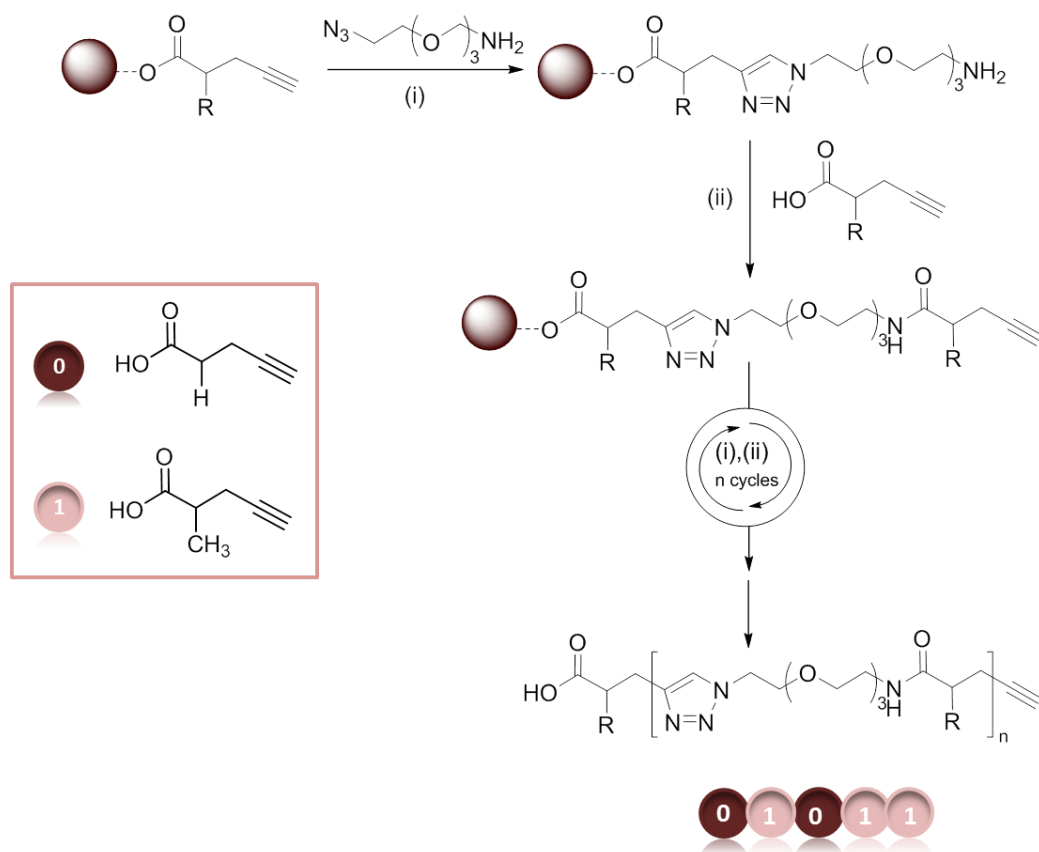
Figure I. 25: Synthesis of uniform information-containing oligo(triazole amide)s. i)Cu-assisted alkyne-azide cycloaddition: CuBr, dNbipy, (CD) spacer ,ii) amidification: PyBOP, DIPEA, N-methyl-2-pyrrolidone, (AB) monomer, 60°C; iii) cleavage from Wang support: TFA, DCM. Abbreviations: 4,4'-di-n-nonyl-2,2'-bipyridine (dNbipy), benzotriazol-1-yl-oxytripyrrolidinophosphonium hexafluorophosphate (PyBOP), N,N-diisopropylethylamine, or Hünig's base (DIPEA)

3.2.2   Poly(alkoxyamine amide)s

Synthetic sequence-controlled polymers which can contain any kind of digital information in their monomer-sequenced chains is also the category of poly(alkoxyamine amide)s synthesized by orthogonal solid phase synthesis[152,153]. Poly(alkoxyamine amide)s synthesis is based on two chemoselective steps without the need of any protective groups, making the synthesis easier and faster. The synthesis is taking place on a solid support alternating two reaction steps. The solid support can be any unmodified Wang resin but it is preferred the Wang resin loaded with glycine as it results in a convenient α-chain end leading to easily traceable fragments mass spectrometry afterwards. The first orthogonal step is the reaction between the primary amine and the symmetric acid anhydride to afford the formation of a bromo-terminated amide. The second orthogonal step is the radical coupling of a carbon-centred radical obtained by copper activation of an alkyl bromide with a nitroxide radical to afford the formation of the alkoxyamine. Two different monomers (anhydride of 2-bromo-isobutyric acid and anhydride of 2-bromopropionic acid) are used in this study and one spacer 2,2,6,6-tetramethylpiperidinyloxy (TEMPO). The one monomer is defined intentionally for information storing purposes as 0 bit (anhydride of 2-bromopropionic acid) and the

other as 1 bit (anhydride of 2-bromo-isobutyric acid). These two monomers differ only in one methyl substituent (case of 1 bit) but this is enough for their MS/MS sequencing that follows the synthesis. To demonstrate the concept, words such as PMC (group name of J.-F. Lutz) or CNRS were written in the poly(alkoxyamine amide)s sequences by attributing the coded monomers to letters[154]. The synthesis is a cycle of these two mentioned iterative steps that can be repeated as many times needed in order to reach the desired polymer length and sequence. Once this is achieved the polymers are cleaved under acidic conditions from the solid support and characterized by NMR in terms of their chemical structure, by SEC as a first proof of monodispersity, by Electrospray high-resolution mass spectrometry (ESI-HRMS) as a very reliable method for the confirmation of monodisperse sample and by tandem mass spectrometry. It was showed that the poly(alkoxyamine amide)s was extremely easy to be decoded by tandem mass spectrometry[130]. Thanks to their labile alkoxyamine C–ON bond the MS/MS fragmentation is really selective.
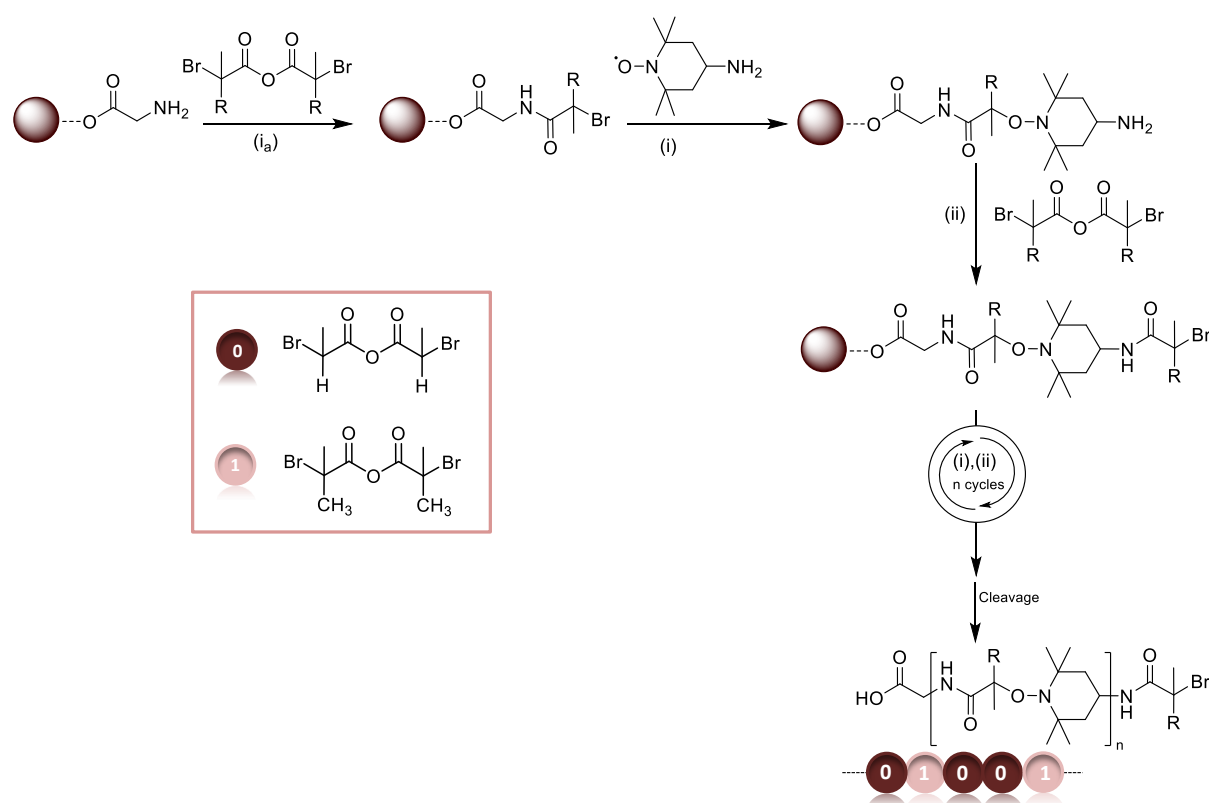
Figure I. 26: General strategy for the solid-phase synthesis of poly(alkoxy amine amide)s. Experimental Conditions: (i$_a$) K2CO3 for 1-bit or DIPEA for 0 bit, THF, RT; (i) CuBr, Me6TREN, DMSO or DMSO, microwaves at 40 °C and cleavage TFA, CH2Cl2.

3.2.3   Poly(phosphodiester)s

Phosphoramidite chemistry is used in this work for the preparation of non-natural sequence-defined polymers and not for nucleic acids[155]. These polymers are prepared to contain information in their chains in the form of binary information as in the previous cases; by defining one monomer as 0 bit

and another as 1 bit, arbitrarily. For this reason, a string of ordered monomers is prepared as a result of sequential attachment of one by one monomer to the growing chain.
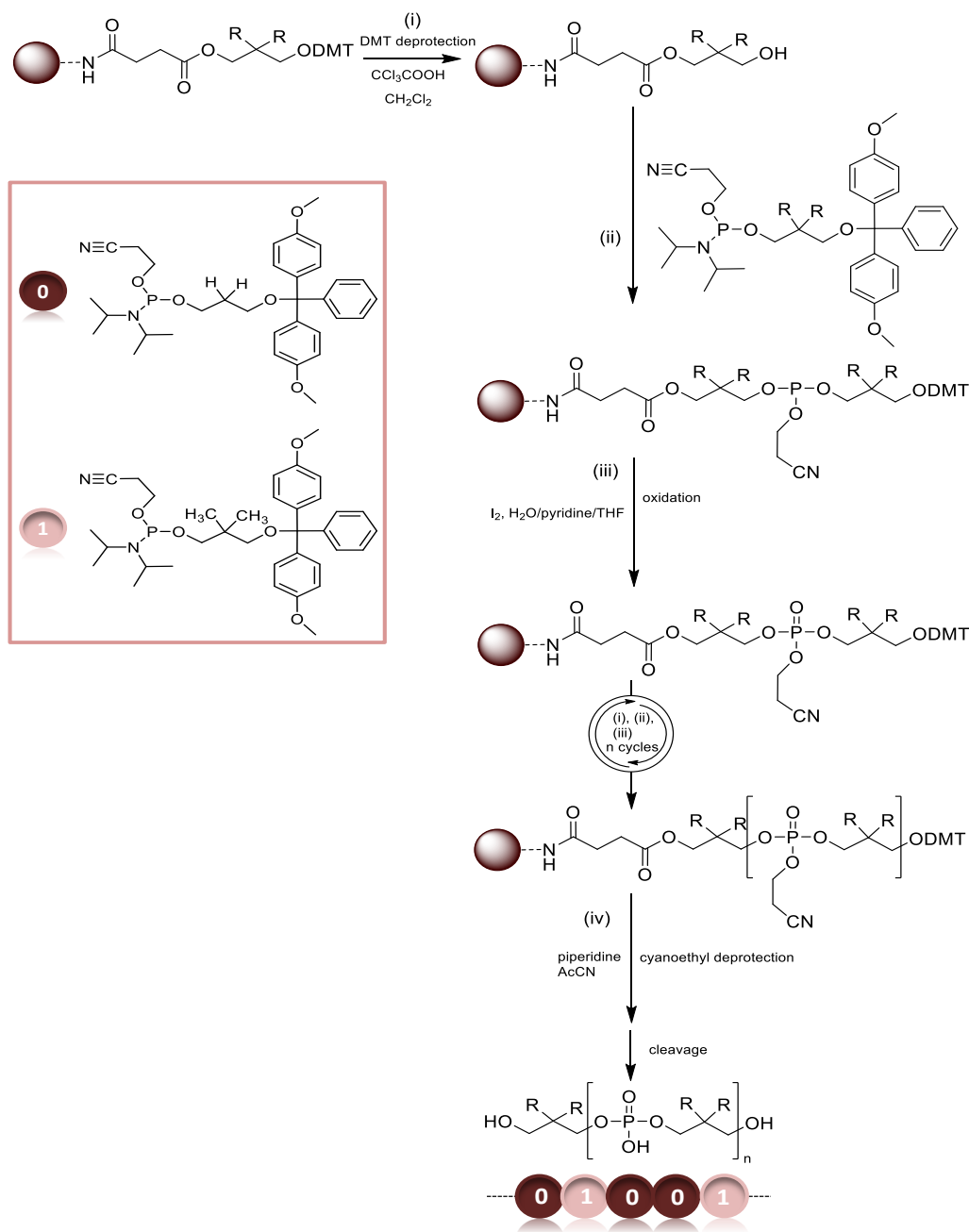
Here, three phosphoramidite monomers are used. The two monomers containing a propyl (2-cyanoethyl (3-dimethoxytrityloxy-propyl) diisopropylphosphoramidite, defined as **0** bit and a 2,2-dimethyl-propyl (2-cyanoethyl (3-dimethoxytrityloxy-2,2-dimethyl-propyl) diisopropylphosphoramidite spacer defined as **1** bit are used in order to introduce the code to the

53

chains and the third one containing a 2,2-dipropargyl-propyl spacer, (2-cyanoethyl (3-dimethoxytrityloxy-2,2-dipropargyl-propyl) diisopropylphosphoramidite defined as **1′** was used to allow post-modification of the polymers such as azide–alkyne Huisgen cycloaddition in our case or other chemistries described in other works(Sonogashira or Castro-Stephens coupling). Except for the phosphoramidite and DMT-protected hydroxy groups, these monomers do not have any structural feature in common with phosphoramidite nucleosides. This iterative synthesis is focused on three main steps, DMT-deprotection, phosphoramidite coupling and iodine oxidation and they are repeated until the desired length of the polymer is achieved. After that deprotection of the cyanoethyl phosphate protecting group, deprotection of the final DMT-group and cleavage under basic conditions are following. The polymers were dried under vacuum and characterized by NMR, SEC. After synthesis, the information encrypted in the chains can be deciphered using sequencing technologies that have been developed for biopolymer analysis, such as tandem mass spectrometry[156]. MS/MS sequencing of poly(phosphodiester)s results in a bit complicated mass spectrum since they typically dissociate via efficient cleavage in all the phosphate bonds positions, leading to four sets of ion products. In this work the maximum information included was 3 bytes so 24 coded monomer units. But in following publication it was proved that also much longer information sequences can be prepared by using automated synthesis[72]. By applying the phosphoramide protocol to a DNA synthesizer and by adjusting it according to DNA conventions, it was achieved the preparation of monodispersed sequence-encoded non-natural polyphosphates with DP more than a hundred. On a 1000 Å controlled pore glass (CPG) as a solid support instead of cross-linked polystyrene beads used in the previous article and with high excess of monomers in each step to acquire quantitative yields, this synthesis was realized. Moreover, it was needed to cap the unreacted amino groups after each step especially when long sequences were aimed. For the synthetic point, instead of starting the sequence from a 1 or 0 monomer addition it had to be started from the addition of three thymine nucleotides. This primer sequence helps for the high performance liquid chromatography (HPLC) characterization of the coded polymers, but also permits to quantify the formed polymer by UV spectroscopy. All the sequences were performed in relatively short times with the longest polymer synthesized in 12 hours. Subsequently the formed polymers were characterized by ion exchange HPLC, UV spectroscopy and electrospray ionization mass spectrometry (ESI-MS) and in all cases they showed a good control of the synthetic process. Three words were able to be encoded in this kind of polymers, the word PMC (Precision Macromolecular Chemistry, name of the research group of J.-F. Lutz) in a length of 3 bytes-24 bits, Maurice (name of the son of J.-F. Lutz) and Macromolecule in a sequence of 104 coded monomer units. This was a proof that big amount of information can be stored in non-natural polyphosphates in short time and gave encouraging perspectives for the future storage applications in the molecular level.

Very recently it was proved that instead of coding a message in relatively short phosphodiesters' sequences, fact that restricts the encoding capacity, it is possible to encode dense messages in long

polymer sequences without facing any sequencing problems[157]. To do so, long polymer sequences were prepared by interrupting them every one byte to incorporate an easy-cleavable identification tag. The alkoxyamine bond of the tag between the two bytes was facilitating the reading out of the coded message making the mass spectrum of the polymer less complicated. In collision-induced dissociation (CID) conditions, the weak NO-C bonds are cleaved first selectively leading to an initial series of mass signals.
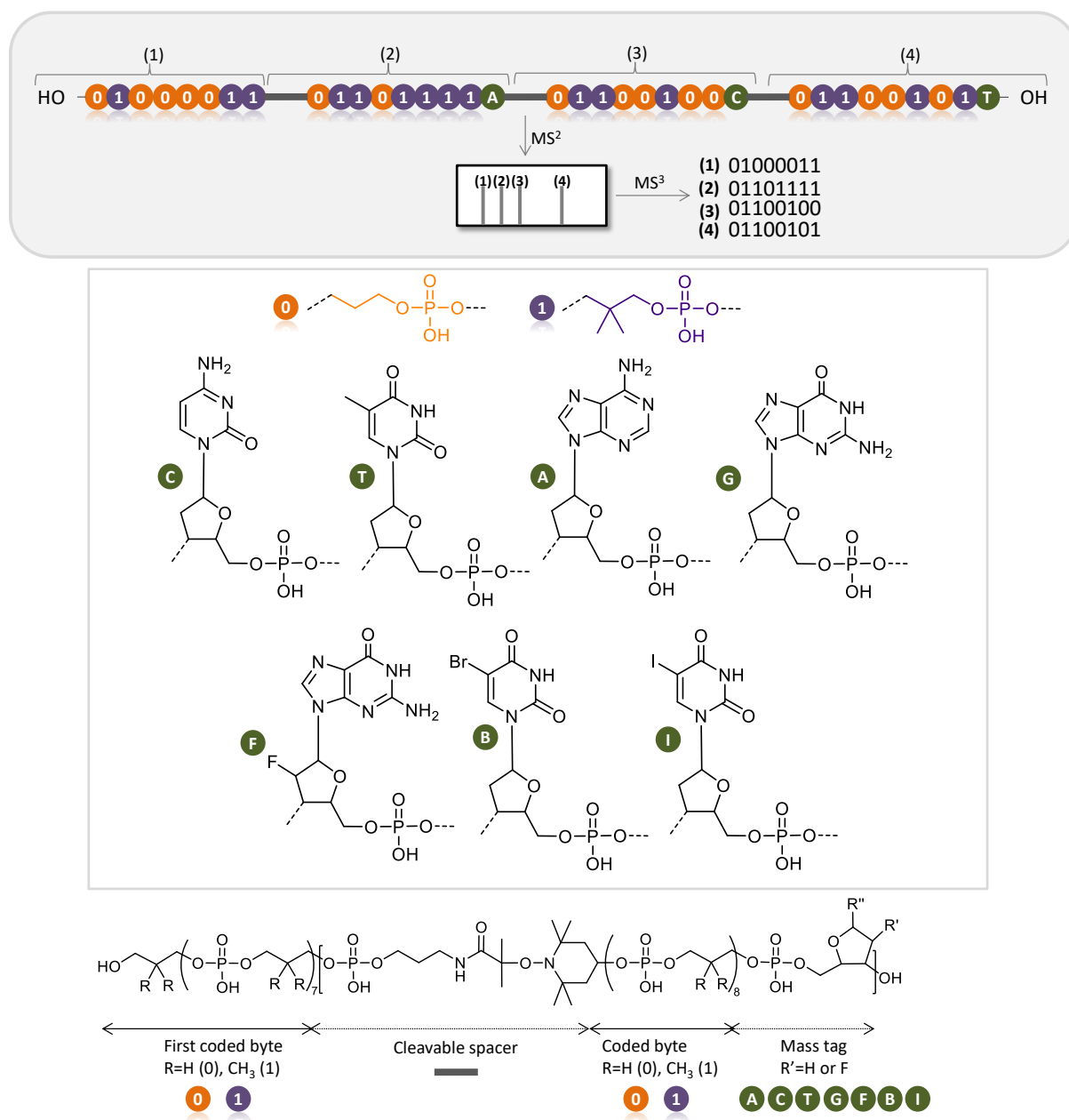
Figure I. 28: Main idea for the sequencing strategy of long digital polymer chains interrupted with easy cleavable identification tags. On the top it is illustrated the sequence of 4 bytes long polymer containing the identification tags every one byte. The polymer is first analyzed in MS/MS conditions in order to have the first fragmentations of the weak NO-C bonds (illustrated as a black spacer) (fragments (1), (2), (3), (4)) and then each signal is sequenced in MS³ to obtain the detailed monomer sequence. In the middle of the figure the chemical structures of the polymer components are shown. And in the bottom the general chemical structure of the polymer prepared by automated phosphoramidite chemistry is depicted.

Afterwards, each mass peak of every byte is individually activated and sequenced to decode the message by MS[3]. As a result complete recovery of the coded information can be achieved in a single measurement with a mass spectrometer of moderate resolution.

3.2.4 Poly(alkoxyamine phosphodiester)s

Poly (alkoxyamine phosphodiester)s synthesis[35] came to improve the two drawbacks of the previous published phosphoramide synthesis[155], the many DMT-deprotection steps needed and the complexity
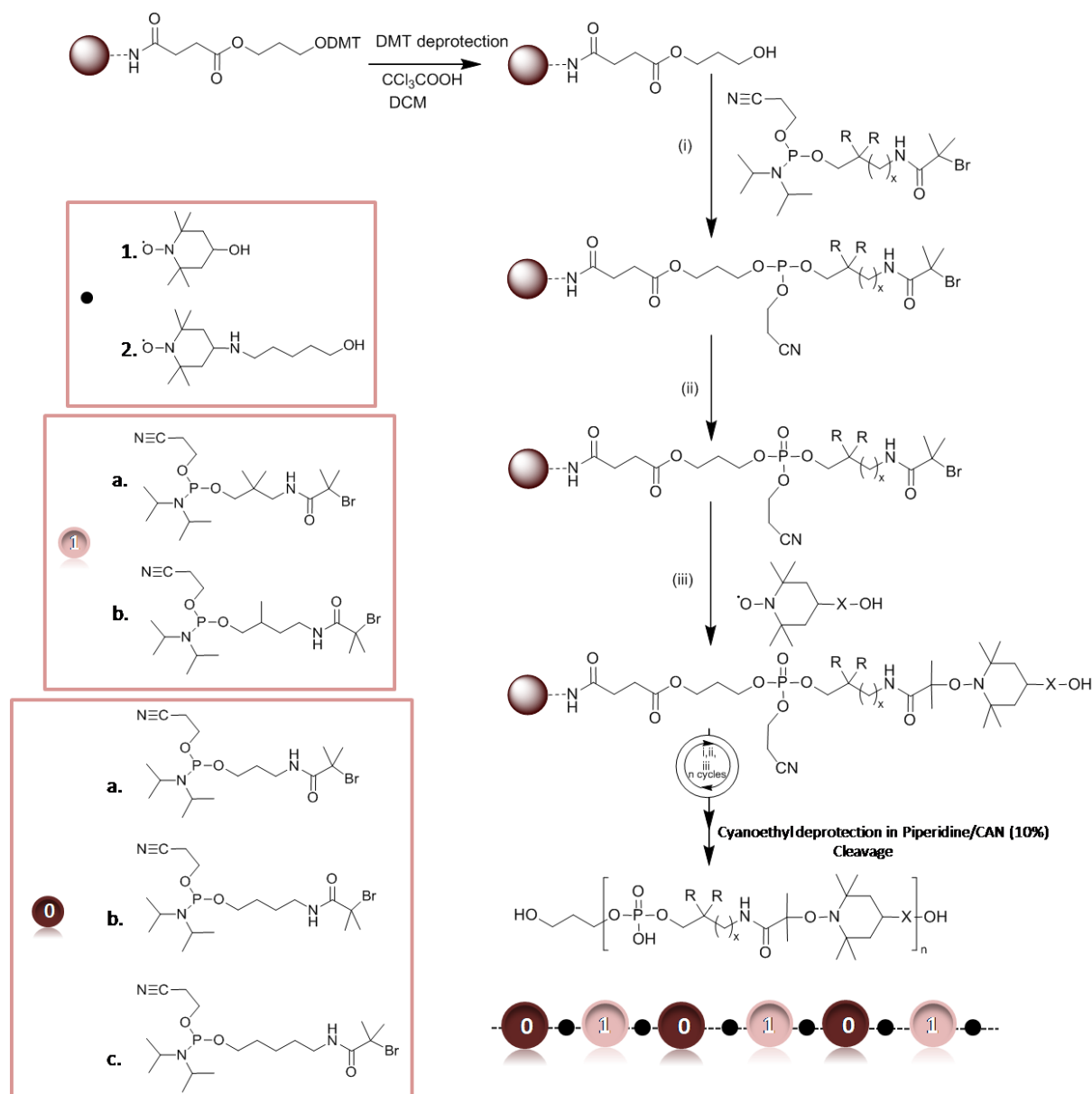
Figure I. 29: Strategy studied for the synthesis of sequence-coded poly(alkoxy amine phosphodiester)s. Experimental conditions: (i) phosphoramidite coupling: RT, AcCN, tetrazole (ii) oxidation: RT, I₂, 2,6-lutidine, THF/H₂O; (iii) radical–radical coupling: CuBr, Me₆TREN, DMSO and cleavage: piperidine, AcCN, RT, then MeNH₂, NH₄OH, H₂O, rt.

in mass spectrometry characterization of the long sequences because they undergo many MS/MS fragmentations. There are other information-containing polymers that are extremely easy to read by MS/MS. This is the case of poly(alkoxy amine amide)s[130]. Due to the weak alkoxyamine bond the sequencing of poly(alkoxyamine amide)s leads to selective C-ON fragmentation. So the introduction of the alkoxyamine bond in the poly(phosphodiester)s structure would help the sequencing. Indeed, in this synthetic procedure it is used one nitroxide as a spacer to facilitate the MS/MS sequencing[151,156]. The iterative strategy is focused on two chemoselective steps, phosphoramidite coupling and nitroxide radical coupling, a reaction between a carbon-centered radical with a nitroxide to afford the formation of alkoxyamine bond. The implementation of information relies on the use of two different types of monomers shown on the insets of the **Figure I.28**.

4. Anti-counterfeit Technologies

The term counterfeit refers to an unauthorized representation of a registered trademark carried on good identical or similar to goods for which the trademark is registered for purposes of misleading the recipient or purchaser into believing he is receiving the original goods (World Health Organization, 2011, Glossary: Counterfeit definition).Counterfeiting products constitute an important threat for our society coming from the ancient years and putting our health and our economy in danger because of their poor quality. It is a phenomenon that is affecting trade for at least 2000 years[158]. It probably started by counterfeiting pottery and ancient Greek vases[159] and of course it was connected very rapidly with the coinage[160]. In our days, e-commerce benefits the growth of forgeries. In this subchapter the size of problem will be presented through its consequences in our life. Then a classification of the existing anti-counterfeit strategies will follow, as well as the ideal characteristics of an efficient anti-counterfeit marker. In the end, the anti-counterfeit taggants will be categorized depending on the different levels of security which could provide.

4.1 Consequences of counterfeit products

Health. In most of the cases counterfeit products are not safe since the European rules concerning the safety are not followed. The use of materials characterized by inferior quality and the not proper installation according to the safety rules can be proved dangerous for human use and shortly to need replacement. Moreover because of the fact that counterfeiters do not always comply with directives and sanitary codes, the composition of the fraud products cannot be certified, resulting in most of the cases in health issues such as allergies or other physical reactions, even fatalities have been reported. Clothes, jewelries, electronics and medicines of healthcare products are the most copied products that are posing our health in risk.

Economy. According to a published report from Frontier Economics, an internationally recognized economics research firm, in January 2017[161] the total amount of cost losses from the international

trade in counterfeit and pirated goods was calculated reaching the \$461 Billion in 2013 and as it is estimated in 2022 it will be \$991 Billion. These tragic values mean that industries worldwide lose billions of dollars because of the forgeries. These costs in not only result of direct losses in sales but also because of losses of reputation and trust from consumers' part and thirdly costs from their involvement in developing new anti-counterfeiting protection methods. And of course this affects people who consequently will lose their job and are led to unemployment. [1]

Environment: Last but not least the issues arising from such a phenomenon are not only the aforementioned. Environment issues including the illegal use of toxic substances for the fraud products manufacture is one of the important problems as well as innovation wound by stealing ideas and fighting with ethics (exploitation of children/ children work). [159]

All these are leading to one thing! Identity is value. Knowledge of the origin, processing and supply chain of a product determines its market price. Product of guaranteed value and methods of assuring for the manufacturer needed to be released in the market to increase once again manufacturer liability. There should be put a stop to the crime of uncontrolled trade by developing efficient and powerful anti-counterfeit opponents.

4.2 Evolution of anti-counterfeit methods

The wild expansion of the problem in many domains, pharmaceutical, aircraft, automobile, tools and luxury goods industries lead to a great demand of powerful and efficient methods for protection from fraud products. The numerous anti-counterfeit techniques are already classified in several categories based in different criteria such as efficiency, security level, pattern, tracking strategy. In this section in order to present as many existing technologies, the categorization relying on the nature of the encoded particles will be used.[162]

1. Graphical encoding strategy: based on the pattern and the shape of the encoded particles.

The conventional macroscopic barcodes made of bars and spaces are part of this class. By varying the width of the space and the one of the vertical lines and their sequential order, a huge variety of codes can be designed[163]. Sometimes they are accompanied by a sequence of numbers and represent a unique product code referring to brand owners and lot number. This kind of barcodes is linear or one-dimensional barcodes and later they were enriched in order to achieve higher security properties. A wide variety of geometrical patterns is introduced in barcodes like rectangles, dots, hexagons. This new category of graphical identity constitutes the two-dimensional barcodes. (**Fig. I. 32a**)

But the graphical encoding methods were not limited to this. Advanced technological achievements were developed to struggle counterfeiting. Sequences of colored layers compacted in micro-particles at a size of 8 μm and made from melamine alkyd polymers allow labeling of food and drugs

packaging. A combination of four to eleven different colored layers equipped with further properties such us UV and magnetic characteristics can produce more than 4 billion possible codes.[164] For the identification of the code a customary microscope or a table microscope is needed. (**Fig. I. 32b**)

Another proposed simple method for fight against fraud products is the random incorporation of silver nanoparticles (AgNWs) in a specific area of a poly(ethylene terephthalate) (PET) film by casting. The random distribution of the nanowires is impossible to create a pattern that can be copied so it constitutes a unique identity for the labeled material like a fingerprint. The observation of the nanowires introduced in the material can be performed by a simple low magnification optical microscope. Moreover it was suggested that the nanowires could be coated by fluorescent dyes to facilitate their detection by a fluorescent microscope.[165]
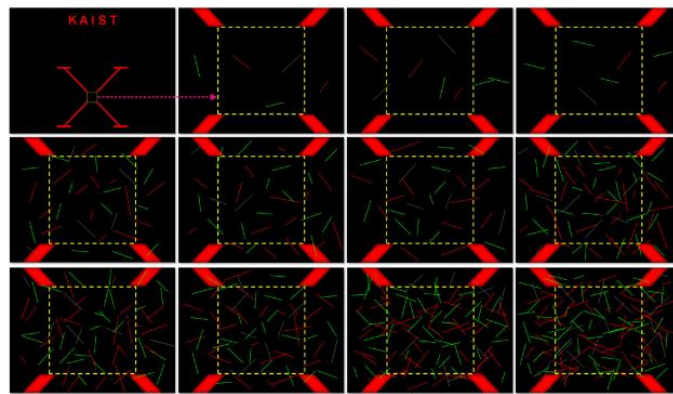
Figure I. 30: Schematic illustration of typical fingerprint patterns (in yellow rectangles) on PET surface. The complexity of the pattern is increased moving from left to the right and from up to down, by increasing the density of the nanowires (Copyright (2014) IOP Publishing Ltd).

Another type of graphical barcode is the preparation of multimetal microrods composed of submicro-sized stripes[166]. Complex stripping patters are prepared by sequential electrodeposition of metal ions into porous membranes, followed by particle release. A silver film deposited on the backside of an Al_2O_3 film works as the electrode for the metal ion reduction of the solution. The pattern of the striped particles depends a) on the pore diameter of the membrane affecting the particle width, b) on the sequence of the metal ions introduced in the solution affecting the number and the pattern of the stripes and finally c) on the charge, passed in each step, dictating the stripe length. The stripped cylindrically shaped metal nanoparticles can be identified by conventional light microscopy through the differential reflectivity of adjacent stripes.

Until today, seven different metals (Pt, Pd, Ni, Co, Ag, Cu, and Au) in segments as short as 10 nm and as long as several micrometers have prepared particles with as many as 13 distinguishable stripes.
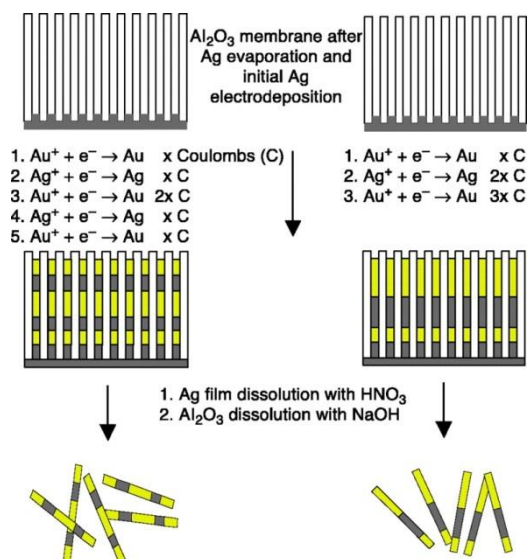
Figure I. 31: Preparation of sequenced metal microrods to be used as taggants (Copyright (2014) IOP Publishing Ltd)

Another method belonging to this approach is the selective photo-bleaching. A barcode pattern can be written in homogeneously fluorescent died microspheres like polystyrene, argogel (polyethylene glycol grafted polystyrene) and dextran beads by a photo-induced process which leads to partial loss of fluorescent properties. The 70% of the bead is available for writing and different line width, symbols and intensities can be designed through an adapted confocal scanning laser microscope (CSLM) in order to develop numerous codes. The reading out of the encrypted codes is performed by a confocal microscope and is facilitated by an orientation given to the particles by a ferromagnetic coating. This alternative, despite the wide applicable field of the biomedical domain in screening and diagnostics, shows some drawbacks like the high cost, long-time process and limited existing bead-based encoding strategies[167].(**Fig. I. 32c**)
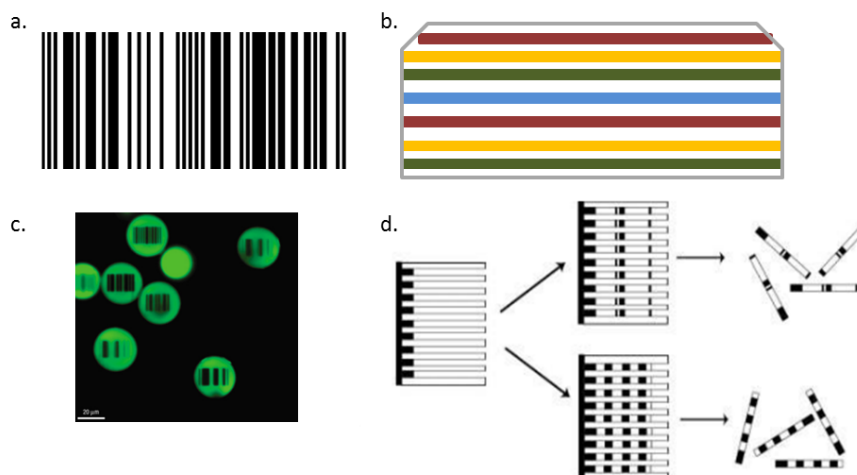
Figure I. 32: Summarizing figure of anti-counterfeit taggants used in graphical encoding techniques: a. conventional space-bars barcodes, b. colour-sequenced maleimide polymers[164], c. fluorescent pattern in polystyrene beads written by photo-bleaching in[167], d. metal stripped nanorods[166]

Holography is a technique of labeling products relying its principle on the pattern. It was invented by Gabor[168] in 1948 and then holographic images where adapted by anti-counterfeit technologies. A hologram is a physical structure that diffracts light into an image. The term 'hologram' can refer to both the encoded material and the resulting image. A holographic image can be in a form of permanently affixed sticker on a product or its packaging and it's altered by using different effects such as kinetic effects (image appears to move or to change colour), depth effects (seems like the image has two or three dimensions) and multi-channel effects[169,170].

2. <u>Optical encoding strategy: based on the unique optical properties of the encoding particles</u>

Particles with interesting optical properties are used as coding medium in this strategy. For this purpose molecules-carriers are used to carry the coding element that can be molecules or nanoparticles with unique characteristics. The carrying is achieved even by encapsulation[171,172] even by attachment to the surface of the cargo beads (covalently or through electrostatic interactions)[173]. Fluorescent organic dyes are the most common coding medium used in such applications[5]. Optical encoding elements differ in the emission of fluorescent signals. Each dye molecule has different emission profile and this can be confirmed by a simple spectrometer and the corresponding intensity ratios can be quantified by a flow cytometer/photo spectrometer to finally decipher the barcode.

Coding with fluorescent dyes is not always so convenient because of their broad emission spectra that overlap when a variety of fluorescent dyes is used and are not long-term stable. Indeed, quantum dots (QDs) are used instead, because of their narrower spectra, covering the entire visible scale range, having the ability of being excited by a single wavelength and can be used for simultaneous excitation of different-sized QDs and exhibit higher photostability against photobleaching[174]. To explain further, quantum dots are semiconducting inorganic nanocrystals with unique photoluminescent properties and they are used for optical encoding, being embedded in polymer beads.

By changing the size of QDs their emission wavelength can be regulated[175,176]. QDs are used broadly in biological systems and can be adapted in vivo and in vitro applications such as cellular labeling and deep-tissue imaging. Water soluble quantum dots were used as biological labels[6,177] but also hydrophobic QDs were introduced in polymeric beads for increased capacity spectral coding (e.g. zinc sulfide–capped cadmium selenide nanocrystals)[171]. The ranging of the intensity levels at a single wavelength and of the color generate the code according the equation $C = n^m - 1$ where n is the intensity levels and m the colors minus one because the level 0 cannot be differentiated from the background. So with the use of 10 different intensity levels and 3 colors resulted in 999 different code possibilities. However, there are still restrictions to their broad use such as the low chemical stability[178] and the cytotoxicity (e.g. CdS, CdSe, CdTe).
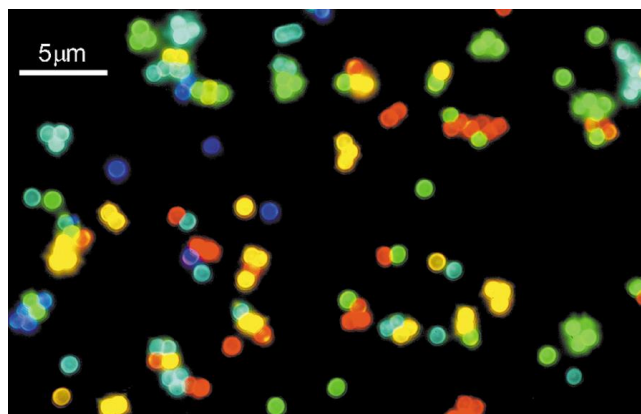
Figure I. 33: Fluorescence micrograph of a mixture of CdSe/ZnS QD-tagged beads emitting single-color signals at 484, 508, 547, 575, and 611 nm. Simultaneous excitation of the beads spread on a glass surface[179]. (Copyright (2001) Springer Nature)

In the frame of optical encoding, except for fluorescent dyes and quantum dots which are made of toxic materials (e.g., CdS, CdSe, CdTe) there have been proposed the use of rare-earth ions. Potential barcoding technologies could rely on oxide nanoparticles or glass rods doped with rare-earth ions to develop exclusive barcode patterns.[7,180,181] The unique characteristics of rare-earth ions connected with their non-toxicity, high-photostability and their exciting by IR or UV photos render them suitable for anti-counterfeit applications. In 2003, micrometer-sized identification tags were generated on glass[182]. Moreover, it was recently developed a method to apply rare-earths as encoding microparticles in many industrial processes and cut down the limitations of encoding capacity/ size by creating unique particle barcodes in nanocrystals architectures [183].

Moreover, europium and terbium tris-dipicolinate complexes were used for their excellent luminescent properties as attractive anti-counterfeit features[11]. The lanthanide complexes were diluted in simple aqueous formula suitable for inkjet printing. The red-emitting luminescent ink containing europium and the green-emitting luminescent ink containing terbium were used to produce accurate full color images which are invisible under white light since they don't absorb it and appeared when they are excited with 254 nm UV light. Documents of increased importance could be potentially tagged to prove their authenticity determined under UV light.

3. Spectroscopic encoding strategy

Drugs containing the wrong active pharmaceutical ingredient (API) or not containing at all the required ingredient are part of the counterfeiters' plan posing a significant threat for the public. A method for the identification of real drug products has been proposed to performed by Raman spectroscopy[184]. The peaks in a Raman spectrum of the known API, desired to be found the medicine under investigation, are compared with the peaks present in the product. So the same the active substance works as a self-barcode to the drug that is incorporated. According to this work the Raman spectrum of the API and of the finished drug product were transformed into barcode representation by

assigning zero intensity to every spectral frequency except the frequencies that correspond to Raman peaks, which are assigned with a value of 1. If the two barcode representations are the same the identity of the finished drug product is the original one and has not been subjected to any alternation. A new algorithm was generated in order to screen antibiotics and antiviral finished drug products (FDPs) with no need of keeping a library of RAMAN spectra of the APIs used in drugs. According to the algorithm only peaks having intensities greater than 20% of the average peak intensity denoted with green in the following Figure 33 where allowed to transformed to barcode bars.
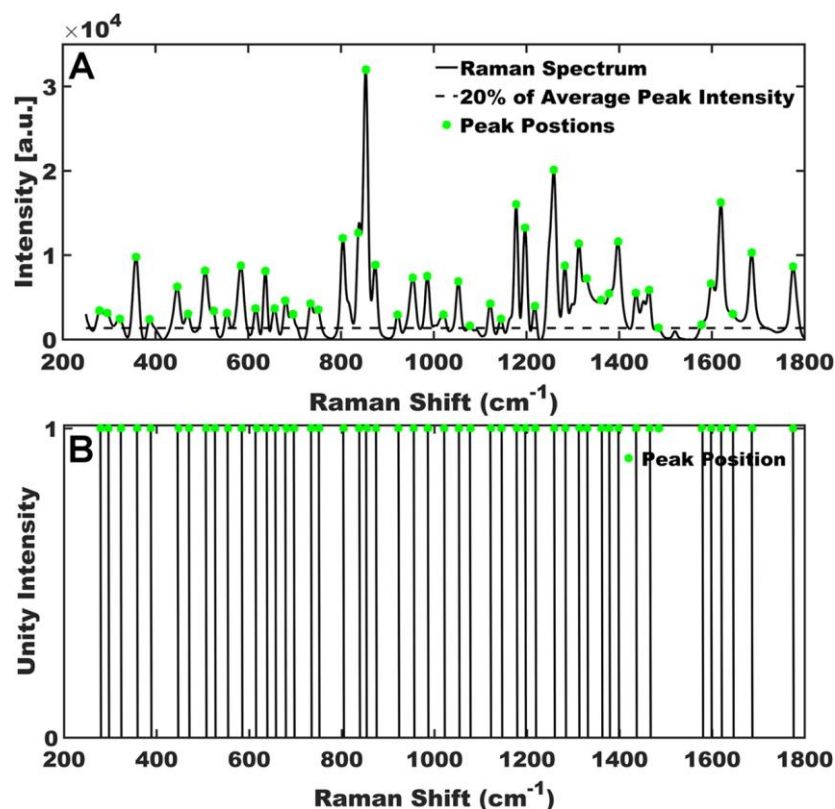
Figure I. 34: Transformation of a Raman spectrum to a barcode. The peaks denoted with green circles were included in the barcode pattern. "Reprinted with permission from (Lawson, L. S. & Rodriguez, J. D. *Anal. Chem.* 88, 4706-4713, (2016). Copyright (2016) American Chemical Society."

4. Electronic encoding strategy

Alloy nanowires Ni-Zn-In were selected to be used as barcodes for their distinct XRF signatures and electrochemical and magnetic properties[185]. The combination of these properties served a multiple reading out of the code. By varying the composition of Zn in the growth solution of nanowires while keeping the other metals concentration constant, the nanowires were alternating their electrochemical behavior giving a unique identity to the materials in which they would be inserted. In brief, in a graph current vs Electric potential (voltage) higher concentration of Zn metal in the alloy nanowires resulted in higher current signal at -1.06 V for the Zn, along with an In peak at -0.59 V of constant height (A).

5. Radio Frequency Identification

This technology has been developed since 1970 and uses radio waves to identify objects. One RFID system comprises a RFID tag, a tag reader equipped with an antenna and transceiver and a host system or connection to an enterprise system as depicted in the **Fig. I. 35**. Typically it is used in anti-counterfeiting of drugs, paper money anti-counterfeiting and vehicle immobilizer[186].

RFID tag   tag reader   Enterprise System
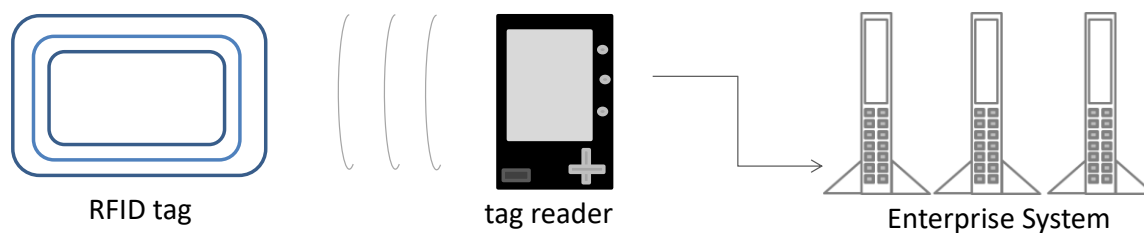
Figure I. 35: A typical RFID system

6. Chemical encoding strategy: based on the chemical "composition" of the particle

The detection and identification of a specific chemical structure or monomer sequence plays the main role in this category. Unique chemical tags are incorporated in the protecting-target product in tiny quantities (some parts per billion)[162] considering the method as more sensitive over spectroscopic techniques.

The biggest English manufacturer of anti-counterfeit markers SmartWater, bases its technology on chemical encoding. Rare-earth lanthanides are utilized as taggants and by combining two detection methods they constitute optical and chemical taggants. Once their fluorescence emission is detected under UV light then they are analyzed in terms of mass by laser ablation inductively coupled plasma mass spectrometry (LA-ICP MS) to determine the elemental composition[187]. The markers were in liquid form composed by water-based polymer solution and one or more Rare-earth elements and were deposed on a variety of materials, left to dry and obtain some traces to analyze them by laser excitation mass spectrometry. Chemical taggants complying also the molecular taggants, rely their detection on sequencing methods. Of course the most popular molecules that are characterized by controlled primary structure, well-defined monomer sequence, as pre-mentioned are the biopolymers: polypeptides[188] and nucleic acids. In the following section DNA taggants will be described in more details since they are included to numerous projects.

Of course, the mentioned techniques can be used individually but a combination of them could be proved more efficient and secure. A practical example is the euro banknotes as depicted in Fig.35. They gather on their surface many different anti-counterfeiting patterns in order to increase their complexity[189]. The tags on euro-banknotes can be printed on the paper (mentioned by blue), engraved in the material (green colour), embedded in it (yellow) or designed by texturing the material (red).
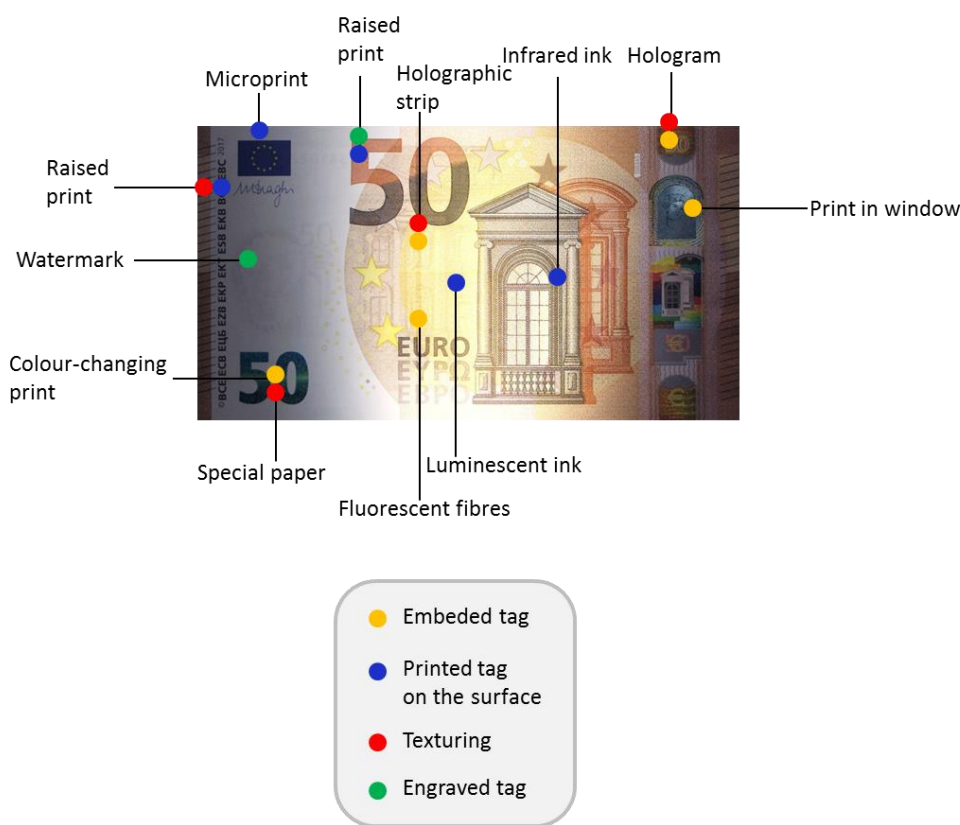
Figure I. 36: A combination of anti-counterfeit methods on a single 50 euros banknote

4.3 DNA labeling

The oldest information storage was generated and exists in nature and is our DNA[190]. Since every biological species carry a unique nucleic acids sequence, this constitutes our identity and the only serious way to be distinguished from the others. Exploiting this property, an entire technology has been set up around crime investigation, forensics and paternity tests. The idea of storing information in DNA strands was further developed and established in the field of anti-forgeries thanks to a huge variety of codes offered by DNA, its straightforward synthesis and the low toxicity of such genetic materials. In academic scale there are many examples of using DNA sequences in order to label materials. In 2004, double-stranded DNA of 100 base-pairs encoding for a specific message was encapsulated in inorganic nanoparticles and sequentially they were mixed with liquids such as body fluid, commercial ink[191] and fuel[192]. Afterwards collection of inorganic-DNA hybrid nanomaterials and decoding of the message followed.

Another example of industrial use of DNA tags was in the domain of pharmaceuticals where Bristol-Myers Squibb company used a DNA sequence of 20 units long to label an anticancer drug to ensure the genuineness of the product through the entire production line up to the final product arrived to the consumer[193,194]. Labels in genomic form were also adjusted in the combat against forgery in the food

industry. More particularly, lactobacilli bacterial genome was inserted in the milk cheese and then it was grown in the cheese body during ripening[195]. All the Swiss cheese makers of the Swiss Emmental cheese used three specific lactobacilli cultures in order to label their cheese production and to distinguish it from other producers through identification of DNA strains by PCR and DNA sequencing.

Of course, since DNA tagging is a breakthrough technology and the possible DNA barcodes are almost uncountable the preparation and the introduction of DNA taggants in various materials is already applied. The pharmaceutical GlaxoSmithKlein (GSK) already prepared one trillion of unique DNA barcodes[196].

But of course, the reading out of the encrypted message it requires one more step before the final acquisition of the information. Due to the fact that tiny amounts of DNA tags are introduced in the products and it is not feasible to investigate their sequence, the amplification by the polymerase chain reaction (PCR) takes place, a procedure that of course increase the analysis time and the cost.

Another alternative way to identify the DNA taggants is through the technique called "FISH" an in situ hybridization method including fluorescence upon hybridization[197,198]. Molecular beacons emit fluorescent signal once they detect and hybridize to their DNA strands targets. Hybridization does not occur when the target DNA does not have the complementary sequence, so this response of the DNA probe is completely selective[199].

4.4 Characteristics of ideal anti-counterfeit markers

The ideal anti-counterfeit taggants should provide the maximum possible protection to the final product and predominate over the counterfeiter's threats. The characteristics that set one marker most appropriate are:

- Limited visibility and detectability with naked eye in order to limit counterfeiters' action
- Uncopiable[200]
- Developed trustworthy authentication techniques to provide certain reading out results
- The technique should offer unlimited number of codes
- Demand relatively easy synthetic protocols, avoiding multistep synthetic routes to keep manufacturing cost in normal standards. They should not add a big additional cost to the final product depending on the needed quantity
- Low detection limit i.e. mass of tracer material required for uniquely tagging a mass of final product)[162]
- Durable, withstands chemical and mechanical alternations
- Versatile, easy integration into a wide variety of carriers

66

4.5 Classification of anti-counterfeit-means based on levels of security needed

There are four different security levels where each tag can belong. According to this categorization the tags which belong to the lowest security level protect the product from counterfeiting less than another belonging to the forth security level. The classification is based on the authentication means of the message encrypted in the barcode and the way a taggant is exposed to our eyes[201].

First security level: This security stage is covered by Overt (visible) features. This means that the anti-counterfeit tags are visible to everyone are especially made to enable the end user to verify the authenticity of the product. The visibility of such features doesn't mean that they are so easy or cheap to be reproduced. But the way that they should be applied on the packaging should be carefully considered in order any trial of removing or reusing the taggant to damage obviously the pack. Otherwise original tags can be recycled with fake package content giving a false impression of authenticity. Parts of this category are: the holograms, Optically Variable Devices (OVD), color shifting security inks and films, security graphics, sequential product numbering, on-product marking. The reading –out method of this anti-counterfeiting strategy is usually simple. The label is detected even by naked eye, or by a small and easily accessible device for such purposes.

Second security level: Serialization/TRACK and TRACE Technologies. This kind of following the original products is under development for the pharmaceutical sector, although it was first considered many years before. This digital technology feature involves the assignment of a unique identity to each stock unit during manufacture, which then is kept though the supply chain until its consumption. The identity will probably include among the others, details on the product name, lot number and expiry date. All the identities will be unique and recorded in a secure database. It is important to note that this method offers the advantage of tracking an item during its entire "life" and of accessing to the history of it (electronic pedigree). Bearing an identity during all the processing stages, an item avoids be modifying by counterfeiters or stealing. Serialization, barcodes, RFID unique surface marking or topography are some of the ways to achieve track and trace technology. The identification of the labeled message is performed by simple hand devices (ex. pen shape) connected sometimes with software.

Third security level: Covert (hidden) features are included in this level. A covert feature needs a specialist 's knowledge in order to be detected and verified. The purpose of this method is to enable to the brand owner to detect the counterfeiters. It's not relevant to the wide audience meaning the customers and if something is published then it will lose its security value. Examples of this case are: invisible printing, embedded image, digital watermarks, hidden marks and printing, anti-copy or anti-scan device, laser coding, substrates, odor. The detection of the labels is getting more complex, as it is hidden and not accessible to everyone if they don't possess the appropriate device.

Forth security level: Forensic Markers are part of this security level. Methodologies of recently developed technologies requiring special equipment and expertise are some of the demands of a high security level for anti-counterfeit features. Laboratory testing and suitable test kits are needed to prove the authenticity of a product bearing anti-counterfeit tags in the frame of the forth security level. Newly developed ways such as chemical, biological and DNA taggants, isotope ratios and micro-taggants are some of the latest technological developments used against forgeries. Equipment like mass spectrometer, PCR machines are some of the expensive machines used for the identification of forth level tags. However, the increased cost they might need, the high security that they can offer compromise the cost especially in some products of high risk or high value products.
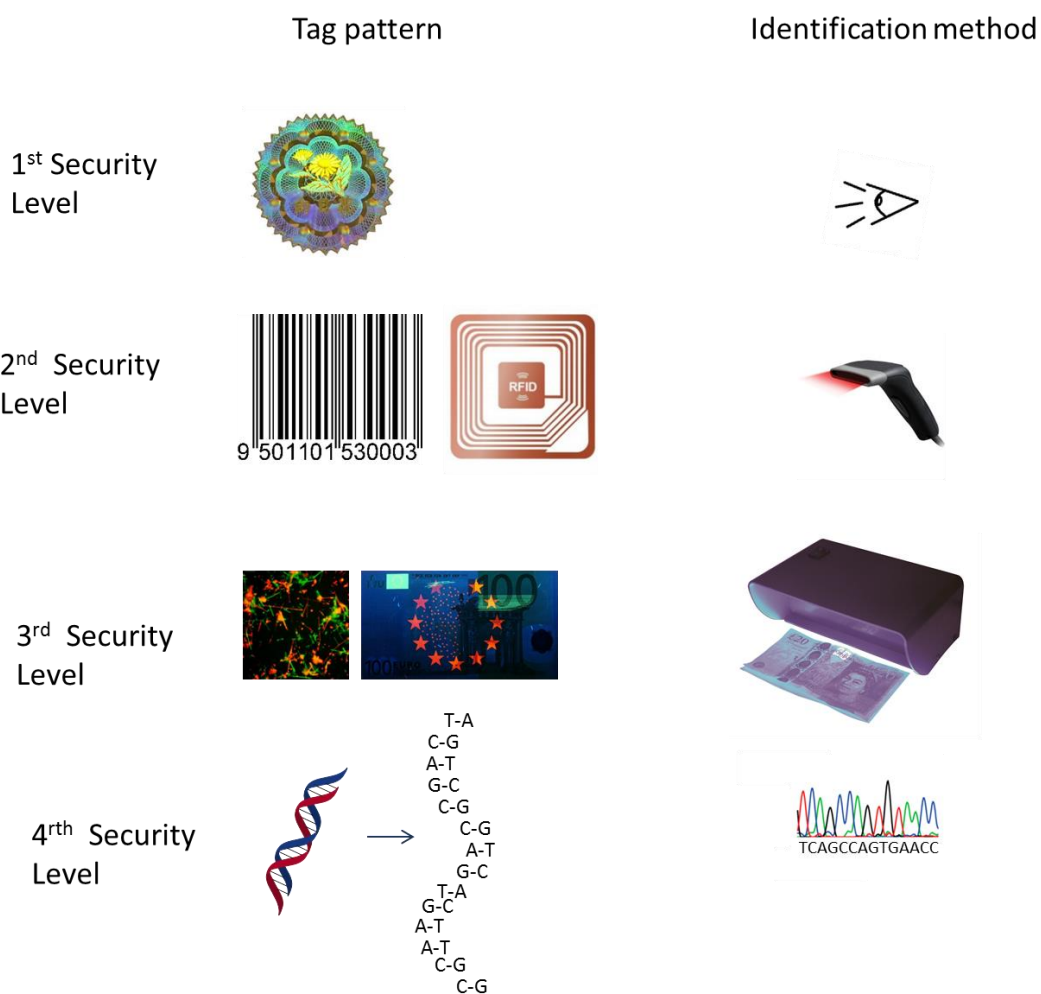

Figure I. 37: Depiction of the four different security levels of anti-fraud technologies and their corresponding identification methods

4.6 Comparison of existing taggants

In order to compare the existing labeling categories, we should consider the aforementioned characteristics of the ideal taggants.

Regarding the factor of number of possible codes it is obvious that chemical encoding methods offer a broader gamma of codes from optical and graphical encodings. Plenty chemical compounds and numerous different chemistries can be combined to produce unlimited unique codes to be applied in tracking and tracing technology. Graphical taggants depending on their shape and geometric motif can generate close to unlimited encoding possibilities but still they are not enough to reach chemical taggants abilities. Similar situation is the case of optical taggants where there are limits because of the fluorescent dyes spectral overlapping. Quantum dots broaden the applicability restrictions of this category adjusting the code numbers towards 10.000-40.000[171]. Possible combination of optical and graphical taggants increase the possible codes number giving a number greater than 10^6 like in the example of rare-earth elements described before [182]. But still this number is not enough. DNA taggants base their code technology on 4 monomers (4 DNA bases) and depending on the length of both primer and probe the potential generated codes are $4\text{\textasciicircum}x$ where x: the length in bases of primer and probe. Other non-natural chemical taggants could increase even more the codes scale by using more than four monomers thus increasing the encoding capacity and the information carried out in the barcode.

Secondly, the detection limit affects the efficiency of one encoding method. This means that the sensitivity of one method depends on the required amount of the taggant in order to be detectable. As it is depicted on the **Fig.I. 38** the detection limits ranges from 0.001 to 10^5 ppm. Higher amount of taggants can change the original properties and functionality of the final labelled products for instance their mechanical properties.
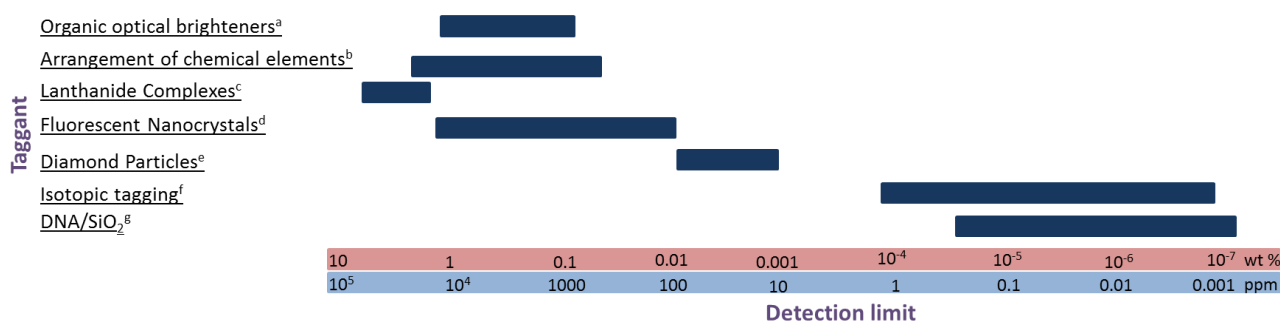
Figure I. 38: Diagram showing the detection limit of several encoding techniques. The colored areas correspond to the required concentration for the depicted taggants as found in published patents.[a]DE102009024685, [b]DE102008060675, [c]CA2881728, [d]US6576155, [e] US2015/0060699, [f]WO2013/143014, [g]US2007/0111314.

5. Conclusions

After this short introduction in the field of sequence-defined polymers, their roots and their evolution, we are still able to say that a so new topic is already so well established in the scientific community and so far introduced in plenty applications. This field is the expansion of the biomolecular sequence-definition. It gave a new breath to the limitations of nature and after so much progress it still seems that it has many more to offer.

However, the field of anti-counterfeiting technologies seems to lack in innovative ideas which can successfully weaken the frauds' impact in our society. We come into conclusion that there is a great need for renewing the anti-counterfeiting strategies and import novel ground-breaking solutions able to struggle the forgeries.

Of course, science can overcome this situation and more particularly sequence-defined polymers can act efficiently to this direction. Linking the new trend of sequence-defined polymers with the trade's wound of counterfeiting; the following pages will be filled with the latest developments on this direction realized in the frame of the current Ph.D. work.

Chapter II:

Identification-tagging of methacrylate-based intraocular implants using sequence-defined polyurethane barcodes

Denise Karamessini, Benoit Eric Petit, Michel Bouquey, Laurence Charles*, Jean-François Lutz*

1. Introduction

In recent years, the increasing production of counterfeit products had a major impact on global world's economy and industry. In this context, the need for protecting consumers, entrepreneurs and manufacturers is becoming more and more indispensable, in particular in pharmaceutical industry and, more generally, in biosciences where the health and life of consumers can be endangered by cheap replicas of genuine products.[202,203] As a consequence, a wide variety of anti-counterfeiting technologies have been described and patented over the last decades. For example, the use of nano or molecular identification tags is not only interesting for distinguishing a genuine product from a counterfeit but also for enabling a manufacturer to track production date and batch number of a given product. Such traceability tags may be particularly relevant for labeling drugs, implants, prosthesis and other *in vivo* materials, which have to comply with strict regulations and norms.[204-208] However, in such demanding applications, important parameters such as the biocompatibility and biodegradability of the identification tag have to be taken into account. Yet, the labeling of biomedical products is crucial when problems occur after a long period of *in vivo* use, in particular in the case of health complications and lawsuits.

Among the wide range of concepts that have been suggested for developing anti-counterfeiting materials, the use of sequence-controlled polymers has been recently proposed as an interesting new option.[12] In such polymers, information is stored at the molecular level in the form of a coded monomer sequence that can be read using a sequencing technology.[13,23] DNA is, of course, the archetypal example of a sequence-coded polymer that can be used as identification barcode for product labeling.[3] However, synthetic information-containing macromolecules may also be used for such a purpose.[39,209,210] Various routes for the preparation of uniform (i.e. monodisperse) sequence-defined polymers have been reported in the literature in recent years.[71,73,211-216] and it has been evidenced that these precision macromolecules open very interesting avenues for materials design.[12,62,217-222] For instance, our group has described in recent years the synthesis and tandem mass spectrometry (MS/MS) sequencing of different classes of non-natural information-containing polymers including poly(phosphodiesters),[31,72] poly(triazole amide)s,[29,30,223] poly(alkoxyamine amide)s,[75,130,224,225] poly(alkoxyamine phosphodiester)s,[35] and polyurethanes(PUs).[39] The latter class of polymers is particularly appealing for anti-counterfeit technologies since PUs constitute a very well-known class of polymer materials with extensively studied physico-chemical properties.[226] For instance, it was shown in previous works that uniform digitally-encoded oligourethanes, which contain a binary sequence built with two monomers defined arbitrarily as 0 and 1 bits (**Figure II.1a**), can be used as molecular barcodes and blended in low amounts in other polymer materials such as casted polystyrene films and methacrylate-based photo-crosslinked 3D prints.[39] In all cases, the barcodes could be easily extracted from the host polymer matrices and readily identified by MS/MS. Thus, these sequence-coded polymers seem promising for tagging a wide variety of materials and, in

particular, biomedical materials since PUs are known to be biocompatible and therefore used in a variety of medical devices ranging from simple catheters to artificial hearts.[227] For instance, PUs constitute the most commonly used class of materials for blood-compatible devices such as artificial heart valves and arteries. PUs are also used in many other bio-applications such a drug-delivery, surgery and ophthalmology.[228,229]
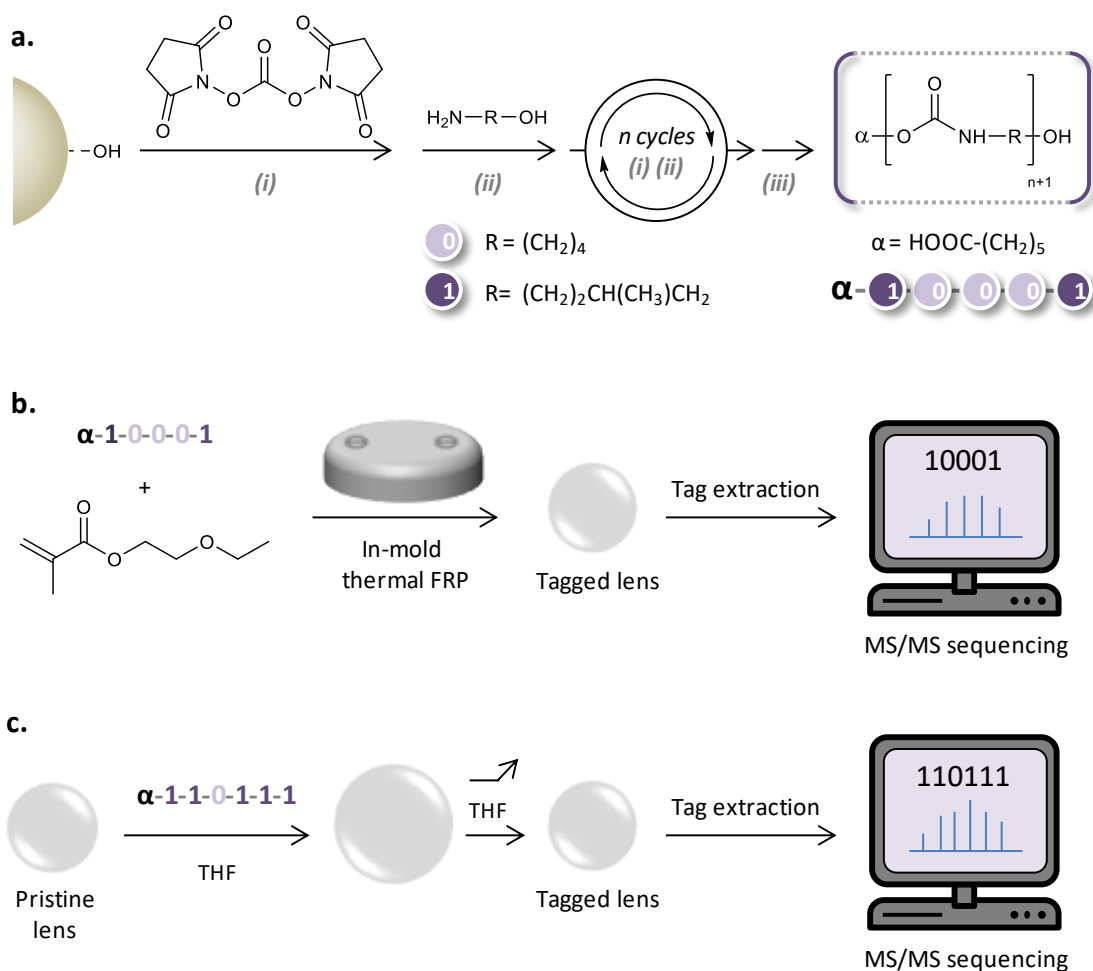
Figure II. 1: (a) General route used for the solid-phase orthogonal synthesis of sequence-coded polyurethanes.[39] Experimental conditions: (i) ACN, triethylamine, microwave, 60°C; (ii) DMF, triethylamine, RT; (iii) Cleavage: TFA/DCM, RT. (b) Direct lens-labelling obtained by *in situ* free radical polymerization (FRP) of 2-ethoxyethyl methacrylate in the presence of a polyurethane tag. (c) Swelling/deswelling strategy used for the polyurethane-labelling of premade lenses.

In this context, the present article describes the use of digitally-encoded polyurethanes as molecular tags for the labeling of hydrophobic intraocular lenses. Ophthalmic implants constitute a widespread class of materials that are very often used after cataract surgery.[230] Although very different types of intraocular lenses are used on the market, these materials are often obtained by free radical polymerization of methacrylates. Historically, the first monomer used for the preparation of intraocular lenses was methyl methacrylate but in order to respect recent surgical procedures requiring a very small incision in the corner of the eye to introduce the lens, the methyl methacrylate was

quickly replaced by a mixture of hydrophobic and hydrophilic methacrylates that can be homopolymerized or copolymerized to obtain the optimal properties, e.g. high refractive index, flexibility, shape memory and biocompatibility.[231] Despite the fact that important technological progress has been made in this field during the last decades, ophthalmic implants have usually an expiration date and their efficiency decreases with use and time. Therefore, the idea to incorporate a molecular identification barcode directly in the polymethacrylate matrix of intraocular implants is relevant since it should enable product identification after long period of times even if the original packaging is lost or thrown away. In order to illustrate the versatility of this concept, digitally-encoded polyurethanes were incorporated in two different types of lenses. In a first approach, the PU tags were dispersed in a methacrylate solution and included *in situ* in the lenses during molded thermal methacrylate polymerization **(Figure II.1b)**. Alternatively, the tags were included in a ready-made commercial implant using a facile swelling/deswelling procedure **(Figure II.1c)**. In both cases, the PU-tagged materials were studied by MS/MS sequencing. In addition, the biocompatibility and the transparency of the modified lenses were tested using standardized tests.

2. Results and Discussion

Sequence-coded polyurethanes were used as readable barcodes for the traceability and anti-counterfeiting labeling of intraocular implants. These sequence-defined oligomers were synthesized by stepwise orthogonal solid-phase synthesis as shown in **Figure II.1 a**.[39] Two successive coupling steps are used in this strategy to form uniform polyurethanes. In a first step, a resin-immobilized alcohol function is reacted with *N,N'*-disuccinimidyl carbonate in order to form an activated succinimide carbonate mono-adduct on the solid support. This reactive function is then selectively reacted in a second step with the primary amine function of an amino alcohol building block to afford a hydroxy-functional carbamate unit. These two consecutive steps can be repeated a certain number of times until a desired chain-length is reached.[39] In order to form readable binary sequences, two amino alcohols building blocks, namely 4-amino-1-butanol and 4-amino-2-methyl-1-butanol, were used and set as coding moieties **0** and **1**, respectively. After synthesis, the sequence-coded polyurethanes are cleaved from the resin and dried. Depending on the amount of information that should be stored in a barcode, coded sequences may be of different size. Thus, five polyurethanes, with different lengths and sequences, were studied in this work as shown in **Table II. 1**. All these polymers were characterized by high-resolution electrospray ionization mass spectrometry (HR-ESI-MS), which indicated in all case formation of uniform polymers **(Table II. 1 and Figures II. 5-9)**. Furthermore, the coded sequences were examined by tandem mass spectrometry (MS/MS), which confirmed that the expected sequences were obtained in all cases **(Figures II. 5-9)**. As indicated in a previous publication, the MS/MS sequencing of sequence-coded polyurethanes is remarkably easy when a negative ionization mode is used.[39]

Table II. 1: HR-ESI-MS characterization of the sequence-coded polyurethanes that were tested as barcodes in the present work.

	Sequence	Yield (%)	m/z_{th}[a]	m/z_{exp}[a]
PU1	α-0-0-0-1	88	605.3403	605.3403
PU2	α-0-0-1-0	60	605.3403	605.3399
PU3	α-1-0-0-0-1	87	734.4193	734.4191
PU4	α-1-1-0-1-1-1	~100	891.5296	891.5286
PU5	α-0-0-1-1-1-1-1-0	77	1121.6562	1121.6557

[a] Theoretical and experimental *m/z* values found by ESI-MS for deprotonated molecules [M-H]⁻.

The incorporation of the sequence-coded polyurethane in intraocular implants was then tested. As discussed in the introduction, one of the interesting advantages of polyurethanes is that their physico-chemistry and miscibility with other polymer materials is well-documented in the literature.[232] In the present case, the intraocular implants are covalently crosslinked networks obtained by free-radical (co)polymerization of polar methacrylates. Thus, two main routes were studied in this work for lens-labeling **(Figure II. 1)**. In the first approach, the polyurethane tags were incorporated *in situ* during network formation **(Figure II. 1b)**. Although various methacrylates can be used to prepare intraocular implants, 2-ethoxyethyl methacrylate was investigated in the present work as a model monomer and ethylene glycol dimethylacrylate was selected as a bifunctional crosslinker. The polymerizations were initiated by a peroxide initiator Luperox® 26 and were performed in bulk at 55°C in a commercial mold that gives a lens-shape to the formed networks. In order to select the best conditions for lens preparation, a series of model experiments was first performed in the presence of different amounts of crosslinker EGDMA ranging from 1-6wt% as compared to EEMA (data not shown). These experiments evidenced that the use of 2wt% of EGDMA is optimal for obtained defect-free intraocular implants. Above that number, the crosslinked poly(2-ethoxyethyl methacrylate) (*c*-PEEMA) lenses may contain pronounced defects such as wrinkles and sometimes white lumps. Below that number, the lenses may become brittle and fragile when swollen in a good solvent like THF. Thus, this optimized amount of EGDMA was used in all further polymerizations conducted in the presence of the polyurethane labels. However, initial attempts to incorporate the tags *in situ* during the thermal copolymerization of EEMA and EGDMA were unsuccessful. In bulk conditions, the polyurethane labels were found to be poorly soluble in EEMA and therefore lenses with tiny macroscopic defects were obtained. To solve this problem, the coded oligomers were first dissolved in a small quantity of warm THF that was afterwards mixed with the reaction medium (THF/EEMA

1:3.1 v/v). In these conditions, defect-free transparent tagged lenses were obtained **(Table II. 2)**. Yet, the incorporation of polyurethane labels in the *c*-PEEMA networks could potentially lead to unwished property changes. Thus, the optical and biocompatibility properties of the polyurethane-loaded implants were studied and compared to those of pristine samples. First of all, a standard transparency test was performed **(Figure II. 2)**. In this test, the tagged and non-tagged lenses were placed in water for several days under intense white light exposure. Non-optimal lenses usually show intense opacity after such a treatment as shown in the reference scale of **Figure II. 2.** However, tagged *c*-PEEMA lenses remain overall transparent, thus suggesting that the polyurethane label do not affect significantly the optical properties of the materials.

Table II. 2: Description of the tagged implants prepared and studied in this work.

	Labeling strategy	Type	Label	Loading (wt%)
L1	*in situ*	*c*-PEEMA	PU1	0.1[a]
L2	*in situ*	*c*-PEEMA	PU2	0.1[a]
L3	*in situ*	*c*-PEEMA	PU3	0.4[a]
L4	*in situ*	*c*-PEEMA	PU4	0.3[a]
L5	Swelling	Artis®	PU1	0.4[b]
L6	Swelling	Artis®	PU2	0.3[b]
L7	Swelling	Artis®	PU4	1.2[b]
L8	Swelling	*c*-PEEMA	PU5	0.14[b]

[a] For tagged lenses prepared by an *in-situ* approach, the loading value represents the weight fraction PU/EEMA. [b] For tagged lenses prepared by a swelling/deswelling approach, the loading value corresponds to the weight fraction PU/THF.

Reference scale

opaque → transparent

PU4-tagged L4

PU5-tagged L8   *PU2-tagged L6*
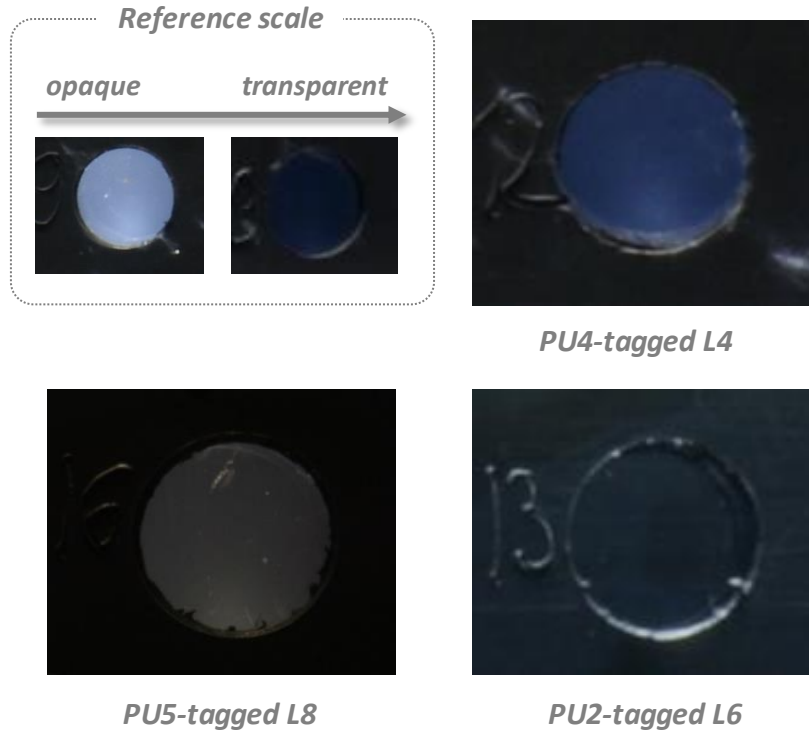
Figure II. 2: Transparency tests performed for samples L4, L6 and L8 that was loaded by swelling with PU4, PU5 and PU2 respectively. The reference scale on the left shows typical opacity of poor and optimal model lenses. The bluish/non-bluish color of the images depends on the distance between the water-immersed lenses and the camera and should not be interpreted as a sign of opacity.

a.

b.

c.

Figure II. 3: Optical microscopy pictures taken after performing the accelerated microvacuole test by using a 18 mm microscope magnification for (a) a pristine c-PEEMA lens used as reference, (b) sample L1 prepared by in situ polymerization in the presence of PU1, and (c) sample L8 labeled by swelling with PU5. The red arrows show typical examples of microvacuoles

Weak whitening was observed in some samples but these defects were not more pronounced than in pristine *c*-PEEMA lenses. Perhaps more importantly, a microvacuole test was performed (**Figure II. 3**). It is well-known that microvacuole-induced glistening effects may significantly impair the properties of (meth)acrylate-based intraocular implants.[233,234] **Figure II. 3** compares optical microscopy images that were taken for the **PU1**-loaded lens **L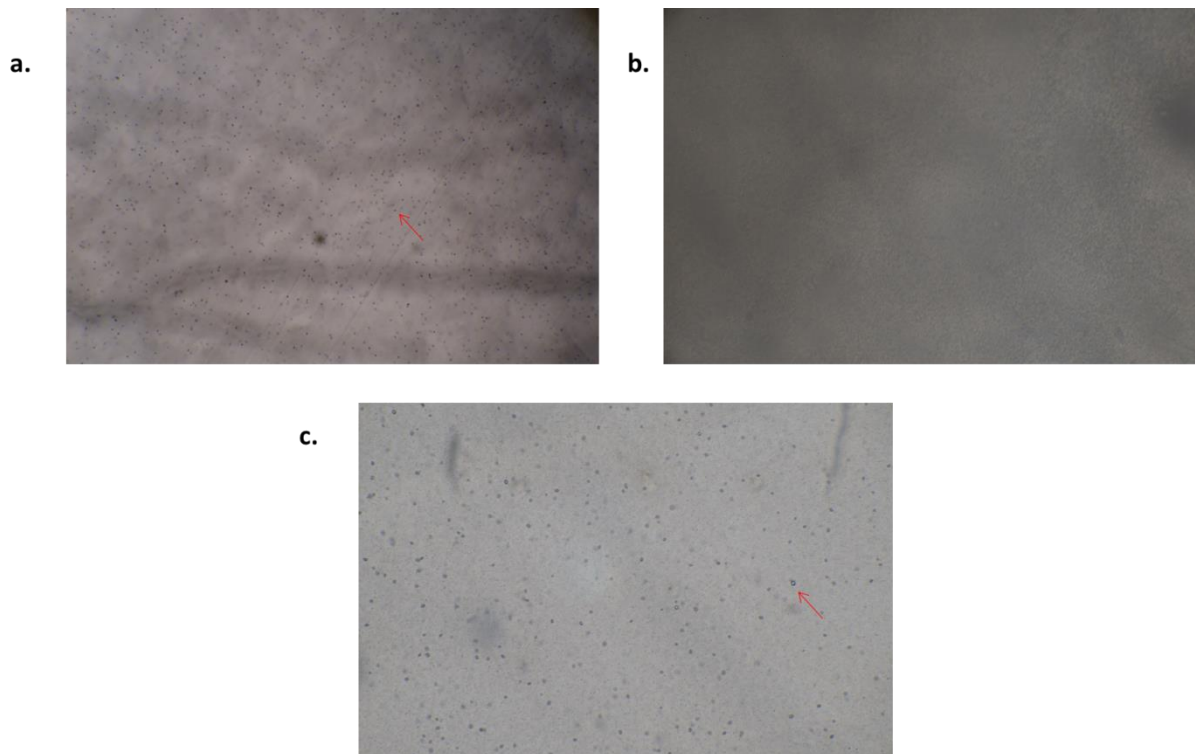1** and for a pristine *c*-PEEMA lens after performing the accelerated microvacuole test. It appears clearly that the presence of polyurethane tags does not influence the diameter and number of observed microvacuoles, thus confirming further that the small amounts of incorporated labels do not alter significantly the optical properties of the implants. Furthermore, an ISO test was done in order to verify the biocompatibility of the tagged-lenses. The aim of this test is to detect traces of monomer, tag or other contaminants that may leak out of the lenses when exposed to aqueous environment and thus lead to eye irritation or other harmful effects. In brief, the lenses were immersed in boiling water for some hours in order to extract potential contaminants and the water was afterwards analyzed by UPLC-MS. The polyurethane labels could not be detected in any cases after performing this test, thus suggesting that *(i)* the label is not leaching out of the lenses in aqueous environment or *(ii)* that it was no incorporated at all in the lenses. The latter scenario was discarded by the mass spectrometry analysis of the tagged lenses. In order to extract the polyurethane labels from the *c*-PEEMA networks, the lenses were placed for 10 minutes in a methanolic solution of ammonium acetate. In all cases, the polyurethane labels were detected by ESI-MS analysis (**Figure II 4a and Figures II. 10-12**). Furthermore, the MS/MS analysis of the found oligomers allowed unequivocal decryption of their coded binary sequences (**Figure II. 4b and Figures II. 10-12**). These results indicate that the polyurethane labels retain their molecular integrity after formation of the network by free radical polymerization and also suggest that they are predominantly physically entrapped in the *c*-PEEMA networks. Perhaps more importantly, mass spectrometry data confirm that the sequence-coded polyurethane barcodes can be stored in biomedical implants and that the information that they contain can be easily recovered.
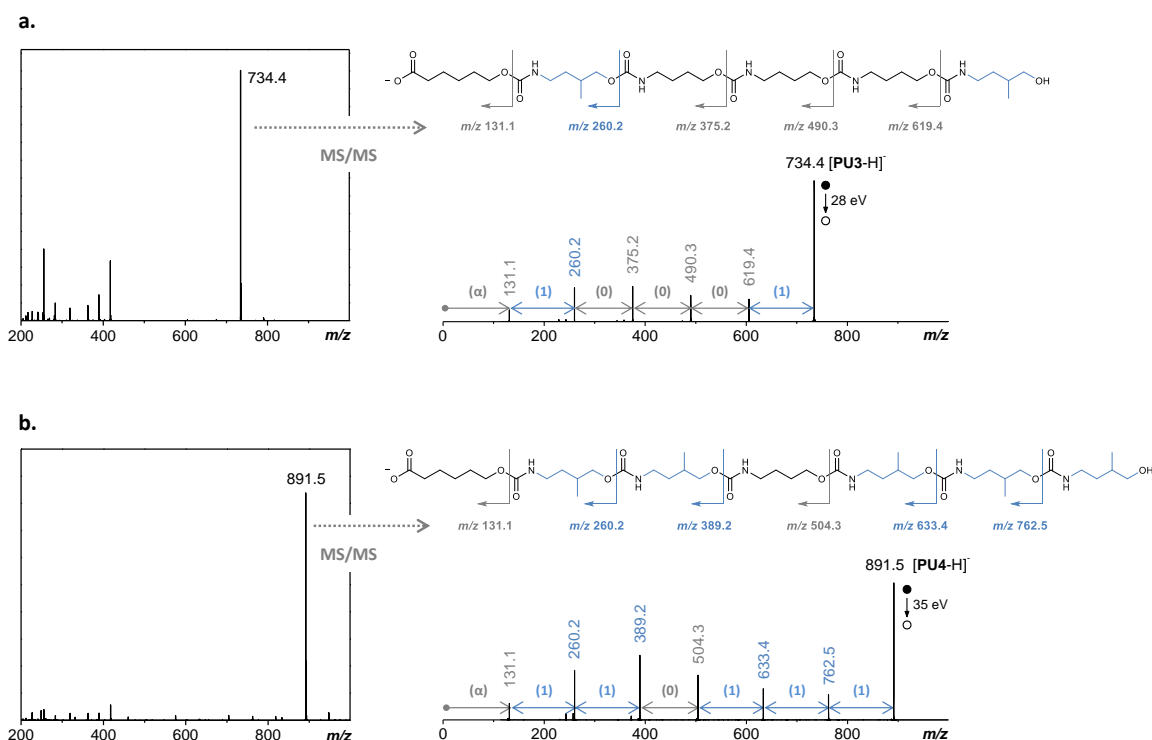
Figure II. 4: ESI-MS (left) and MS/MS (right) characterization of polyurethane tags extracted from (a) sample L3 prepared by free-radical polymerization of 2-ethoxyethyl methacrylate in the presence of PU3 and (b) from the Artis® intraocular lens L7 that was loaded with PU4.

In order to demonstrate further the versatility of this concept, a swelling/deswelling approach was also tested for lens labeling **(Figure II. 1c)**. As shown in **Table II. 2**, this strategy can be applied to *c*-PEEMA lenses but also to other types of methacrylate-based implants such as commercial Artis® lenses. In this approach, the lenses are simply swollen in THF and afterwards exposed to a THF solution containing a polyurethane label. After some hours, the THF-swollen lenses were dried in order to entrap the labels in the networks. It is important to note that this drying process should be performed slowly since fast drying may result in cracks and even complete breakage of the fragile lenses. The modified lenses were also subjected to optical and biocompatibility tests. Transparency and microvacuole tests evidenced formation of highly transparent materials **(Figure II. 2 and Figure II. 3)** and suggested that the swelling/deswelling approach is probably even more suitable than the *in situ* approach, although it should be considered that polyurethane-loading is probably about four times lower when the labels are incorporated by swelling rather than by *in situ* polymerization. On the other hand, traces of the polyurethane labels were detected by UPLC-MS after performing the biocompatibility tests. These findings are probably due to the fact that the polyurethane labels are not only incorporated inside the methacrylate networks but also physically adsorbed on the external surface of the lenses after THF drying. In order to solve that problem, the surfaces of the loaded lenses were first cleaned by immersion in hot water and afterwards rinsed with clean water. The cleaned up lenses were subjected to the biocompatibility test again and no polyurethane leakage could be detected anymore. All the lenses tagged via the swelling/deswelling procedure were also analyzed

by MS and MS/MS (**Figure II. 4 and Figure II. 12**). As shown in **Figure II. 13.b**. and **II. 14.b**, the polyurethane tags were efficiently extracted from the lenses and sequenced by MS/MS.

Figure II. 5: (a) Negative ion mode ESI mass spectrum of PU1, α-0-0-0-1. (b) MS/MS sequencing of [PU1 − H]⁻ at *m/z* 605.3 (collision energy: 25 eV) and corresponding dissociation scheme.

Figure II. 6: (a) Negative ion mode ESI mass spectrum of PU2, α-0-0-1-0. (b) MS/MS sequencing of [PU2 − H]⁻ at *m/z* 605.3 (collision energy : 25 eV) and corresponding dissociation scheme
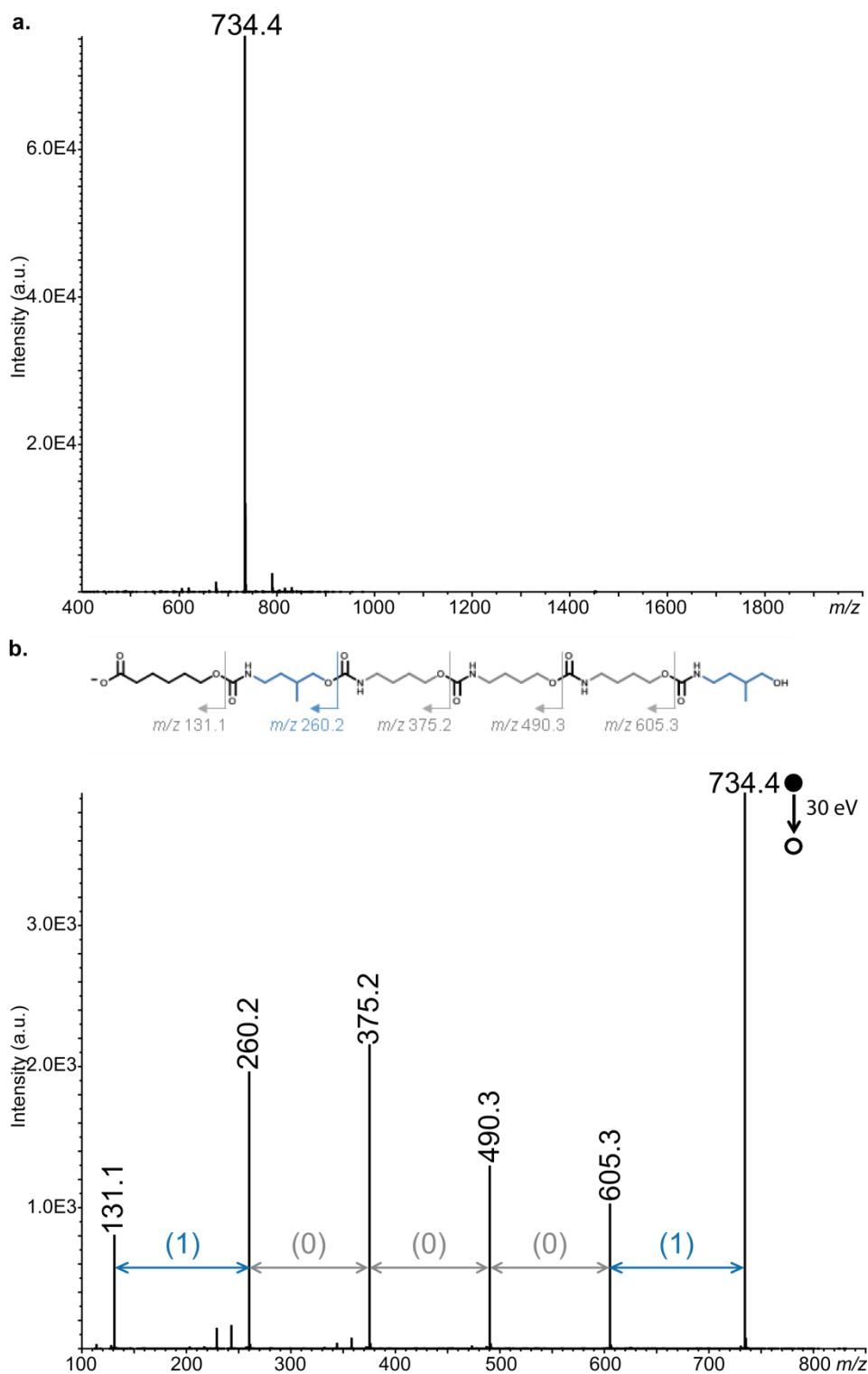
Figure II. 7: (a) Negative ion mode ESI mass spectrum of PU3, α-1-0-0-0-1. (b) MS/MS sequencing of [PU3 − H]⁻ at *m/z* 734.4 (collision energy : 30 eV) and corresponding dissociation scheme.
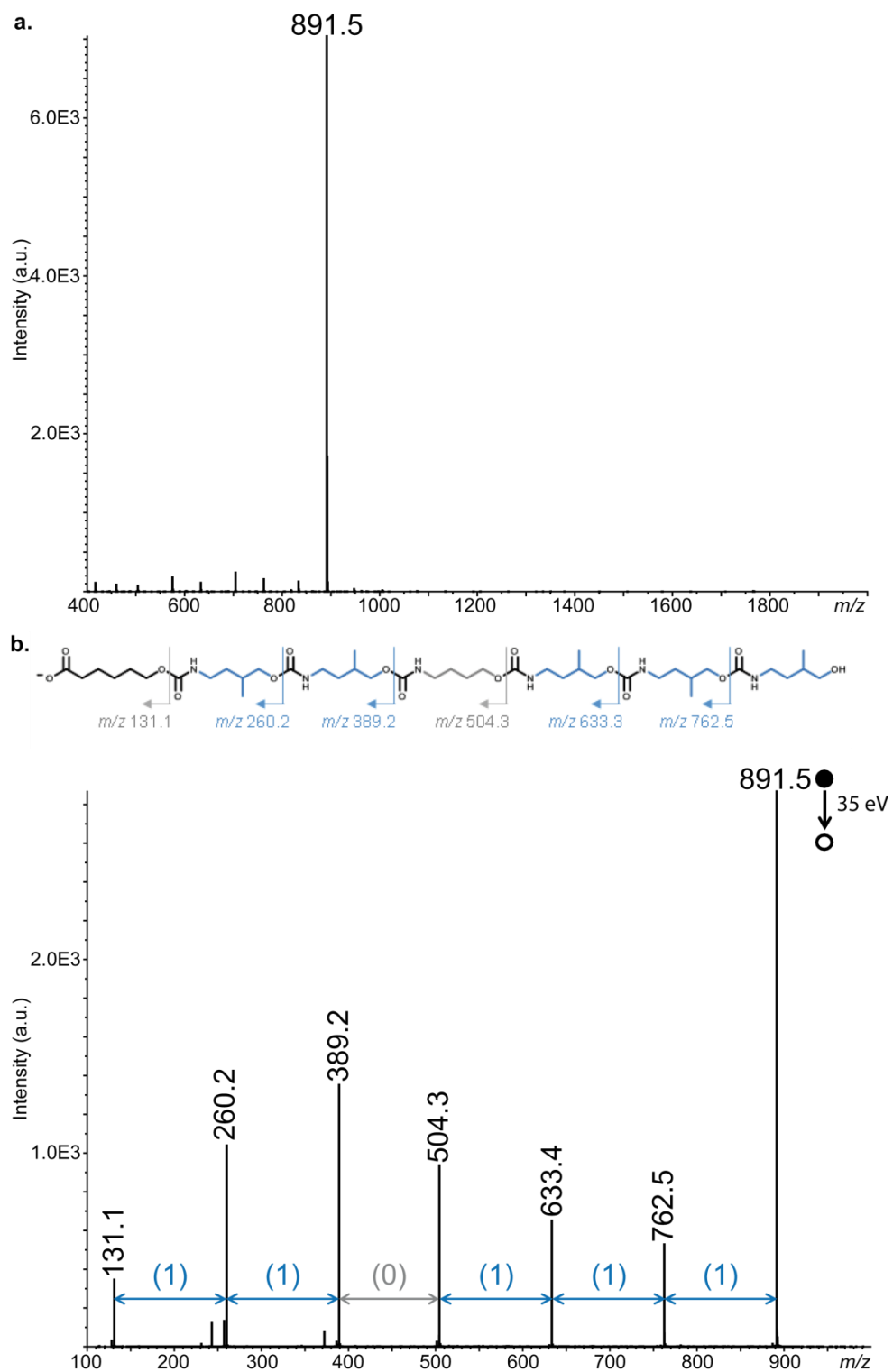
Figure II. 8: (a) Negative ion mode ESI mass spectrum of PU4, α-1-1-0-1-1-1. (b) MS/MS sequencing of [PU4 − H]⁻ at *m/z* 891.5 (collision energy : 35 eV) and corresponding dissociation scheme.
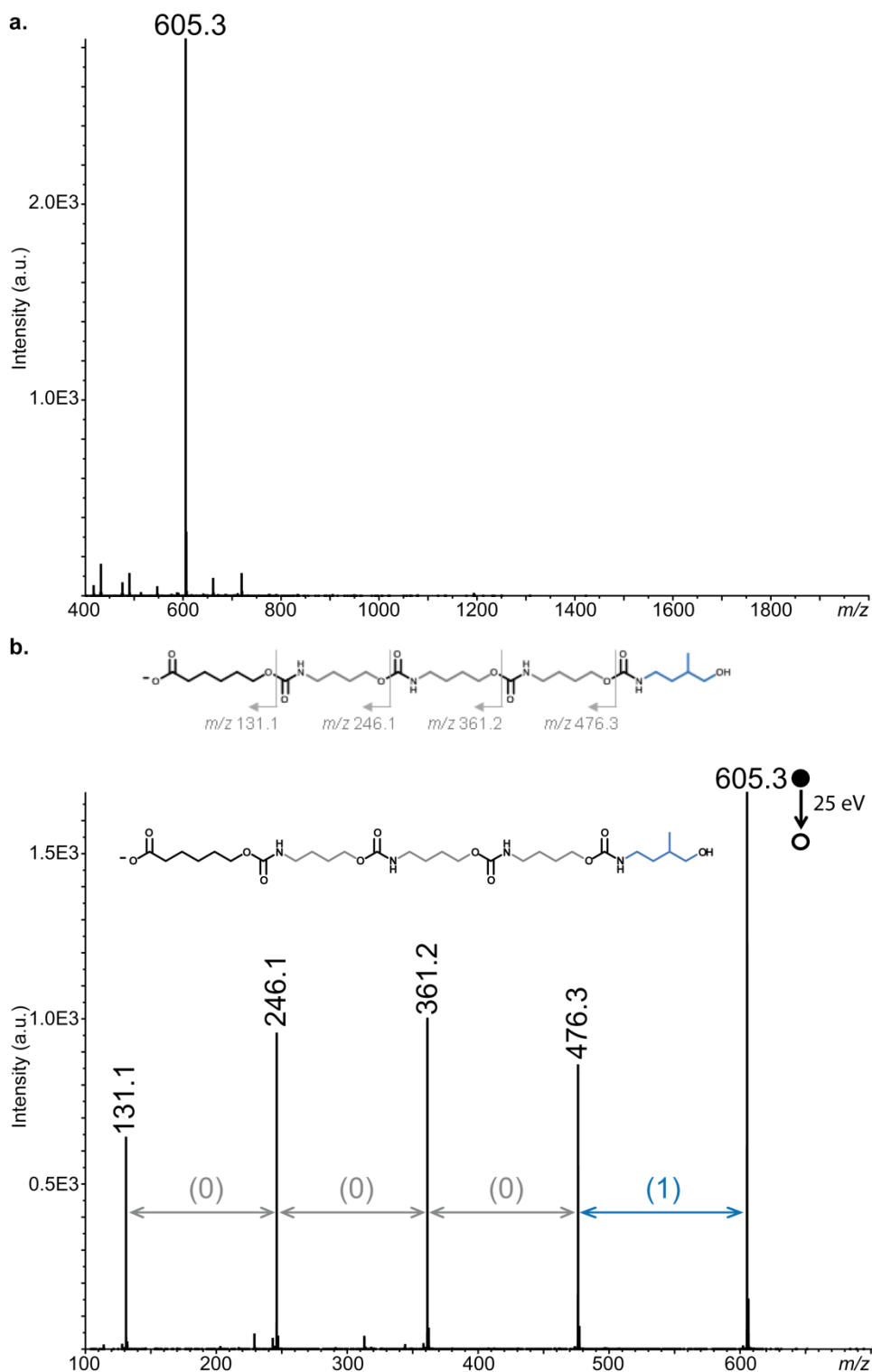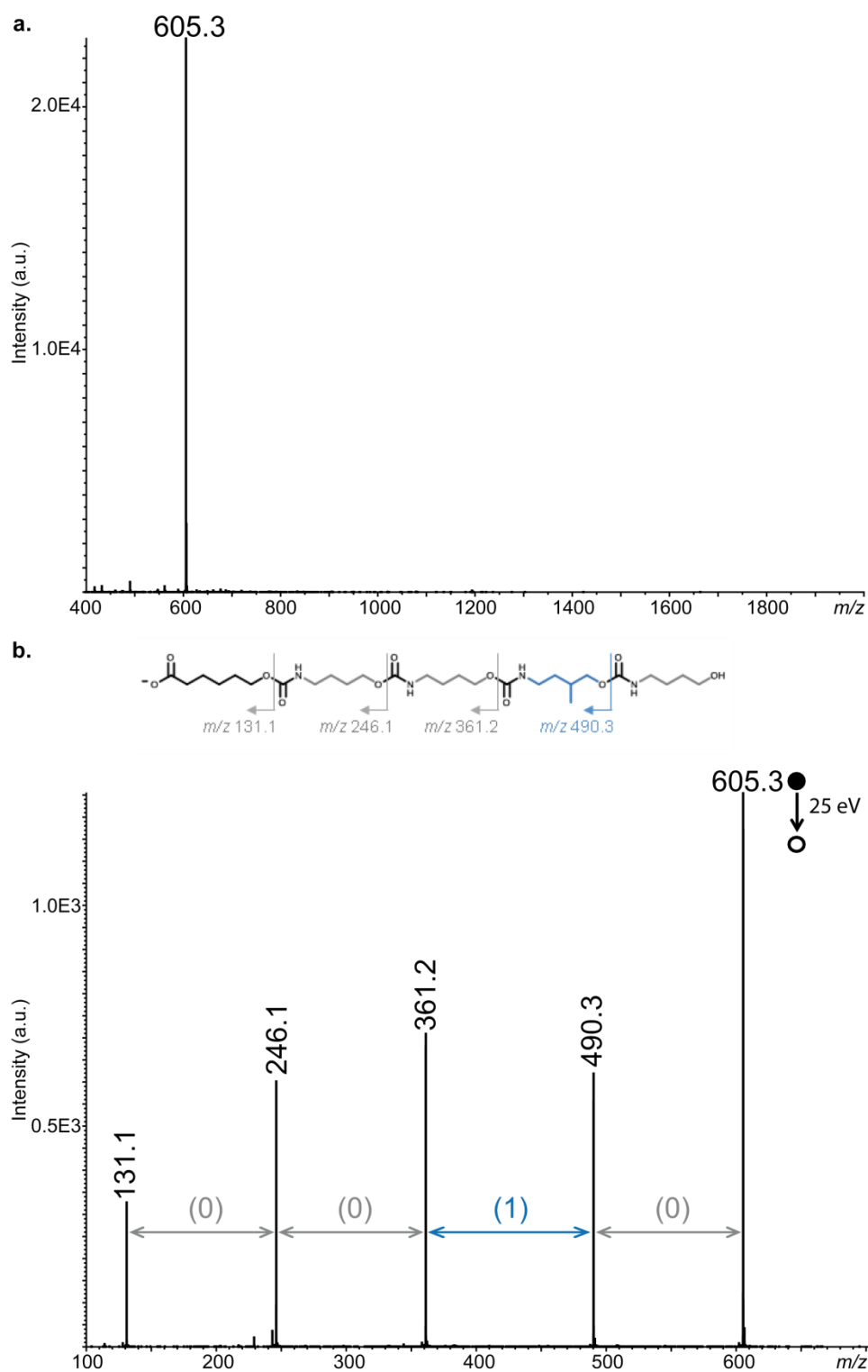
Figure II. 9: (a) Negative ion mode ESI mass spectrum of PU5, α-0-0-1-1-1-1-1-1-0. (b) MS/MS sequencing of [PU5 − H]⁻ at *m/z* 1121.7 (collision energy : 40 eV) and corresponding dissociation scheme
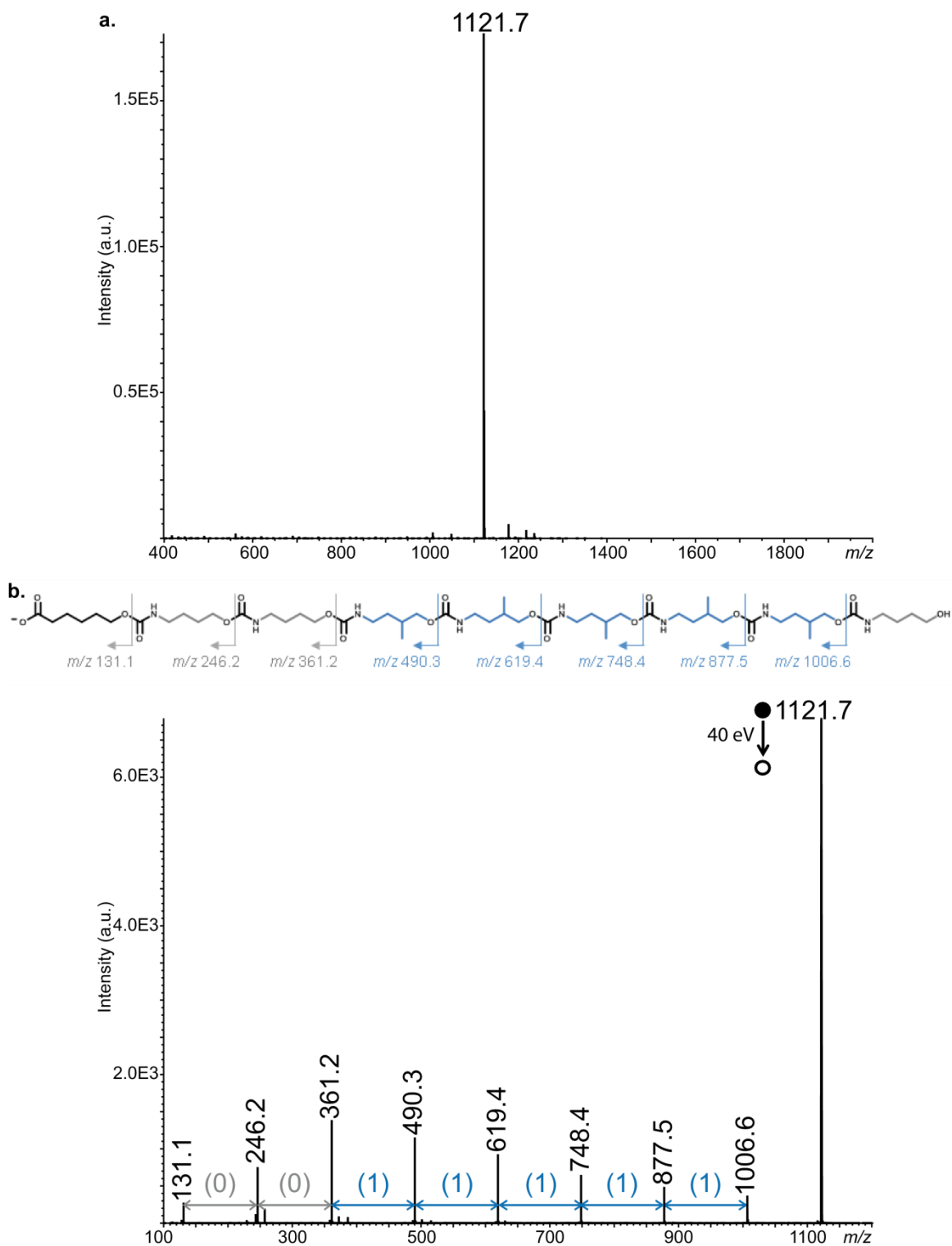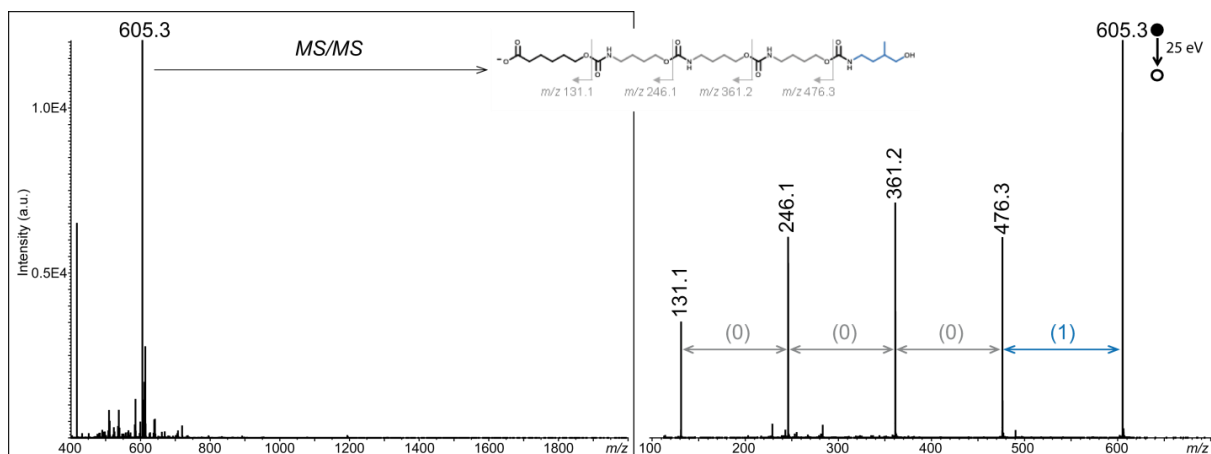
Figure II. 10: ESI-MS (left) and MS/MS (right) characterization of the polyurethane tag extracted from sample L1 prepared by free-radical polymerization of 2-ethoxyethyl methacrylate in the presence of PU1.
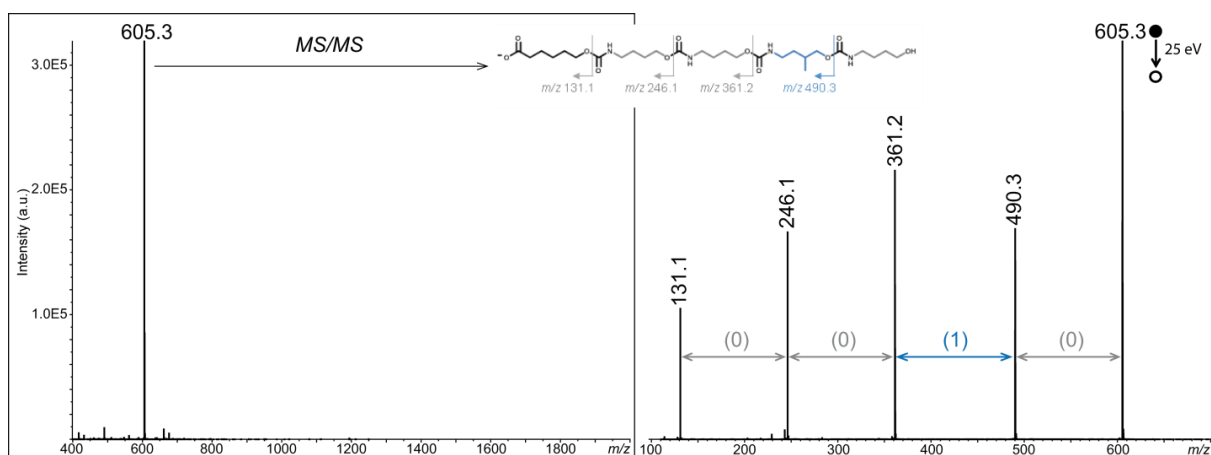
Figure II. 11: ESI-MS (left) and MS/MS (right) characterization of the polyurethane tag extracted from sample L2 prepared by free-radical polymerization of 2-ethoxyethyl methacrylate in the presence of PU2.
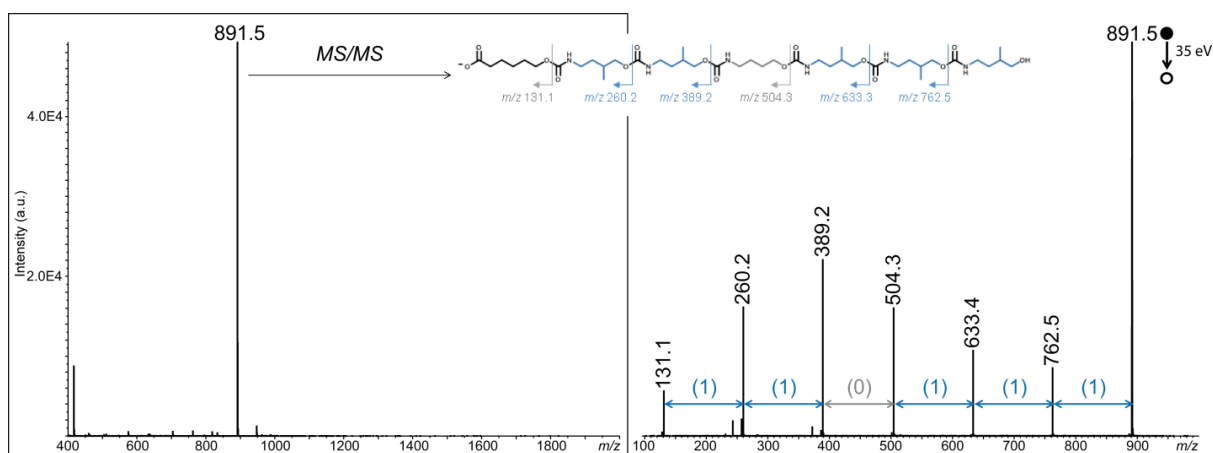
Figure II. 12: ESI-MS (left) and MS/MS (right) characterization of the polyurethane tag extracted from sample L4 prepared by free-radical polymerization of 2-ethoxyethyl methacrylate in the presence of PU4.
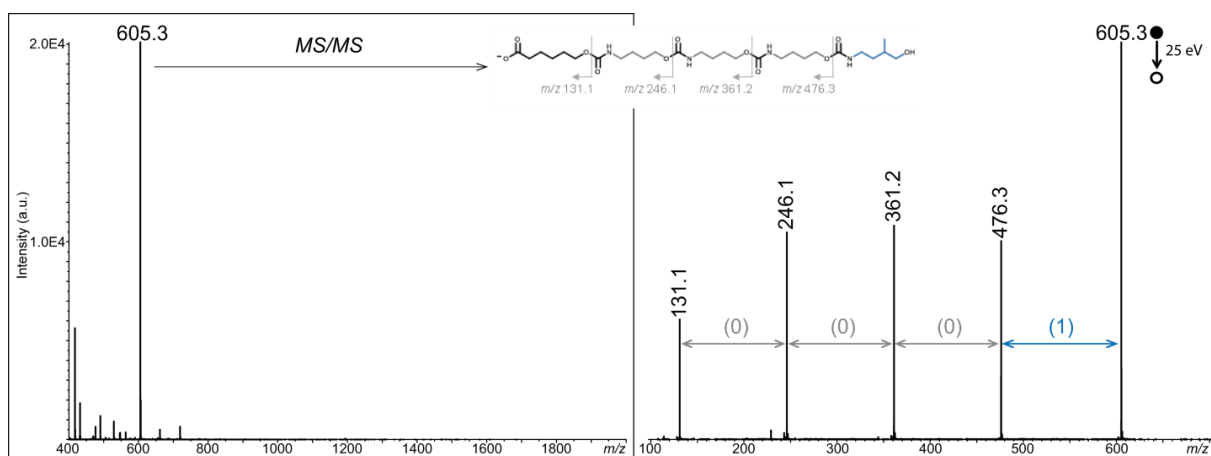
Figure II. 13:ESI-MS (left) and MS/MS (right) characterization of the polyurethane tag extracted from the Artis® intraocular lens L5 that was loaded with PU1.
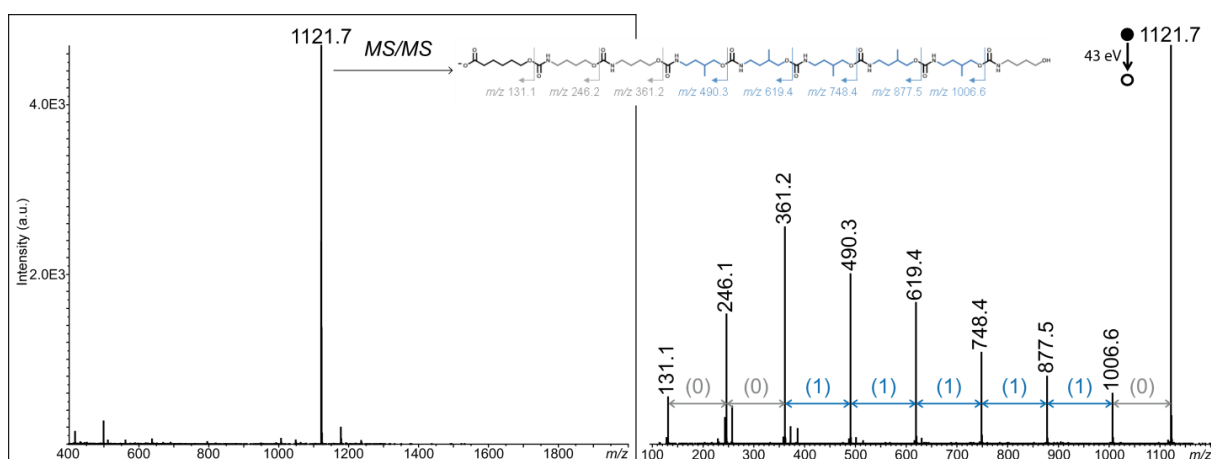
Figure II. 14: ESI-MS (left) and MS/MS (right) characterization of the polyurethane tag extracted from the *c*-PEEMA lens L8 that was loaded with PU5.

3. Conclusions

Methacrylate-based intraocular implants were labeled with small amounts of sequence-coded polyurethanes that can be used as traceability and anti-counterfeiting barcodes. Two different strategies were investigated for incorporating the sequence-defined oligomers in the lenses. In a first approach, the label was included *in situ* during the formation of the crosslinked methacrylate network. In an alternative strategy, the polyurethane barcode was included in a premade lens using a simple THF swelling/deswelling procedure. Both approaches led to the successful preparation of polyurethane-tagged intraocular implants. In all cases, it was verified that the incorporation of the polyurethane barcodes does not modify drastically the optical properties of the lenses and also does not lead to significant aqueous release of contaminants that could be potentially irritant or harmful to the eyes. Furthermore, it was demonstrated that the polyurethane tags can be easily extracted from the lenses and characterized by mass spectrometry. In particular,

87

their coded sequences can be easily deciphered by MS/MS, thus opening interesting opportunities for traceability and anti-counterfeit labeling of intraocular implants. Yet, it should be noted that only short model sequences were studied in the present work. For real industrial applications, longer barcodes containing a higher amount of information may be needed. Furthermore, before thinking about biomedical use, the toxicity of these new PUs oligomers shall also be carefully assessed. Nevertheless, this first proof-of-concept underlines the relevance of these materials for implant tagging. More generally speaking, sequence-coded polyurethane barcodes could be relevant for labeling a wide range of biomaterials and biomedical devices.

Chapter III:

Abiotic sequence-coded oligomers as efficient in vivo taggants for the identification of implanted materials.

Denise Karamessini[‡], Teresa Simon-Yarza[‡], *Salomé Poyer, Evgeniia Konihcheva, Laurence Charles,*

Didier Letourneur* and Jean-François Lutz*

1. Introduction

The certification of biomedical and pharmaceutical products is a major health and economical challenge. Currently, the World Health Organization estimates that more than 8% of the medical devices in circulation are counterfeits. The widespread circulation of these products, which do not meet international safety regulations, may greatly put at risk the health and life of consumers.[235] This is particularly true in the case of *in vivo* materials such as plastic implants, which shall be safe, biocompatible and traceable. In the last few years, the US food and drug administration and the EU Commission have defined the requirements for the implementation of a Unique Device Identification (UDI) to avoid counterfeits and ensure medical device traceability. Labelling requirements include the UDI information on the label and/or the packages of medical devices. Nevertheless, this strategy does not completely eliminate the risk of counterfeit. Strategies to incorporate the UDI directly inside the medical device shall reduce considerably the risks, making also possible to identify a device after implantation. However, although a wide variety of anti-counterfeiting technologies are available,[4] only a few of them can be applied *in vivo*. Indeed, a valid anti-counterfeiting solution for long *in vivo* use shall be biocompatible and bio-stable. Therefore, relatively simple technologies, such as colored markers, are currently used to label implants.

Among all anti-counterfeiting technologies that have been reported in the literature, sequence-controlled polymers represent a new and interesting option.[12] In particular, uniform polymers containing a perfectly-defined monomer sequence can be used as a molecular barcode.[209,210,236] For instance, DNA, which contains specific sequences of the four nucleotide monomers A, T, G and C, has been extensively studied for practical anti-counterfeiting and traceability applications.[3,236] It can be sprayed on or included in a host material and decoded using a next-generation sequencing technology.[13,237] Furthermore, DNA taggants can be employed in trace amounts because they can be amplified by the polymerase chain reaction. However, DNA molecules are sensitive to chemical and thermal degradation and therefore cannot be employed in all processing conditions.[238] Similarly, bare DNA is far from being ideal for being applied as taggant *in vivo*. Indeed, genetic polymers are not bio-inert and may interfere with the biology of a host organism and *vice versa*, the genetic material of the host may contaminate the taggant and lead to false identification results. Thus, as demonstrated by Grass and coworkers, DNA taggants have to be encapsulated in silica nanoparticles for efficient anti-counterfeiting use.[17,239,240]

We have recently shown that abiotic sequence-coded polymers constitute an interesting alternative to DNA for anti-counterfeiting applications.[210,241,242] Indeed, using solid-phase iterative strategies, it is possible to write monomer-coded information on non-natural polymer chains.[32,72,243] Moreover, this information can be easily and very rapidly decoded by tandem mass spectrometry (MS/MS).[32,131,244] Among the different types of non-natural sequence-defined polymers that have been described,[33,214,215,223,245] oligocarbamates[246-248] (i.e. short polyurethanes) appear to be very interesting

candidates for materials labeling.[39] Indeed, these oligomers are chemically- and thermally-robust and can therefore be dispersed in a wide variety of materials, including 3-D printed resins,[39] casted plastic films[39,242] and intraocular lenses.[241] In all these examples, it was demonstrated that oligourethane taggants can be homogeneously included and stored in the host materials but can also be selectively extracted and decoded by tandem mass spectrometry. Moreover, standard polydisperse polyurethanes are usually biocompatible and therefore used in numerous biomedical applications.[227] Although some isocyanate monomers used in conventional step-growth polymerizations can be carcinogenic, polyurethanes by themselves were never evidenced to be harmful to living hosts.[38] In this context, it was tempting to evaluate the *in vivo* potential of sequence-coded oligourethane taggants. **Figure III.1a** shows the general strategy that was investigated in this work. A sequence-defined oligourethane, containing a monomer-coded binary sequence, was synthesized and used as taggant for the labeling of poly(vinyl alcohol) (PVA) model implants. PVA has been used for over four decades for numerous medical applications, such as surgical sponges, contact lenses, as well as implantable materials such as cartilage substitutes, meniscus tissues and vascular grafts.[249-254] For instance, the PVA crosslinked sponge Ivalon® was one of the first PVA products marketed for duct replacement, articular cartilage replacement and pharmaceutical release. Hence, oligourethane-tagged crosslinked PVA films were implanted *in vivo* in eight rats for three months. Some films were explanted at different time intervals and their authentication was tested by mass spectrometry.
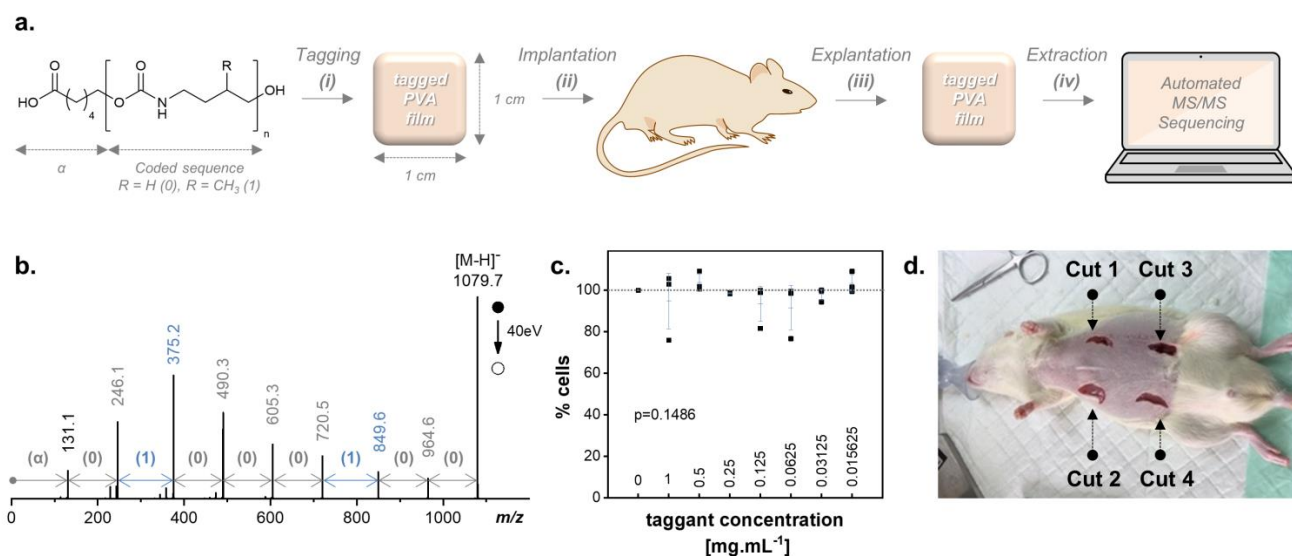
Figure III. 1: (a) General strategy studied in this work. Experimental conditions: *(i)In situ* **tagging during PVA crosslinking: Taggant, PVA, sodium trimetaphosphate, NaOH, H₂O/DMF 90°C;** *(ii)* **Implantation: UV-sterilization, invasive surgery;** *(iii)* **Explantation: surgery, H₂O swelling, drying;** *(iv)*Taggant-extraction: MeOH, **ammonium acetate. (b) ESI-HR-MS/MS spectrum obtained in negative mode for the pure oligourethane-taggant, containing the coded sequence α-01000100, obtained after its synthesis. (c) Cytotoxicity assay obtained for endothelial cells incubated for 48h in the presence of the oligourethane taggant at different concentrations. These results were obtained with three independent experiments. Bars correspond to the standard error of the mean. (d). Photography of an anesthetized rat during surgery. The arrows show the four incisions, two intramuscular (cuts 1-2) and two subcutaneous (cuts 3-4), in which the model PVA implants were placed.**

2. Results and Discussion

The sequence-defined oligourethane taggant was synthesized *via* an orthogonal solid-phase procedure that has been previously reported.[39] It is performed on an OH-functional resin and involves two successive steps: the reaction of the OH group with *N,N'*-disuccinimidyl carbonate (DSC) in the presence of triethylamine and then the reaction of the resulting succinimide-carbonate with the amine group of a coded amino-alcohol. The repetition of this two-steps cycle allows synthesis of oligourethanes. Here, a model taggant, containing a coded sequence of eight monomer units was prepared (Figure III.2). In the present study, a binary language was used to encode the oligomers. As described in earlier works,[39,241,242] monomer synthons containing either a butyl or a 2-methylbutyl linker are detected in MS/MS sequencing as 0 or 1units, respectively. In addition, the hexanoic acid chain-end resulting from solid-phase cleavage is denoted as α, following previously established conventions.[39] It shall be remarked that binary coding is only used here as a proof-of-concept. For real anti-counterfeiting applications, more complex monomer codes are developed.[209,255] In the present work, the coded taggant was synthesized by both manual and automated synthesis. **Figure III.2.a** shows a typical electrospray (ESI) mass spectrum measured for an oligourethane synthesized by manual synthesis. Although near-uniform, the oligomer contains minor impurities. For instance, a species with a mass that is 56 Da heavier than the targeted oligomer, which probably results from a base-catalyzed insertion-mechanism occurring during the DSC/Et$_3$N step, is often detected in these syntheses.[242] This problem was solved through the use of a weaker base, i.e. pyridine, which enables manual synthesis of perfectly-uniform oligomers. These conditions were then tested on a Chemspeed automated synthesis platform (see exper. section. **Fig. S.1**).[256,257]In this case, microwave irradiation, which is in general used during the DSC step was replaced by a simpler heating procedure. Nevertheless, the robotic instrument allowed successful automated synthesis of uniform taggants **(Figure III.2b).** The MS/MS spectrum obtained for the oligourethane taggant after its synthesis. In the negative ion mode,[40] the sequence of the oligomer α-01000100 can be easily decoded. It can be obtained by manual sequencing, i.e.by measuring the fragment-to-fragment distance corresponding to the mass of either 0 or 1 synthons that are successively found in the sequence, as shown in **Figure III.1.b,** but it can also be deciphered in a few milliseconds using the software MS-DECODER.[131] Moreover, the cytotoxicity of the oligourethanes was tested using two cell lines, namely human umbilical vein endothelial cells and NIH3T3 fibroblasts **Figure III. 3**. These cell lines were chosen according to potential PVA applications, e.g. vascular grafts and surgical sponges. The doses studied in the cytotoxic assay were selected assuming that the tagged implants tested *in vivo* (see below) contain about 0.5 mg of oligourethane taggant. The studied concentrations were comprised between 0.01 and 1 mg·mL^{-1}, which is greater than the concentrations that would potentially be reached *in vivo* by progressive release. **Figure III.1.c** shows the results of cell viability assays obtained with endothelial cells incubated for 48h in the presence of different concentrations of the taggant.

Statistical analysis of three independent experiments demonstrated lack of acute cytotoxicity at the studied doses of the sequence-coded oligourethane.
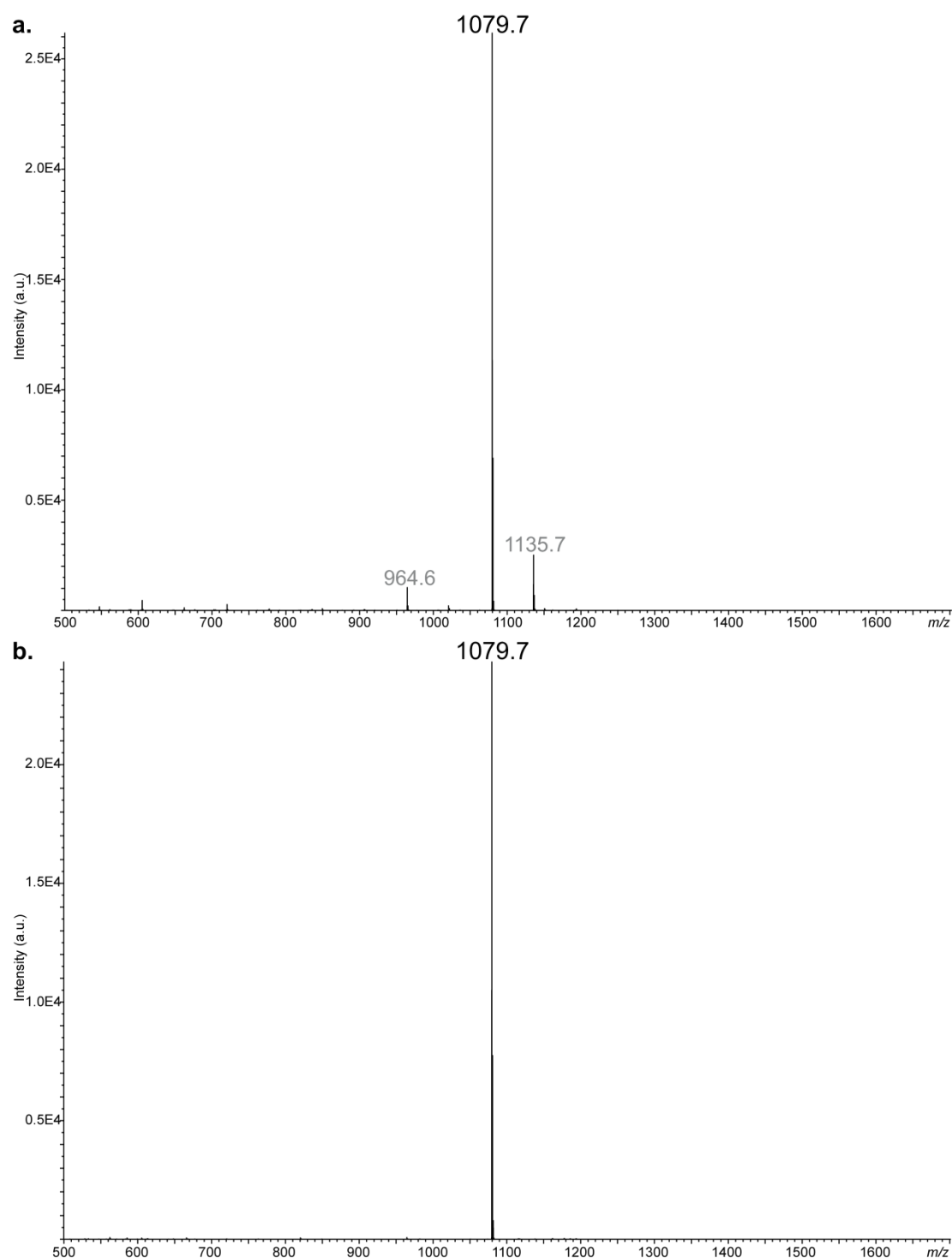
Figure III. 2: Negative ion mode ESI mass spectrum of the α-01000100 oligourethane prepared by (a) manual or (b) automated synthesis and detected as a deprotonated molecule at *m/z* 1079.7. This assignment was supported by accurate mass data recorded in the positive ion mode for the doubly protonated molecule ($C_{48}H_{90}N_8O_{19}^{2+}$, *m/z*$_{th}$ 541.3156, *m/z*$_{exp}$ 541.3155). Peaks annotated in grey at *m/z* 964.6 and *m/z* 1135.7 in part (a) correspond to the α-0100010 oligourethane (i.e., with the missing last synthesis step) and to the impurity with a mass that is 56 Da heavier than the targeted oligomer, respectively.
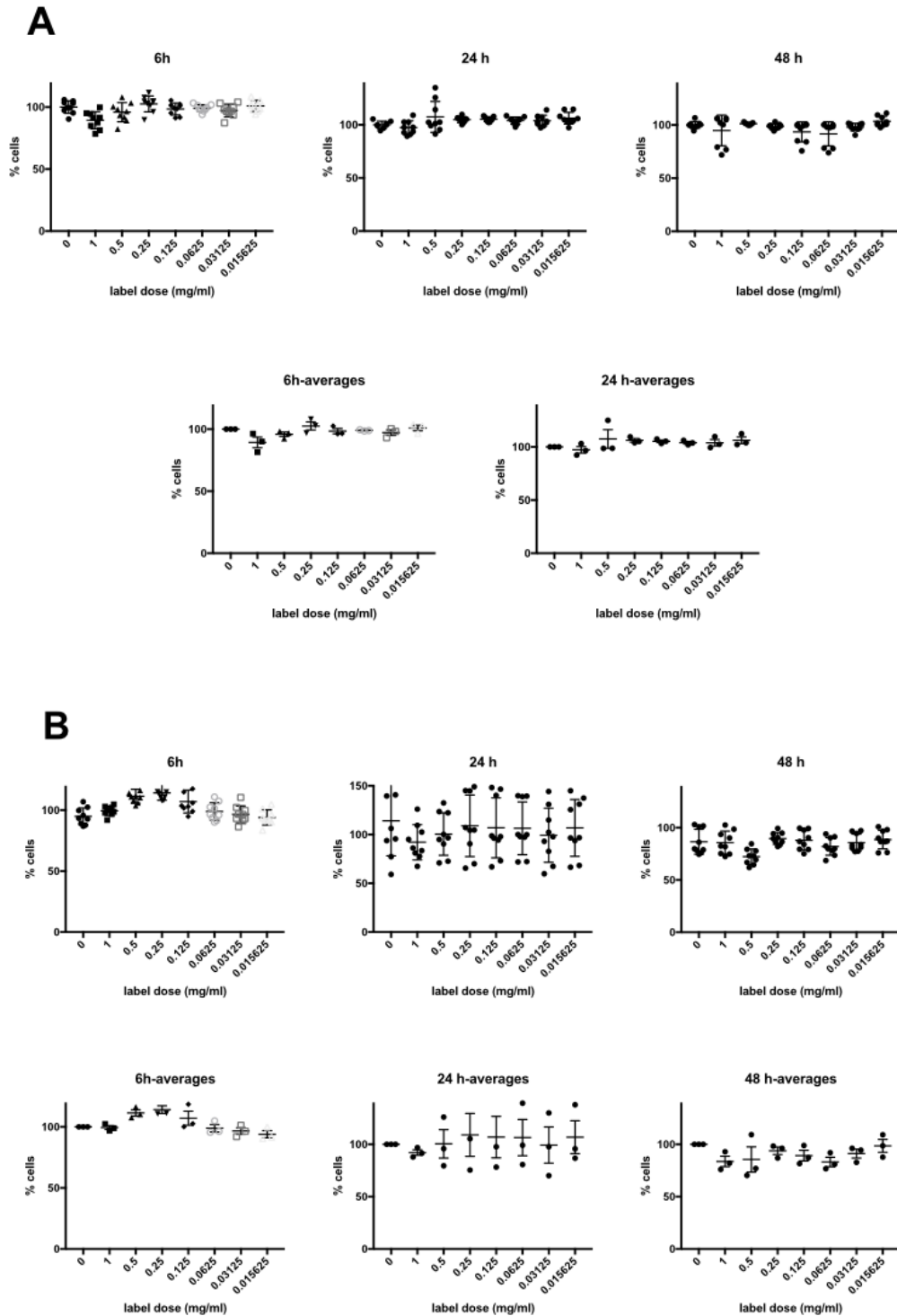
Figure III. 3: Results of cytotoxicity test conducted A) in endothelial cells (HUVEC) and B) in NIH3T3 fibroblasts. Graphs represent cell survival after 6, 24 and 48 hours of incubation with different concentrations of the oligourethanes. Upper graphs show all the points of the three experiments; in the graphs below each point represents the average of an independent study (n=3) and bars correspond to the standard error of the mean of three independent studies at 6 and 24 hours. The 48h-average is shown in Figure III. 1c of the main document. Cell viability was in all cases higher than 70 % of the control group, meaning that the material can be considered as non-cytotoxic.

The oligourethane taggant was then incorporated in small amount (1 wt%) in model crosslinked PVA films with a thickness of about 250 μm. Taggant-inclusion was performed *in situ* during PVA film formation. The oligourethane was first dissolved in DMF and the obtained solution was mixed with an aqueous solution of PVA and sodium trimetaphosphate.[250] After obtaining crosslinking in basic conditions, the membranes were washed several times with water and analyzed by ^{1}H NMR (**Figure III. 4**) and electrospray (ESI) mass spectrometry.
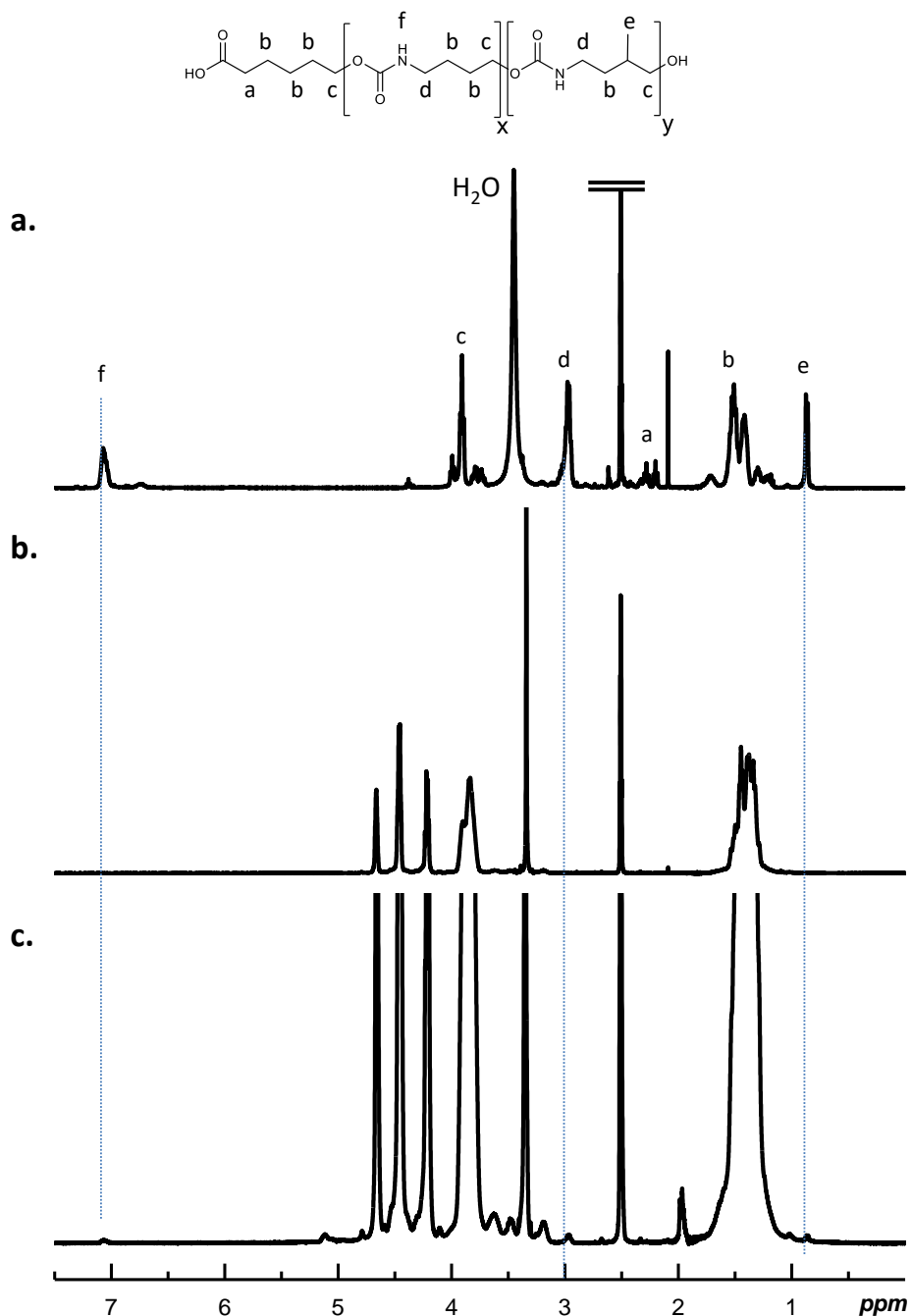
Figure III. 4: ^{1}H NMR spectra recorded in DMSO-*d6* for (a) the coded oligourethane α-01000100; (b) a pristine PVA cross-linked film; and (c) a portion of a PVA crosslinked film labeled with the oligourethane. The latter measurement was performed on different film portions in order to evidence the homogeneous distribution of the oligourethanes in the PVA films. For clarity, only a single example is shown in this figure. All other measurements were comparable.

These measurements indicated that the taggant was homogeneously dispersed inside the PVA films. Furthermore, the taggant can be selectively extracted from the films using a methanol/ammonium acetate incubation procedure and its sequence was identified by ESI-MS/MS (**Figure III. 5**).
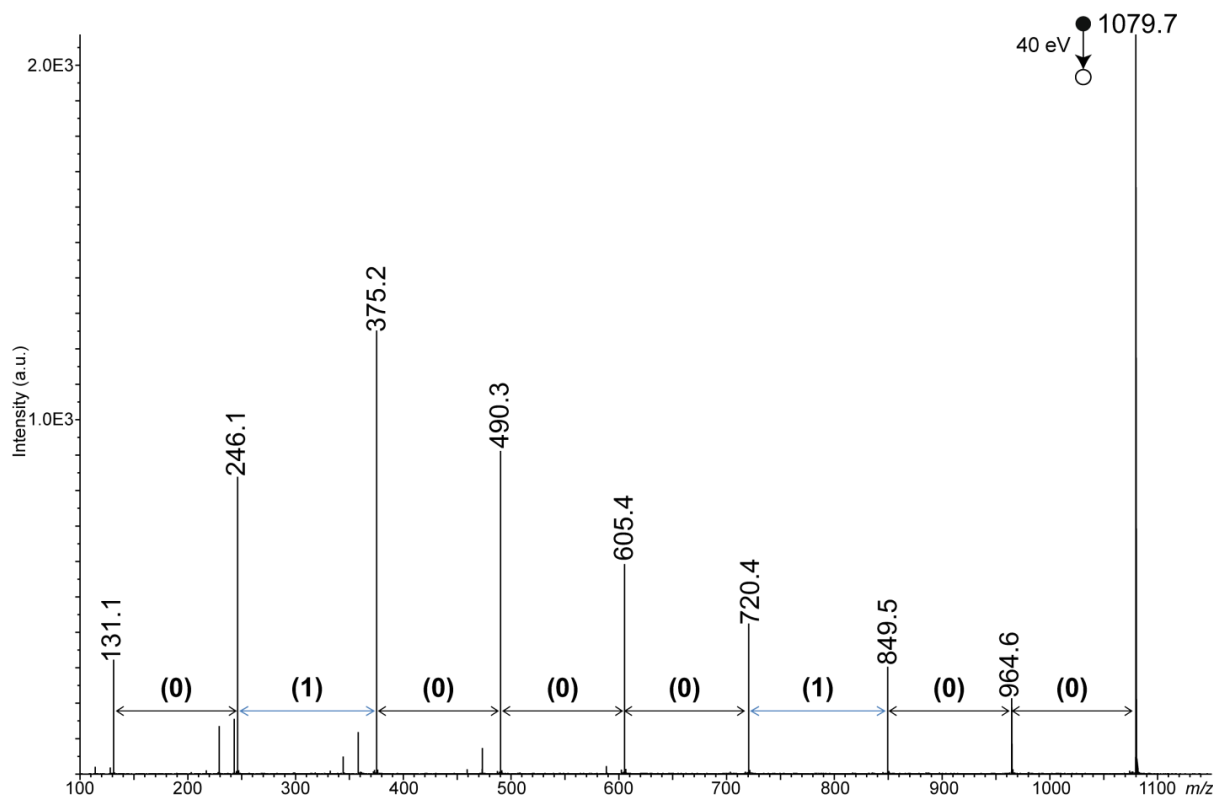
Figure III. 5: ESI-MS/MS of the _m/z_ 1079.7 precursor ion detected in the methanolic extract of a PVA film tagged with the α-01000100 oligourethane.

The PVA films were then cut into1 cm^{2}implants (about 50 mg each, thus containing about 0.5 mg of taggant), sterilized by a UV treatment and placed inside live rats. **Figure III.1.d** shows a picture of an anesthetized rat during surgery. Four abdominal incisions were performed - two intramuscular (cuts 1-2) and two subcutaneous (cuts 3-4) - and a PVA sample was placed in each of them. Both oligourethane-tagged and control non-tagged films were implanted. The location of the tagged and control implants was intentionally varied in some animals (**Table III.1**)**.** After one week, one month and three months of _in vivo_ storage, rats were sacrificed and the corresponding PVA films were explanted. After one week of implantation, the inserted samples were easily separated from the rat tissues, whereas for longer periods of implantation the PVA films appeared integrated in a newly-formed tissue. There were no noticeable differences between oligourethane-tagged films and non-tagged control samples, thus suggesting that the taggants are not harmful and probably not leaching out of the implants. The latter claim was supported by an _in vitro_ experiment, in which an oligourethane-tagged PVA film was stirred at 37°C in a phosphate-buffered saline (PBS) solution. The mass spectrometry analysis of aliquots of the aqueous phase over a period of 14 days indicated

that there is almost no release of the poorly-hydrophilic oligourethane from the PVA film (**Figure III. 6**).
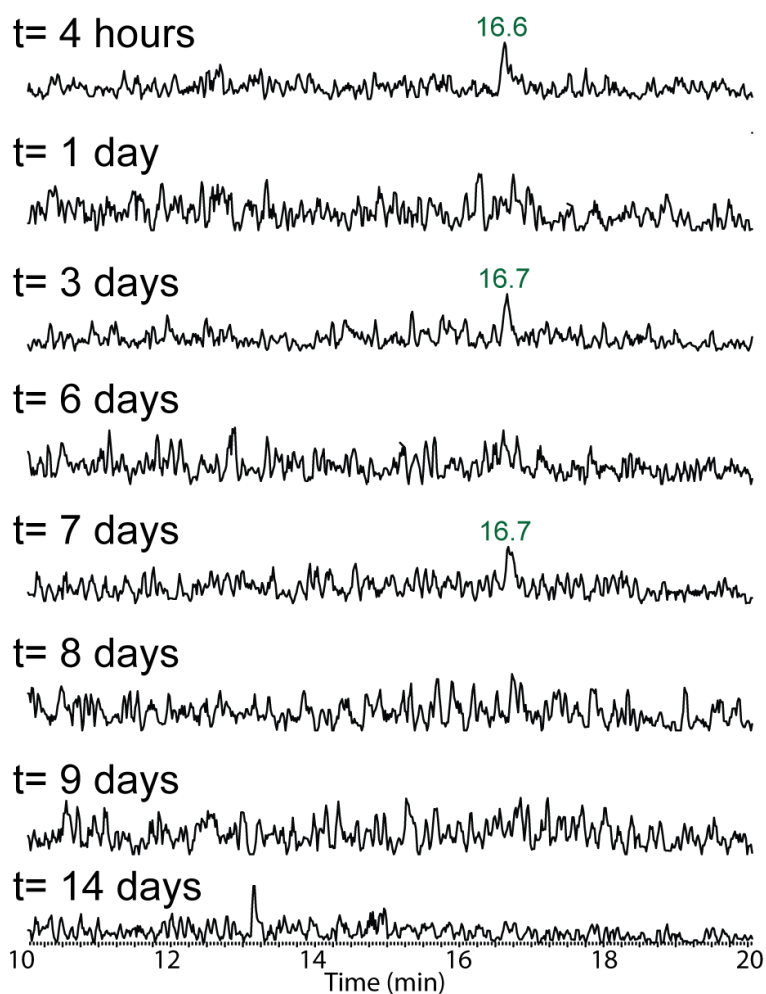
Figure III. 6: Extracted ion chromatogram (*m/z* 1079.6) recorded by HPLC-ESI-MS analysis of PBS solutions sampled at different times during the leaching *in vitro* test. When observed, the targeted oligourethane taggant, expected at a 16.7 min retention time, was always detected with a very low signal-to-noise ratio (S/N ≈ 3), that is, at or below its detection level.

Furthermore, histological examination of organs (**Figure III. 7**) and hematological tests (**Figure III. 8**) were performed after 3 months and gave no noticeable signs of toxicity.
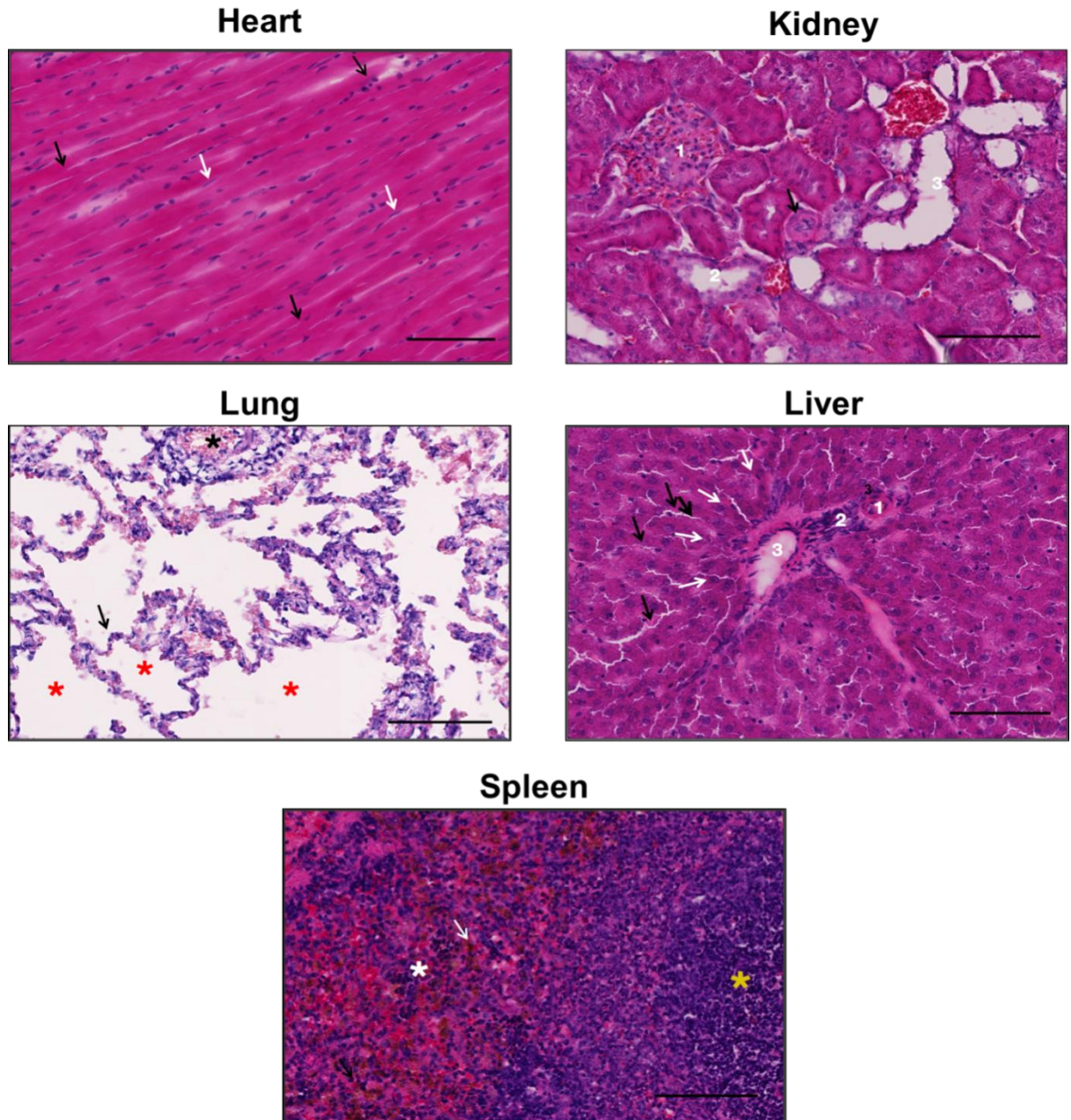
Figure III. 7:Hematoxilin eosin staining of tissues 3 months after implantation showed no signs of toxicity. Heart: transverse plane of the heart tissues with characteristic branching fibers (black arrows) and central nucleus (white arrows). Kidney: renal cortex section characterized by the presence of 1) renal corpuscules, 2) proximal convoluted tubules, 3) distal convoluted tubules and blood vessels (black arrow). Lung: a simple squamous epithelium (black arrows) constitutes the alveoli (red stars) next to a blood vessel (black arrow). Liver: portal triad constituted by 1) the hepatic artery, 2) bile duct and 3) portal vein. White arrows show hepatocytes arranged in rows and in radial disposition from the portal triad; black arrows show sinusoids between adjacent rows of hepatocytes. Spleen: tissue section evidences normal red pulp (white star) and white pulp (yellow star) regions.

Importantly, the explanted PVA films were analyzed by ESI mass spectrometry. Prior to these measurements, the films were rinsed with water and dried. Afterwards, the methanol/ammonium acetate extraction procedure described above was applied. Extracts from both tagged and non-tagged films were analyzed. It should be specified that these measurements were conducted as a blind study. In other words, the mass spectrometry experimenters did not have hints about which film contained a

taggant or not. Nevertheless, as shown in **Figure III. 9**, the oligourethane taggant was detected in all labelled films and undetected in all control films (**Table III.1**). The *m/z* 1079.7 deprotonated oligourethane was measured with different abundances in mass spectra shown in **Figure III. 9**, as a result of different amount of membrane being extracted in each case. However, when relating this peak intensity (in arbitrary units a.u.) to the mass of the extracted membrane, the oligourethane MS response were similar (40-50 a.u./mg, on average). Furthermore, the coded sequence of the taggants could be recovered by MS/MS in all cases.
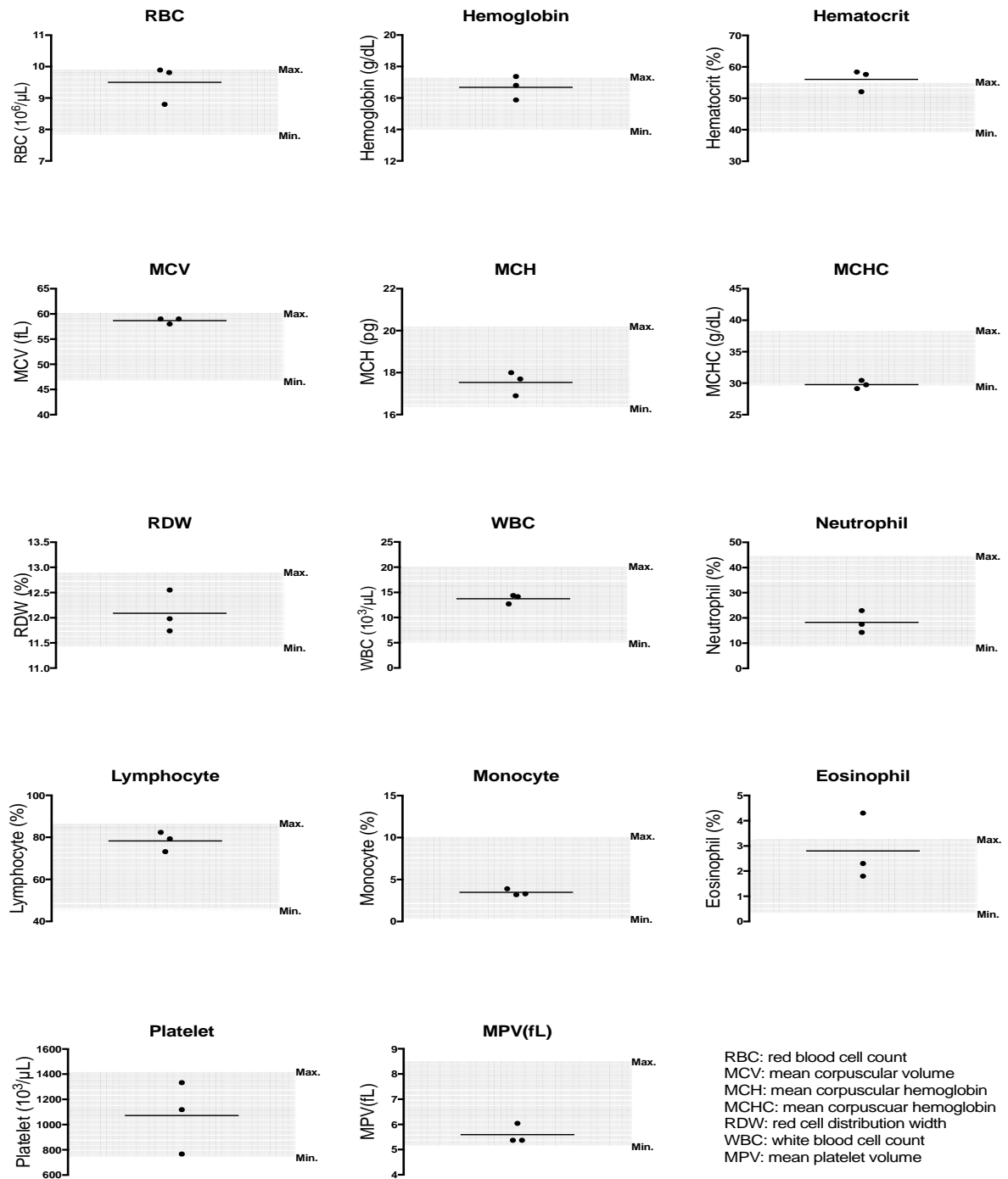
Figure III. 8: Results of hematological parameters of rats after 3 months of implantation (n=3). Horizontal bars represent the mean and region in grey shows the reference ranges reported for adult rats.[258]

Table III. 1: Localization of the tagged and non-tagged PVA implants in the different rats. [a]

	Cut 1	Cut 2	Cut 3	Cut 4
1 week				
Rat 1	non-tagged	tagged	non-tagged	tagged
Rat 2	non-tagged	tagged	non-tagged	tagged
Rat 3	non-tagged	tagged	tagged	tagged
1 month				
Rat 4	non-tagged	tagged	non-tagged	tagged
Rat 5	tagged	non-tagged	tagged	non-tagged
3 months				
Rat 6	non-tagged	tagged	non-tagged	tagged
Rat 7	non-tagged	tagged	non-tagged	tagged
Rat 8	non-tagged	tagged	non-tagged	tagged

[a]See Figure 1d in the main text for the body localization of the four different cuts.
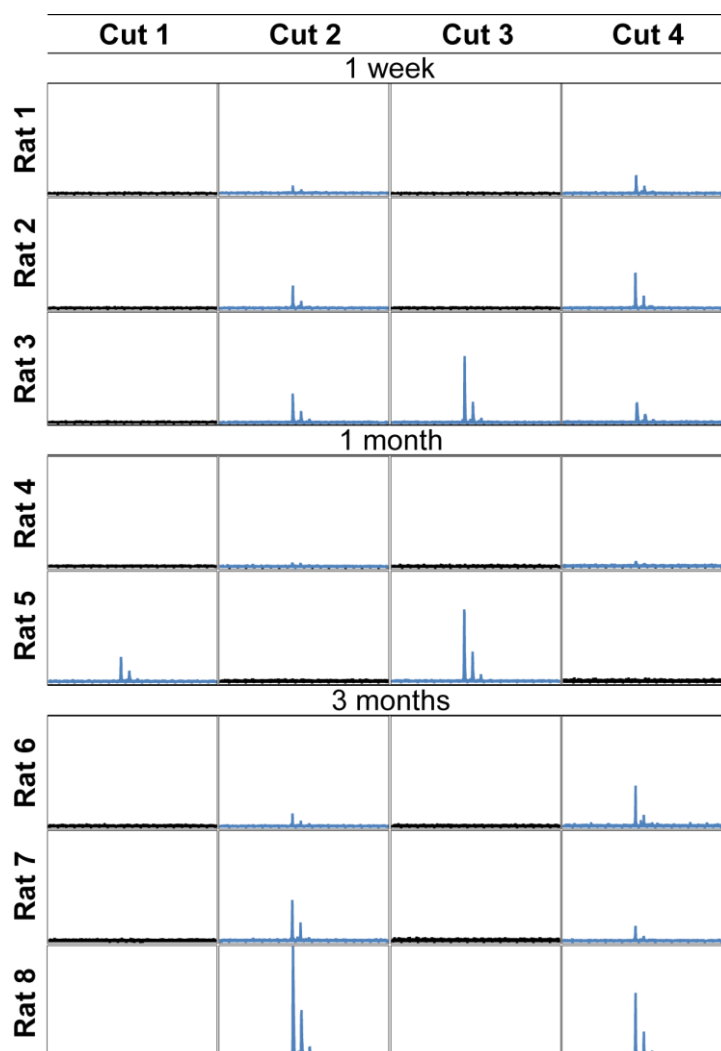
Figure III. 9: Normalized ESI mass spectra (expanded on the 1071-1091 *m/z* range) recorded for methanolic extracts of explanted PVA, showing that the oligourethane label was systematically recovered from tagged implants (as revealed by the whole isotopic pattern of the *m/z* 1079.7 anion, in blue) while it remained undetected from control non-tagged films (in black).

For instance, **Figure III. 10** shows a MS/MS spectrum obtained after three months of *in vivo* implantation. Very interestingly, after such a period of time *in vivo*, MS/MS analysis yields the same dissociation pattern as the one shown in **Figure III. 1. b**, thus evidencing the robustness and usefulness of oligourethane taggants. Additionally, the sequence of the oligomer can also be decoded after *in vivo* implantation with the help of the MS-DECODER software. For instance, the analysis of the spectrum shows in **Figure III. 10** required about 20 milliseconds. Comparable results were obtained for all tagged films after one week, one month or three months. Even at the lowest detection level (see for example Rat 4 in (**Figure III. 9**), the coded sequence of the oligomer was efficiently decoded (see exp. sect. **Fig.S.2**).
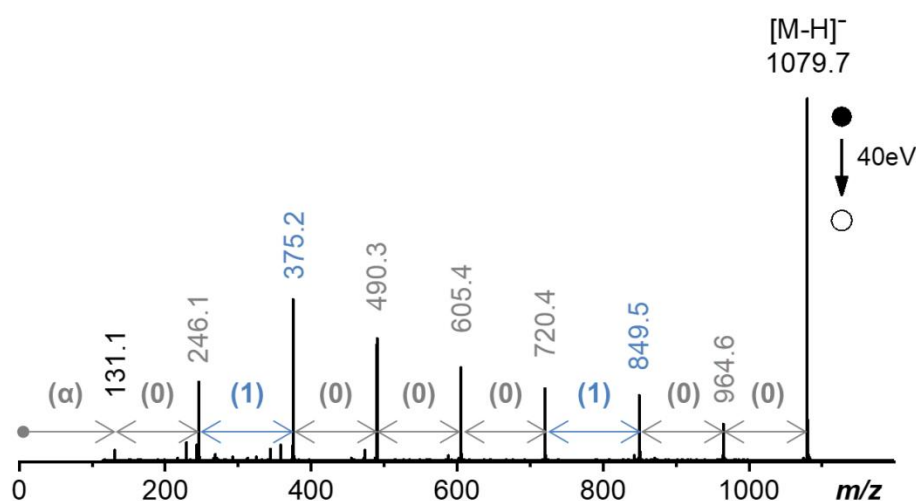
Figure III. 10: ESI-HR-MS/MS spectrum recorded for the oligourethane taggant α-01000100 after 3 months of *in vivo* implantation and selective extraction from the host PVA film. This particular spectrum corresponds to the film that was implanted in the subcutaneous cut 4 of rat 6 (Table III.1 and Figure III.9).

3. Conclusions

In summary, it was shown in this study that information-containing oligourethanes can be used as molecular taggants for the identification of implants. Such sequence-coded oligomers can be easily dispersed in plastic implants and applied *in vivo*. Quite remarkably, after several months of *in vivo* implantation, the taggant can be recovered and unequivocally decoded by mass spectrometry. Furthermore, the taggant did not induce toxicity or inflammatory tissue reactions in the host organisms. These new findings open up interesting perspectives for the development of traceable biomedical products, which could be useful for forensics and medical lawsuits. It shall be stated that the scope of utilization of the oligourethane taggants is definitely not limited to the model PVA materials tested in this work. Beyond this first proof-of-principle, personalized oligourethane taggants could be useful for the authentication of a wide variety of plastic implants, including intravascular stents, artificial heart valves, surgery screws and breast implants. Yet, for each new type of host material, taggant dispersion, storage, extraction and detection shall be carefully studied and optimized.

Nevertheless, when used in small amounts, sequence-coded oligourethanes can potentially be included in a wide variety of host plastics. Therefore, the present results broaden the scope of applicability of so-called precision polymers.[62]

Chapter IV:

Sequence-defined polyurethanes as molecular taggants for wood labeling

1. Introduction

Anything that is collectible and expensive is a potential forgery. Not only objects made of plastic as described before are threatened by the counterfeiters but plenty others, made of stone, marble, metal, glass, textiles and wood. Very trustful-like replicas of vases, copies of statues, paintings and precious artifacts are prepared even in the same studio as the original, renders their distinction very hard.[259]

For instance wood and its derivatives constitute an appealing target. Furniture, musical instruments, doors and paintings are some potential forgeries' victims. During the last years, much furniture have been copied and sold illegally in the market by unauthorized dealers[260]. Poor quality, deterioration of the brand and risk of the consumers' safety around counterfeiting pose the real threat.

In 2015 it was reported the RFID system application on furniture for tracking the product during the entire supply chain and transportation procedure[260,261]. The common barcodes in a sticker form are not the most appropriate taggants for this purpose, since they can be removed and the information written on them is accessible to everyone, fact that makes them easily falsified. To this direction, it has been already discussed the need of wood labeling for providing control over the chain of custody systems of the logs in order to prevent illegal logging. It is important to track and trace the route of the wood from its forest origin through the whole process until it turns to the primary wood products[262,263]. Hammer branding, paper or plastic labels with barcode information, imprinted nail-based labels, magnetic stripes, RFID labels[264,265], microtaggant tracers, tracer paint, chemical and genetic fingerprint[266] are some of the existing techniques for tracking wood from stranding trees to preliminary products.

Concerning the chemical and genetic fingerprints only preliminary work has been done, like the use of fluorescent tags or the analysis of the DNA of the wooden logs in order to find out some special characteristics of the origin of the wood logs. However, all of the described methods are not used yet for the marking of wooden products existing in the market.

In the spectrum of the present work, the incorporation of the molecular taggants in the wood material is proposed as a secure anti-counterfeit solution. There are two potential ways of labeling wood with molecular taggants. The first includes anti-counterfeiting coating by use of varnishes containing the taggant dissolved in their mixtures. The second deals with the enclosing of sequence-coded PUs within the wood fibers. Here, we selected to invest on the second approach as a more homogeneous labeling solution for the wood piece. In this context, the molecular barcode was proposed to be introduced in the wood during the preparation of the final product. However, here we show just a proof of concept for the labeling of some untreated wooden parts. The research is focused on the investigation of the efficient wood labeling and the taggant reading-out. Molecular barcodes made from resistant poly(urethane)s bearing an encrypted message in their well-defined primary structure

were used for this purpose. Three different types of wood were used as samples to be tagged with encoded sequence-defined PUs in order to investigate potential differentiation in the labeling behavior and during the taggant extraction procedure. The reading-out of the coded message of the barcode was also investigated, proposing an alternative non-destructible method for the tagged material (Desorption Electrospray Ionization-MS).

DESI was first described by Cooks[267] as a new method to analyze various compounds (including peptides and proteins) from metal, polymer and mineral surfaces. DESI-MS is performed by directing charged droplets and solvent ions onto the surface to be analyzed. Then, the compound on the surface is ionized producing gaseous ions which are directing to the distant mass spectrometer via an atmospheric pressure ion-transfer line. The DESI-MS resulting spectra are similar to ESI-MS spectra and they show singly or multiply charges ions of the analytes.

2. Results and Discussion

2.1 Taggants preparation The taggants were prepared as mentioned in the previous chapters following the two iterative steps process. The solid phase synthesis was performed either manually or on the robotic platform. For this project, sequence-defined oligourethanes were synthesized, constituted from 5 to 8 monomers. The two monomers used to encrypt ASCII messages in the oligomers chains, 4-amino-1-butanol codes for 0 bit and 4-amino-2- methyl-1-butanol coded for 1-bit The oligomers where subjected to characterization techniques for the determination of their uniformity, m/z ratio and monomer sequence.

-Mass spectrometry. The synthesized oligomers were always tested by ESI-MS and MS/MS. Through these two techniques the monodispersity and the exact sequence of the oligomer are well confirmed, thus they are ready to be used for their purpose as taggants. All the oligo-urethanes used in this project are presented on the **Table IV. 1** constituting the taggants library.

Table IV. 1: Contains all the samples used as molecular barcodes for the labeling of wood. Their ASCII-coded sequence, *m/z* theoretical and *m/z* experimental

Sample	Sequence	Synthetic method	m/z_{th}	m/z_{exp}
PU1	01001	manual	736.4339[c]	736.4342 [c]
PU2	000001	manual	854.5081[a]	854.5073[a]
PU3	01000100	manual	541.3156[c]	541.3172[c]
PU4	01010110	manual	555.3312[c]	555.33134[c]
PU5	01000111	manual	555.3312 [b]	555.3310 [b]

PU6	01000100	robot	541.3156^c	541.3165^c

-Nuclear Magnetic Resonance (NMR). The oligo-urethanes were characterized by ^{1}H-NMR and ^{13}C-NMR in deuterated-DMSO. Two indicative examples are shown on the **Figure IV.1** and **IV.2** where the ^{1}H-NMR and the ^{13}C-NMR are presented, respectively.
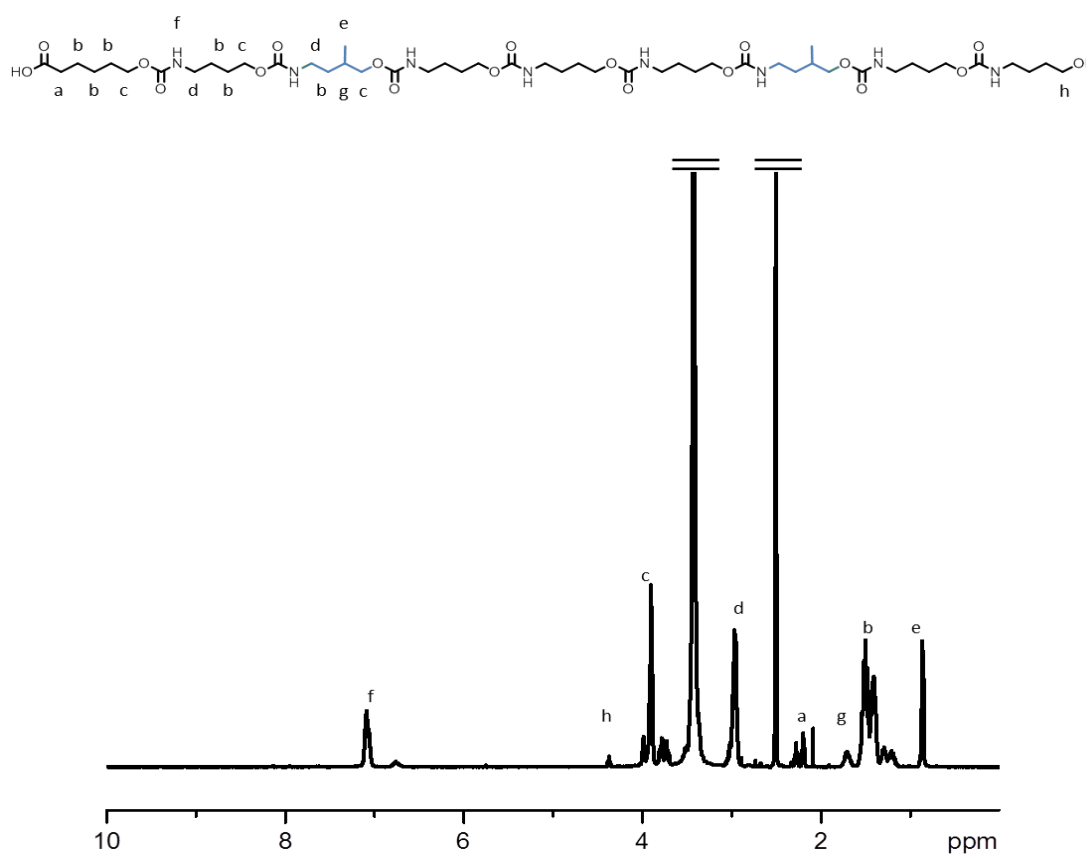
Figure IV. 1: ^{1}H-NMR spectrum of the oligo –urethane (PU6)
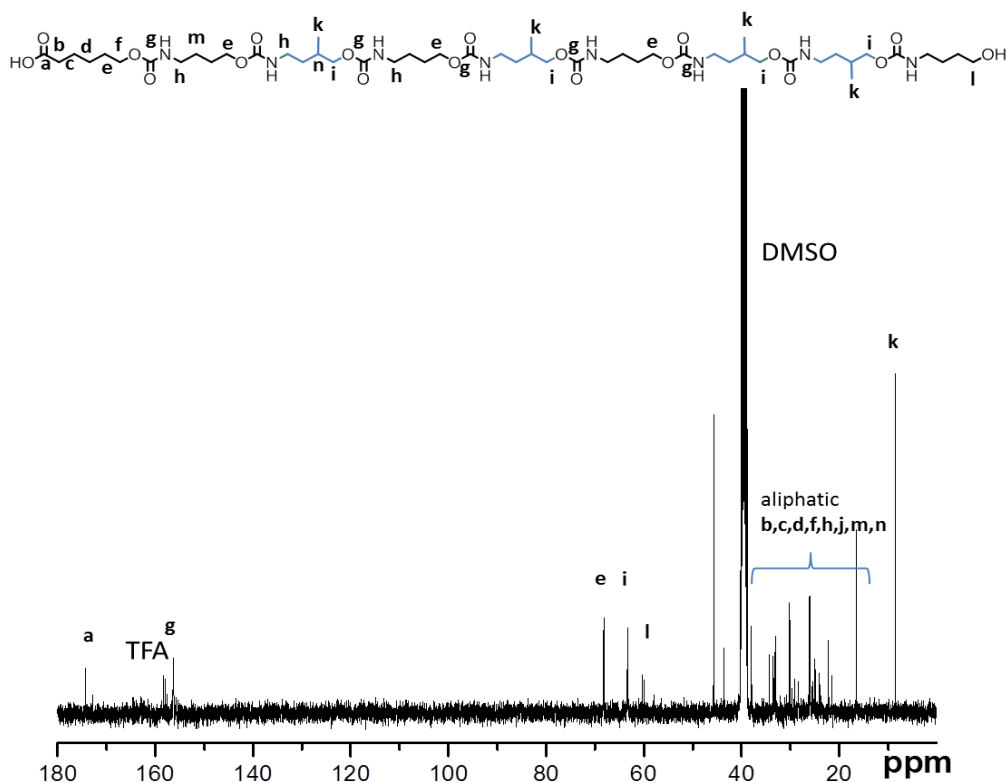
Figure IV. 2: ^{13}C-NMR in *d6*-DMSO for the oligourethane with monomer sequenceα- 0-1-0-1-0-1-1-0-ω(PU4)

-Size-Exclusion Chromatography (SEC). The oligo-urethanes were also analyzed by Size-Exclusion Chromatography performed in THF, in order to examine their molar mass distribution. The shortest sequences were dissolved very easily in THF and characterized by SEC, the longer needed ultra-sounds and temperature to be dissolved whereas the longest (more than 8 monomers on the sequence) were not any more able to be characterized by SEC since they were insoluble in THF. On **Figure IV.3** the SEC chromatogram of three oligomers of different length is depicted.
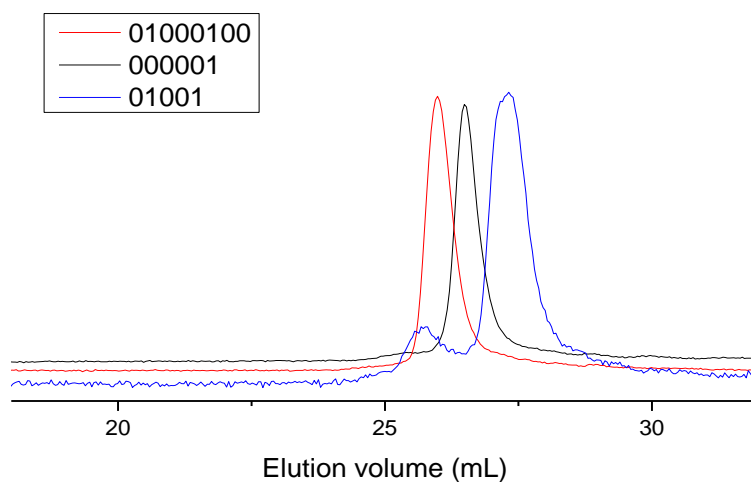
Figure IV. 3: SEC Chromatography for the nearly monodispersed oligo(urethane)s. Comparison of three samples of different length

110

From the above **Figure IV.3** it is possible to estimate the length of the sequences from their elution volume. The longer the sequence, the bigger their molecular weight is, the faster the molecules are eluted from the chromatographic columns. Consequently, the volume elution peaks from the right to the left represent the oligomers of increased molecular weight. The SEC chromatography gives also an estimation of the level of polymer dispersity. If the peak corresponds to a narrow and monomodal signal, then the sample is uniform without incomplete intermediate steps or other impurities (which should belong to a second peak of lower molecular weight).

2.2 Labeling

The labeling of the wood was performed by immersion. The procedure is based on the swelling of the wood under the appropriate conditions, which were investigated in this work. The maximum possible swelling would help the oligomer to penetrate the wood and once this is done, during the wood drying, the label would be trapped inside it. The procedure was the following: the small pieces of wood were immersed in the solution of the oligomer (0.2 w/v%). The samples were kept in the solution for 8 hours and then removed to let them dry and proceed with the MS analysis for the detection of the label. The taggant reading-out was performed following two possible approaches as depicted on the **Figure IV.4**. The first method was ESI-MS. After the extraction of the label from the wood, the extract solution was analyzed by ESI-MS and then by MS/MS. Alternatively, the detection of the label was also realized by DESI-MS and sequentially by MS/MS. DESI-MS was applied directly on the wood without need of label extraction.
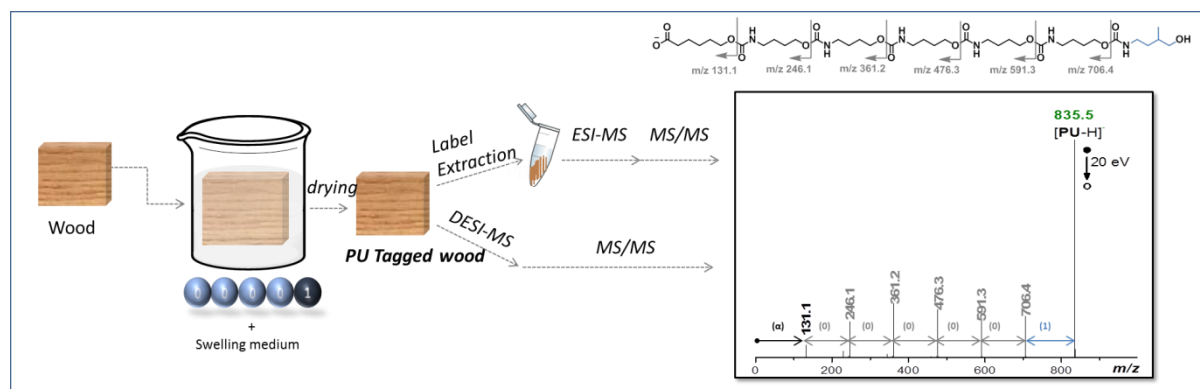
Figure IV. 4: Schematic representation of the labeling process of the wood. First step: immersion in oligourethane solution, second step: drying, Third Step: extract of label, Final Step: MS/MS analysis of tag solution

2.2.1   Selection of wood type

The swelling of wood measured by its external dimension changes depends on several parameters as mentioned. It has been reported in the literature that swelling varies with the wood species, structure and density. For instance, it was found that two hardwood species (sugar maple and aspen) exhibit greater maximum swelling ability compared to softwoods (spruce averaged from 6.5 to 7.3%,

Douglas fir from 7.3 to 9.3%, sugar maple varied from 10.0 to 12.0% and aspen from 9.1 to 10.0%). This is highly related to the higher density of hardwoods [268].

According to the literature and the preferences of wood species in commercial wooden products, three different wood species were chosen for this work. The selected species were of varying characteristics like their hardness (: Janka Hardness): walnut: 4.5kN, beech:5.8kN, oak:~ 6kN, and density: walnut:40-43 lb/ft^3, 650-700 kg/m^3, beech:32-56 lb/ft^3, 700-900kg/m^3, oak: 37-56lb/ft^3, 600-900 kg/m^3.

Figure IV. 5: Photo of the three wood species used in the wood labeling investigation

2.2.2   Selection of solvents

The dimensional changes in wood are owed to the swelling of the cells or of the fibers from which the wood is composed[269]. The swelling of wood both in water and in organic solvents has been investigated many years ago as it constitutes one of the fundamental experimental processes in wood industry including wood pulping, preservation, removal of extractives, dimensional stabilization and chemical modification. The successful wood swelling can also be affected by elevated temperatures[270] which was applied in the work (60ºC).

As it was showed in bibliography dimethyl sulfoxide (DMSO) is the best organic polar swelling solvent for wood, that means that in this solvent the wood takes the maximum dimensions increase but dimethylformamide (DMF) leads to a more rapid wood swell. DMF could be efficiently used with simple immersion whereas DMSO requires a vacuum impregnation process[271]. On the **Table IV.2** the data ,according to the literature, show the swelling difference depending on swelling medium and time parameter. DMF reaches 17% increase wood dimensions after swelling after the period of 6 hours whereas DMSO 4%.

Table IV. 2:Comparison of swelling solvents for beech-versus time in days

Wood	Solvent	Time (days)	Swelling (%)
	DMSO	1/4	~4
		6	22
beech	DMF	1/4	17
		6	20

So the solvent DMF was selected for the swelling of the wood as the most appropriate for the taggant penetration, since in industrial application the factor of time plays an important role. However, because of the high boiling point of DMF it is not easy to deal with it since the wood is not drying so easily. For this reason THF was also chosen for the labeling even if its swelling coefficient (7.2) is not as high as this of DMF (12.5), still this value is efficient for the desired swelling activity[272,273]. Tetrahydrofuran can help in the easy processing of wood labeling since its boiling point is much lower.

2.2.3   Solution concentration

Another parameter which was tested in terms of immersion was the solution concentration in oligourethane. So instead of using 0.2 w/v % solution for the immersion of wood, it was attempted to lower to the half, meaning 0.1 w/v %. (W4). As it was shown, the detection of the label was limited but still possible (data not shown). However, the more concentrated solution was used in the study to facilitate the results observation

To summarize, all the mentioned parameters which affect the swelling of wood were taken under account for our research in order to achieve the maximum possible anti-counterfeit label absorbance in the wood.

Table IV. 3: List of tagged wood. Decryption for each sample: label, solvent, immersion time and reading-out method used.

Sample	Label	Wood	Solvent	Detection	Time
W1	PU1	beech	THF	ESI-MS (layers)	8 hours
W2	PU2	beech	DMF	DESI-MS+ESI-MS	8 hours
W3	PU3	walnut	THF	ESI-MS (layers)	12 hours
W4	PU5	beech	THF	DESI-MS+ ESI-MS (layers)	8 hours
W5	PU5	walnut	DMF	desi+ ESI-MS (layers)	8 hours
W6	PU7	oak	THF	ESI-MS (layers)	8 hours

-ESI-MS Spectrometry. The barcode reading-out was achieved by two mass-spectrometry methods, the conventional ESI-MS and the DESI-MS. With the first approach the wood was sanded and the sawdust was immersed in a methanolic solution with ammonium acetate (3 mM). The solution of the

extracted tag was measured by electrospray MS and sequenced by MS/MS. On the **Figure IV.6** the entire procedure is depicted.
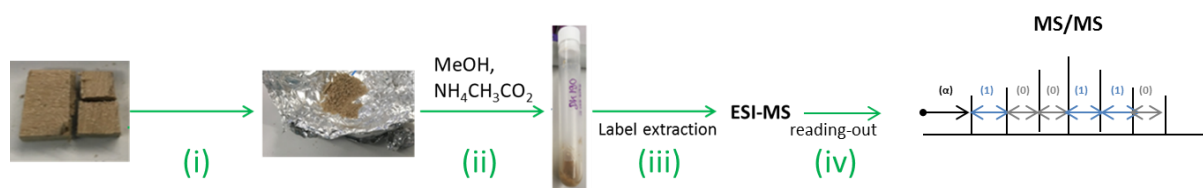
Figure IV. 6: Procedure of label extraction by i) sanding the wood, ii) added in methanolic solution of ammonium acetate (3mM) and iii) and through the centrifugation iii) the supernatant was isolated to be analyzed by ESI-MS for the label characterization

A piece of beech labeled by the PU2 with monomer sequence α-**000001**-ω and mass 836.5 Da was analyzed by ESI-MS (**Figure IV.7**). The wood was labeled by its immersion in the oligourethane's solution in DMF (0.2 w/v %). After wood drying for 24 hours, the entire piece was subjected to DESI-MS analysis for the label detection. The signal annotated in green corresponds to the PU ion was analyzed further by MS/MS (**Figure IV.8**)
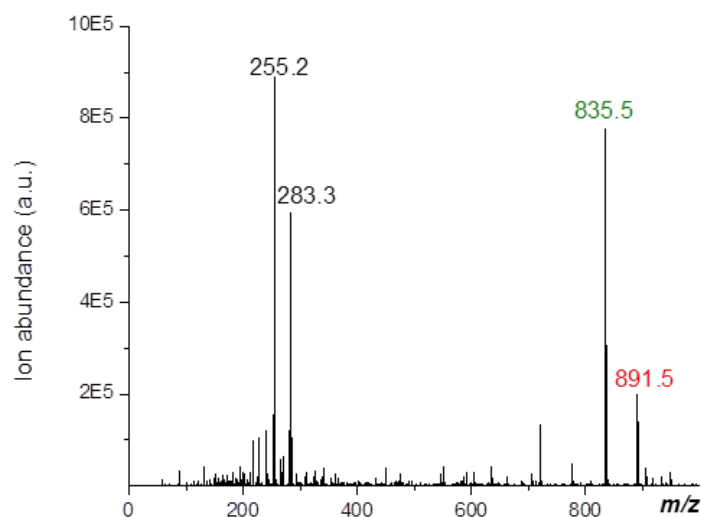
Figure IV. 7: Negative ion mode ESI mass spectrum of the sample W2, α-000001 oligourethane prepared by manual synthesis, and detected as a deprotonated molecule at *m/z* 835.5. This assignment was supported by accurate mass data recorded in the positive ion mode for the doubly protonated molecule ($C_{48}H_{90}N_8O_{19}2+$, *m/z*$_{th}$ 541.3156, *m/z*$_{exp}$ 541.3155). The peak annotated in red corresponds to the impurity with mass +56 Da heavier than the targeted oligomer. Peaks marked in black at *m/z* 255.2.6 and *m/z* 283.3are known peaks coming from background analysis.

Figure IV. 8: ESI-MS/MS of the *m/z* 835.5 precursor ion detected in the methanolic extract of a beech tagged with the α-000001 oligourethane.(W2)

Desorption Electrospray-MS Spectrometry. An alternative way was also applied without destroying the surface of the wood, the label could be identified with the Desorption Electrospray mass spectrometry. The piece of wood was placed on the DESI plate and sprayed by the solution 90% MeOH-ammonium acetate (3 mM)/10% THF. By analyzing the wood surface, the label was detected easily.

On the **Figure IV.9** it is depicted the method of label reading by DESI-MS carried out for the same sample analyzed on the **Figure IV.7** and **8** by ESI-MS and ESI-MS/MS.
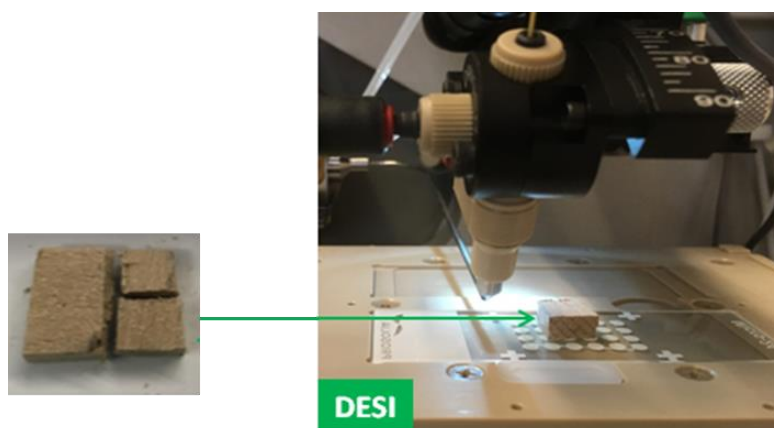
Figure IV. 9: DESI-MS analysis of the labeled beech with the sequence α-000001-ω

On the **Figure IV.10** it was shown that the detection of the PU ion is feasible by DESI-MS since the PU ion at *m/z* 835.5 is observed. Still the spectrum is a bit noisy coming from the matrix of the wood.

Nevertheless, the peak corresponding to the *m/z* of the targeted oligomer is distinct, concluding that the method is efficient enough to be used as a taggant reading out technique. A method which could be followed in order to identify the non-corresponding peaks and consequently make the detection of the label even easier is first to characterize by DESI-MS a non-tagged wood surface. As a result, all the mass peaks attributed to the unlabeled wood could be noted and the only difference comparing to the labeled wood would be the signal corresponding to the PU ion. **Figure IV.11** shows the sequencing of the coded-information of the PU2 used as a taggant in the sample.
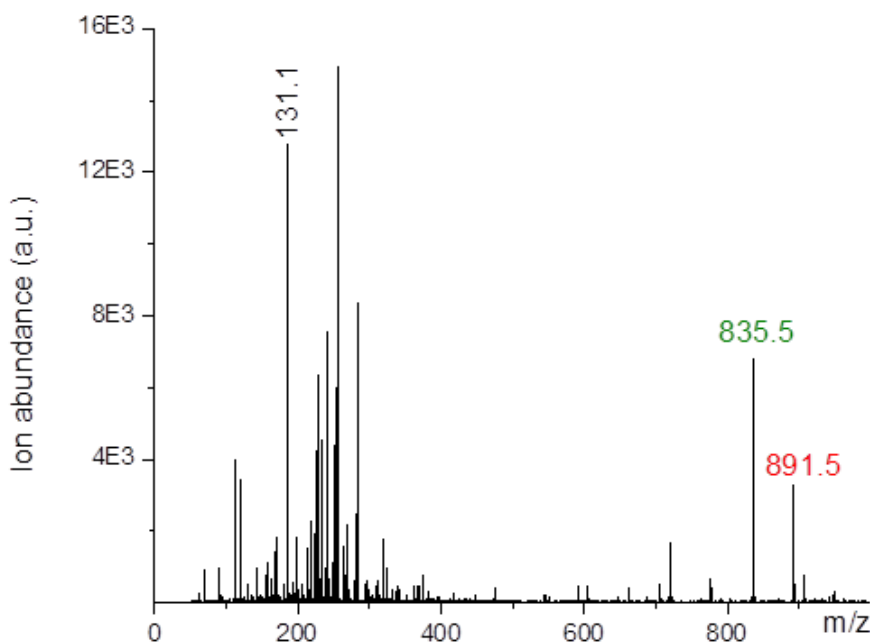
Figure IV. 10: Negative mode DESI-MS of the *m/z* 835.5 precursor ion detected on the surface of the beech tagged with the α-000001oligourethane (W2).
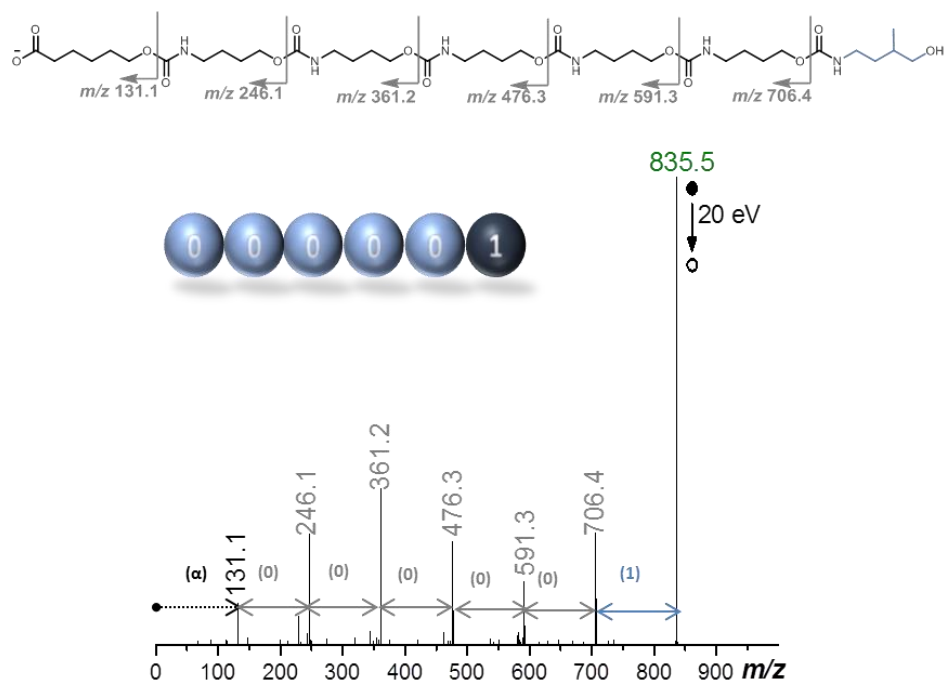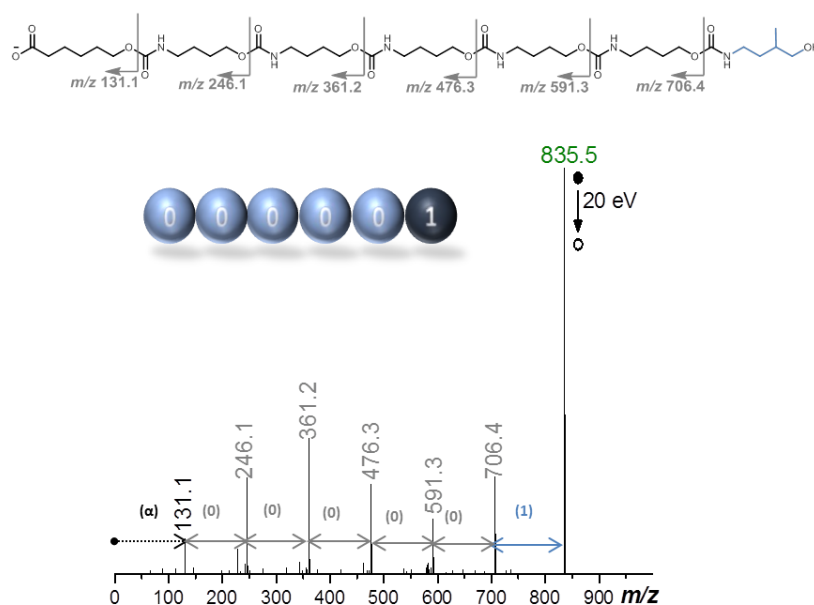

Figure IV. 11:DESI-MS/MS of the *m/z* 835.5 precursor ion detected in the methanolic extract of a beech tagged with the α-000001 oligourethane (W2).

Investigation of labeling depth. In order to investigate the degree of labeling, meaning if the label absorption is only superficial or deeper, a special analysis of the interior layers was performed. As it is shown on the **Figure IV.12** the wood with dimensions2cm x 2 cm x 0.5 cm in shape of cuboid, was subjected to a special procedure called milling. The exterior layer, Layer 0, of 1mm thickness was first put away. The following layers were all of the same thickness 0.375 mm and were named from the exterior to interior 1st, 2nd, 3rd, and 4th. These four layers were cut in this thickness in order to reach the middle of the piece (in thickness). The layers were not anymore in a planar surface form but in the form of wood pulp as depicted on the **Figure IV.13**
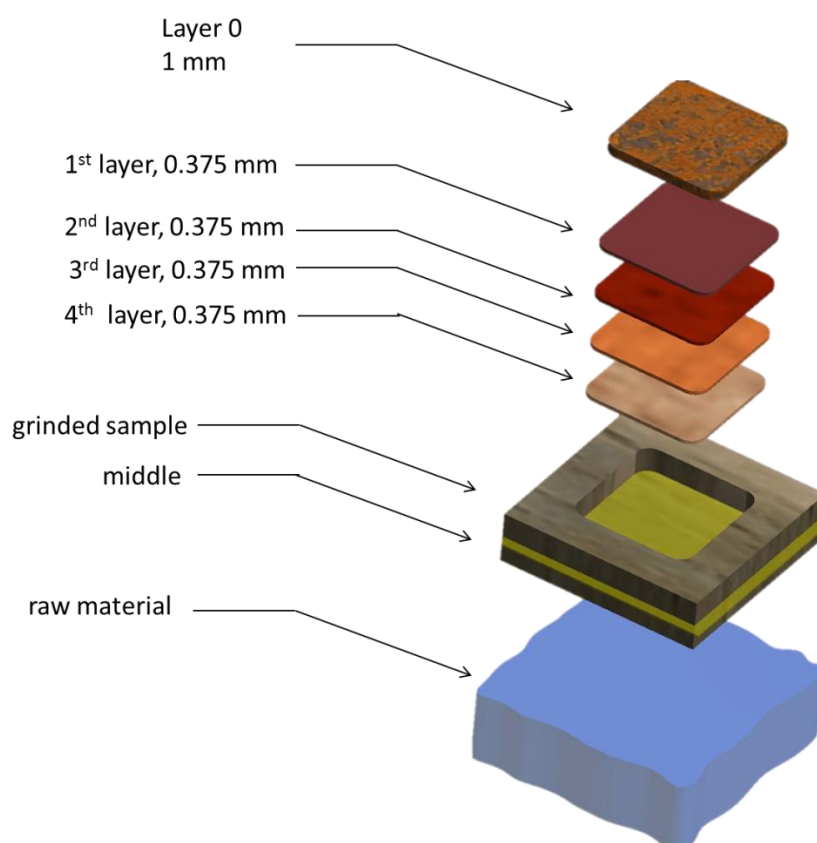
Figure IV. 12: 3D representation of the cutting procedure of a wooden piece with dimensions 2cm*2cm*0.5cm for the isolation of 4 inner layers for the labeling depth test

Each layer was treated afterwards a solution of methanol and ammonium acetate for the label extraction. The entire mixture was placed for 10 minutes in the ultra-sounds bath with the aim to extract the absorbed molecular tag. The supernatant solution was analyzed by ESI-MS for the detection of the label and by MS/MS sequencing for the decryption of the coded message.
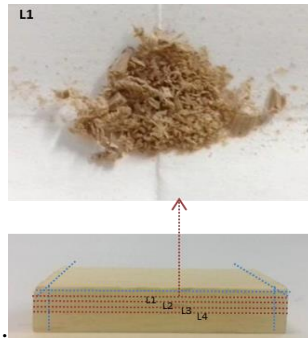
Figure IV. 13: Illustrates the walnut wood pulp corresponding to the layer 1 during the investigation of labeling depth.

The following figures correspond to the ESI-MS analysis of each layer, by naming layer 1 the upper layer to layer 4 the wood layer closer to the middle of the piece. The layers were labeled by the oligomer PU3 (α-**01000100**-ω, 1080.6 Da).
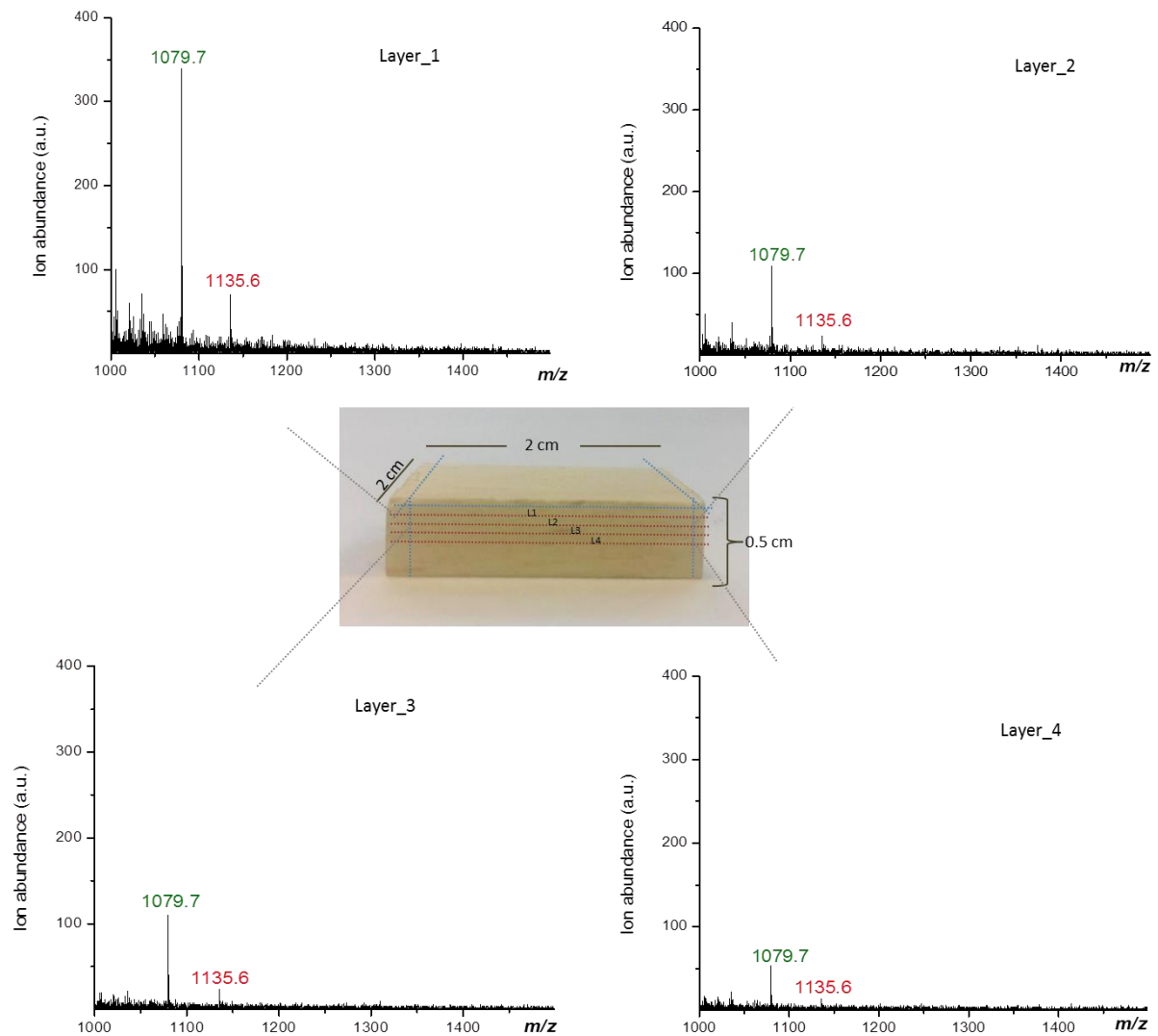
Figure IV. 14:Investigation of the labeling process on walnut. Isolation of four layers with different depth and analysis of the extract solutions by negative mode ESI-MS spectrometry (W3).

On the **Figures V.14,** the four layers of the treated piece of walnut are analyzed by negative mode ESI-MS and the extracted label is well detected in all of them with ion mass *m/z* 1079.6 (annotated in green) corresponding to the deprotonated marker. It is also visible that the mass peak annotated in red and corresponding to the Δ=+56 *m/z* of the oligomer is also present in the mass spectrum as part of the oligomer fingerprint.

It is obvious that even though the signal is losing its intensity moving to the deeper layers, it is still there, easily detectable and sequenced by tandem mass spectrometry. Fact that proves that the wood swells efficiently absorbing the PUs tag and capturing them while the wood dries. The **Figure IV.15** shows the tandem mass spectrometry that is applied on the desired oligomer mass peak to find the exact oligomer sequence through the generated fragment ions due to the increased collision energy. The selective fragmentation of the oligomers in negative mode on the position of C-O carbamate bond leads to easy to read MS/MS spectra. Indeed, the distance between the consecutives fragment ions is equal to the mass of a coded unit in combination with the fact that the two monomers have different masses; the attribution of the presence of a 0 or 1 monomer is very facile.
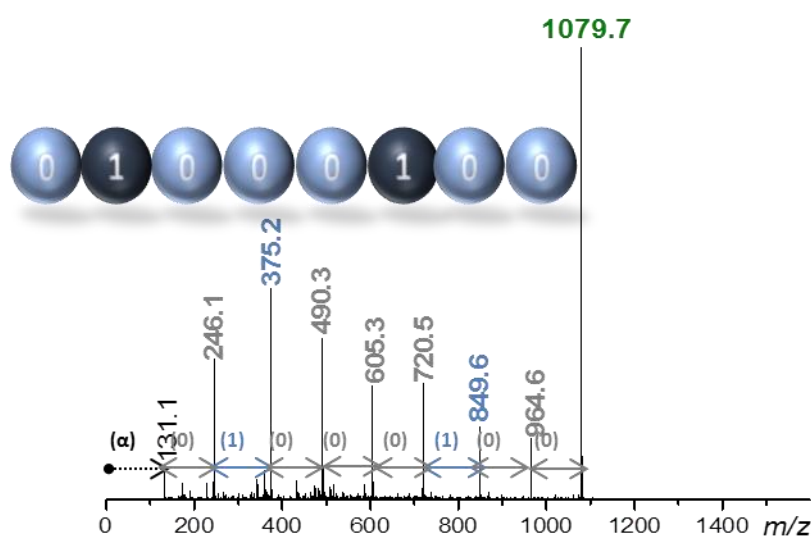
Figure IV. 15: ESI-MS/MS of the *m/z* 1079.9 precursor ion detected in the methanolic extract of a walnut tagged with the α-01000100 oligourethane.(extract of W3)

The same test was applied to all the three species of wood chosen for this work. The following **Figure IV.16** concerns the labeling of beech with oligourethane barcode of monomer sequence **α-01001-ω (PU1)** written on the C4 language. The immersion was realized in THF solution of the oligomer used in the same conditions as above. The results show the same positive conclusion that the label penetrated in the inner side of the wood as it was detected in all the four layers by ESI-MS.

Each oligomer signal detected by negative mode ESI-MS was further sequenced by MS/MS. In all the cases there was no problem in decoding the monomer sequence as it's shown on the **Figure IV.17.**
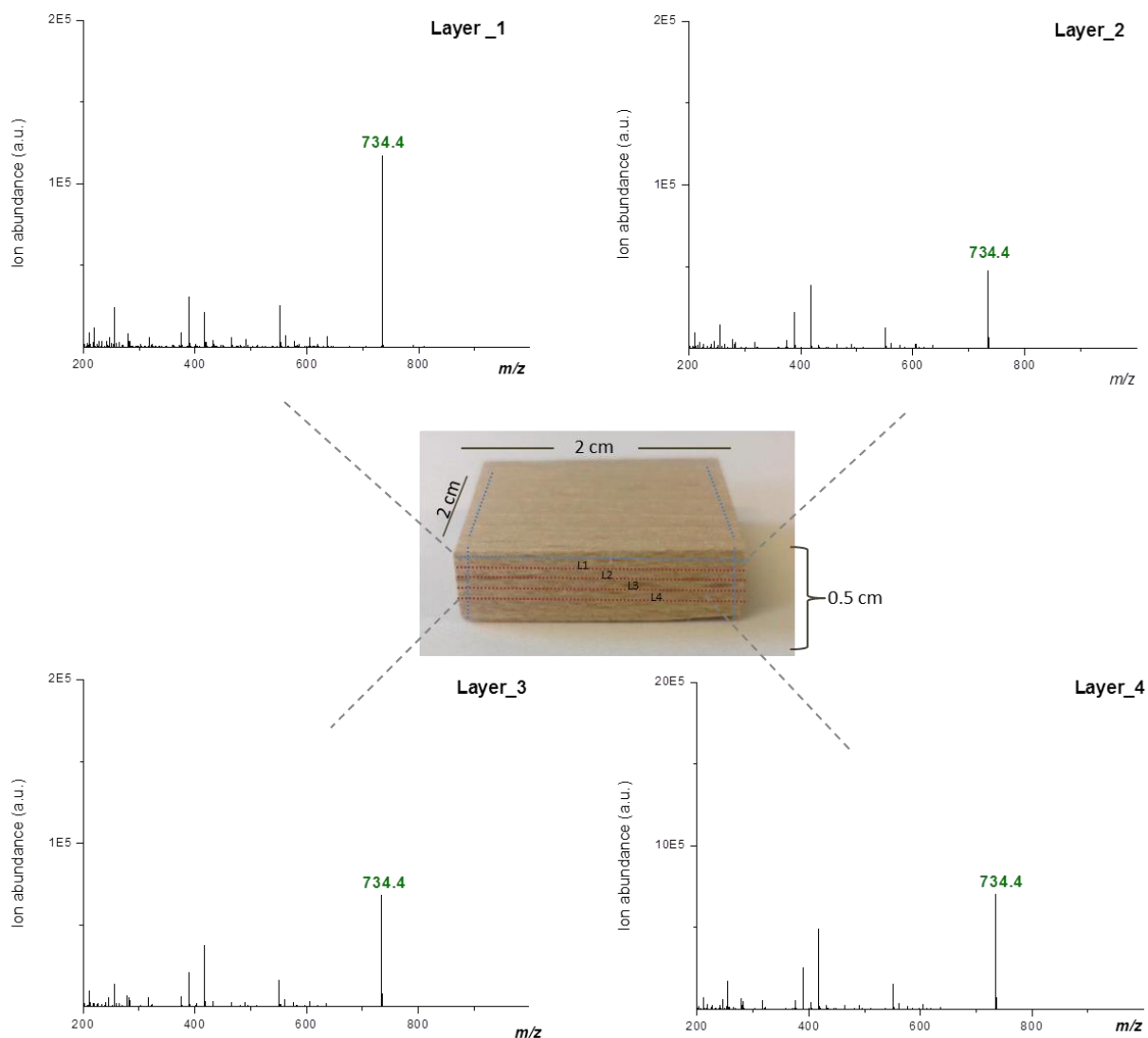
Figure IV. 16: Investigation of the labeling process on beech. Isolation of four layers with different depth and analysis of the extract solutions by negative mode ESI-MS spectrometry. (W1)
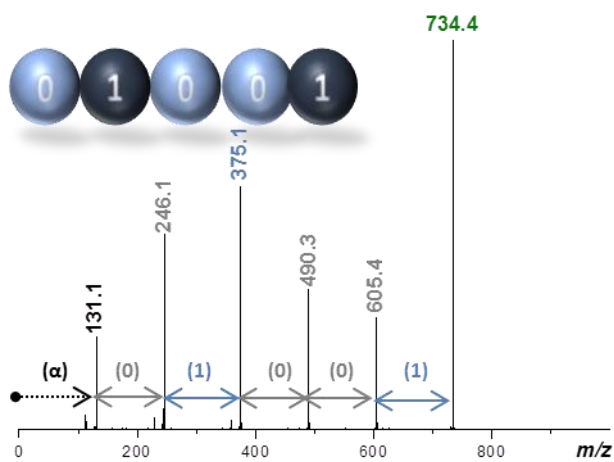
Figure IV. 17: Indicative ESI-MS/MS spectrum of the *m/z*734.4 ion of the extract of one of the beech layers. Meanwhile, the *m/z*734.4 ion of the extracts of all the layers was sequences (extract of W1).

In the last case of oak the oligourethane sequence **α-01000100-ω,**1080.8 Da, was dissolved in THF at the same concentrations as before. ESI mass spectra were recorded in negative ion mode for the four layers shown on the **Figure IV. 18**. The targeted deprotonated PU expected at *m/z* 1079.6 was only detected with very low abundance in the layers 3 and 4.
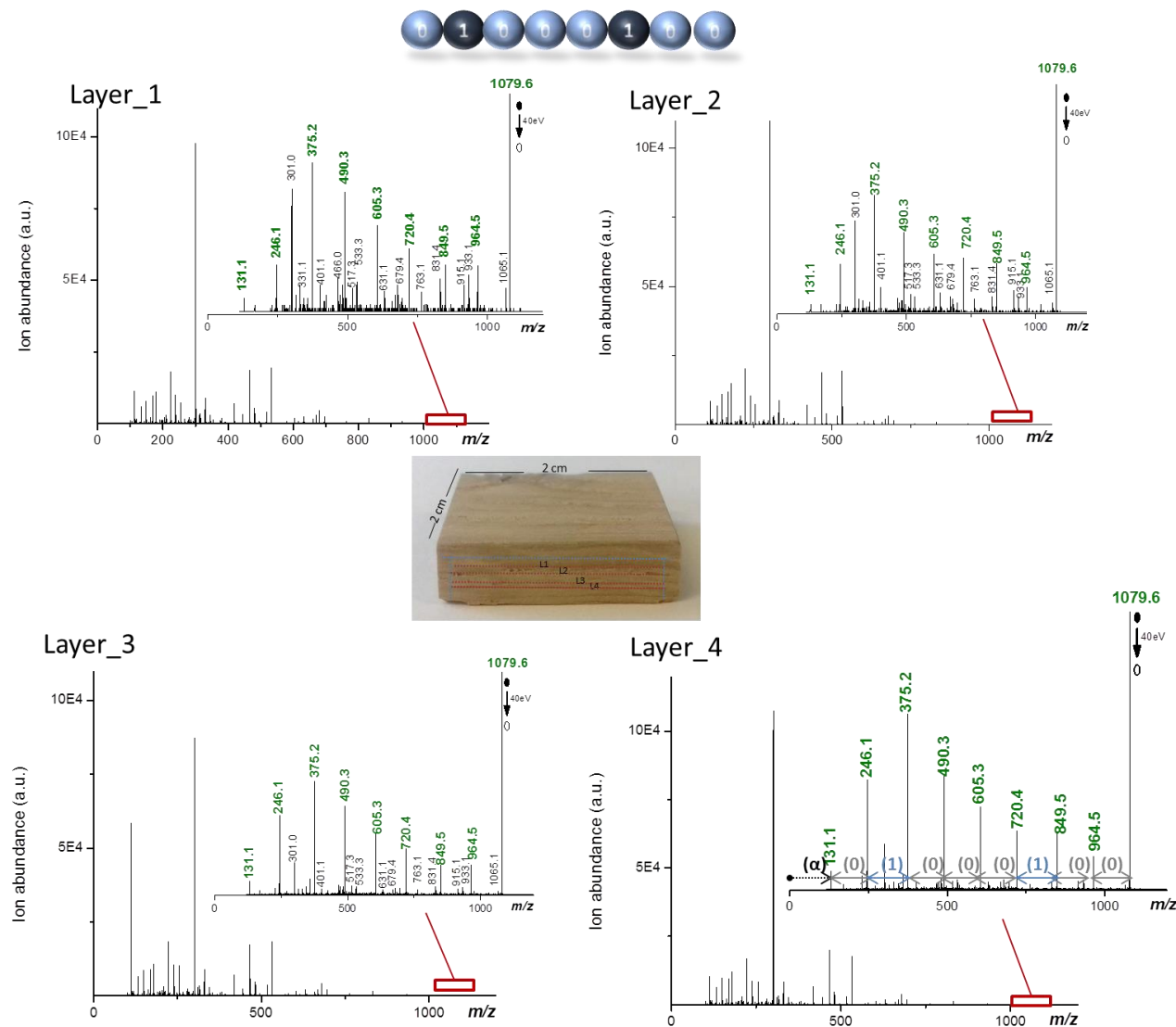
Figure IV. 18: Investigation of the labeling process on oak. ESI-MS analysis was applied in negative mode on the extract solutions of the different layers. Inset: ESI-MS/MS of the *m/z* 1079.6 ion in the extracts of the different labeled oak layers. Signals annotated in green correspond to the fragments expected for this α-01000100-ω PU. (W6)

The oligomer might not have been detected by ESI-MS, nevertheless; MS/MS analysis of *m/z* 1079.6 ion was performed for all the different grinded layers to confirm the results. Surprisingly, the desired deprotonated PU at *m/z* 1079.6 was clearly evidenced in all the samples, proved by the MS/MS spectra of the **Figure IV.18**. There, it's shown all the contained fragments of the sequence (peaks annotated in green).

From the **Figure IV.18** we could assume that the labeling of oak with anti-counterfeiting taggants seems less efficient than the labeling of walnut and beech. DMF (higher swelling coefficient) was used alternatively for the investigation of the depth layers in order to exclude that the problem origins from the solvent. Similar results were recorded. Potential explanation to this phenomenon is that oak is harder and denser wood comparing to the two other species, with higher activation energy[270,274]. This fact could explain that probably the used temperature of the impregnation procedure was inadequate to swell enough the wood piece in order to absorb the label of the solution. Another explanation could be that the quantity of the extractives (sugars) comparing to the two other wood (beech and walnut) was low, thus its swelling[270] was limited resulting in not-adequate absorption of label.

3. Conclusions

In summary, in this research chapter sequence-defined polyurethanes were used to label wood for protection against counterfeiting. The molecular taggant was able to tag the surface of the wood piece as it was proved by its detection via DESI-mass spectrometry. The absorption of the anti-counterfeiting label from the entire wood mass was also examined. By cutting the wood in different depth layers it was evidenced by MS that the taggant was also diffused in the inner part of the wood complying with the demands of a secure anti-counterfeiting labeling. Overall, the wood labeling by sequence-defined PUs taggant was proved to be one more very interesting application, related to a new material which is threatened and highly used in furniture, musical instruments, floor carpet, in wooden canvas and in the frames of high value paintings.

Chapter V:

2D sequence-coded oligo-urethane barcodes for plastic materials labeling.

Denise Karamessini, Salomé Poyer, Laurence Charles, and Jean-François Lutz**

1. Introduction

Among the potential applications of sequence-controlled polymers,[12] it has been suggested that anti-counterfeiting technologies could be an interesting area of use.[32] Indeed, a macromolecule containing a perfectly defined sequence of monomers can potentially be used as a label or "barcode",[275] in which molecular information certifying authenticity can be included. For instance, DNA, which contains a defined sequence of nucleotides, is sold by several companies as an anti-counterfeiting solution for the labeling of high-value materials. Since DNA strands can be selectively hybridized and amplified by polymerase chain reaction, DNA tags can be used in trace amounts for materials labeling. However, DNA is not stable in all conditions and may degrade during materials processing, e.g. in hot-melt extrusion, thermoset curing, photo-curing, 3D printing or sol-gel process. Thus, for many applications, DNA barcodes have to be encapsulated, for example in processable nanoparticles as developed by Grass and coworkers.[3,276] Alternatively, non-natural sequence-defined polymers may also be used as anti-counterfeiting barcodes.[32] Over the last years, we[30,32,35,71,72,277] and others[33,105,214,278] have demonstrated that a wide variety of uniform sequence-defined synthetic macromolecules can be synthesized using multi-step growth approaches.[62] In particular, our group has evidenced that such polymers can be used to store information. For instance, binary information can be easily written in synthetic sequence-defined macromolecules using two monomers that are defined as 0 and 1-bits. In addition, the digital sequences can be easily read using a sequencing methodology[13] such as tandem mass spectrometry (MS/MS).[29,130,151]

Among all the different types of digital polymers that have been reported by our group, sequence-coded oligourethanes (or oligocarbamates) appear as a very interesting class of polymers for anti-counterfeiting technologies. Uniform sequence-defined oligocarbamates can be synthesized using a variety of solid-phase iterative approaches.[33,246,248,279] In a publication reported last year,[39] our group has shown that digital oligourethanes can be synthesized using a simple protecting-group-free iterative approach.[223] Furthermore, it was found in this study that the COOH-terminated oligomers prepared via this orthogonal approach are particularly easy to decode by negative-mode MS/MS sequencing.[39] In other words, sequence-defined oligourethanes can easily be both coded and decoded. Furthermore, classical polyurethanes constitute a well-known class of plastics with widely-described physico-chemical properties, including for example chemical resistance and thermal stability. Therefore, sequence-coded oligourethanes appear as ideal candidates for materials labeling. For instance, we have already demonstrated that oligourethane barcodes can be included in small amounts (typically less than a weight percent) in casted polystyrene films,[39] 3D-printed photo-cured methacrylate resins[39] and acrylate-based intraocular implants[241]. In all cases, it was also demonstrated that the barcodes can be selectively extracted from the host polymer materials and sequenced by MS/MS. Yet, in all these examples, the information sequence was included in a single oligomer chain

(i.e. 1D-coding). In another recent study, our group has shown that information can also be written in a set of oligomers of different mass (i.e. 2D-coding).[210] In such a strategy, digital information is stored in a library of chains. The electrospray mass spectrometry (ESI-MS) analysis of these mixtures leads to an intentionally-polydisperse spectrum (i.e. first dimension fingerprint) and the MS/MS sequencing of each individual peak of this mass distribution gives access to the sequence-information included in each oligomer (i.e. second dimension fingerprint). This concept is powerful because *(i)* it does not require the synthesis of long coded oligomers and *(ii)* it gives access to an increased security level for anti-counterfeiting applications, as compared to standard 1D barcodes. However, this interesting 2D approach was not tested so far for materials labeling, mostly because the reported proof-of-concept was obtained with sequence-coded oligo(alkoxyamine amide)s,[210] which are thermolabile and thus very fragile oligomers.[32] Hence, in the present work, the 2D-coding strategy was applied to sequence-defined oligourethanes and tested for the labelling of different commodity plastics such as polystyrene (PS), polyvinylchloride (PVC) and polyethylene terephthalate (PET).

2. Results and Discussion

Two libraries of sequence-coded oligourethanes were used as 2D barcodes for the labelling of thin plastics films (**Figure V. 1**). Each oligomer was prepared via a solid-phase orthogonal iterative process, as described in an earlier publication.[39] In this approach, two monomers are used as a binary alphabet. In the formed oligourethanes, a 1-bit corresponds to a methylated synthon, whereas a 0-bit corresponds to its non-methylated analogue (**Figure V. 1**).

Combining this 14 Da mass difference with the specific dissociation pattern of sequence-defined oligourethanes in the negative ion mode, the nature of these synthons as well as their respective locations along these oligomeric chains can readily be distinguished in MS/MS sequencing, as reported earlier.[39] In the present work, the model digital sequence 01000001 01000010 was encoded in oligurethanes. In order to show the versatility of the 2D barcoding concept, this sequence was written in two different libraries, containing either three of four components, as shown in **Figure V.1**. The four components library contained the oligomers **P1**-**P4** (**Figure V. 1** and **Table V. 1**), with sequence α-01, α-000, α-0010 and α-1000010, to be combined from the smallest to the largest one in order to compose the model digital sequence.[210]

Coded library 1:

(P1) α- 0 - 1

(P2) α- 0 - 0 - 0

(P3) α- 0 - 0 - 1 - 0

(P4) α- 1 - 0 - 0 - 0 - 0 - 1 - 0

Coded library 2:

(P1) α- 0 - 1

(P5) α- 0 - 0 - 0 - 0 - 0 - 1

(P6) α- 0 - 1 - 0 - 0 - 0 - 0 - 1 - 0

α

Coded sequence
R = H (0), R = CH$_3$ (1)

Bit 0 =

115.1 Da

Bit 1 =

129.1 Da
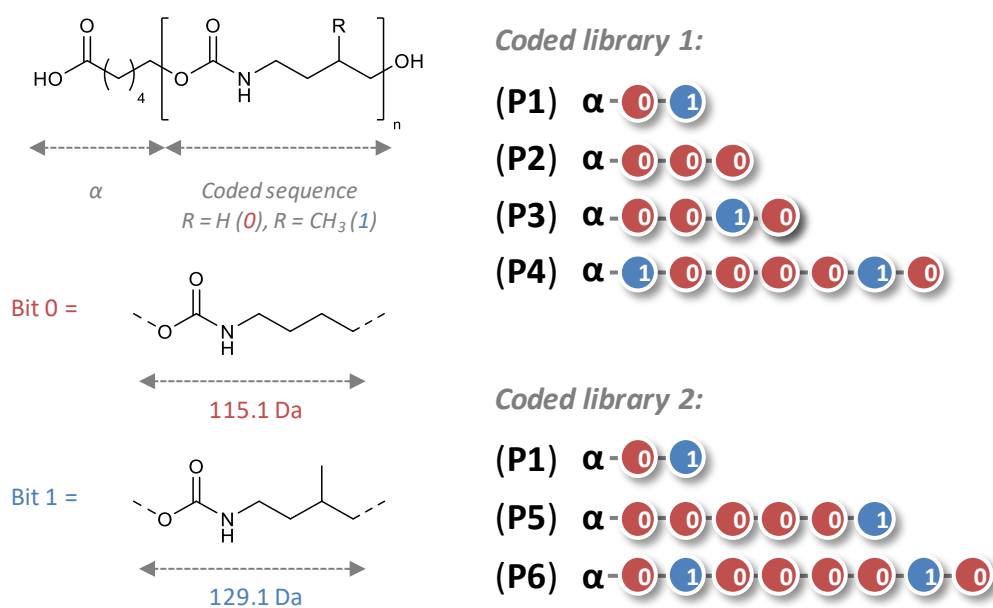
Figure V. 1: Alternatively, but using the same writing rules,[210] this sequence was generated with oligomers from the three components library, namely P1, P5 and P6 (Figure 1 and Table 1), with sequence α-01, α-000001 and α-01000010, respectively. In all oligomers, the prefix α in these sequences denotes a short spacer obtained after resin cleavage, as defined in previous works.[39,241]

Table V. 1: HR-MS characterization of the sequence-coded oligourethanes.[a]

	Sequence	Theoretical mass m/z_{th}	Experimental Mass m/z_{exp}	Yields (%)
P1	α-0-1	377.2282	377.2287[b]	89
P2	α-0-0-0	478.2759	478.2768[b]	96
P3	α-0-0-1-0	607.3549	607.3563[b]	66
P4	α-1-0-0-0-0-1-0	966.5605	966.5612[b]	53
P5	α-0-0-0-0-0-1	854.5081	854.5091[c]	96
P6	α-0-1-0-0-0-0-1-0	1098.6504	1098.6530[c]	68

[a]All accurate mass measurements were performed in positive mode ESI-MS, for either b [M+H]+ or c[M+NH4]+.

All the oligomers composing these libraries were first individually analyzed by electrospray ionization high resolution mass spectrometry (ESI- HRMS). In all cases, the main signal could be assigned to the desired oligomer based on elemental composition derived from accurate measurements performed in the positive ion mode (**Table V.1**). Moreover, all samples were highly

monodisperse, although some impurities were sometimes detected as shown by mass spectra recorded in the negative ion mode (**Figures S13-S18**). Furthermore, the monomer sequence of each digital oligourethane was confirmed by negative mode ESI-MS/MS (**Figures S19-S24**).

As mentioned in the introduction, three model commodity polymers were tested as host-matrices for the 2D-coded oligourethane libraries, namely polystyrene, poly(vinyl chloride) and polyethylene terephthalate. In order to show the versatility of the 2D-barcoding concept, both the three-component and the four-component oligourethane libraries were tested for labelling these three different polymers (i.e. six different samples were studied). For optimal anti-counterfeiting and traceability applications, the amount of barcodes that is included inside a product shall be as low as possible in order to not alter the physico-chemical properties of the host materials and to not be too easily spotted by potential infringers. Still, the embedded amount of the molecular barcode shall be sufficiently high to allow its extraction from the host matrix and its analytical detection. Following these prerequisites, the global oligourethane content was kept below 1 wt% in all studied films (i.e. 0.6-0.7 wt% for the three-component library and 0.7-0.9 wt% for the four component library). The sequence-coded libraries were incorporated in the polymer matrices using a simple solvent casting procedure. Typically, the host matrix and the oligourethanes constituting the chosen coded library were dissolved in a common good solvent (i.e. tetrahydrofuran for PS and PVC, phenol for PET) and mixed together. In most cases, it was necessary to heat the solutions in order to obtain a good dissolution of the oligourethanes, and eventually of the host matrix (e.g. for PET in phenol). The solutions were then poured into glass plates and the solvents were evaporated to form homogeneous thin films. For PS and PVC, evaporation was performed at room temperature, whereas heating was necessary to form the PET films. It shall be noted that these mild thermal treatments (i.e. in the 50-90°C range) are not leading to noticeable oligourethane degradation. Indeed, as demonstrated in an earlier work,[39] the thermal decomposition of sequence-coded oligourethanes starts to occur around 150°C. In all cases, dried polymer films - transparent for PS and PVC and white for PET - were easily obtained via this solvent casting procedure.

The formed films were then analyzed in order to verify the presence and the readability of the 2D barcodes within the host matrices. First, it was important to verify that the oligourethanes were homogeneously dispersed within the films. Taking into account the very low weight fraction and the very short chain-length of the oligourethanes that were embedded in the host matrices, phase segregation shall not occur within the films. Nevertheless, homogeneity was verified using a simple qualitative ^{1}H NMR analysis. For this, small pieces of the films were cut at different locations and placed in a deuterated solvent. It shall be noted that the chosen deuterated solvent shall not necessarily fully solubilize the host films but shall solubilize the oligourethanes. The PET and PVC membranes were studied in DMSO-d_6, whereas the PS membrane was studied in THF-d_6.For all types of host matrices, the NMR spectra indicated the presence of the oligourethanes in all studied regions of the

films, thus ruling out the possibility of an inhomogeneous distribution(Figures S25-S27).More importantly, the possibility to extract the 2D-oligourethane mixtures from the films was studied. To do so, all films were incubated in a methanolic solution of ammonium acetate (3 mM) for 10 min. Methanol is a non-solvent for PS, PVC and PET but it partially solubilizes oligourethanes at room temperature. Composition of this incubation solution allows optimal ionization of oligourethanes in the negative ion mode and was hence specifically selected to enable direct injection of extracts in the ESI source with no prior dilution. Figure 2 shows the MS spectrum that was obtained for the PET membrane labeled with the three-component oligourethanes library. It appears clearly that the three oligomers **P1**, **P5** and **P6** of the library can be clearly identified as deprotonated species [M-H]$^-$ at m/z values of 375.2, 835.5 and 1079.6, respectively. Due to their intentional mass differences, these three oligomers lead to a detectable first-dimension fingerprint in MS[210]. Furthermore, each peak of this mass distribution can be individually sequenced by MS/MS. Figure 2a-c shows the MS/MS spectra that were obtained for the three oligomers. Their digital sequence can be very easily deciphered, showing that neither solvent casting nor matrix-storage affected their structural integrity. In the present case, the model protection sequence 01000001 01000010 was unequivocally found, as evidenced in **Figure V. 2.**
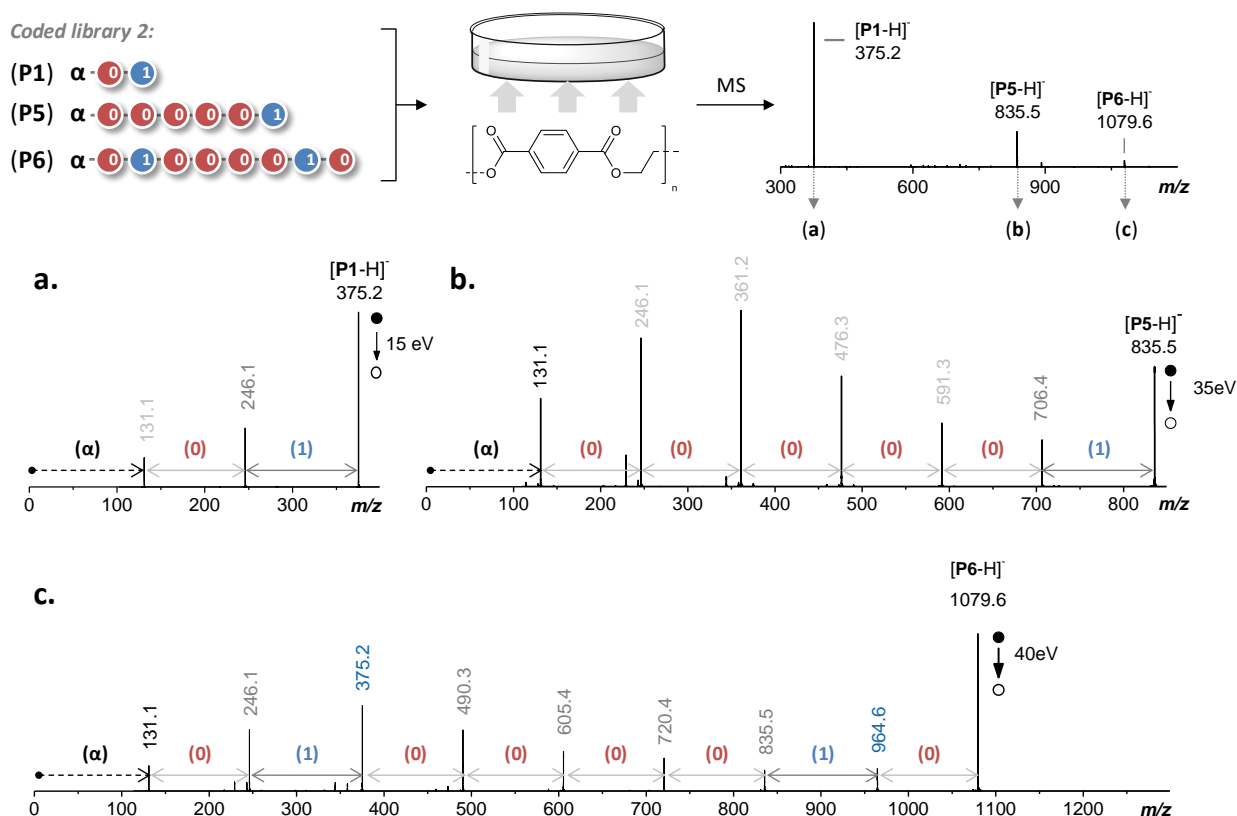
Figure V. 2: Mass spectrometry analysis of a PET membrane labeled with the three-component oligourethanes library. The three oligomers were first included in a PET film through a solvent casting procedure. Through selective methanol extraction, the oligomer mixture was extracted from the film and analyzed by ESI-MR (top left). All oligomers are detected in this spectrum and can therefore be individually

Comparable results were obtained for all types of films and all coded libraries (**Fig. V. 3-V. 7**)

Figure V. 3: Mass spectrometry analysis of a PET membrane labeled with the four-component oligourethanes library. a) ESI-MS of the extract, showing signals (in green) expected for deprotonated P1 (*m/z* 375.2), P2 (*m/z* 476.3), P3 (*m/z* 605.3) and P4 (*m/z* 964.5). Peaks annotated in black correspond to impurities previously detected in some oligomer samples. ESI-MS/MS sequencing of b) [P1 − H]⁻ at *m/z* 375.2 (E_coll: 15 eV), c) [P2 − H]⁻ at *m/z* 476.3 (E_coll: 20 eV), d) [P3 − H]⁻ at *m/z* 605.3 (E_coll: 25 eV), and e) [P4 − H]⁻ at *m/z* 964.5 (E_coll: 40 eV) after solvent extraction from the PET film. The *m/z* 283.3 fragment (italicized value) in b), which cannot be generated from an oligourethane typically reveals an interfering *m/z* 375.2 precursor ion. Non-labeled peaks in MS/MS spectra correspond to secondary fragments.

Figure V. 4: Mass spectrometry analysis of a PS membrane labeled with the four-component oligourethanes library. a) ESI-MS of the extract, showing signals (in green) expected for deprotonated P1 (*m/z* 375.2), P2 (*m/z* 476.3), P3 (*m/z* 605.3) and P4 (*m/z* 964.5). Peaks annotated in black correspond to impurities previously detected in one or the other oligomer samples. ESI-MS/MS sequencing of b) [P1 − H]$^-$ at *m/z* 375.2 (E$_{coll}$: 15 eV), c) [P2 − H]$^-$ at *m/z* 476.3 (E$_{coll}$: 20 eV), d) [P3 − H]$^-$ at *m/z* 605.3 (E$_{coll}$: 25 eV), and e) [P4 − H]$^-$ at *m/z* 964.5 (E$_{coll}$: 40 eV) after solvent extraction from the PET film. In b), the *m/z* 260.1 fragment (in red) measured at a 115.1 *m/z* distance from the *m/z* 375.2 precursor ion could indicate the alternative 10 sequence for P1. However, this assumption could readily be rejected owing to the relative abundance of this *m/z* 260.1 ion. Instead, it reveals the presence of a 10 oligourethane impurity present as traces in P4 (see Figure S16). Similarly, the *m/z* 260.1 and *m/z* 375.2 fragments (in red) in d) reveal the presence of a 1000 oligourethane impurity present as traces in P4 (see Figure S4) but, since their relative abundance is not consistent with that of other fragments, their presence does not invalidate identification of P3. Non-labeled peaks in MS/MS spectra correspond to secondary fragments.
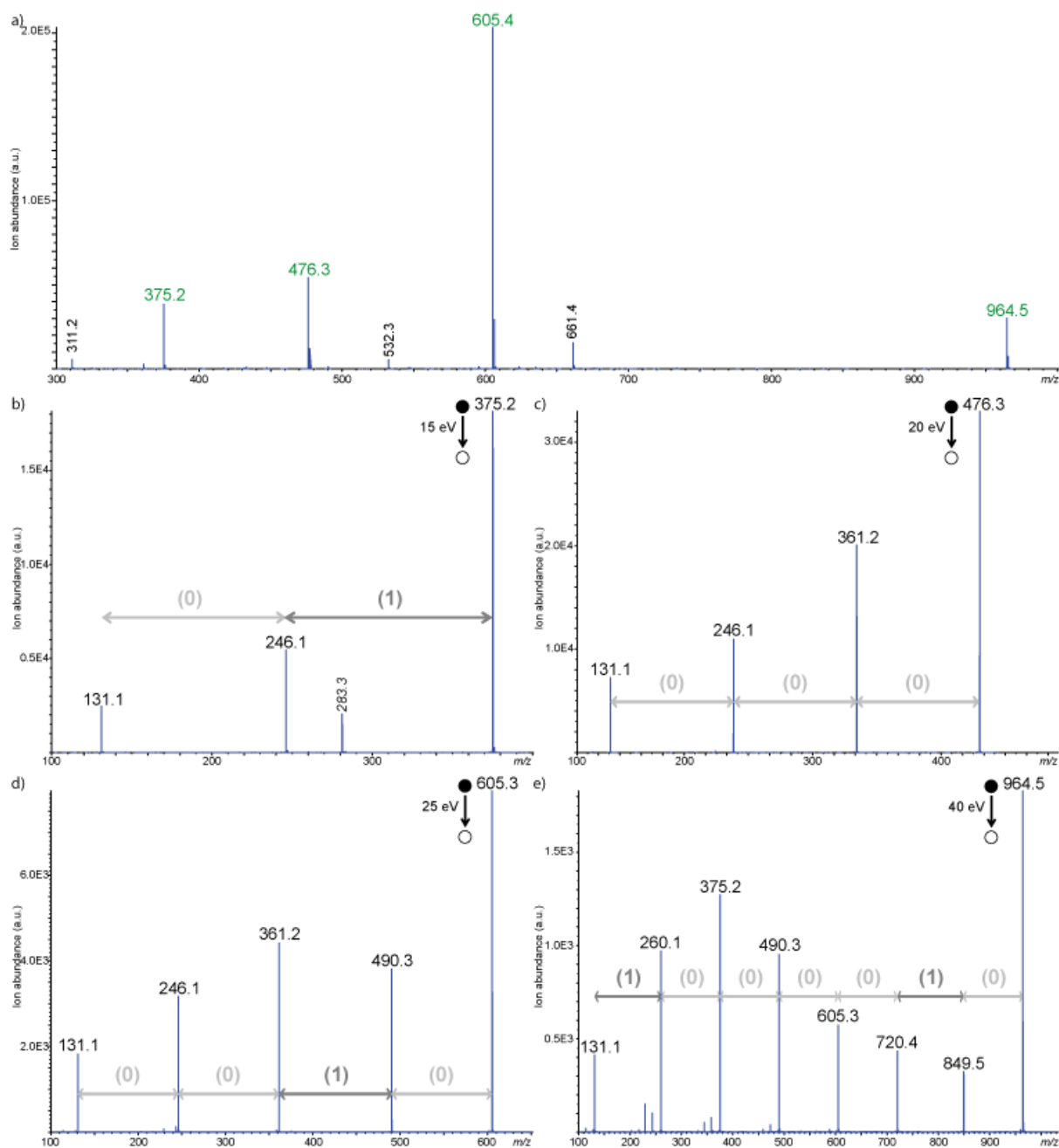
Figure V. 5: Mass spectrometry analysis of a PS membrane labeled with the three-component oligourethanes library. a) ESI-MS of the extract, showing signals (in green) expected for deprotonated P1 (*m/z* 375.2), P5 (*m/z* 835.5), and P6 (*m/z* 1079.6). Peaks annotated in black correspond to impurities previously detected in one or the other oligomer samples. ESI-MS/MS sequencing of **b)** [P1 − H]⁻ at *m/z* 375.2 (E_{coll}: 15 eV), **c)** [P5 − H]⁻ at *m/z* 835.5 (E_{coll}: 30 eV), and **d)** [P6 − H]⁻ at *m/z* 1079.6 (E_{coll}: 40 eV), after solvent extraction from the PS film. The *m/z* 283.3 fragment (italicized value) in b), which cannot be generated from an oligourethane, typically reveals an interfering *m/z* 375.2 precursor ion. Non-labeled peaks in MS/MS spectra correspond to secondary fragments.
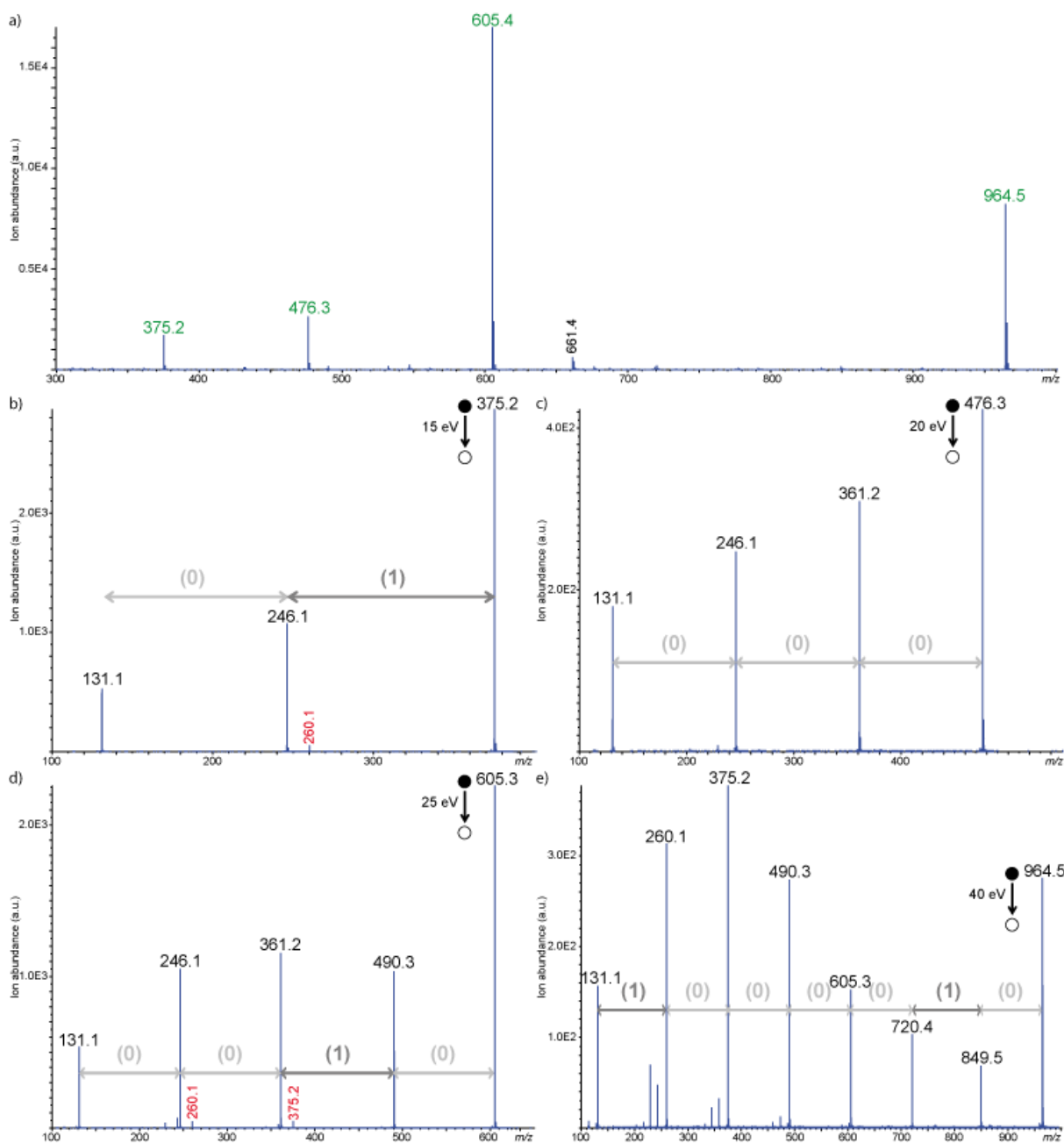
Figure V. 6: Mass spectrometry analysis of a PVC membrane labeled with the three-component oligourethanes library. a) ESI-MS of the extract, showing signals (in green) expected for deprotonated P1 (*m/z* 375.2), P5 (*m/z* 835.5), and P6 (*m/z* 1079.6). Peaks annotated in brown correspond to impurities extracted from the PVC membrane (see Figure S21). ESI-MS/MS sequencing of **b)** [P1 − H]⁻ at *m/z* 375.2 (E_{coll}: 15 eV), **c)** [P5 − H]⁻ at *m/z* 835.5 (E_{coll}: 30 eV), and **d)** [P6 − H]⁻ at *m/z* 1079.6 (E_{coll}: 40 eV), after solvent extraction from the PVC film. Fragments at *m/z* 217.0, *m/z* 283.3, and *m/z* 315.1 (italicized values) in b), which cannot be generated from an oligourethane, typically reveal an interfering *m/z* 375.2 precursor ion. Non-labeled peaks in MS/MS spectra correspond to secondary fragments.
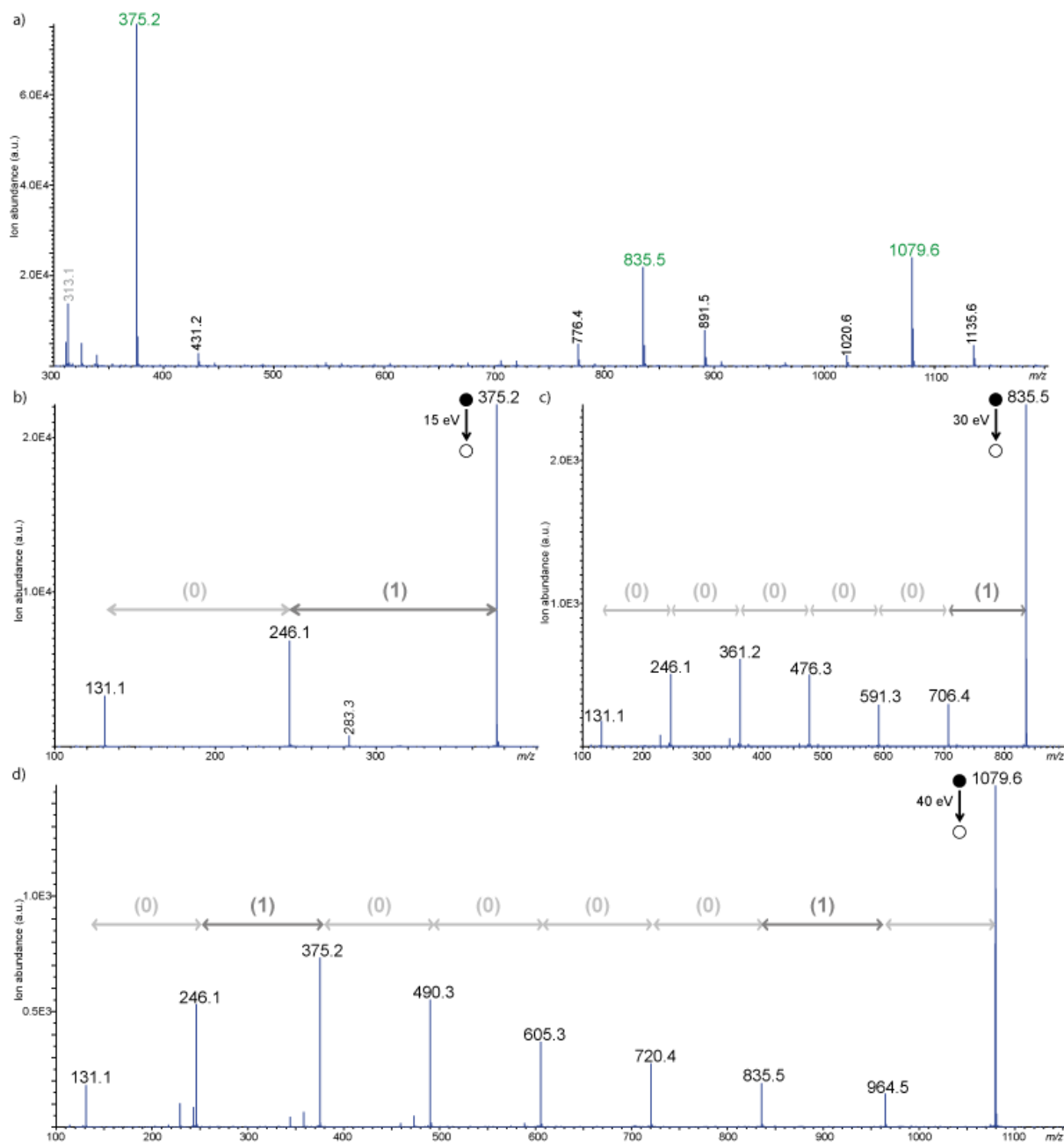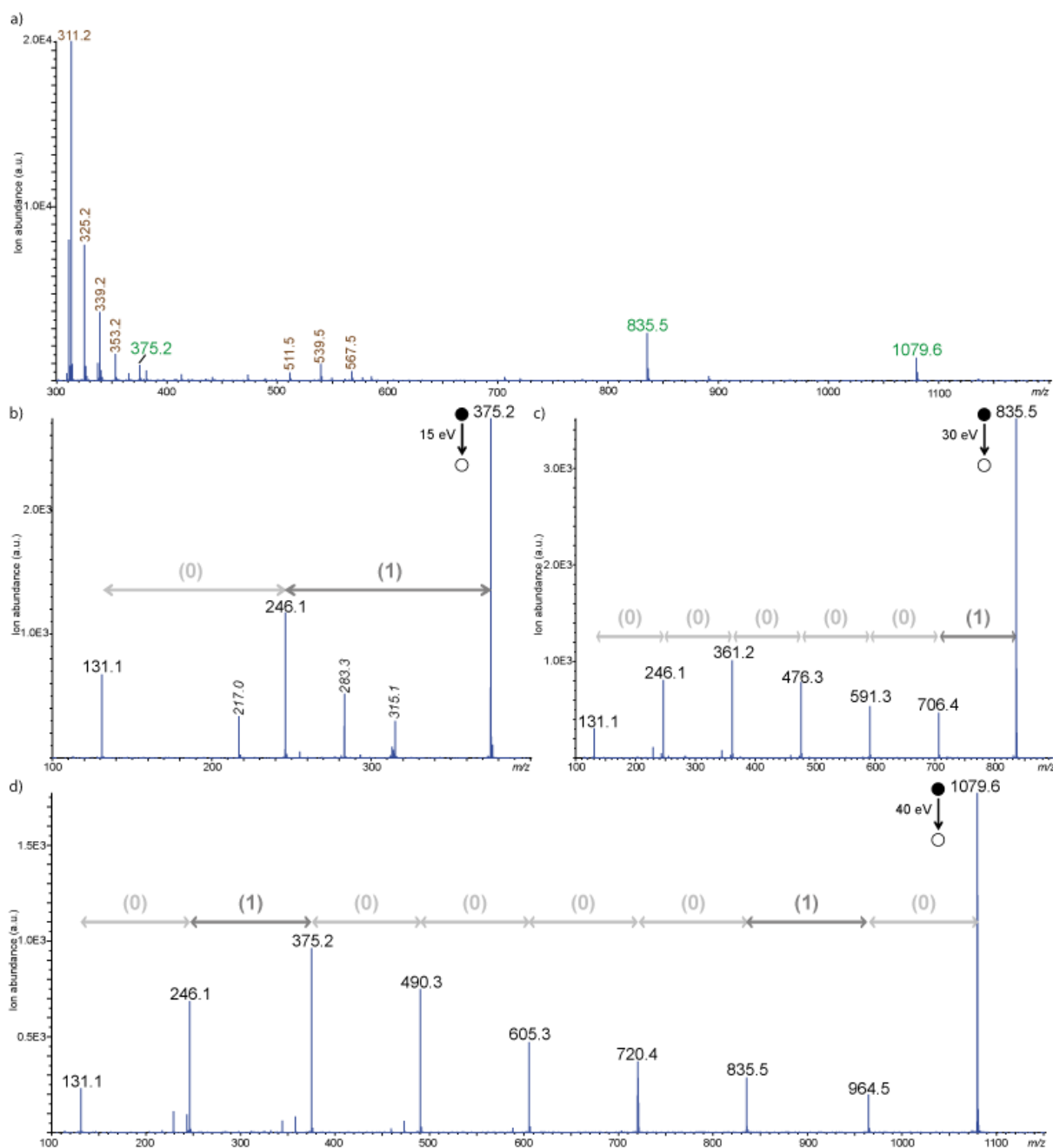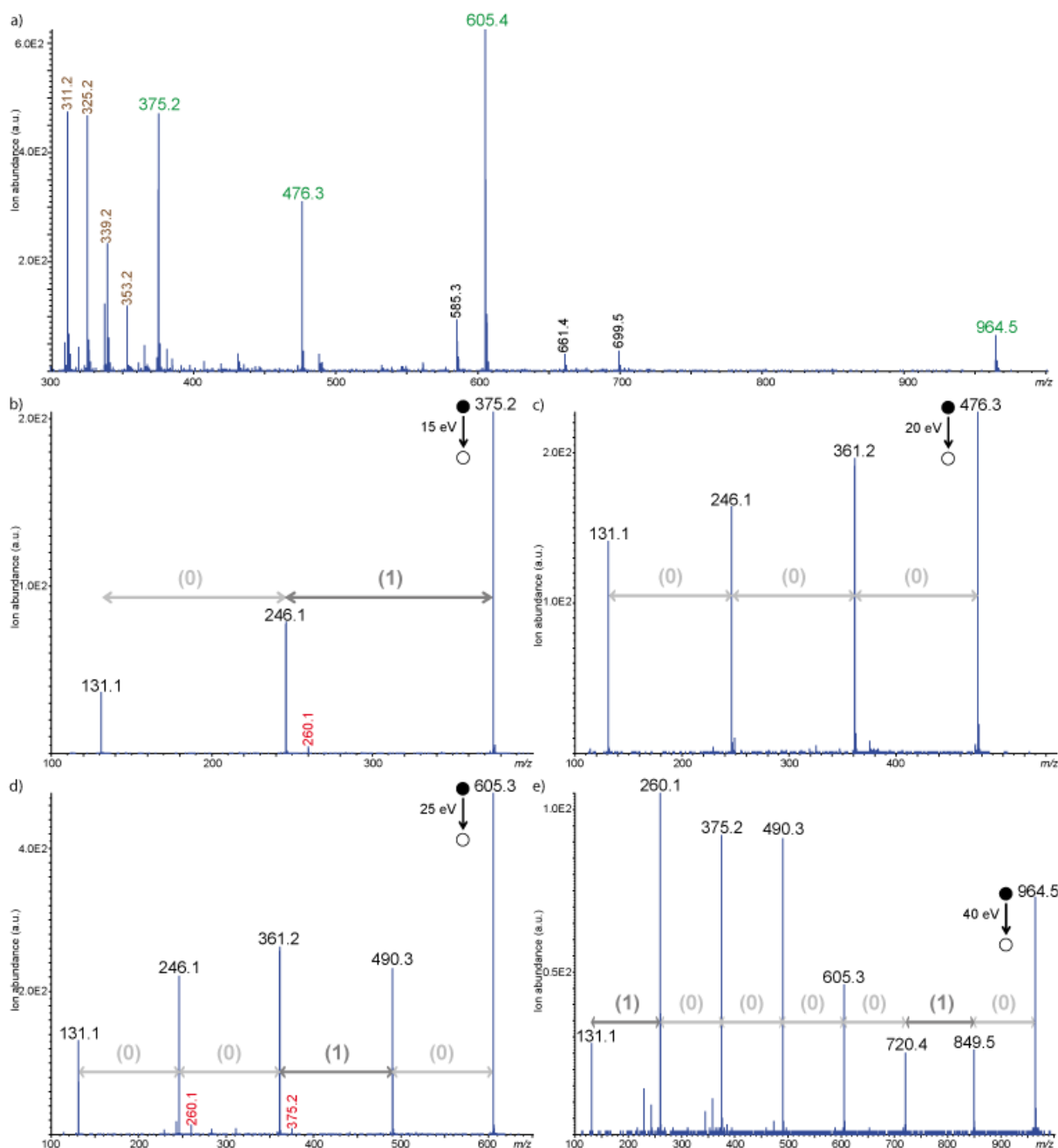
Figure V. 7: Mass spectrometry analysis of a PVC membrane labeled with the four-component oligourethanes library. a) ESI-MS of the extract, showing signals (in green) expected for deprotonated P1 (*m/z* 375.2), P2 (*m/z* 476.3), P3 (*m/z* 605.3) and P4 (*m/z* 964.5). Peaks annotated in brown correspond to impurities extracted from the PVC membrane (see Figure S21). Peaks annotated in black correspond to impurities previously detected in some oligomer samples. ESI-MS/MS sequencing of b) [P1 – H]⁻ at *m/z* 375.2 (E$_{coll}$: 15 eV), c) [P2 – H]⁻ at *m/z* 476.3 (E$_{coll}$: 20 eV), d) [P3 – H]⁻ at *m/z* 605.3 (E$_{coll}$: 25 eV), and e) [P4 – H]⁻ at *m/z* 964.5 (E$_{coll}$: 40 eV) after solvent extraction from the PVC film. For fragments annotated in red in b) and d), see discussion in caption of Figure S18. Non-labeled peaks in MS/MS spectra correspond to secondary fragments.

It shall be mentioned that MS spectra obtained for PVC films showed oligourethanes signals of with much lower intensity compared to the other two membranes and exhibited noticeable impurities, which were initially present in the commercial PVC samples as supported by MS data recorded for the extract of a non-labeled PVC film (**Figure V.8**).

134
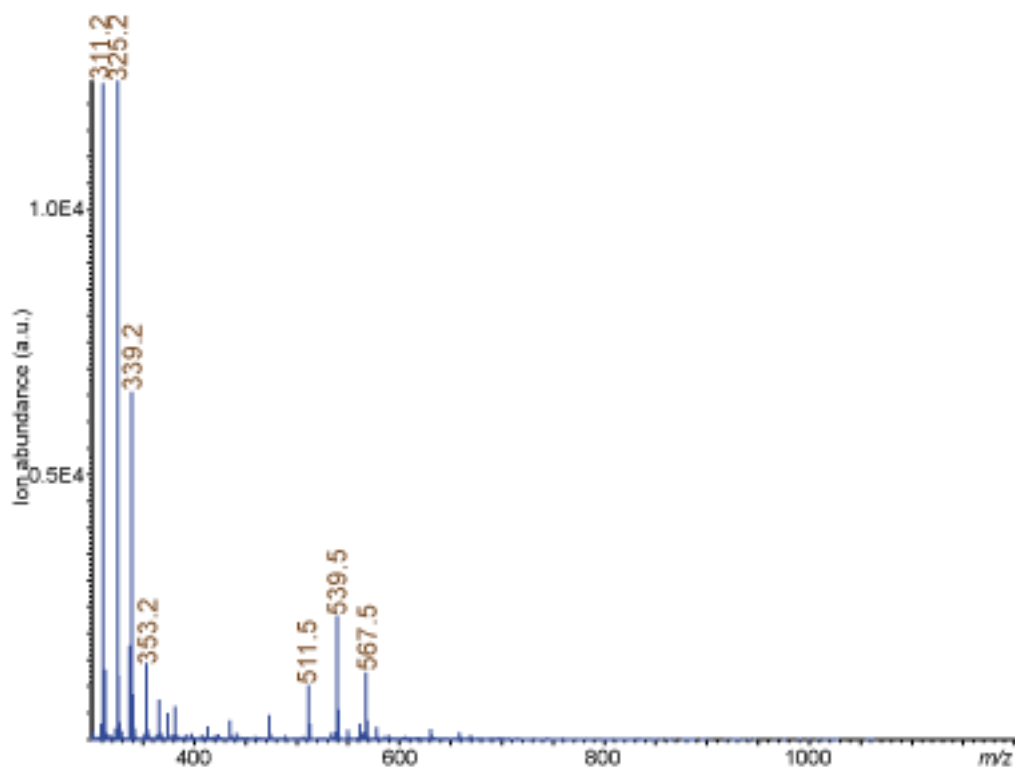
Figure V. 8: ESI-MS of the extract of a non-labeled PVC membrane.

3. Conclusions

In summary, uniform sequence-coded oligourethanes were used as anti-counterfeit tags in commodity polymer matrices, i.e. PS, PVS and PET. However, instead of using one type of coded oligomer as reported before,[241] multicomponent libraries containing oligomers with different chain-length, sequence and mass were used. These coded libraries could be dispersed in all types of polymer matrices using facile solvent casting procedures. Furthermore, the oligomer mixtures could be extracted in all cases from the films and analyzed by mass spectrometry. In particular, a combination of MS and MS/MS analysis allows reconstructing a complex digital sequence included in the whole library. These results are important because they indicate that oligourethane barcoding is not restricted to single-coded-chains but can be extended to more complex oligomer mixtures. Furthermore, the results of this communication evidence that the concept is relatively universal and can be applied to very different types of host plastics. Indeed, the selective solvent-extraction protocols described in this work are practical and allow direct MS analysis of the sequence-coded barcodes (i.e. without requiring barcode amplification or other pre-analysis treatments). These results open up interesting new horizons for the identification and traceability of plastic-based or plastic-containing products.

Chapter VI:

Covalent incorporation of sequence-defined polyurethanes taggants in cross-linked polymer networks

Unpublished data

1. Introduction

As mentioned in the Introduction, anti-counterfeiting taggants have to fulfill many different criteria in order to be optimal. The enclosure of the molecular barcode has already been achieved in the chapters II-V by covering a wide frame of materials. In addition, their incorporation in polymer networks has been proved in the methacrylate-based networks for the labeling of intraocular lenses and in the PVA-based implants. In all these cases, the taggant was not chemically linked to the matrix but its incorporation was performed physically. They constitute important applications in the evolution of anti-counterfeiting but they are still lacking in some taggants' characteristics.

Although, the two proceeding routes used for the labeling of polymer networks, were rapid, efficient and with high potentials for their use in industrial labeling applications, here we want to show that the covalent attachment of the PU barcode in the polymer network is possible as an alternative solution for more secure applications. By covalent attachment, there are no big chances that the PU taggant could move out of the tagged material. The fact that the PU taggant is bounded on the material makes its use more suitable for high-security demanding applications. Furthermore, its detection was developed by the introduction of a specific linker. Thus, DESI-MS can denote directly the PU after cleaving it from the polymeric network with the help of chemical treatment.

This chapter focuses on the switch from the non-covalent labeling to the covalent attachment of the taggant in the polymeric material and for this purpose a model material p-NIPAM gel was labeled. To make all the described things work, the synthesized sequence-defined PU label is modified including a cleavable linker. The linker is specially designed to be cleavable through DESI-MS spectrometry in order to set free the taggant from the gel and be sequenced by DESI-MS/MS. Except for the cleavable bond the molecule of the linker was including methacrylamide end-group, necessary for the gel-formation and its incorporation in it. On the **Figure VI.1** the general concept of the project is depicted.

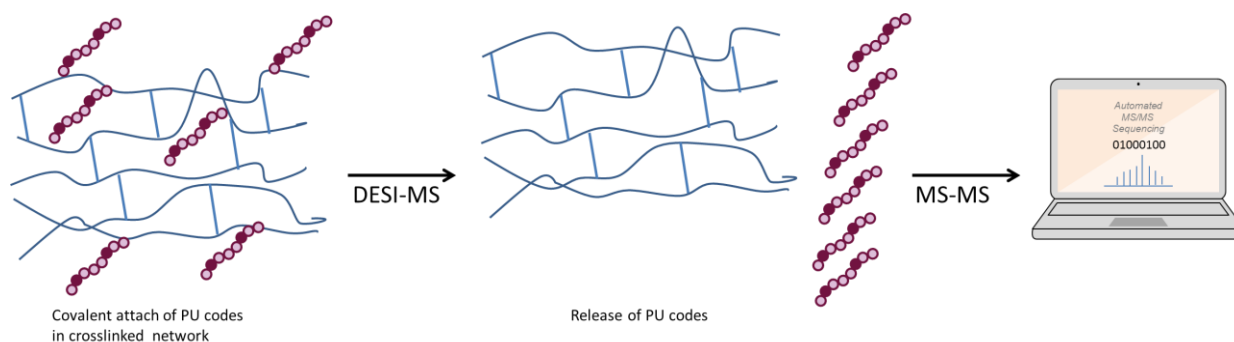**Figure VI. 1: Schematic representation of the general idea of the current chapter. The PU barcodes are covalently incorporated in a cross-linked polymer network unable to be detected without cleaving them from it. The key to unlock the encrypted information of the sequence-defined poly(urethane)s is the DESI-MS. Through the later method the information-containing polymers are free to be detected and read-out by MS/MS.**

2. Results and Discussion

2.1 Selection of materials to be tagged

This chapter deals with covalent attachment of coded poly(urethane)s molecular markers to polymer gels. It is well known that polymer gels find applicability to a plethora of fields including food and chemical processing, pharmaceuticals, medicine, agriculture, civil engineering and electronics[280]. Their wide applicability might put them under the risk of counterfeiting making necessary their marking and tracking by using the appropriate labels. Free-radical polymerization are commonly used to prepare gels by reacting the monomers with multifunctional cross-linkers[281].

Furthermore, poly(N-isopropylacrylamide) since its discovery in 1986[282] has been used to a plethora of applications such as sensing and biosensing[283,284], drug delivery[285-287], tissue engineering[288] and smart optical systems[289]. p-NIPAM has the property to form gel, i.e. cross-linked polymer networks , which exhibit similar behavior as the neat p-NIPAM [290].So, in order to covalently incorporate the PU sequences in a polymer network, p-NIPAM gel prepared through radical polymerization was chosen as interesting material.

2.2 Synthesis of a model PU macromonomer

To do so, the urethane sequences after their preparation, following the two repetitive chemoselective steps synthesis, were modified with methacrylate end-group. The sequence-defined polyurethanes were prepared as described in previous chapters.[39]

Once the coded message is written by the alternation of the two amino alcohol building blocks on the polymer chains, the oligomer is not cleaved from the resin but still anchored there, it is activated once more with its reaction with DSC in microwaves reactor. The final block instead of being one of the previously used amino alcohols (amino-butanol or amino-methyl-butanol) was an amino methacrylate monomer to introduce the methacrylate function to the oligo(urethane) as its terminus. This reaction step was carried out with 2-aminoethyl methacrylate hydrochloride in the presence of trimethylamine and DMF dry. After one hour of reaction, the mixture was rinsed with water, DMF and diethylether. The sequence-coded modified oligo(urethane)s were cleaved from the resin in TFA/DCM (1/1 (v/v)) solution. The strategy was first tested with a simple amino methacrylate in order to confirm the concept and then was differentiated to methacrylamide end-group. in paragraph 2.3.
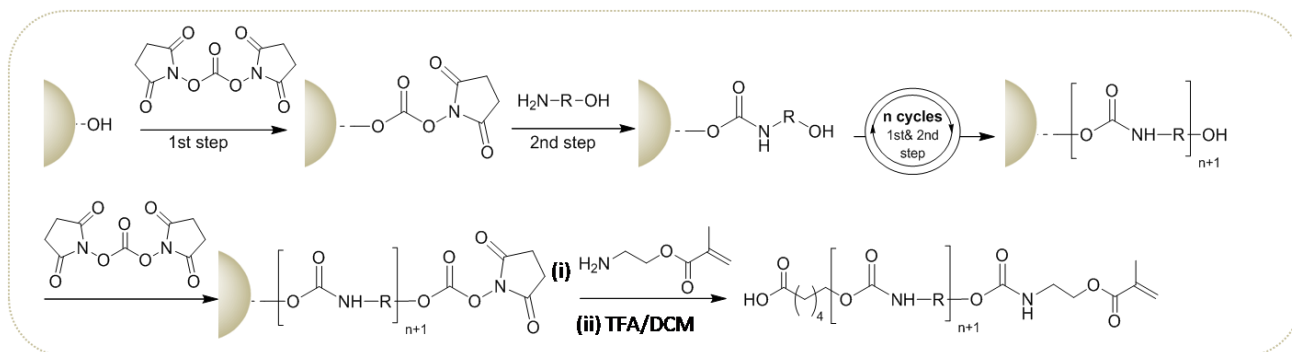
Figure VI. 2: Representation of the synthetic procedure for the preparation of methacrylate-ended oligo(urethane) barcodes. The two consecutive steps for the synthesis of sequence-defined oligo(urethane) followed by the reactivation step by DSC and reaction with 2-aminoethyl methacrylate on the solid support. The final cleavage from the resin terminates the preparation of sequence-coded PUs with methacrylate terminus.

The oligomers were characterized by SEC and MS-spectrometry to confirm their structure and their purity. Following, on the **Figure VI. 3**, it is shown an indicative modified oligo(urethane) with the sequence α-0-1-0-1-ω. The 0 bit corresponds to the 4-amino-1-butanol, m_0=115.1 Da, and the 1 bit to the 4-amino-2-methyl-1-butanol, m_1=129.1 Da.

$M_{n,SEC}$:1180 g mol^{-1}
$Đ_{SEC}$:1.01
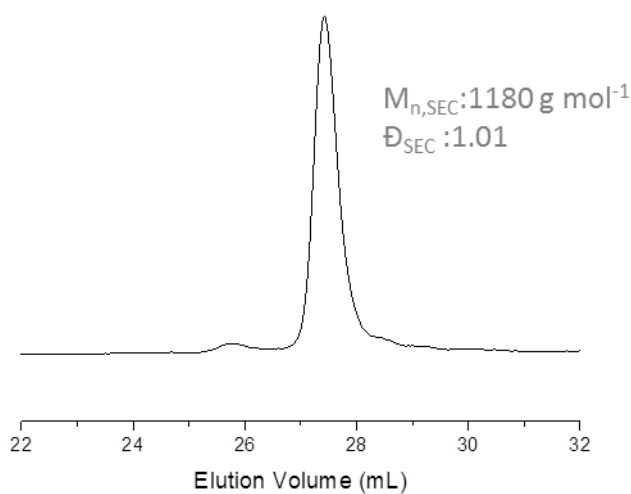
Figure VI. 3: SEC chromatogram of the oligomer α-0-1-0-1-ω with α= $C_6H_{11}O_2$ ($m_α$=115.0759 Da) and ω= $C_7H_{10}NO_4$ ($m_ω$=172.0610 Da)

141

Figure VI. 4: ESI-MS spectrum in negative mode on the left of the figure. With green it is noted the desired oligomer and in orange the impurity with Δm=+56 Da.

As shown in the **Figure VI. 4**, the sample with monomer sequence α-0-1-0-1-ω with α= $C_6H_{11}O_2$ (m_α=115.0759 Da) and ω= $C_7H_{10}NO_4$ (m_ω=172.0610 Da) was monodisperse with the only minor impurity of Δm=+56 Da probably because of the use of a strong base for the couplings, trimethylamine. This peak is observed in many oligomers when this base is used, whereas when we switch to pyridine, the +56 signal disappears (see **Ch .III, Fig. III.2**)

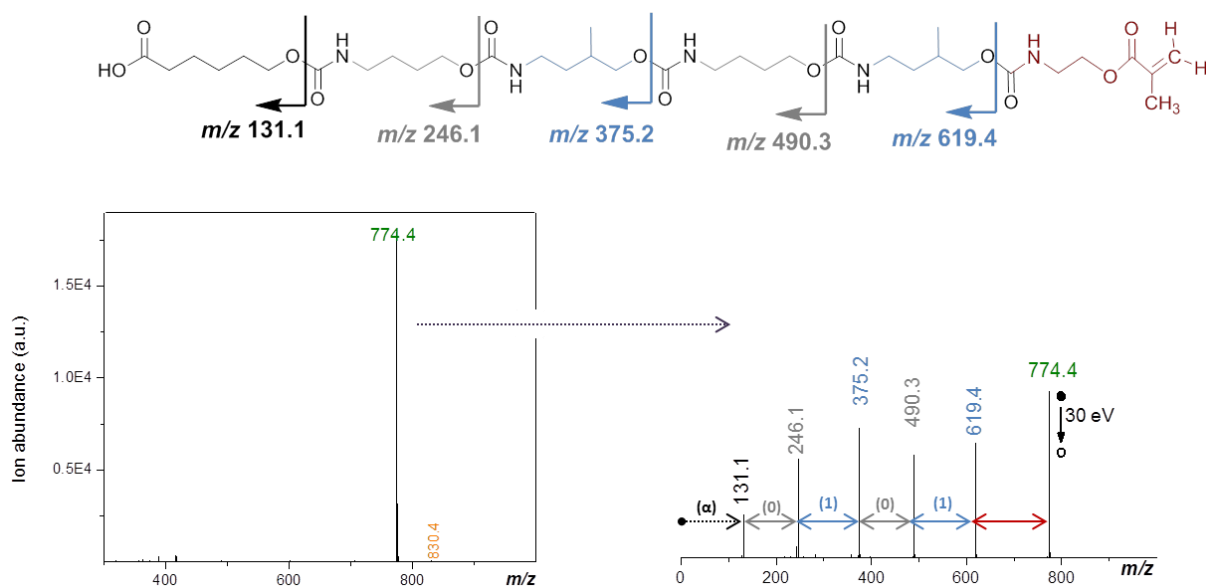It was proved that such modification of the oligo(urethane)s is feasible and very easy by just replacing the amino-alcohols blocks with the amino methacrylate monomer, allowing in a further step co-polymerization of the oligo-urethanes with MMA. (data not shown) The results showed that modified oligo(urethane)s can be incorporated through polymerization to the polymer matrix.

2.3 Selection of DESI-cleavable bond

As an extension of the previous investigation, it had to be found a way to isolate the coded-information from the polymer network and analyzing it in the simplest way possible. The solution to the problem gave the insertion of a DESI-MS cleavable bond.

Cleavable bonds by DESI have been described in the literature[291-294]. More particularly, they are very useful for the study of proteins conformation because the understanding of the protein three-dimensional structures and the protein-protein interactions is essential for the knowledge around their biological function. In these cases, the disulfide bond bridge in inter- or intra peptides undergoes selective cleavage by DESI-MS method. The latter in combination with MS spectrometric analysis of the generated products provide structural insights in proteins. Furthermore, it has been showed that disulfide bonds survive under mild condition radical polymerizations[295,296] allowing its incorporation

in the oligourethane macromonomer through radical polymerization technique. In our case, the DESI-MS cleavable bond is integrated in the oligo(urethane) sequence before the methacrylamide terminus (**Fig. VI.5**). Like this, it is allowed to proceed to the copolymerization and the formation of a polymer cross-linked network, but with possible sequential-information recovery thanks to the cleavable bond.

2.3 Synthesis of S-S linker

The synthesis of the disulfide linker is depicted on the following **Figure VI. 5**. The synthesis of N'-methacryloyl cystamine is a series of reactions starting with cystamine dihydrochloride. In a first step the cystamine is monoprotected by tert-butyloxycarbonyl. Then, the other free amine group is modified by methacryloyl chloride in a second step. As a third step the Boc protected N'-methacryloyl cystamine is deprotected and ready to react with the sequence-defined oligourethane.
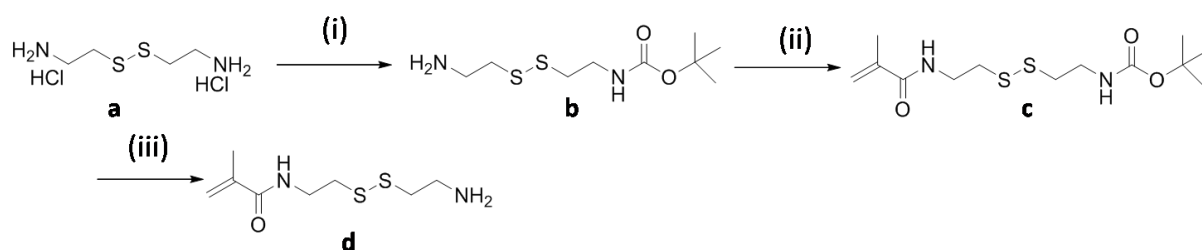
Figure VI. 5: Schematic representation of the synthesis of cleavable monomer (d), N-Methacryloyl cystamine: (i) di-tert-butyl dicarbonate/triethylamine, MeOH, (ii) methacryloyl chloride/ N,N-diisopropylethylamine, CH₂Cl₂, (iii) TFA/ CH₂Cl₂.

The N'-methacryloyl cystamine was characterized by ^{1}H-NMR, ^{13}C-NMR and ESI-MS to determine its purity and chemical structure. The NMRs were recorded in deuterated DMSO and the ESI-MS in positive mode.

However, the compound **d** after the deprotection from the protecting group is not at the depicted form. It is in a TFA salt form, $C_7H_{11}O_2NS_2NH_3^+/CF_3COO^-$. The latter is not causing any problem for further oligourethane modification, instead the amine is protected from being oxidized and thus degraded. The anion of the N-methacryloyl cystamine can be further supported by the ^{1}H-NMR spectrum and the signal at 4.9 ppm.
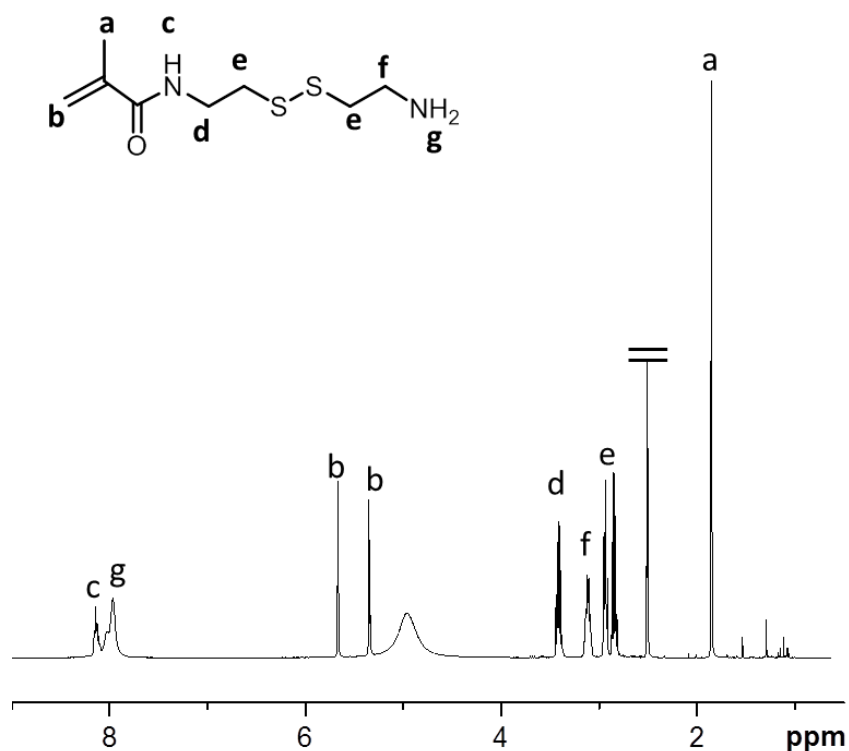
Figure VI. 6: ^{1}H-NMR of linker in d_6-DMSO
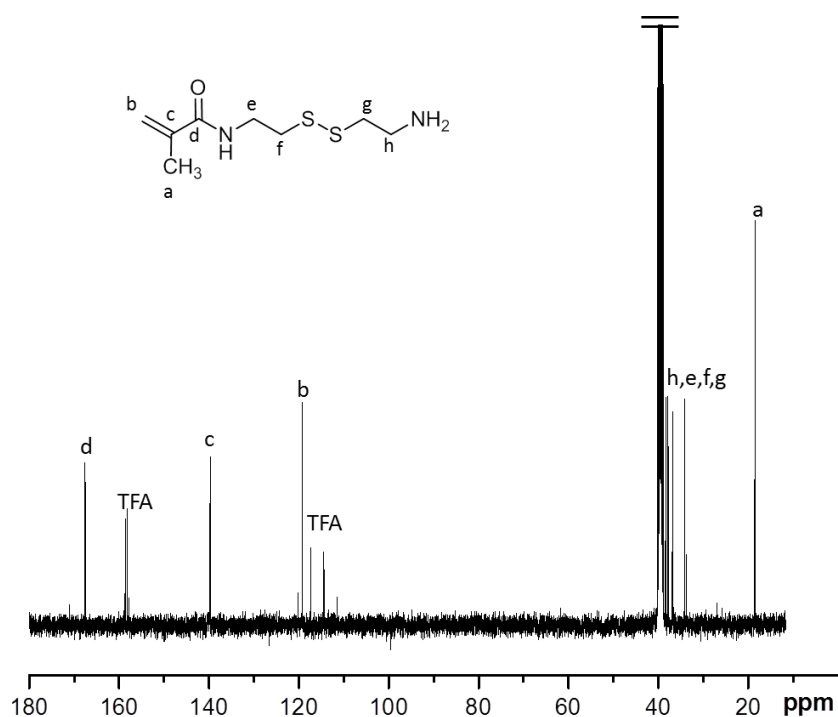
Figure VI. 7: ^{13}C-NMR of linker in d_6-DMSO

The ESI mass spectrum recorded in the positive ion mode for the linker shows a main peak corresponding to the targeted compound as a protonated molecule, $[M + H]^+$ at m/z 221.1 (in green, **Figure VI. 8**). This assignment is supported by both accurate mass measurements and MS/MS (green

inset of **Figure VI. 8**). A less abundant species is also detected at *m/z* 289.1 (in red, **Figure VI. 8**). This ion corresponds to a bifunctional cystamine with methacrylamide end-group. This ion derives from potential traces of unprotected cystamine by Boc in the (i) step of the synthesis of the linker (**Figure VI.5**) which then leads to a N,N' Methacryloyl cystamine. The presence of this impurity is not a problem for the oligomer modification because only the primary amine reacts with the activated resin. The red inset constitutes the MS/MS spectrum recorded for this ion suggests a 288.1 Da molecule.
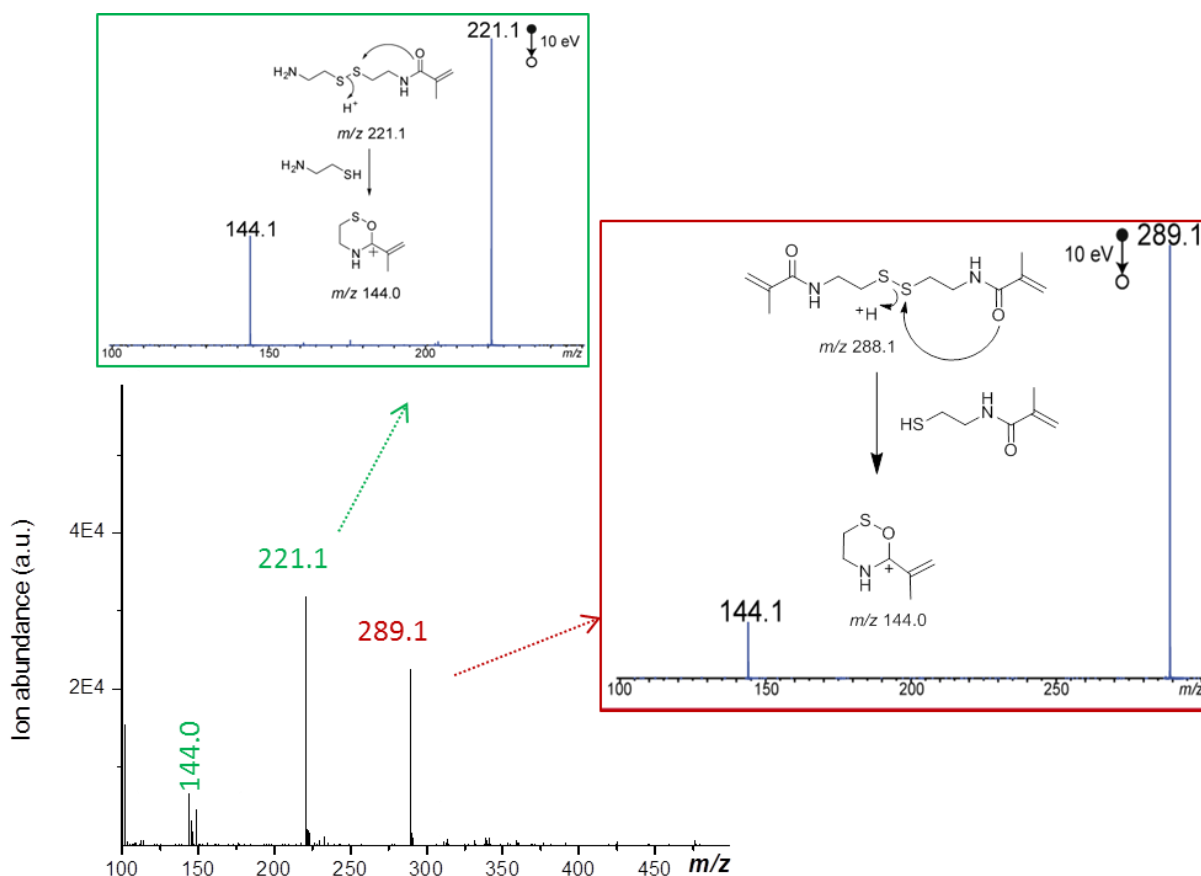
Figure VI. 8: ESI-MS in positive mode of N-Methacryloylcystamine. The ion *m/z* 144.0 is an in-source fragment of both *m/z* 221.1 and *m/z* 289.1.

2.4 Synthesis of the oligo(urethane) containing S-S linker

Following all the previous research, the attachment of the S-S linker to the oligomer was straightforward. **Figure VI. 9** shows the modification of the oligomer from –OH terminus to methacrylamide terminus including the S-S DESI cleavable bond. In the first step of the modification the alcohol function of the oligomer on the resin reacts with the *N,N'*- disuccinimidyl carbonate leading to the formation of the activated unsymmetrical active carbonate. This reacts with the amino group of the N-Methacryloyl cystamine to afford the methacrylamide-function on the oligo(urethane).
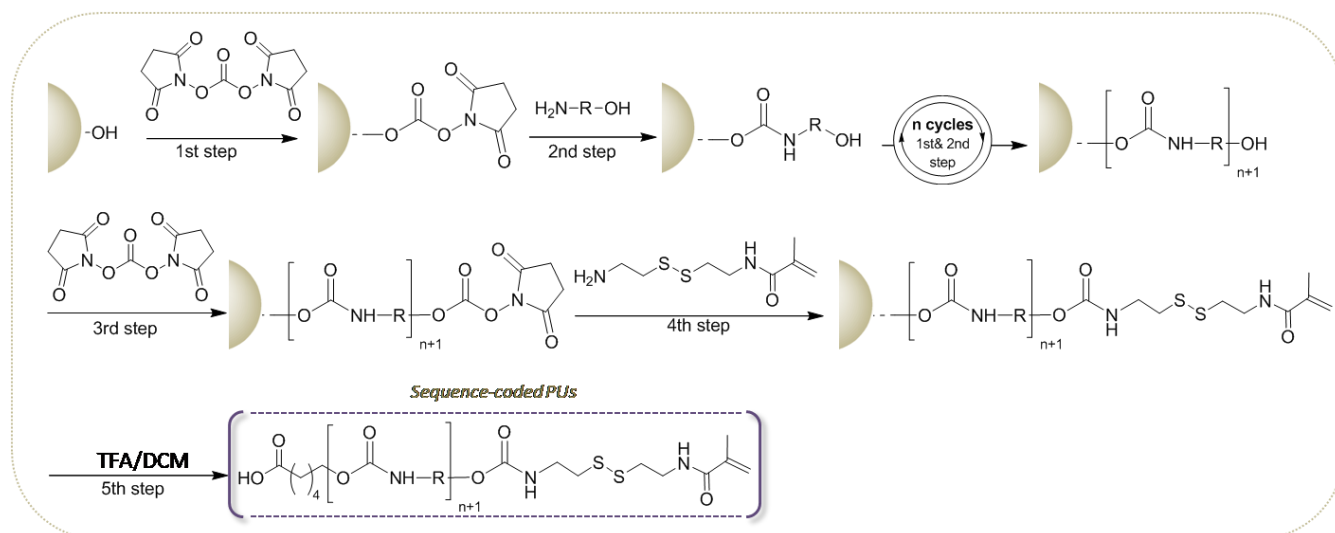
Figure VI. 9: The construction of the methacrylamide-ended oligo(urethane) barcode. The synthesis of the sequence follows the two chemoselective steps, 1st step: DSC,dry pyridine, dry acetonitrile, 2nd step: amino-alcohol, dry pyridine, dry DMF. The resin is activated once more at the 3rd step (DSC, dry pyridine, dry acetonitrile) to be ready to be coupled with the N-Methacryloyl cystamine at the 4th step (triethylamine, dry DMF).
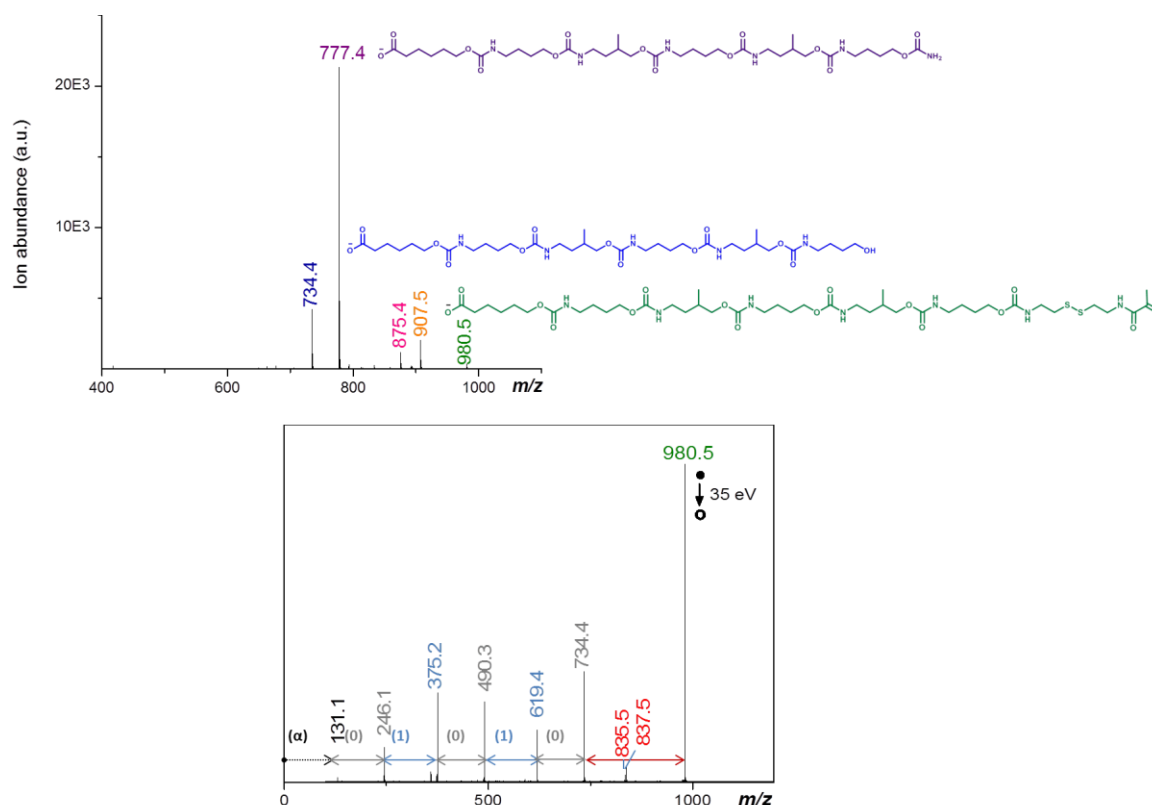
Figure VI. 10: ESI-MS spectrum in negative mode of the coupled oligomer with the N-methacryloyl cystamine above. Below MS/MS analysis of the desired molecule. The peak at m/z 835.5 and m/z 837.5 are products of the S-S bond cleavage and their mechanism is explained in the Figure VI. 11

As depicted on the **Figure VI. 10.** The coupling of the N-Methacryloyl cystamine with the oligo(urethane) was a bit tricky. In the first trials as proved from the mass spectrometry the

146

methacrylamide oligomer was formed in low yield. Non-reacted oligomer was also present in ESI-MS spectrum as well as several other impurities, products of the inefficient coupling.

In fact, by exchanging the dry pyridine with the triethylamine during the synthesis, the desired molecule was formed. The **Figure VI. 11** shows the nearly pure ESI-mass spectrum and MS/MS spectrum. Instead of using anhydrous pyridine as base, the coupling required a stronger base like triethylamine, and this possibly because of the protonated amine generated after the acidic di-BoC cleavage. As a result, the ESI-MS spectrum of the product was polydisperse with several impurities being present (**Figure VI. 10).**
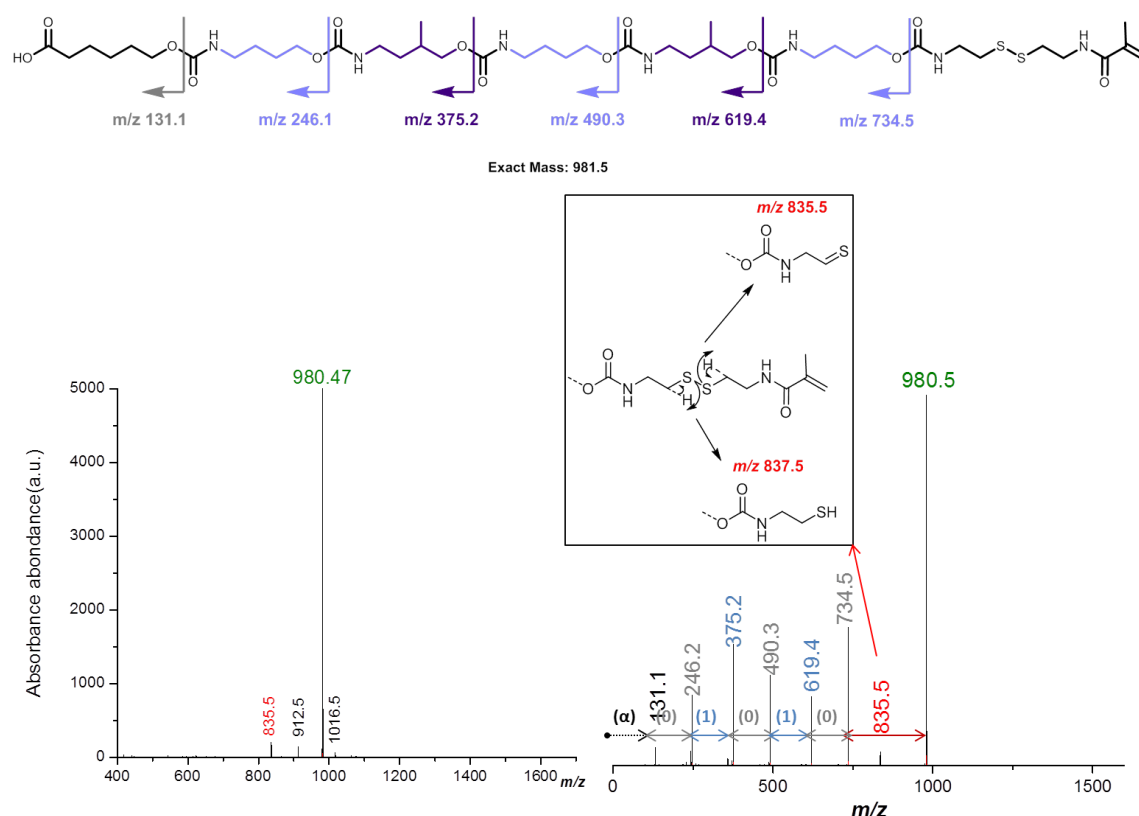
Figure VI. 11: MS-Characterization of the modified oligomer. Oligo(urethane) with monomer sequence α-0-1-0-1-0-ωwhere ω:$C_9H_{15}N_2O_3S_2$. ESI-MS spectrum revealed the mass of the expected composition with minor impurities. MS/MS spectrum on the right side shows the monomer sequence. The minor fragment denoted in red at *m/z* 835.5 is due to the S-S bond break, showed in the small window.

2.5 Incorporation of the modified oligomer in model polymer networks

The modified oligomer is ready to constitute a co-monomer for the co-polymerization of NIPAM for the preparation of cross-linked polymer networks. NIPAM, N,N'-Methylene bis (acrylamide) and methacrylamide-end oligourethane in a weight ratio of 85/10/5 take part to the controlled radical co-polymerization. The bis-acrylamide plays the role of the cross-linker leading to p-NIPAM gels with information-containing oligomers incorporated though the radical polymerization of its methacrylamide bond (**Figure VI.8**). After 18hours of reaction the gel point was reached. The entire

mixture was solidified. The gel was washed three times by DMF in SPE tube and let dry under vacuum.
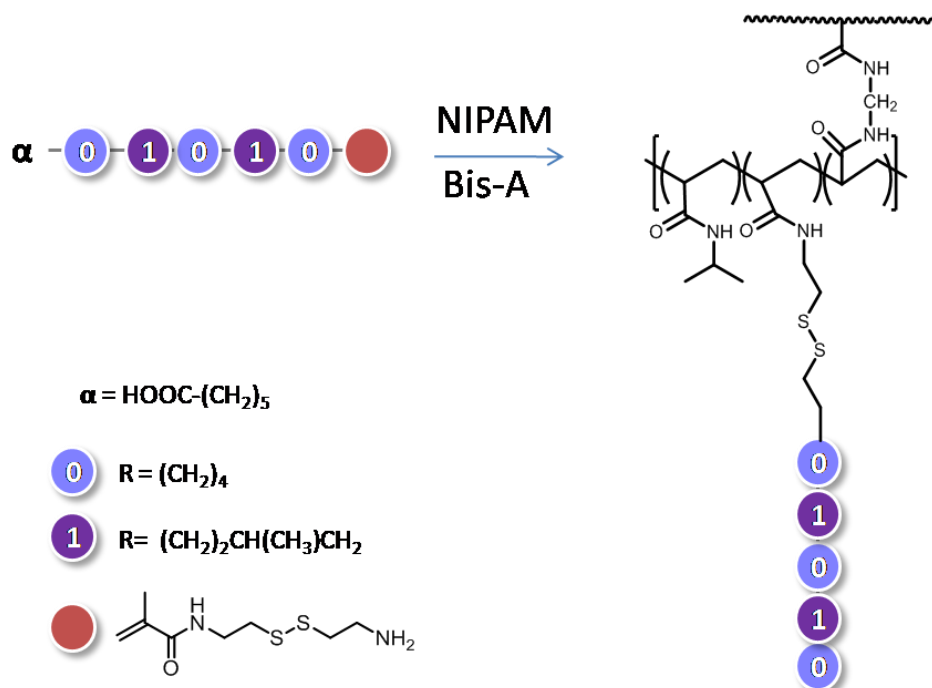
Figure VI. 12: Preparation of p-NIPAM cross-linked networks bearing information-containing oligomers through radical polymerization with Bis-Acrylamide as cross-linker.

2.6 DESI-MS for the release and reading out of oligomer

The p-NIPAM gel was subjected to DESI analysis. The idea is to perform reactive DESI-MS to induce the dissociation of the S-S linker which is present between the sequence-coded information and the polymers matrix. Hence, the sequence-defined oligomer is free to be read-out by MS/MS as shown on the (**Fig. VI.13**).

So, a small piece of the cross-linked polymer network was placed onto the DESI plate and sprayed by a slightly basic solution: H_2O + 0.1% NH_4OH (for pH adjustment). It was first analyzed under these conditions as a blank test, in order to examine if the presence of non-attached polymer is obvious or if any signal from S-S cleaved oligourethane is detected. In first analysis trials, it was visible that non-covalent S-S modified oligourethane was present in the DESI-MS spectrum of the gel as a deprotonated molecule at *m/z* 980.5. So it was evidenced that either the oligourethane was not attached at all on the polymer gel or the radical polymerization was not of 100% conversion and the gel was not rinsed enough in order to remove all the monomer traces.
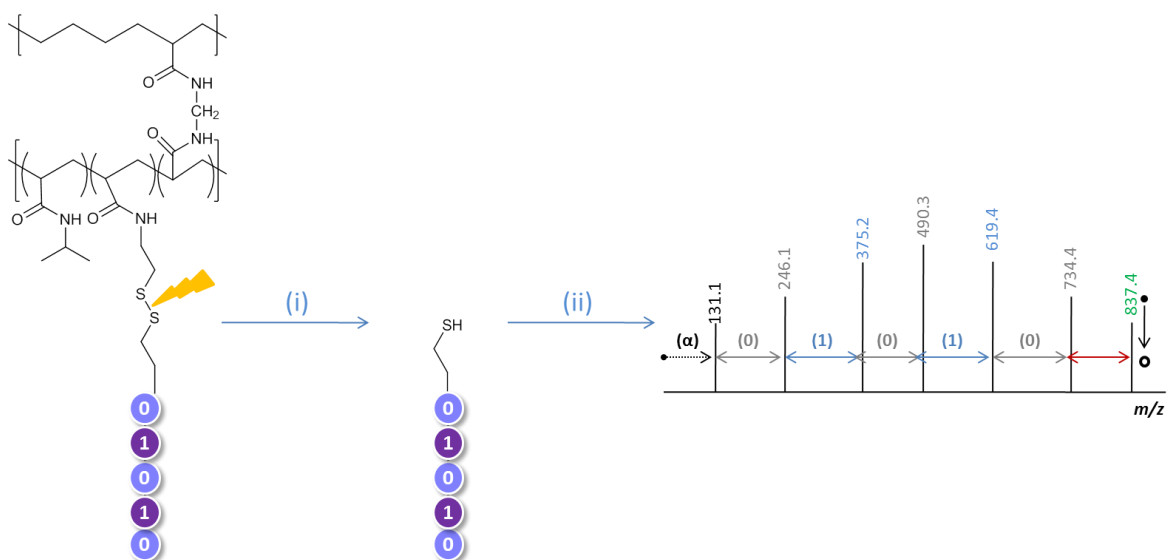
Figure VI. 13: Theoritical representation of the reading-out of the sequence-coded polymer is following the S-S bond breaking by DESI-MS. The coded-oligomer is then free to be sequenced by tandem mass spectrometry to decrypt the stored message.

Thus, the gel was washed further, for two days in DMF with changing the solvent 4 times. Second analysis showed that our initial hypothesis for non-complete conversion was right. This time there was no evidence of non-covalent attached oligourethane when the gel was analyzed by DESI-MS performing the blank test. Following, the sample was subjected to DESI-MS where in the sprayed solution was included dithiothreitol (DTT). DTT is an often used reagent for the reduction of the S-S bond[297,298]
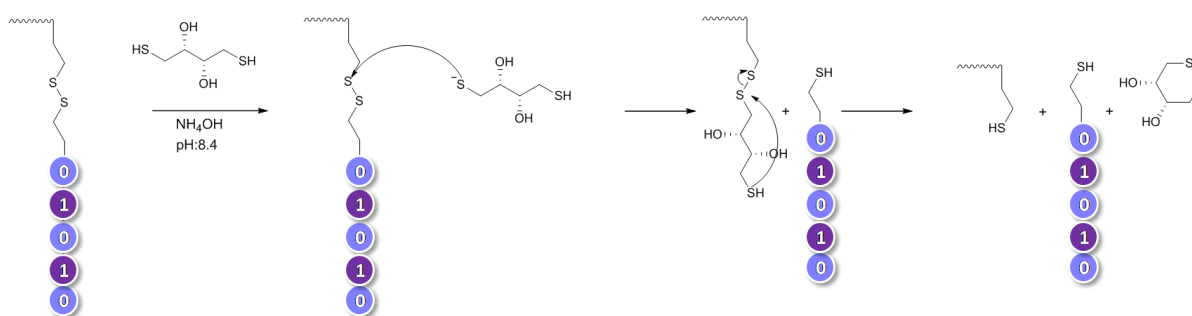
Figure VI. 14: Mechanism of the DTT in the S-S cleavage

Indeed, the reduction of the S-S bond of the linker took place and the signal corresponding to the oligourethane resulting from the S–S bond cleavage is clearly detected as a deprotonated molecule at *m/z* 837.5 (**Fig. VI.15.b).**

The reactive DESI product at *m/z* 837.5 was sequenced by MS/MS for the reading-out of the coded-message (**Fig. VI.16**).

149
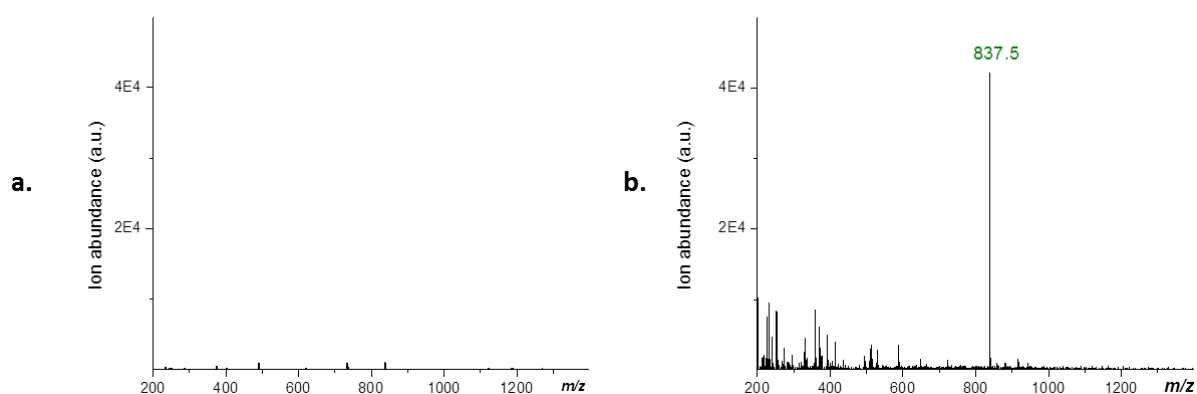
Figure VI. 15: Negative mode DESI-MS of the gel including the oligourethane covalently attached. a. DESI-MS of the sample with sprayed solution H₂0 + NH₄OH (blank test). b. DESI-MS of the sample with the sprayed solution including DTT (+ H₂0 + NH₄OH). In the first case there is no free oligourethane *m/z* 980.5 neither signal of the oligourethane resulted from the S-S reduction at *m/z* 837.5, whereas in the second case the spectrum exhibits the *m/z* 837.5.
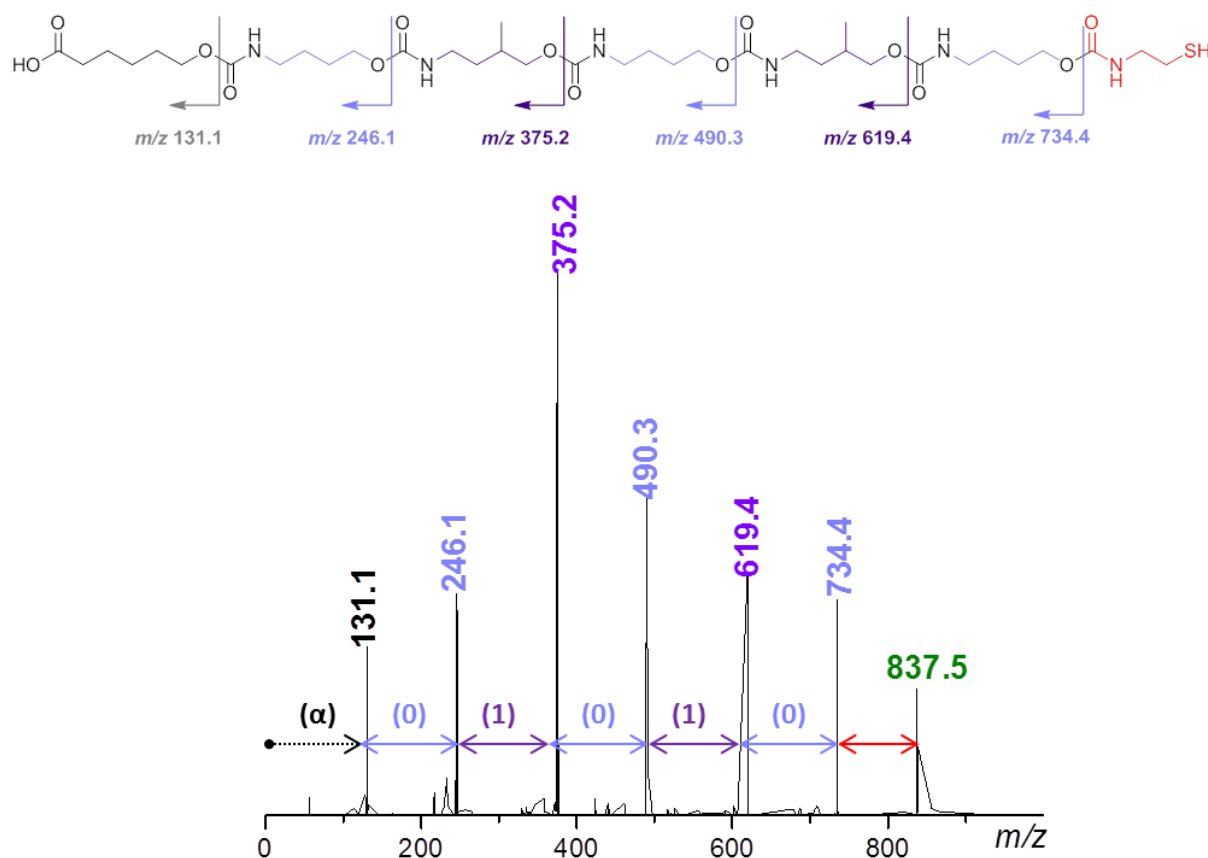
Figure VI. 16: Negative mode DESI-MS/MS [M − H]⁻ ion at *m/z* 837.5 of the spectrum in figure IV.12

From the **Figure VI.15** it is clear that simple DESI-MS (**Fig.IV.15.a**) cannot detect any PU signal thus reactive DESI-MS is necessary for its detection. This fact renders the covalent attachment even more secure anti-counterfeiting method, demanding from the analyst to use the suitable strategy for the taggant detection.

3. Conclusions

In summary, this chapter focuses on the covalent incorporation of the molecular taggants in polymer networks. PNIPAM gels were used as a model material for this work. Sequence-defined oligo(urethane)shave already shown their efficacy as anti-counterfeiting taggants. Another step forward was made through this work to the direction of high-security anti-counterfeit solutions. The oligomers were slightly modified for the introduction of a DESI-MS cleavable bond and the methacrylamide end-group. The modified information-containing oligomer was covalently incorporated in a poly (N-isopropylacrylamide) network during the radical polymerization of N-Isopropyl Acrylamide. The resulted polymer gels constituted mainly from p-NIPAM (85wt%), bisacrylamide (10 wt%) as crosslinker and the modified molecular tag (5 wt%). The resulting gel was washed away from the non-reactant monomers and subjected to reactive DESI-MS for the release of the taggant. DTT cleaved the S-S bond of the linker through reduction allowing us to proceed with the decryption of the binary message via MS/MS. The immobilization of the taggant in the polymer cross-linked network and its following reading out were successful opening the frame of anti-counterfeiting applications of the synthetic sequence-defined polymers.

General Conclusions

To conclude, a new anti-counterfeit technology has been developed in the frame of this Ph.D. thesis. Sequence-defined oligourethanes taggants, synthesized on solid support through an iterative protocol, were used for this purpose. Their synthesis was based on two chemoselective steps on a hydroxyl modified Wang resin: the activation of the resin with disuccinimidyl carbonate and the subsequent reaction of the resulting activated carbonate with an amino-alcohol monomer unit. In this work, two amino-alcohols monomers with different side groups were used to code the polymers, i.e. giving access to binary identification sequences. Each oligourethane had therefore a unique monomer sequence and therefore constitutes an exclusive product identity that can be deciphered by tandem mass spectrometry. In this work, the oligourethane taggants were tested in different host materials. It shall be noted that the taggant methodology described in this thesis is not restricted to binary sequences, which were only used as models in this work. Indeed, monomer alphabets containing more symbols can also be employed for increasing coding possibilities[23,255].

In **Chapter II**, it was shown that oligourethane taggants can be used as anti-counterfeit taggants for biomedical implants. Sequence-defined oligourethanes were incorporated in intraocular lenses. This part of the work was performed as an informal collaboration with the company Acrylian, which is specialized in the production of poly(2-ethoxyethyl methacrylate)intraocular implants. The incorporation of the taggants in the lenses was achieved through two different approaches: a) it was included in situ during the formation of the crosslinked methacrylate network or b) it was included in a premade lens using a simple solvent swelling/deswelling procedure. In both cases, homogeneous labeling was achieved as confirmed by oligourethane detection via NMR and mass spectrometry. The label detection was performed after its extraction from the implant. Moreover, transparency and biocompatibility tests of the labeled ophthalmic implants showed no significant modification of the optical properties and no leaching out of contaminants. Overall, it was showed that the sequence-defined oligourethane taggants can be used as anti-counterfeit markers in ophthalmic implants, without affecting the utility and biocompatibility of the product.

Chapter III dealt with the *in vivo* applicability of oligourethane-tagged model implants. In this particular project, the sequence-defined oligourethanes were used to tag a PVA-based model of a vascular implant. This study was performed in collaboration with the group of Didier Letourneur at INSERM U1148, Paris, where all animal studies were performed. The challenge was to introduce the labeled plastic implant in alive rats and investigate the detectability of the oligourethane label after three different implantation periods. For this reason, the oligourethanes were tested in terms of cytotoxicity. The cells viability showed lack of cytotoxicity and great potentials for the imminent work. Indeed, the inclusion of an 8-bit-coded oligomer in the plastic implant was realized *in situ* during PVA film formation. The oligourethane was dissolved and mixed with the PVA mixture

resulting in a labeled cross-linked PVA network. The labeled plastic implants were introduced in living organisms. From the shortest to the longest implantation period, the label of the explanted film was detected and the encrypted message decoded via tandem mass spectrometry proving further the robustness of the taggant technology.

The use of oligourethane taggants is not restricted to plastics labeling. The study presented in **Chapter IV** shows how products made of wood could also be tagged by sequence-coded oligourethanes. To begin with, the investigation of all the parameters affecting the labeling procedure through impregnation was indispensable. Indeed, different solution solvents and wood species were tested. Small pieces of beech, walnut and oak were immersed in the label solution. The confirmation of the label absorption came with the MS analysis of the different depth layers of the wood piece. From the exterior up to the deepest/ interior layer, the detection of the oligomer mass was achieved, denoting the efficiency of wood labeling by sequence-defined oligourethanes via impregnation.

Beside the achievement of introducing the abiotic sequence-defined taggants in materials of different nature, it was of equal importance to provide increased anti-counterfeiting protection for demanding applications. To this direction, **Chapter V** described the development of a two dimensional fingerprint pattern designed to increase the security level of the taggants. Until now, all the used oligourethane taggants constitute the simplest labeling design, providing information in a 1D linear chain of sequenced-monomers. In order to increase the information volume included in a taggant, we reported the mixing of multiple shorter uniform monomer-sequences. Monodisperse sequence-defined oligourethanes of different chain length and molecular weight were mixed and included in three polymer matrices through casting procedure. Following their extraction, their ESI-MS fingerprint was a polydisperse pattern (1st dimension fingerprint) which in a second phase each mass peak was sequenced individually to decode the message (2nd dimension fingerprint) of each uniform oligourethane. This study indicates that the polymer sequence-defined taggants are not restricted to single polymer chains but can be extended to more complex designs with increased coded-information.

Finally, **Chapter VI** dealt with the covalent attachment of the oligourethane taggants in cross-linked polymer networks. To do so, the oligourethanes were simply modified in order to be able to take part in free radical vinyl polymerization as macromonomers. However, the extraction of the sequence-coded oligourethane from the co-polymer matrix would not work without any further modification of the macromonomer. So, the introduction of a disulfide DESI-cleavable bond in the polymer chains was carried out. The successful insertion of modified oligourethanes in the polymer network was done by radical polymerization. Reactive DESI-MS was used as a tool to reduce the S-S bond of the linker and enabled the MS/MS sequencing for the decoding of the oligourethane. The work showed that PU

taggants can be chemically linked to the polymer matrix and read-out without any difficulty, broadening their application spectrum even more.

Overall, new perspectives in the domain of anti-counterfeiting technologies were described in the chapters of this PhD thesis. Recapitalizing the research progress made, new anti-counterfeiting solutions were developed and pushed the field some steps forward. The use of binary language to encode the oligomers was used to enrich them with ASCII information enabling their encryption of important information for anti-counterfeit markers. Their application for labeling of plastic and wooden materials, as well as their in vivo testing, proved their broad usefulness and robustness. In addition, the possibility of interfering in their fingerprint pattern (2D taggants) as well in their chemical structure (introduce polymerizable end-group and S-S cleavable bond), whereas their utility as anti-counterfeit taggants remains, showed the wide applicability's opportunities. Consequently, it is logical to think that non-natural sequence-defined polymers could constitute in the next years a potential commercial solution to struggle forgeries.

Experimental section

CHAPTER II: IDENTIFICATION-TAGGING OF METHACRYLATE-BASED INTRAOCULAR IMPLANTS USING SEQUENCE DEFINED POLYURETHANE BARCODES

A. CHEMICALS

Compounds	Suppliers	Purity (%)
4-Amino-1-butanol	TCI	98
4-amino-2-methyl-1-butanol	TCI	98
N,N'-disuccinimidyl carbonate (DSC)	TCI	>98.0
Triethylamine (TEA)	Merck	>97%
2-ethoxyethyl methacrylate (EEMA)	Sigma-Aldrich	99%, stabilized with hydroquinone monomethyl ether
ethylene glycol dimethylacrylate (EGDMA)	Sigma-Aldrich	98%, stabilized with monomethyl ether hydroquinone
Luperox® 26 (LC26)	Arkema	-
anhydrous acetonitrile (dry ACN)	Sigma-Aldrich	99.8%
anhydrous dichloromethane (dry DCM)	Sigma-Aldrich	≥99.9%, 40-150 ppm amylene
dichloromethane (DCM)	Sigma-Aldrich, Carlo Erba	≥99.9%
diethyl ether	Carlo Erba	-
anhydrous N,N-dimethylformamide (dry DMF)	Sigma-Aldrich	99.8%
N,N-dimethylformamide(DMF)	Sigma-Aldrich	≥99.0%
Tetrahydrofuran (THF)	Aldrich	99%, stabilized with BHT
Trifluoroacetic acid (TFA)	Sigma-Aldrich	99%

All the above chemicals were used as purchased. Trimethylamine was kept dry under KOH pellets. Commercial Artis® intraocular lenses were kindly provided by Acrylian (Strasbourg, France). The Wang resin used for sequence-defined polyurethane synthesis was modified with a cleavable linker as

described in the literature. Methanol (Fisher Chemical) and ammonium acetate (Sigma-Aldrich) were used as received for mass spectrometry experiments.

B. Measurements

B.1 Nuclear Magnetic Resonance

The lenses were analyzed by ^{1}H NMR spectrometry on a Bruker Avance 400MHz spectrometer equipped with Ultrashield magnet. This technique was performed in order to check the homogeneous dispersion of the PU label on the entire surface of the lens. The spectra were recorded inTHF-*d8*.

B.2 Mass Spectrometry (ESI-MS and MS/MS)

High resolution MS and MS/MS experiments were performed using a QqTOF mass spectrometer (QStar Elite, Applied Biosystems SCIEX, Concord, ON, Canada) with the ESI source operated in the negative mode (capillary voltage: -4200 V; cone voltage: -75 V). Ions were accurately mass measured in the orthogonal acceleration time-of-flight (oa-TOF) mass analyzer, using PEG oligomers adducted with an acetate anion (in MS) or the precursor ions (in MS/MS) as internal standards. In this instrument, air was used as nebulizing gas (10 psi) while nitrogen was used as curtain gas (20 psi) and collision gas. Instrument control, data acquisition and data processing were achieved using Analyst software (QS 2.0) provided by Applied Biosystems.

C. Experimental procedures

C.1 Solid-phase synthesis of sequence-coded polyurethanes

Digitally-encoded polyurethanes were synthesized following a recently-described orthogonal iterative protocol.[299] In brief, these polymers were prepared on a hydroxy-functionalized crosslinked polystyrene resin using the coupling steps shown in Figure 1a. In a first step, the resin (100 mg, 1 Eq.) was reacted for 1h with di(*N*-succinimidyl) carbonate (6 Eq.) in the presence of TEA in dry ACN under microwave irradiation (Monowave 300, Anton Paar, 60°C, 8W). Afterwards, the resin was transferred into a solid-phase extraction tube and washed several times with DMF. In a second step, the activated resin was reacted for 20 min at RT with an excess amino-alcohol (i.e. 4-amino-1-butanol **0**, or 4-amino-2-methyl-1-butanol **1**, 10 Eq.) in the presence of TEA in dry DMF. Then, the resin was washed with DMF, diethyl ether and transferred back to a microwave tube. These two coupling steps were repeated successively a given number of times in order to reach a desired sequence and chain-length. The final polyurethanes were cleaved from the resin using a TFA/CH$_2$Cl$_2$ mixture (5:5 v/v). After filtering-off the resin, TFA and CH$_2$Cl$_2$are evaporated under reduced pressure to afford the desired polyurethanes as a white solid.

C.2 DIRECT LENS LABELING BY IN SITU FREE RADICAL POLYMERIZATION IN THE PRESENCE OF A POLYURETHANE TAG

The free radical polymerization was performed in a commercial mold (Acrylian, Strasbourg, France) allowing synthesis of a lens-shaped crosslinked methacrylate network. A digitally encoded polyurethane (0.1-0.4%wt as compared to EEMA) was first dissolved in 1 mL of warm THF and then gently mixed in a mixture of 2-ethoxyethyl methacrylate (3 g, 18.96 mmol, 1 Eq.), the crosslinker EGDMA (0.06 g, 0.303 mmol, 0.02 Eq.) and the radical initiator LC26 (0.03 g, 0.139 mmol, 0,01 Eq.). The mixture was left for 1h in order to avoid the formation of bubbles, poured in the mold and placed in an oven at 55°C for 18 hours. It should be noted that degassing is not strictly necessary in these experiments. After polymerization, the mold was opened and the crosslinked transparent lens was removed from it.

C.3 LABELLING OF PREMADE LENSES USING A SWELLING/DESWELLING STRATEGY IN THE PRESENCE OF A POLYURETHANE TAG

The following strategy can be used to label commercial Artis® lenses or non-commercial ones obtained by in-mold free radical polymerization of EEMA. In all cases, the lenses were first swollen in THF for 15 minutes. Afterwards, pure THF was removed and replaced by a solution of a digitally encoded polyurethane in THF (the oligomer was previously dissolved in warm THF). The lens was kept in the solution for 5-8 hours and it was then placed in a closed vial with holes in the cap. Deswelling and drying was performed by letting THF evaporate slowly at RT for approximately two days.

C.4 POLYURETHANE TAGS EXTRACTION AND ANALYSIS BY ELECTROSPRAY MASS SPECTROMETRY

Extraction of PU tags from lenses was performed in an ultrasonic bath (10-15 min) and using a methanol solution of ammonium acetate (3 mM). This solution composition was selected to fit requirements for best ionization of PUs in case the extracts could not be diluted prior to ESI-MS. Different experimental conditions were tested, all allowing sufficiently concentrated extracts to be obtained. Either a piece (5-25 mg) or the whole tagged lens (5-25 mg) was immersed in a minimum solvent volume (200-500 µL or 1-3 mL, respectively). So-obtained solutions were perfectly clear and eventually further diluted (1/10 to 1/100, v/v) prior infusion in the ESI source at 10 µL/ min using a syringe pump. PU oligomers (1-2 mg) were dissolved in methanol (300 µL) in an ultrasonic bath (15 min). Samples were further diluted (1/100 to 1/1000, v/v) in a methanolic solution of ammonium acetate (3 mM) and injected in the ESI source at 10 µL/min using a syringe pump.

C.5 Biocompatibility tests

In order to check their biocompatibility, the polyurethane-tagged lenses were tested using the standard ISO 11979-5:2006 procedure that permits to detect extractible additives. First, the lenses were dried at $60^{\circ}C \pm 5^{\circ}C$ under vacuum for 48h in order to remove traces of moisture. Then, a piece a lens of approximately 0.1 mg was weighed and placed in the extraction cartridge of the Soxhlet apparatus. The flask was filled with deionized water (70% of its capacity) and placed in a heated oil-bath to reflux water vigorously. After 4 hours, the water was allowed to cool down to RT and the sample was taken out. The water was concentrated to a final volume of 10 mL and analyzed by UPLC-MS using a Waters apparatus equipped with a PDA and a single quadrupole mass spectrometer (3100 SQ Waters). The measurements were performed on a RP18 column (1.7 µm, 2.1x50 mm) using water with 0.1% of formic acid and acetonitrile with 0.1 % of formic acid as eluents; gradient 95/5 and 5/95 in 5 minutes. Similar results were obtained after direct ESI-MS analysis by infusing water extracts (after a 1/10 dilution in methanol supplemented with 3 mM ammonium acetate) into the ionization source using a syringe pump. The lens piece was left drying for several days and weighed in order to assess its weight loss.

C.6 Transparency test

The lenses were immersed in a black walled aquarium equipped with 220V LED white light and filled with deionized water. The lenses were left at $35^{\circ}C$ for 10 days. A Nikon D7100 camera covered with black curtain was placed in a distance of 40 cm from the center of the front glass of the aquarium. Pictures from all the lenses were captured at the same time.

C.7 Accelerated microvacuole test

The lenses were immersed in a bottle filled with deionized water that was closed and placed in an oven at 45 ± 1 °C for 24 hours. Afterwards, the lenses were transferred to another bottle filled with water. The bottle was placed in a closed box made from expanded polystyrene. The temperature in the box and in the water was 37 ± 1 °C and a B1 series microscope equipped with a Nikon D7100 camera was placed next to the bottle at the same temperature. After 2.5 hours, each lens was observed through the microscope and several photos were captured from the entire surface.

CHAPTER III: ABIOTIC SEQUENCE-CODED OLIGOMERS AS EFFICIENT IN VIVO TAGGANTS FOR THE IDENTIFICATION OF IMPLANTED MATERIALS

A. MATERIALS

Compounds	Suppliers	Purity (%)
4-Amino-1-butanol	TCI	98
4-amino-2-methyl-1-butanol	TCI	98
N,N'-disuccinimidyl carbonate	TCI	>98
anhydrous acetonitrile	Sigma-Aldrich	99.8%
dichloromethane (DCM)	Fisher Scientific	≥99.9% with amylene
	Carlo Erba	-
trifluoroacetic acid (TFA)	Alfa Aesar	99
diethyl ether	Carlo Erba	
anhydrous N,N-dimethylformamide(dry DMF)	Sigma-Aldrich	99.8
N,N-dimethylformamide(DMF)	Sigma-Aldrich	≥99.0
anhydrous pyridine	Sigma-Aldrich	99.8 %, in Sure/ Seal™
polyvinyl alcohol (M.W.~ 125000 [Mowiol® 20-98]),	Aldrich	-
Trisodium tri-metaphosphate(STMP)	Sigma Aldrich	≥95
KOH pellets	VWR Chemicals	99
Triethylamine(TEA)	Merck	>97

Triethylamine (TEA, Merck, >97%) was stored on KOH pellets in dark. The Wang resin (0.94 mmol/g, IRIS Biotech) used for sequence-defined oligourethane synthesis was modified with a cleavable linker as described in the literature.[299] The microwave instrument used for the first step of the oligourethane synthesis was a Monowave 300 from Anton Paar. The second step of

the oligourethane synthesis was conducted in solid phase extraction (SPE) tubes using a KS 130 basic (IKA) shaker. A SWING Synthesizer SLT II from Chemspeed Technologies AG was used for the automated synthesis of oligourethane tags. The platform is equipped with a Huber Unistat Tango thermostat and a vacuum pump CVC 3000 Vacuum brand PC 3000 series. Methanol (Fisher Chemical) and ammonium acetate (Sigma-Aldrich) for mass spectrometry experiments were used as received. Cell culture reagents were purchased from Gibco. Resazurin sodium salt powder was obtained from Sigma-Aldrich (R7017). Mayer Hematoxylin was obtained from Diapath (Ref C0303) and Eosin Y from from Richard-Allan Scientific-Thermo Scientific (Ref 711).

B. Measurements

B.1 Nuclear Magnetic Resonance.

The polymer film was analyzed by ^{1}H NMR spectrometry on a Bruker Avance 400MHz spectrometer equipped with Ultrashield magnet. The spectra were recorded in DMSO-*d*6.

B.2 Electrospray Mass Spectrometry for membrane extracts.

High resolution MS and MS/MS experiments were performed using a QqTOF mass spectrometer (QStar Elite, Applied Biosystems SCIEX, Concord, ON, Canada) with the ESI source operated in the negative mode (capillary voltage: -4200 V; cone voltage: -75 V). Ions were accurately mass measured in the orthogonal acceleration time-of-flight (oa-TOF) mass analyzer, using the precursor ions as internal standards to calibrate MS/MS data. Samples were injected in the ESI source at 10 µL/min using a syringe pump. In this instrument, air was used as nebulizing gas (10 psi) while nitrogen was used as curtain gas (20 psi) and collision gas. Instrument control, data acquisition and data processing were achieved using Analyst software (QS 2.0) provided by Applied Biosystems. One part (a few mg) of each membrane explanted from rats was cut in small pieces and sonicated for 10 min in 300 µL of a methanolic solution of ammonium acetate (3 mM). Ammonium acetate assists the deprotonation process during ESI of the oligourethane taggant, and its presence in the extractive solution allows direct injection of the extracts with no prior dilution. For useful comparison, all MS and MS/MS data were recorded in the same conditions (100 cumulated spectra, 1.7 min acquisition).

B.3 High-Performance Liquid Chromatography-Mass Spectrometry (HPLC-MS) for leaching test samples.

In contrast to explanted film extracts, samples collected during leaching tests contained a large amount of PBS which would affect the ionization yield of the targeted taggant. To avoid direct injection in the ESI source, PBS solutions were analyzed with a HPLC-ESI-MS coupling that allowed the PBS buffer to be eluted in the void volume. These measurements were performed using

a Zorbax eclipse plus phenyl-hexyl column (4.6*100 mm, 3.5 µm, Agilent Technology, Santa Clara, CA) held at 35°C in the oven of an Agilent Series 1100 HPLC system equipped with a binary pump and an autosampler (V_{inj} = 10 µL). The mobile phase was delivered at a 1 mL min^{-1} flow rate, as follows: eluent A: H_2O + 0.1% formic acid; eluent B: MeOH + 3 mM ammonium acetate; gradient: 80% A from t=0 min to 2 min, then 50% A from t=4 min to 6 min, then 0% A from t=26 min to 28 min (return to initial conditions in 2 min and kept stable for 5 min). The column effluent was directed to the ESI source to t=6 min after a flow split of 1/50. In these experimental conditions, the PU taggant was measured at a 16.6 min retention time.

B.4 **AUTOMATED SEQUENCING WITH MS-DECODER.** MS-DECODER is a platform-independent in-house developed software that can run on any computer with Java8 installed (Windows, macOS, Linux derivatives…). [131] The software source code is freely available on github: https://github.com/LSMBO/MS-Decoder.

C. EXPERIMENTAL PROCEDURES

C.1 SYNTHESIS OF THE OLIGO-URETHANE TAGGANT.

Sequence-coded oligourethanes were prepared on a hydroxy-functionalized crosslinked polystyrene resin using two iterative coupling steps, as previously reported. [39] In a first step, the modified resin (100 mg, 1 Eq) was placed in a microwave glass tube. A solution of DSC (145 mg, 6 Eq) in acetonitrile anhydrous (2 mL) and (0.2 mL, 1.4 mmol) triethylamine or (0.1 mL, 1.2 mmol) pyridine was added in the tube. The tube was sealed under argon flow and the mixture was stirred in the microwave reactor for 1 hour at 8 Watt, 60°C. After reaction, the resin was washed five times with DMF. In the second step, a solution of an amino alcohol (either 84 mg for 0 or 97 mg for 1, 10 Eq), triethylamine (0.3 mL, 2.1 mmol) either pyridine (0.15 mL, 1.8 mmol) in 2 mL DMF anhydrous was added to the resin in a SPE plastic tube and the mixture was shaken for 20 minutes at room temperature. At the end of the reaction, the resin was washed five times with DMF, washed with diethyl ether and then was transferred back to the microwave tube. These two coupling steps were repeated a certain number of times until a desired chain-length and coded sequence were attained. The cleavage of the oligomers from the resin was achieved by using a TFA/CH_2Cl_2 (1:1 v/v). After filtering-off the resin, TFA and CH_2Cl_2 were evaporated under reduced pressure to afford the desired oligourethanes as solids.

C.2 AUTOMATED SYNTHESIS OF THE OLIGOURETHANE TAGGANT.

The stepwise oligourethane chemistry described in section C.1 was also performed automatically on a SWING platform from Chemspeed Technologies AG. The molar ratios between reactants were the same as in A.2 unless noted. All the required steps of the iterative synthesis were recorded as computer commands in the Autosuite Editor Program (version 2.0.16.1) and carried out on the automated platform by the Autosuite Executor module of the software. The Chemspeed synthesizer is equipped with a variety of blocks and tools (Figure S2) allowing liquid cold chemicals storage (A), warm storage (B), solid phase synthesis (C), inert gas use, heating, filtration and automated transfer of liquids in the resin reactors through a 4-channel liquid handling unit with 4 syringe pumps (D) (transfer values used: air gap volume: 10 μL, source and destination speed: 10 mL/min). The glass reactors of (A), (B) and (C) were connected to an argon line (0.2 bar). Modified resin was weighed and put in the one vessel of the Solid Phase block (C). The reactants, 4-amino-1-butanol (0-bit), 4-amino-2-methyl-1-butanol (1-bit), anhydrous pyridine, diethyl ether and anhydrous DMF were placed in vials on the storage rack (A) on the left of the platform. DSC was dissolved in anhydrous acetonitrile (same quantity of DSC as in A.2 in 2.5 mL dry ACN) and placed in the reactors of the reaction block (B), where warm oil circulation can be applied if necessary. Before each addition of DSC solution in the reaction mixture, the area (B) was heated for some minutes at 60°C to favor complete DSC dissolution in ACN. For the first reaction step, pyridine and a warm solution of DSC in ACN were transferred to the solid-phase reactor in (C) with the help of an automated syringe (D). Instead of microwave irradiation used in conventional manual synthesis (see A.2), this step was performed upon simple heating at 60°C for 1 hour under vortex shaking (speed used=500-600 rpm). After performing this step, vacuum filtration was applied to the reactor to remove the solvents and DMF was added several times for washing the resin. For the second reaction step, 4-amino-1-butanol (or 4-amino-2-methyl-1-butanol), pyridine and anhydrous DMF were added in (C) with the help of an automated syringe (D). The reaction was then performed at room temperature for 30 minutes, followed by solvent removal and successive DMF (4 times) and diethyl ether (1 time) washing. The two steps were repeated a given number of times until the desired length and sequences were reached. Once the synthesis is finished, the oligomer anchored on resin was removed from the robot and added in the TFA/ DCM (1/1) cleavage solution to detach it from the solid support and then left to dry to afford the oligourethanes as solids.

C.3 PREPARATION OF TAGGED AND NON-TAGGED CROSSLINKED PVA FILMS.

Crosslinked PVA films (about250 μm thick) were prepared based on a method previously reported.[250]For the oligourethane-tagged films, PVA (2 g) was first dissolved in hot deionized water (20 mL) at 90ºC. The solution was stirred for 3 hours until complete dissolution of the polymer. 20 mg of the oligourethane taggant (1% wt comparing with PVA) were dissolved in 2 mL DMF and the resulted solution was added to the PVA solution and left stirring for one hour more. Then the

temperature of the solution was cooled down to room temperature before the addition of the sodium trimetaphosphate solution in distilled water (0.15 mL, 15% w/v). When a homogeneous mixture was obtained, an aqueous solution of NaOH (0.06 mL, 30% w/v) was poured into the mixture. The mixture was poured into glass plates and left for 48 h for the complete evaporation of the solvents at 40°C. The prepared films were rinsed with water for one day by changing the water three to four times and stored at 4°C. Non-tagged crosslinked PVA films were prepared following the same procedure but without incorporating the taggant. Although not necessary, DMF (2 mL) was also employed in this procedure in order to prepare fully comparable samples.

C.4 CONTROL OF THE HOMOGENEITY OF THE TAGGANT DISPERSION IN PVA.

The homogeneity of the taggant dispersion in crosslinked PVA was characterized by ^{1}H NMR. The films were cut in different sub-pieces that were solubilized in DMSO-d_6 and individually analyzed. The obtained spectra were compared to a reference spectrum of a non-tagged PVA films in order to detect typical signals of the taggant.

C.5 IN VITRO CHARACTERIZATION OF TAGGANT-LEACHING FROM THE PVA FILMS.

A small piece of an oligourethane-tagged PVA film was incubated in PBS solution in order to investigate the potential release of the taggant from the model implant. To do so, a square centimeter tagged film was immersed in 20 mL phosphate-buffered saline solution with pH=7.4 and kept at 37°C for 14 days. Periodically, 1 mL of the supernatant solution was taken and analyzed by HPLC-MS.

C.6 CELL CULTURE

Human umbilical vein endothelial cells (HUVECs) and NIH3T3 fibroblasts were obtained from ATCC. Cells were cultured in Dulbecco minimum essential medium-L-glutamine (DMEM), supplemented with 10% (v/v) fetal bovine serum (FBS) and 1% penicillin-streptomycin-amphotericin (PSA). Cells were seeded in a T75 cell culture flask and kept under controlled conditions (5% CO_2 at 37°C) throughout the whole experiment.

C.7 IN VITRO TOXICITY TESTS.

The taggant was dissolved in MeOH under magnetic stirring at 55°C at 10 mg/ml and then diluted in cell culture media at different concentrations. Cell viability was assessed using a Resazurin assay. Cells were seeded in 96-well plate (10,000/well) and cultured overnight to assure cell adhesion. Then, cell culture was removed and cells were treated with 7 different concentrations of the taggant (1, 0.5, 0.25, 0.12, 0.06, 0.03, 0.01 mg/mL; n=3; 100 µL/well). After 4 hours, 24 hours and 48 hours, cells supernatant was removed, cells were washed once with PBS, and then incubated with 100 µL/well of a solution containing 10% of resazurin in cell culture medium. 1.5 hours later, the optical density was

recorded at 560 nm (590 nm reference wavelength; i-control microplate reader software, TECAN Männedorf, Switzerland). Cells treated with culture medium were included as negative controls. Also the toxicity of the MeOH at the doses present in the treatment groups was assessed using solutions prepared only with MeOH and culture medium. For statistical analysis, 3 independent experiments were performed.

C.8 IMPLANTATION IN WISTAR RATS.

TheprocedureandtheanimalcarecompliedwiththePrinciplesofLaboratoryAnimal Care formulated by the National Society for Medical Research. All animals were kept at 20-26°C controlled temperature, under a regular 12 hour light cycle. Food and water wereprovided *ad libitum* and environmental enrichment was assured. The studies were carried out under authorization number 006235 of the Ministere de l'Agriculture, France. In total, 8 male Wistar rats (15 weeks) were assigned to three groups (1 week n=3; 4 weeks n=2; 12 weeks n=3). Immediately before implantation, PVA films were cut (1 cm x 1 cm) and were submitted to UV irradiation for 30 minutes. Implantation was performed under general anaesthesia with inhaled isofluorane. Two different abdominal implantation methods were used for each animal, namely intramuscular and subcutaneous. Intramuscular implantation was done into the space between external and internal muscle layer, created by small incision between two muscle layers. In the case of subcutaneous implantation, the implants were inserted far away from the cutaneous incision, to minimize the trauma around the implant. The incisions were then sutured using a 4.0 Prolene suture. Each animal was implanted with both tagged and non-tagged PVA films. At the end of the study, 12 weeks after implantation, organs were collected for histological examination and blood was collected for hematological analysis.

C.9 EXPLANTATION.

One week, one month, and three months after implantation, animals were sacrificed under general anesthesia with inhaled isoflurane and implants harvested for further analysis. Newly formed tissue surrounding the material was removed to collect just the implant that was dried and cut in two parts of same size, one of which was used for selective extraction and MS analysis.

C.10 TAGGANT EXTRACTION AND MS/MS SEQUENCING.

Blind analysis was performed in order to prove the efficiency of the oligourethane-tagging of *in vivo* implanted films. The analyst was not aware of the type of implant (tagged or non-tagged) that was measured. Tagged and non-tagged films were macroscopically not distinguishable from another. The explanted implant was cut in tiny pieces and immersed in 300 µL of a methanolic solution with ammonium acetate (3 mM). The mixture was placed for 10 minutes in ultrasonic bath for taggant extraction. Each extract was then injected in the electrospray ionization source operated in the negative mode.

C.11 Histological tests.

Organs harvested at the end of the study were fixed in 4% paraformaldehyde solution, embedded in OCT (Optimal Cutting Temperature compound) and frozen in isopentane cooled in a liquid nitrogen bath. A cryo-microtome was used to prepare 10 μm thick sections of the tissues. Samples were stained with hematoxylin eosin following a common protocol: Mayer hematoxilin for 4 minutes, rinsing in tap water, immersion in 1% acid acetic solution, rinsing in tap water, stain in eosin for 2 minutes, rinsing in tap water, dehydration and mounting. NanoZoomer digital slide scanner was used for image analysis.

C.12 Hematological tests.

After 3 months of implantation, plasma samples were collected in heparinized tubes and analyzed using a Vet ABC ™ Hematology Analyzer.

C.13 Statistical analysis.

Unpaired nonparametric Kruskal-Wallis test was used; $p<0.01$ was considered as significant.
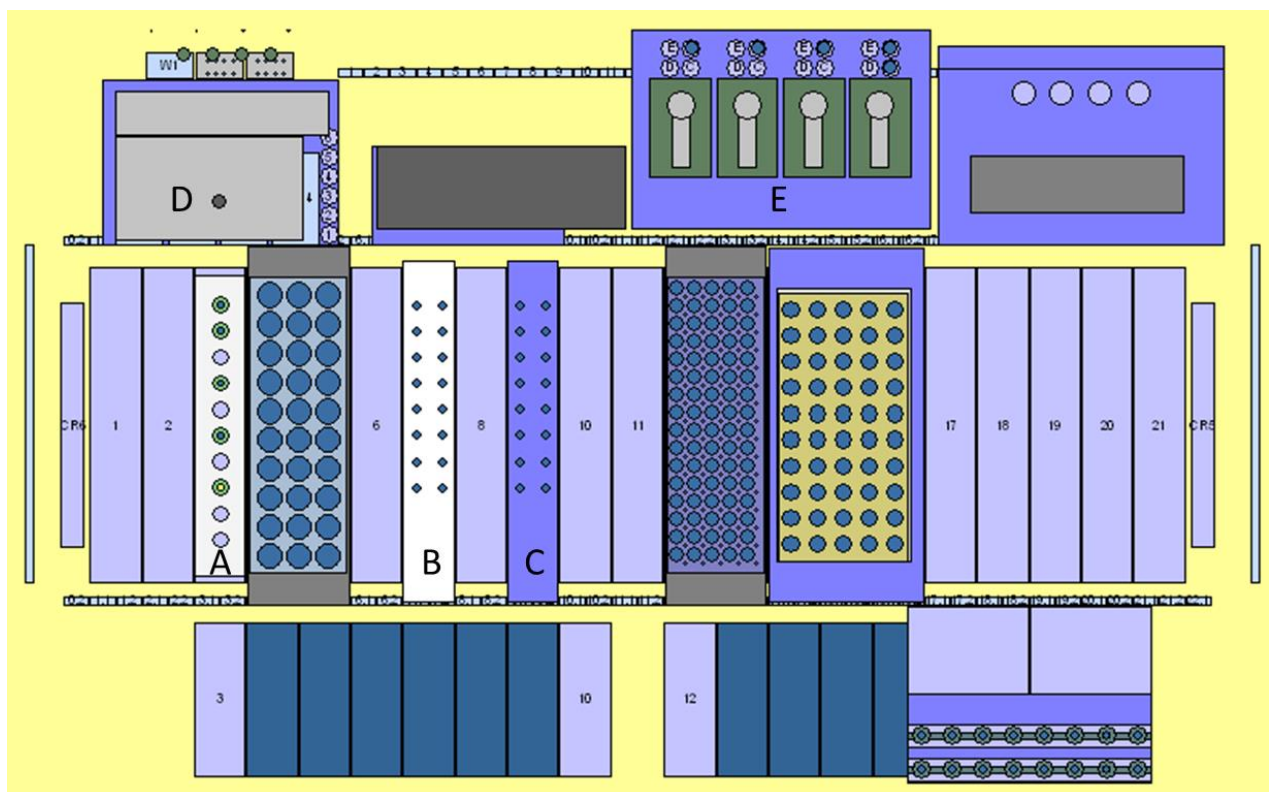
D. Supplementary Figures

Figure S. 1 : Configuration of the automated platform used in this study: A = stock solution rack, B = reaction block, C = solid phase block, D = 4-channel liquid handling unit, E = syringe pumps.
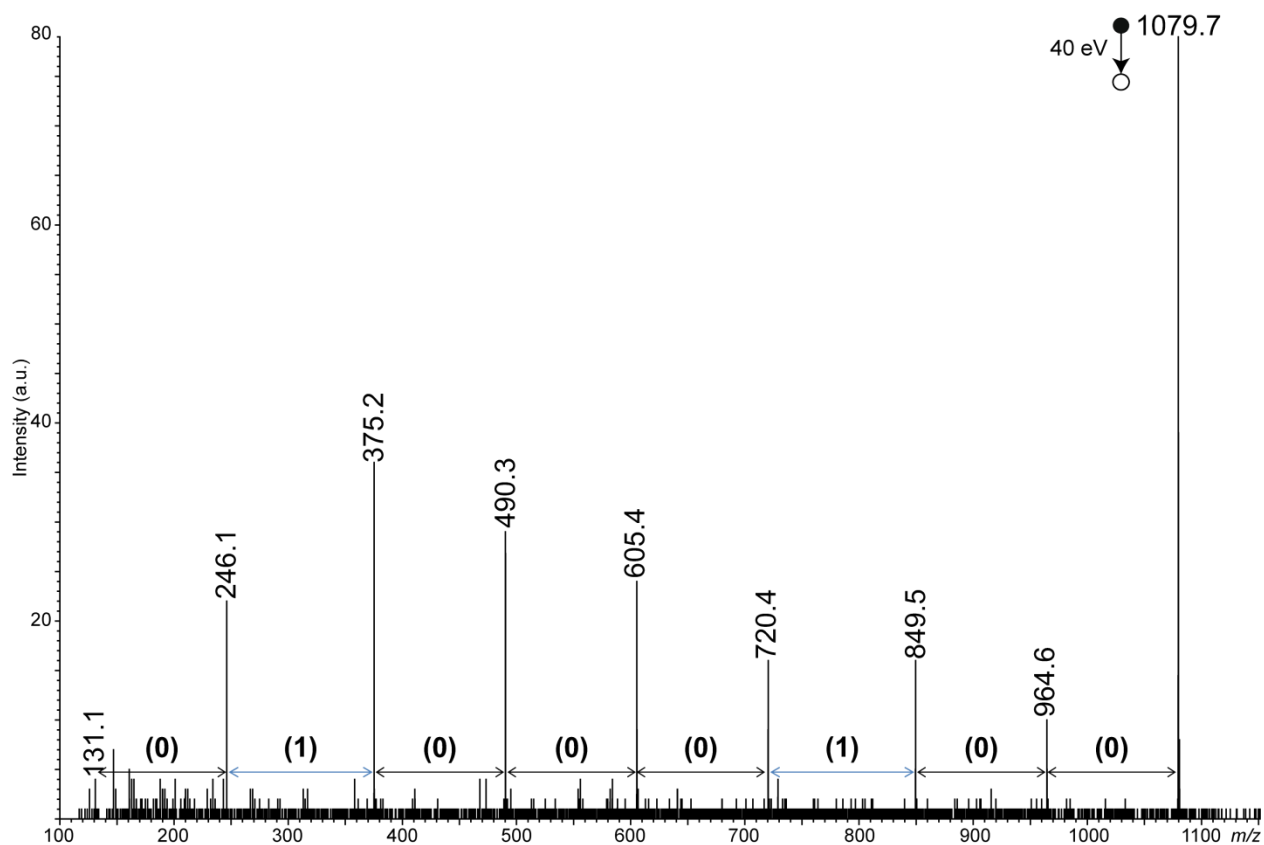
Figure S. 2 : ESI-MS/MS of the *m/z* 1079.7 precursor ion detected in the methanolic extract of the PVA film explanted from cut 2 of Rat 4: in spite of the very low abundance of this ion in MS (see Figure III. 9 in main document), its fragmentation pattern still allowed unambiguous reading of the α-01000100 code stored in the oligourethane taggant.

CHAPTER IV: SEQUENCE-DEFINED POLYURETHANES USE AS TAGGANTS FOR WOOD LABELING

A. CHEMICALS

Compounds	Suppliers	Purity (%)
4-Amino-1-butanol	TCI	98%
4-amino-2-methyl-1-butanol	TCI	98%
N,N'-disuccinimidyl carbonate (DSC)	TCI	>98.0%
Triethylamine (TEA)	Merck	>97%
Pyridine anhydrous	Sigma-Aldrich,	99.8% in Sure/Seal™
anhydrous acetonitrile (dry ACN)	Sigma-Aldrich	99.8%
dichloromethane (DCM)	Sigma-Aldrich, Carlo Erba	≥99.9%)
diethyl ether	Carlo Erba	-
anhydrous N,N-dimethylformamide(dry DMF)	Sigma-Aldrich	99.8%
N,N-dimethylformamide(DMF)	Sigma-Aldrich	≥99.0%
Tetrahydrofuran(THF)	Aldrich	99%, stabilized with BHT
Trifluoroacetic acid (TFA)	Sigma-Aldrich	99%

Triethylamine was kept on KOH pellets in dark. All the rest reactants and solvents were used as purchased.

B. MEASUREMENTS

B.1 DESI-MS AND DESI-MS/MS

DESI-MS analyses were performed on a Synapt-G2 (Waters, UK) equipped with a 2D DESI ion source (Prosolia, USA) operated in the negative ion mode using the following parameters: capillary voltage: -3.5 kV; sampling cone voltage: -40 V source temperature 100°C. Solvent is sprayed at 2 µL min^{-1} under a desolvation gas (N$_2$) flow of 10 bars. The entire wood piece was directly placed on

the DESI plate without any previous preparation and analyzed by DESI-MS with sprayed solution 90%MeOH/3 mM ammonium acetate/10% THF. Data analyses were conducted using the MassLynx 4.1 and DriftScope 2.1 programs provided by Waters and OmniSpray 2D for the DESI source (Prosolia).

B.2 ESI/MS AND MS/MS

High resolution MS and MS/MS experiments were performed using a QqTOF mass spectrometer (QStar Elite, Applied Biosystems SCIEX, Concord, ON, Canada) with the ESI source operated in the negative mode (capillary voltage: -4200 V; cone voltage: -75 V). Ions were accurately mass measured in the orthogonal acceleration time-of-flight (oa-TOF) mass analyzer, using PEG oligomers adducted with an acetate anion (in MS) or the precursor ions (in MS/MS) as internal standards. In this instrument, air was used as nebulizing gas (10 psi) while nitrogen was used as curtain gas (20 psi) and collision gas. Instrument control, data acquisition and data processing were achieved using Analyst software (QS 2.0) provided by Applied Biosystems. One part (few mg) was scratched to obtain the wood dust and sonicated for 10 min in 500 μLof a methanolic solution of ammonium acetate (3 mM). The supernatant was recovered from the4 minutes certification at 13000 rpm. The later was further diluted to the 1/10v/v and analyzed by ESI-MS.

B.3 SEC CHROMATOGRAPHY

The SEC setup used in this work was equipped with a Shimadzu RiD-10A refractometer, a Shimadzu SPD-10Avp UV detector, and four monoporosity PLGel columns (5 mm, 30 cm, diameter = 7.5 mm): 50, 100, 500, and 1,000 A°. This setup was used for characterization of oligomers and short polymers (100–20,000 g/mol). In both setups, the mobile phase was THF with a flow rate of 1 mL/min. Toluene was used as the internal reference. The calibration was based on linear PS standards from Polymer Laboratories.

C. EXPERIMENTAL PROCEDURES

C.1 MOLECULAR ANTI-COUNTERFEIT TAG PREPARATION

By automatic or manual solid phase synthesis the poly(urethane)s containing information used as anti-counterfeiting markers were prepared as presented page (160-161).

C.2WOOD LABELING

The tagging process of the molecular anti-counterfeit labels on the wood was achieved by impregnation. Several solvents were tested for the labeling of the wood based on their swelling effect on the wood species. DMF, THF, methanol were used to dip small wood pieces. The wood weighed ranging from 1.3 to 1.6 g depending on the species and its dimensions were 2 cm*1.8 cm*0.5 cm. A

piece was immersed in 10 mL of poly(urethane)solution (~0.2 %w/w)(poly(urethane) compared to wood weight was varying from 1.3 % v/v to 1.6% v/v). The wood in the taggant solution was stirring for 8 hours in order to keep the entire surface in the solution. One hour with accompanied with heating at 60 °C and the rest in R.T. Afterwards, it was removed from the solution and let dry for 24 hours.

C3. LABEL EXTRACTION FROM THE WOOD

The taggant used anti-counterfeit label for the wood was analyzed by ESI-MS and MS/MS. But first in order to acquire the label two different procedures took place. On the one hand, a piece from the entire wood was sawn in order to recover the sawdust. The latter (120.6 mg) was immersed in a solution (500 μL) of MeOH with ammonium acetate (3 mM). The mixture was subjected to ultrasound for 10 minutes for the oligomer extraction. The supernatant was recovered and then centrifuged for 4 minutes at 13,000 rpm. After a 1/10th dilution, this extract was analyzed by ESI-MS. On the other hand, a massive piece was analyzed directly by DESI-MS spectrometry with solvent mixture of 90% MeOH / ammonium acetate (3Mm)- 10% THF)

C.4 INVESTIGATION OF TAGGANT ABSORBANCE DEPTH.

After the 24 hours wood drying it was cut in layers with the help of the technique called milling. Two kinds of appliances were used to cut the wood in four layers. At the beginning, a Hure 301 manual milling machine, then a PMER 3AC CNC milling machine programmed by ANILAM software (to automatize the machining of the different layers of the square hollow). The screws and wedges (devices to hold the piece of wood) as well as the cutter (tool used to cut the hollow) were cleaned with ethanol before use.

By removing 1 mm of the thickness of the upper layer of the piece and leaving 4 mm of each of the four sides around the cut square apart, it was possible to isolate the inner part of the wood. In the continue, 4 different layers of 0.375mm thickness each were cut in order to reach the middle of the wood. The four different layers were used for the ESI/MS and MS/MS analysis in order to investigate the depth of the taggant absorbance.
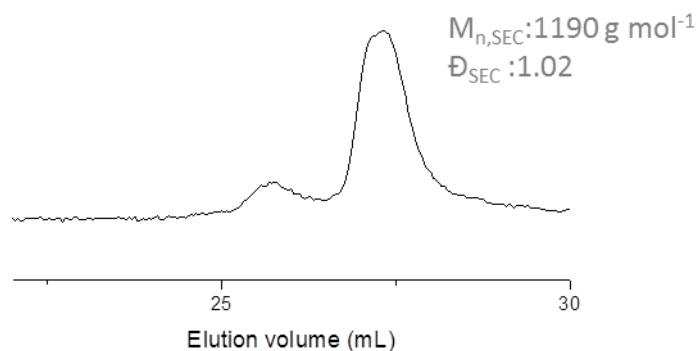
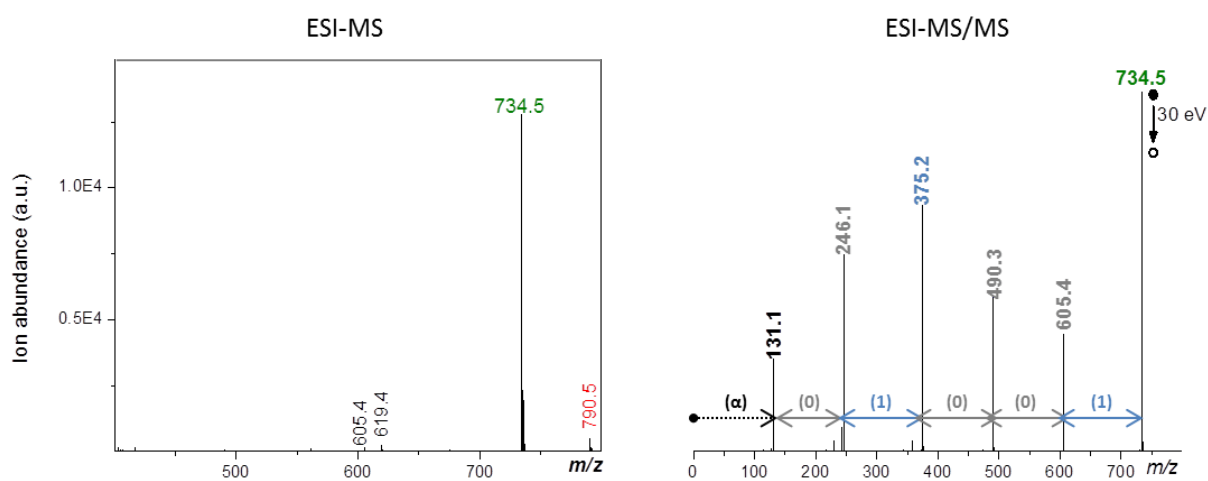**Figure S. 3 : SEC spectrum of the PU3 with monomer sequence 01001 (PU1).**

Figure S. 4 :ESI-MS spectrum in negative mode of the sample PU1 used for the labeling of beech (W1). The peak annotated with red corresponds to the Δ=+56 Da and the rest are small missteps.
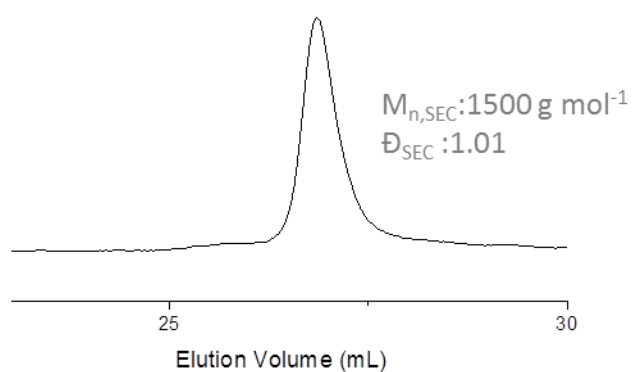

Figure S. 5: SEC spectrum of the PU2 with monomer sequence 000001

Figure S. 6 : ESI-MS spectrum (on the left) in negative mode and ESI-MS/MS (on the right) of the sample PU2 synthesized through manual solid phase synthesis and used for the labeling of beech (W2).

Figure S. 7 : SEC spectrum of the PU3 with monomer sequence01000100

Figure S. 8 :ESI-MS spectrum (on the left) in negative mode and ESI-MS/MS (on the right) of the sample PU3 synthesized through manual solid phase synthesis and used for the labeling of walnut (W3). Peaks annotated in red corresponds to the Δ=+56 Da of the miss step (964.6 *m/z*) and of the targeted oligomer (1079.6 *m/z*).
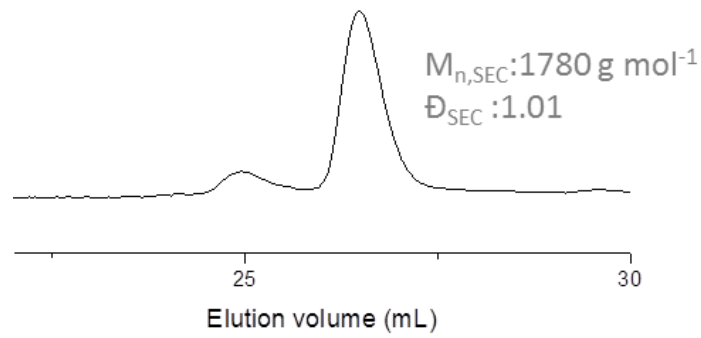
Figure S. 9 : SEC spectrum of the PU4 with monomer sequence01010110
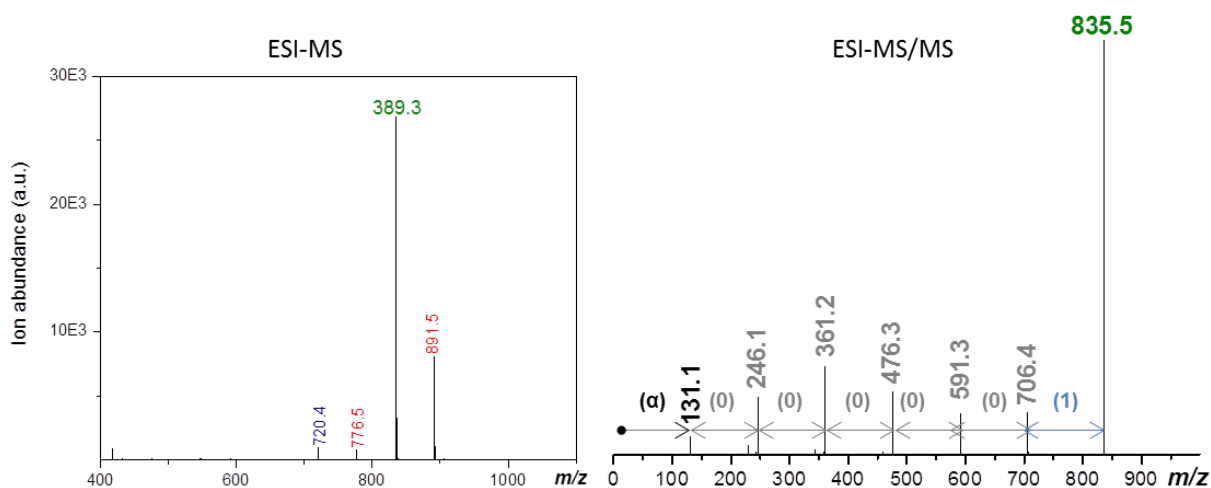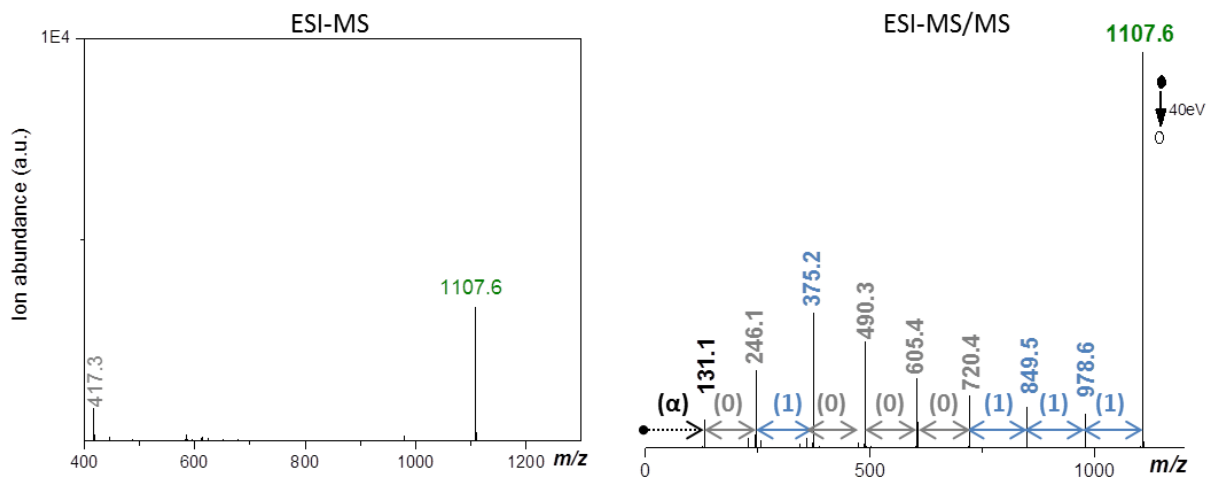

Figure S. 10 : ESI-MS spectrum (on the left) in negative mode and ESI-MS/MS (on the right) of the sample PU4 synthesized through manual solid phase synthesis and used for the labeling of oak (W4). Signal in grey from the background.
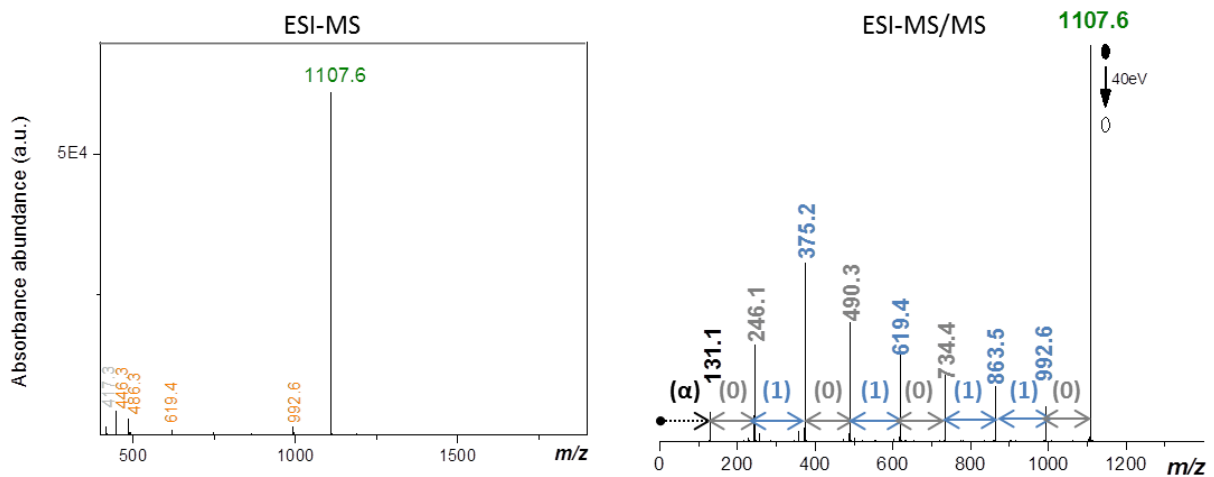
Figure S. 11 : :ESI-MS spectrum (on the left) in negative mode and ESI-MS/MS (on the right) of the sample PU5 synthesized through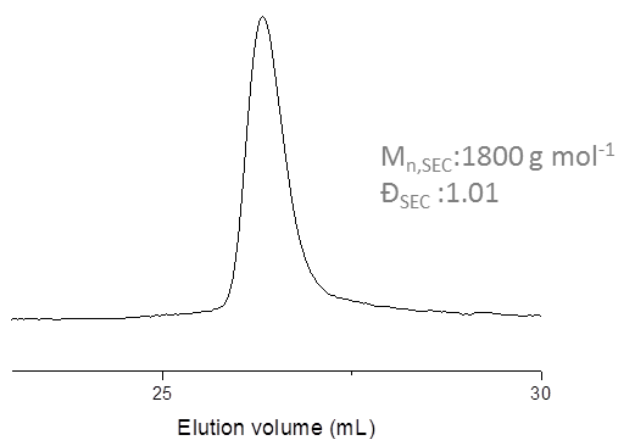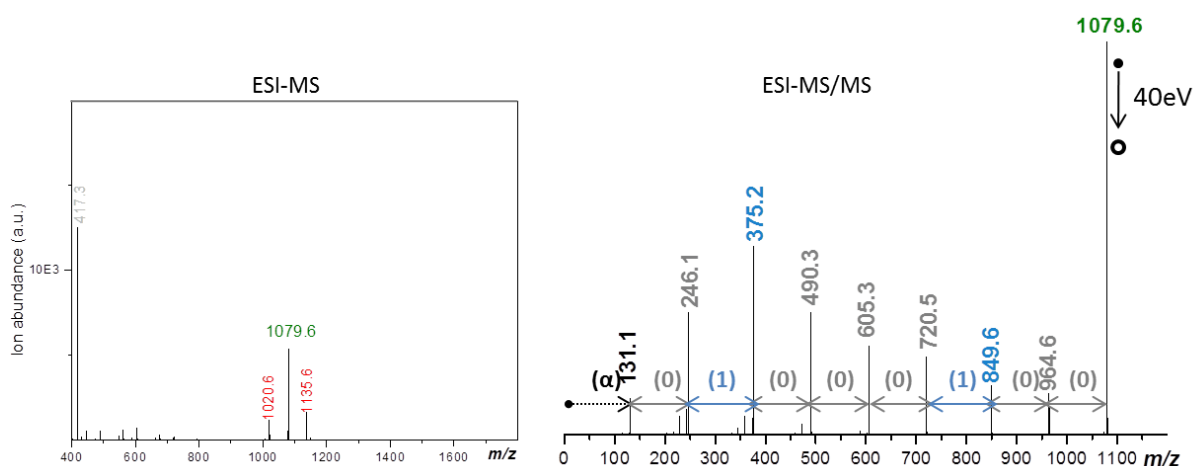 manual solid phase synthesis and used for the labeling of walnut and beech (W5 & W6). The peaks annotated in orange correspond to miss steps. Signal in grey from the background
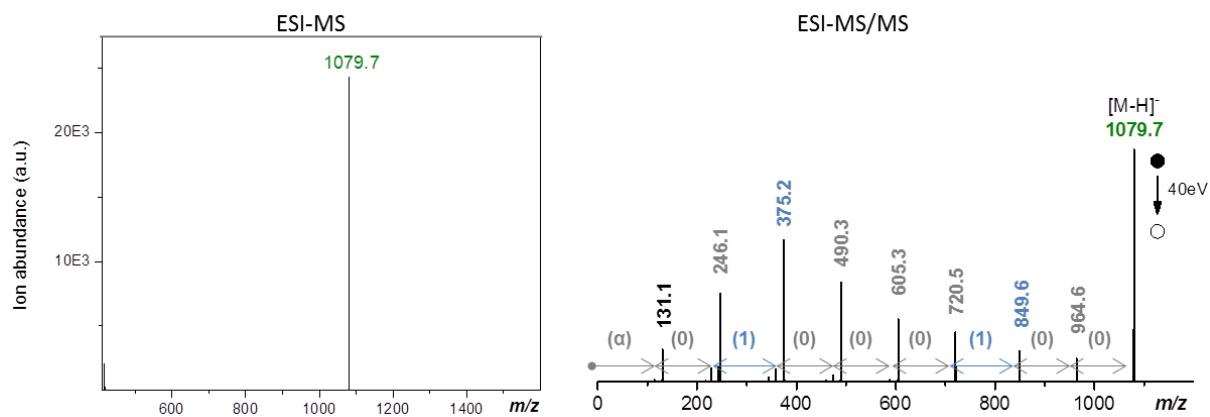
Figure S. 12: ESI-MS spectrum in negative mode of the sample PU6 synthesized through the automated approach used for the labeling of oak (W7).

CHAPTER V: 2D SEQUENCE-CODED OLIGO-URETHANE BARCODES FOR PLASTIC MATERIALS LABELING

A. CHEMICALS

| Compounds	Suppliers	Purity (%)
4-Amino-1-butanol	TCI	98%
4-amino-2-methyl-1-butanol	TCI	98%
N,N'-disuccinimidyl carbonate (DSC)	TCI	>98.0%
Triethylamine (TEA)	Merck	>97%
N, N, N', N', N''-pentamethyldiethylenetriamine (PMDETA)	Aldrich	99%
(1-bromoethyl)benzene	Alfa Aesar	97%
Phenol detached crystals	Alfa Aesar	99 %
poly(vinyl chloride) (PVC, high molecular weight)	Sigma-Aldrich	-
poly(ethylene terephthalate) (PET, granular)	Sigma-Aldrich	-
Styrene	Sigma-Aldrich	99%
Copper (I) bromide (CuBr)	Alfa Aesar	98%
anhydrous acetonitrile (dry ACN)	Sigma-Aldrich	99.8%
anhydrous dichloromethane (dry DCM)	Sigma-Aldrich	≥99.9%, 40-150 ppm amylene
dichloromethane (DCM)	Sigma-Aldrich, Carlo Erba	≥99.9%)
diethyl ether	Carlo Erba	-
anhydrous N,N-dimethylformamide(dry DMF)	Sigma-Aldrich	99.8%
N,N-dimethylformamide(DMF)	Sigma-Aldrich	≥99.0%

Tetrahydrofuran (THF)	Aldrich	99%, stabilized with BHT
Trifluoroacetic acid (TFA)	Sigma-Aldrich	99%

CuBr was purified by stirring in acetic acid and rinsed with ethanol and diethyl ether, then dried. Styrene was distilled over CaH2. Triethylamine was stored on KOH pellets in dark. The Wang resin (0.94 or 1.8 mmol/g, IRIS Biotech) used for sequence-defined oligourethane synthesis was modified with a cleavable linker as described in the literature.[299] The microwave instrument used for the first coupling step of the oligourethane synthesis was a Monowave 300 from Anton Paar. The second step of the oligourethane synthesis was conducted in solid phase extraction (SPE) tubes using a KS 130 basic (IKA) shaker. Methanol (Fisher Chemical) and ammonium acetate (Sigma-Aldrich) were used as received for mass spectrometry experiments.

B. MEASUREMENTS

B.1 SIZE EXCLUSION CHROMATOGRAPHY.

The SEC set-up used in this work was equipped with four PLGel Mixed C columns (5 mm, 30 cm, diameter: 7.5 mm), a Wyatt Viscostar-II viscometer, a Wyatt TREOS light-scattering detector, a Shimadzu SPD-M20A diode array UV detector and a Wyatt Optilab T-rEX refractometer. This set-up was used for polystyrene characterization (1,000–3,000,000 g·mol-1). The mobile phase was THF with a flow rate of 1ml/min. Toluene was used as the internal reference. The calibration was based on linear PS standards from Polymer Laboratories.

B.2 NUCLEAR MAGNETIC RESONANCE.

The homogeneity of the oligourethane libraries inclusion in polymer films was analyzed by ^{1}H NMR spectrometry on a Bruker Avance 400MHz spectrometer equipped with Ultrashield magnet. The spectra were recorded either in THF-*d6* or in DMSO-*d6*.

B.3 ELECTROSPRAY MASS SPECTROMETRY.

High resolution MS and MS/MS experiments were performed using a QStar Elite mass spectrometer (Applied Biosystems SCIEX, Concord, ON, Canada) equipped with an electrospray ionization (ESI) source. The capillary and cone voltages were respectively +5500 V and +75 V when operated in the positive ion mode, and - 4200 V and -75 V in the negative ion mode. In this hybrid instrument, ions were measured using an orthogonal acceleration time-of-flight (oa-TOF) mass analyzer. In the MS mode, accurate mass measurements were performed in the positive ion mode using reference ions from a poly(propylene glycol) or a poly(ethylene glycol) internal standard. In the MS/MS mode, a

quadrupole was used for selection of precursor ions to be further submitted to collision-induced dissociation (CID) in a collision cell. In this instrument, air was used as the nebulizing gas (10 psi) while nitrogen was used as the curtain gas (20 psi) as well as the collision gas. Instrument control, data acquisition and data processing of all experiments were achieved using Analyst software (QS 2.0) provided by Applied Biosystems.

C. EXPERIMENTAL PROCEDURES

C.1 SOLID-PHASE SYNTHESIS OF SEQUENCE-CODED OLIGURETHANES.

Digitally-encoded oligourethanes were prepared on a hydroxy-functionalized crosslinked polystyrene resin using two iterative coupling steps, as previously reported.[39] In a first step, the modified resin (100 mg, 1 Eq, loading: 1.8 mmol/g) was placed in a microwave glass tube. A solution of DSC (277 mg, 6 Eq) in acetonitrile anhydrous (4 mL) and (0.3 mL, 2.16 mmol) trimethylamine was added in the tube. The tube was sealed under argon flow and the mixture was stirred in the microwave reactor for 1h at 8 watt, 60ºC. After reaction, the resin was washed five times with DMF. In the second step, a solution of an amino alcohol (either 168 mg for 0 or 194 mg for 1, 10 Eq), trimethylamine (0.5 mL, 3.6 mmol) in DMF anhydrous was added to the resin in a SPE plastic tube and the mixture was shaken for 20 minutes at room temperature. At the end of the reaction, the resin was washed five times with DMF, washed with diethyl ether and then was transferred back to the microwave tube. These two coupling steps were repeated a certain number of times until a desired chain-length and digital sequence were attained. The cleavage of the oligomers from the resin was achieved by using a TFA/CH2Cl2 (1:1 v/v). After filtering-off the resin, TFA and CH2Cl2 were evaporated under reduced pressure to afford the desired polyurethanes as white solids. All oligomers were characterized by HR-ESI-MS as described in the main text. In some cases, in particular in the case of oligomers containing less than 5 coded bits, small peaks corresponding to dimer [2M-H2O-H]- and trimer [3M-2H2OH]- can sometimes be found in the final ESI-MS spectra. The species are probably formed by esterification of the COOH-, OH-terminated oligomers in the cleavage conditions. However, these peaks can be removed using a simple KOH treatment.

C.2 SYNTHESIS OF POLYSTYRENE BY ATOM TRANSFER RADICAL POLYMERIZATION.

To a 25mL round flask, purified CuBr (0.0114g, 0.0797 mmol) was added and then the flask was degassed through argon-vacuum cycles. Styrene (11 mL, 95.69 mmol) and PMDETA (0.016649 mL, 0.0797mmol) were poured into the round flask through the septum and stirred under argon flow for 20 min. Then, (1-bromoethyl)-benzene (0.010883 mL, 0.0797 mmol) was added and the reaction was conducted at 85oC for 44 hours. The final reaction mixture was precipitated in 100 mL of cold methanol, filtrated, washed with cold methanol and dried. The polymer formed was dissolved in THF and pass through a neutral alumina column in order to remove copper traces. The solution was

precipitated again in cold methanol to afford the desired polystyrene as a white solid. Size exclusion chromatography in THF: Mn = 58·700 g·mol-1, Đ= 1.24.

C.3 PROCEDURE FOR INCORPORATING 2D-CODED LIBRARIES IN PLASTIC FILMS.

The tagged polymer films were prepared in a glass Petri dish using a solvent casting procedure. A polymer (either PS, PVC or PET) was dissolved in an appropriate solvent (see below) at a concentration of 6% w/v. The oligourethane libraries (coded library 1: molar ratio **P1/P2/P3/P4** ~ 1/1/1/1.5; coded library 2: molar ratio **P1/P5/P6** ~ 1/1/1) were dissolved in the same solvent and both solutions were mixed. PS and PVC membranes were prepared in THF at 50oC, whereas PET was dissolved in phenol at 90oC for 1-2 h. The obtained PET solution was poured into a glass plate and kept at 70°C for 20 h. The PS and PVC mixtures were left at r.t. until complete evaporation of the solvent. After evaporation, the casted polymer thin films were detached from the glass substrate by adding water. For films labeled with the three-component and four component libraries, the global oligourethane content embedded in the dried films was 0.65 and 0.75 wt%, respectively.

C.4 PROCEDURE FOR BARCODE EXTRACTION.

Sequence-defined oligourethanes were extracted using the same protocol independently of the polymer matrix. Films were slightly cut into 1-5 mm² pieces and a few mg (2-5) were sonicated for 10 min in 300 μL of methanol containing 3 mM of ammonium acetate. Resulting extracts were injected in the ESI source at a 10 μL min-1 flow rate using a syringe pump.

D. ADDITIONAL FIGURES

Figure S. 13 : Negative mode ESI-MS of oligomer P1 **(α-01) detected as a deprotonated molecule at** *m/z* **375.2. Additional peaks correspond to sample impurities (in black) or background signals (in grey).**
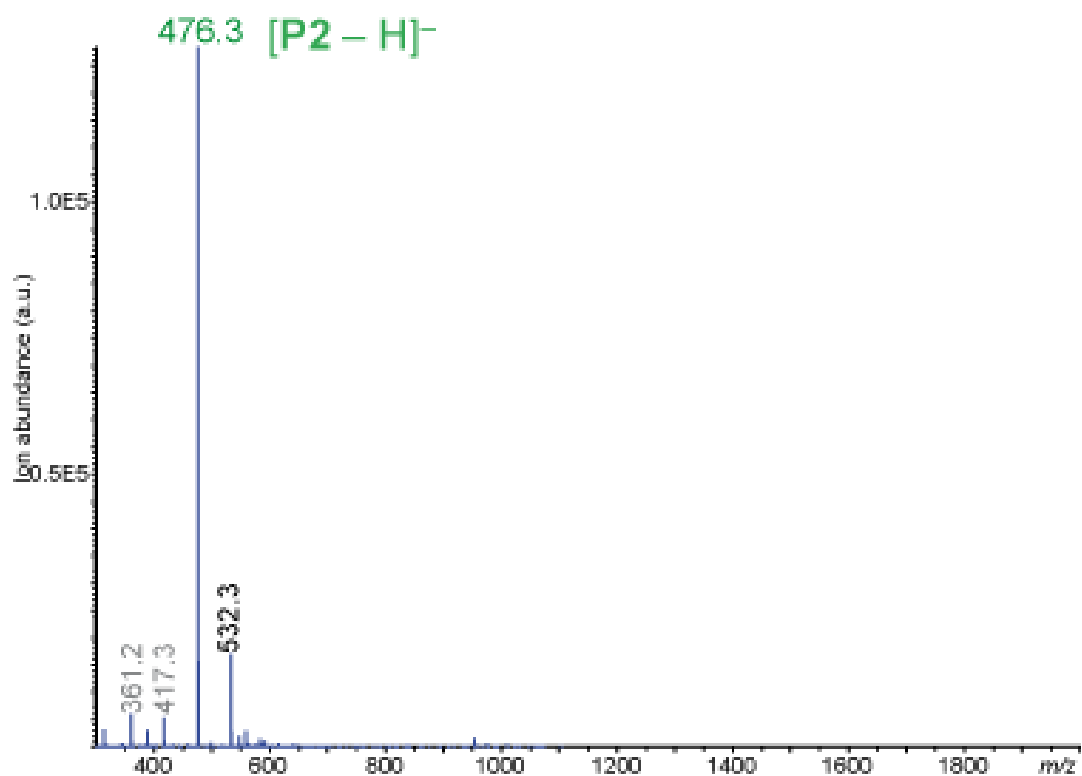
Figure S. 14: Negative mode ESI-MS of oligomer P2 **(α-000) detected as a deprotonated molecule at** *m/z* **476.3. Additional peaks correspond to sample impurities (in black) or background signals (in grey).**
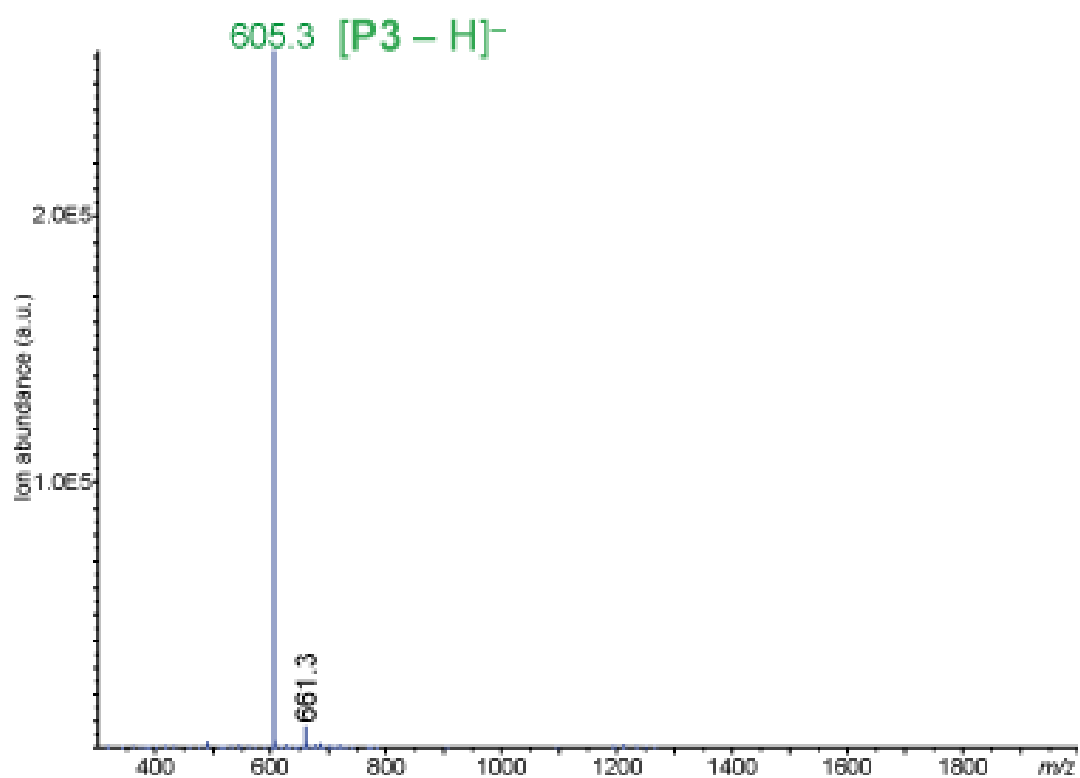
Figure S. 15: Negative mode ESI-MS of oligomer P3 **(α-0010) detected as a deprotonated molecule at** *m/z* **605.3. Additional peak corresponds to a sample impurity (in black).**
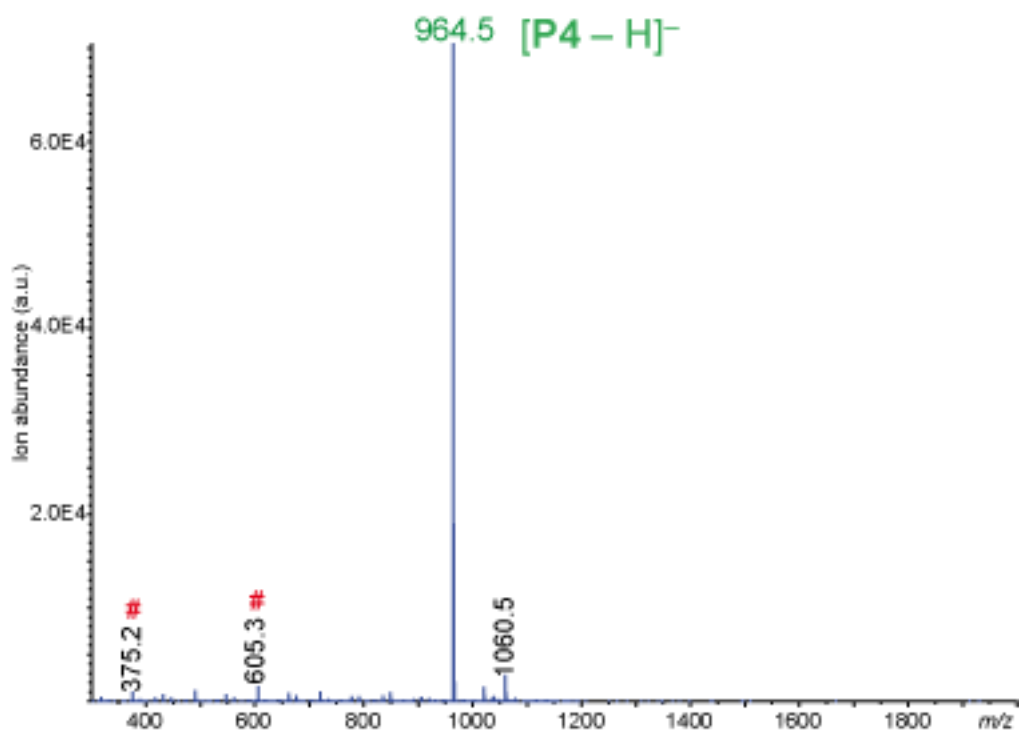
Figure S. 16: Negative mode ESI-MS of oligomer P4 (α-1000010) detected as a deprotonated molecule at *m/z* 964.5. Additional peaks correspond to sample impurities (in black). # : see discussion related to Figures V.5 & V.7
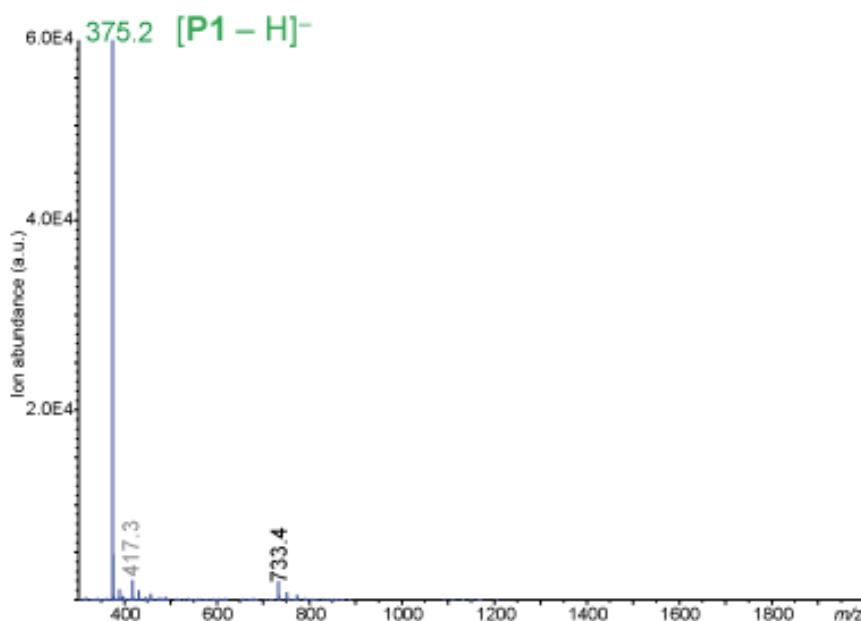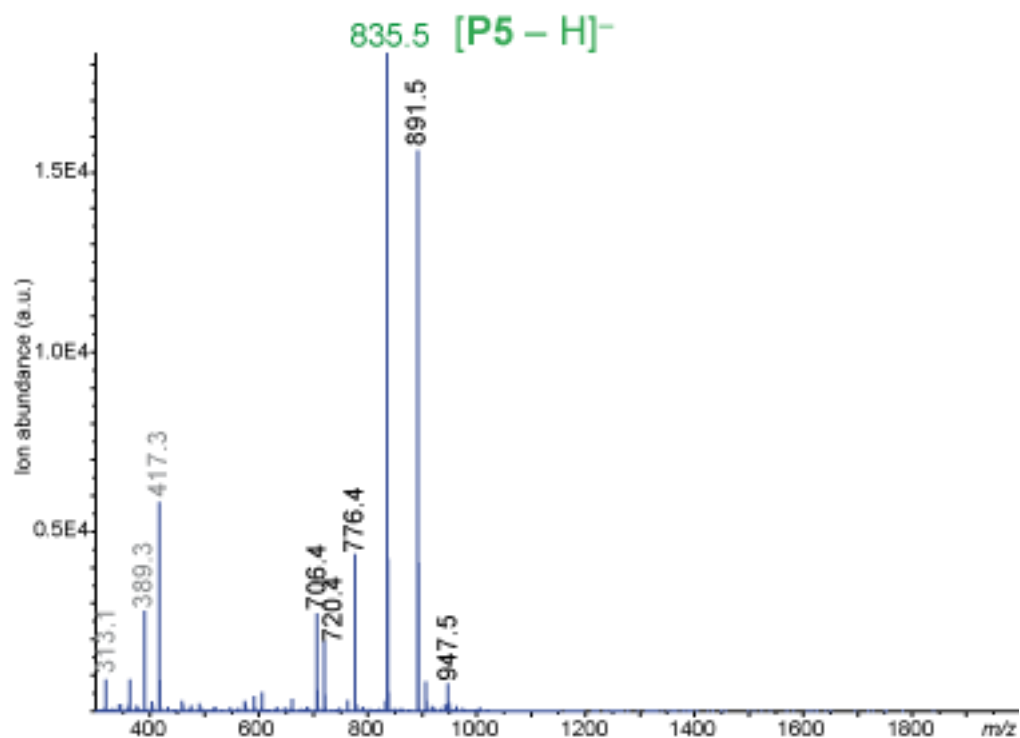

Figure S. 17 : Negative mode ESI-MS of oligomer P5 (α-000001) detected as a deprotonated molecule at *m/z* 835.5. Additional peaks correspond to sample impurities (in black) or background signals (in grey).
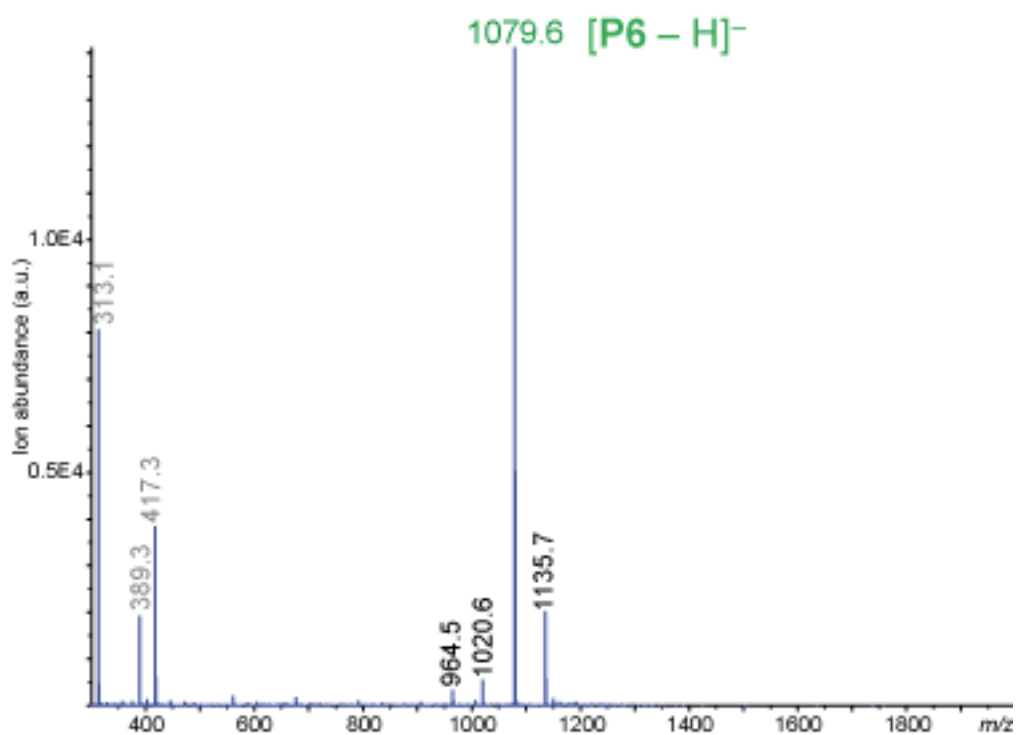
Figure S. 18 :. Negative mode ESI-MS of oligomer P6 **(α-01000010) detected as a deprotonated molecule at** *m/z* **1079.6. Additional peaks correspond to sample impurities (in black) or background signals (in grey).**
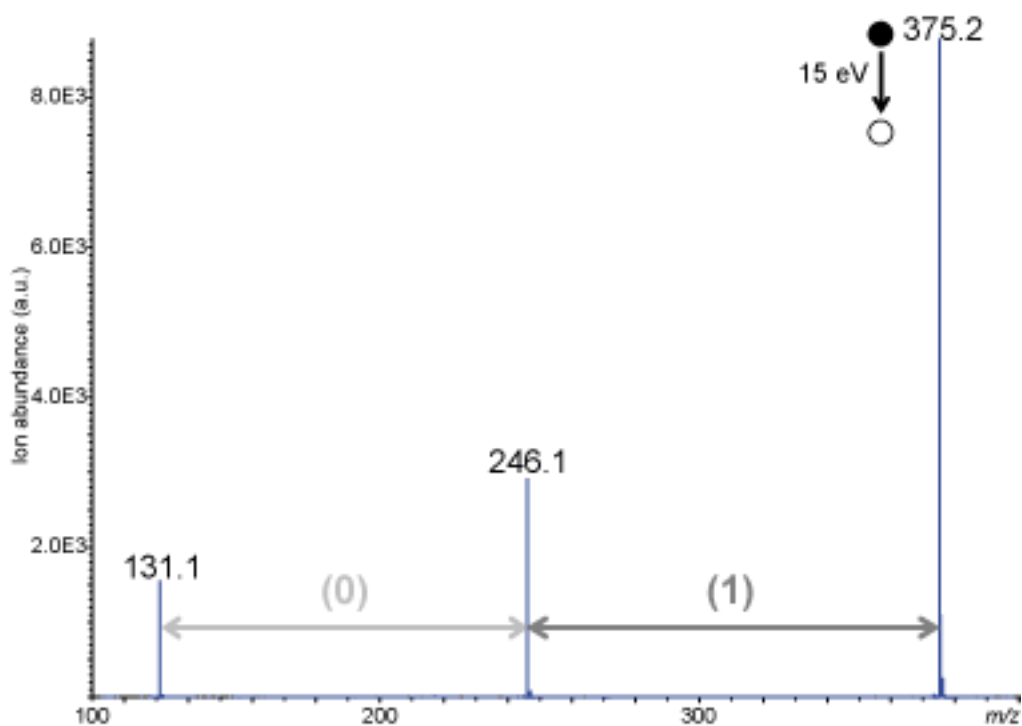

Figure S. 19 : MS/MS spectrum of [P1 – H]⁻ at *m/z* **375.2 using a 15 eV collision energy, allowing the 01 sequence expected for** P1 **to be validated.**
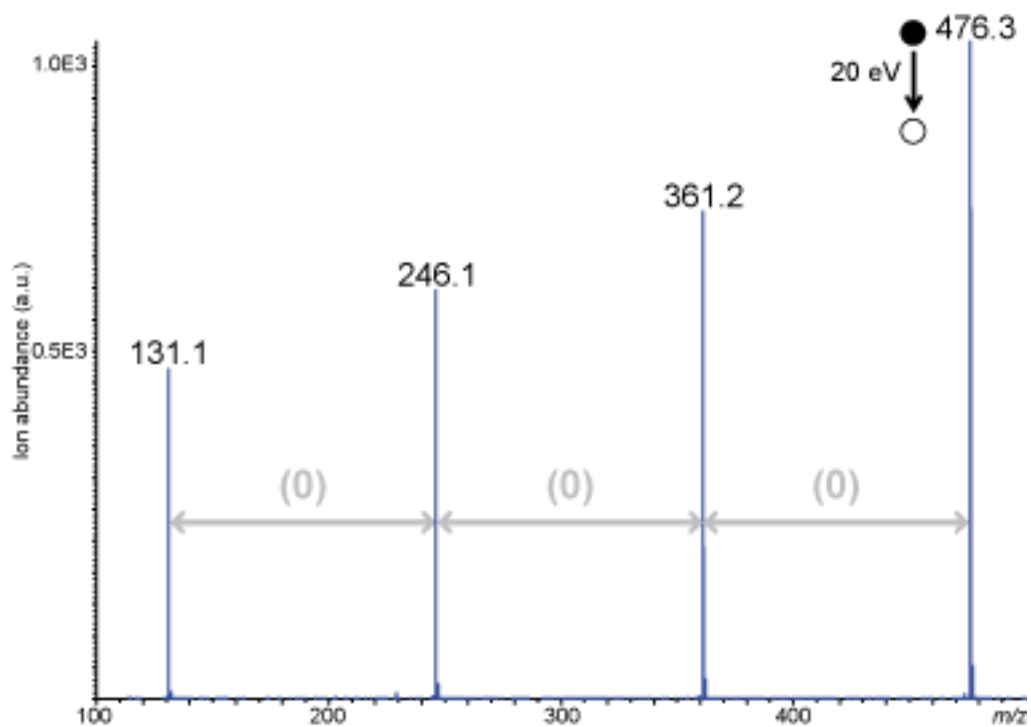
Figure S. 20 : MS/MS sequencing of [P2 − H]⁻ at _m/z_ 476.3 using a 20 eV collision energy, allowing the 000 sequence expected for P2 to be validated.
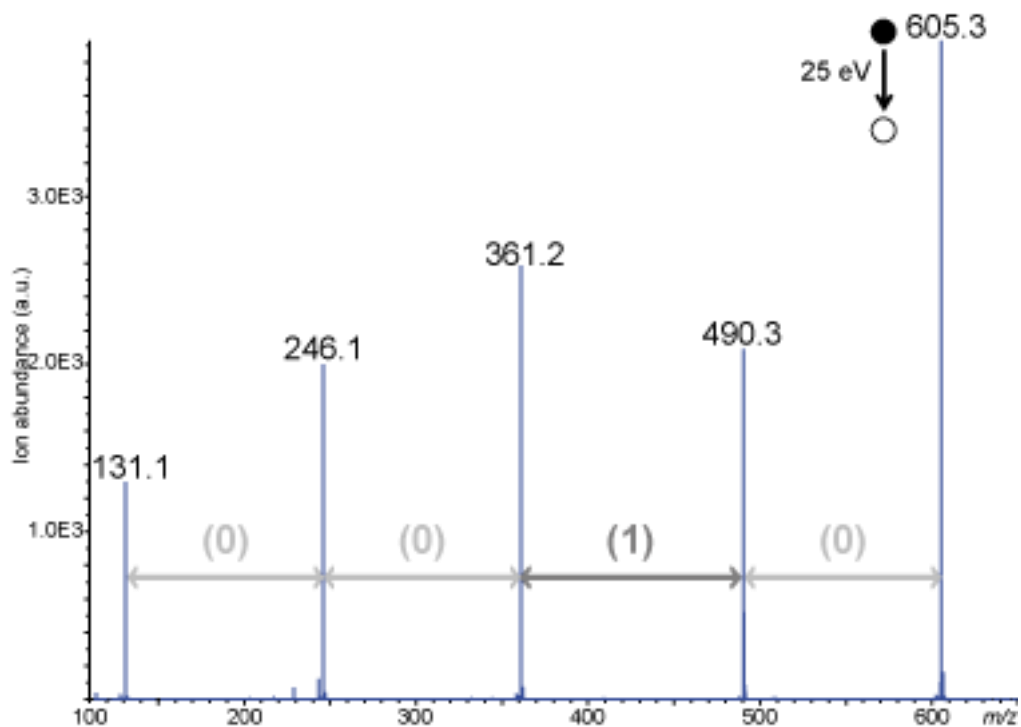
Figure S. 21 : MS/MS sequencing of [P3 − H]⁻ at _m/z_ 605.3 using a 25 eV collision energy, allowing the 0010 sequence expected for P3 to be validated.
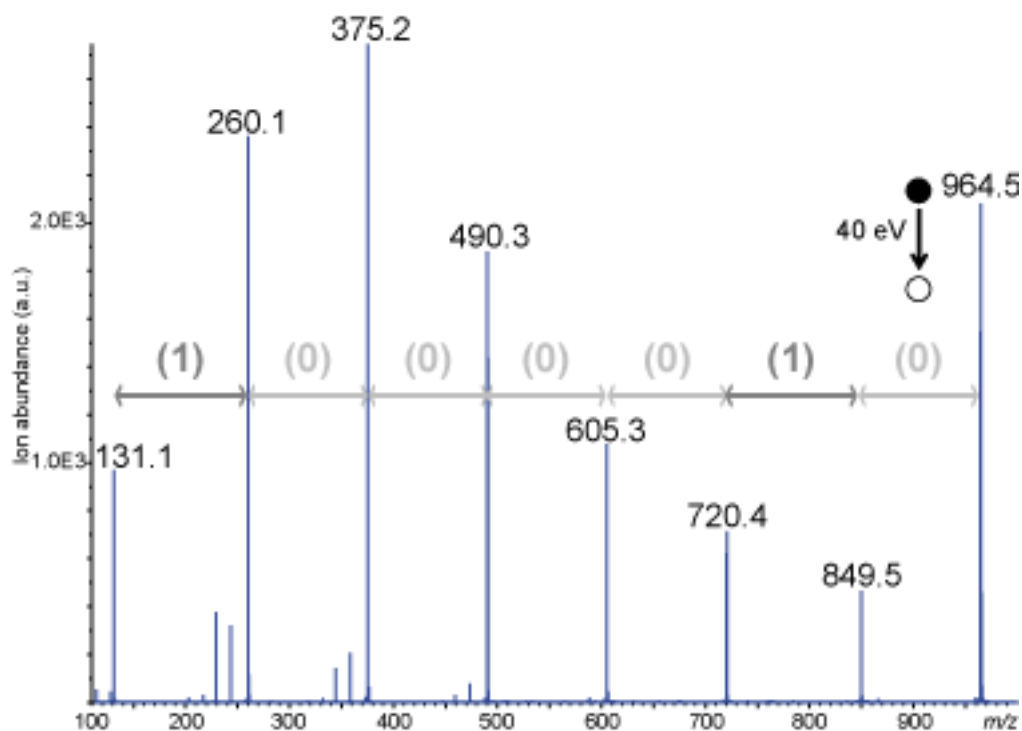
Figure S. 22 : MS/MS sequencing of [P4 – H]⁻ at *m/z* 964.5 using a 40 eV collision energy, allowing the 1000010 sequence expected for P4 to be validated.
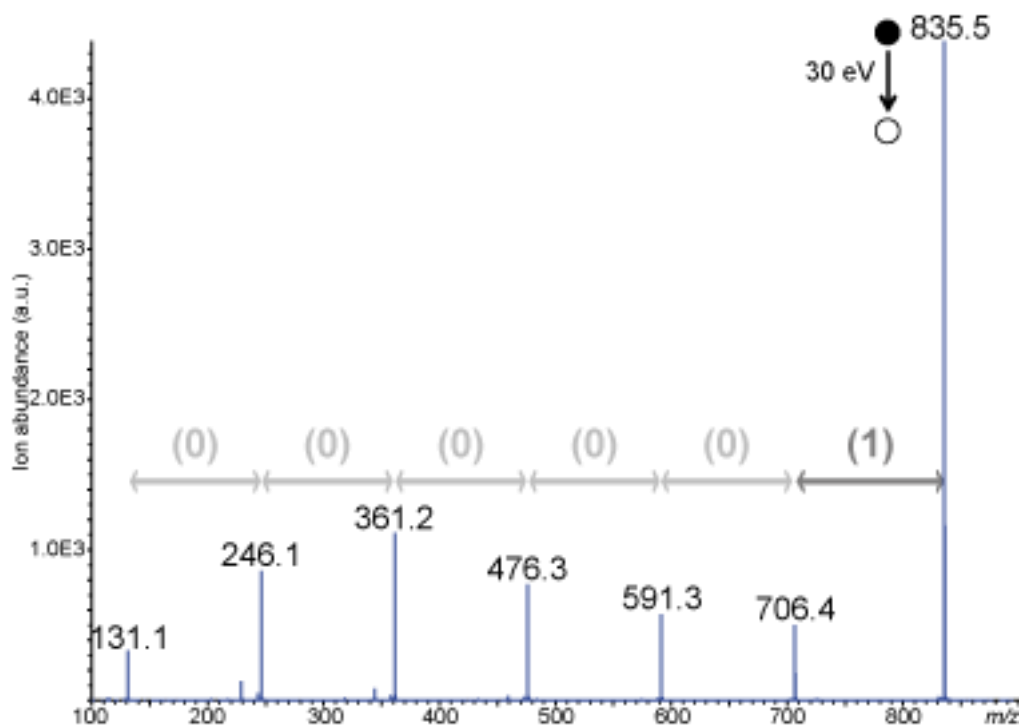
Figure S. 23 : MS/MS sequencing of [P5 – H]⁻ at *m/z* 835.5 using a 30 eV collision energy, allowing the 000001 sequence expected for P5 to be validated.
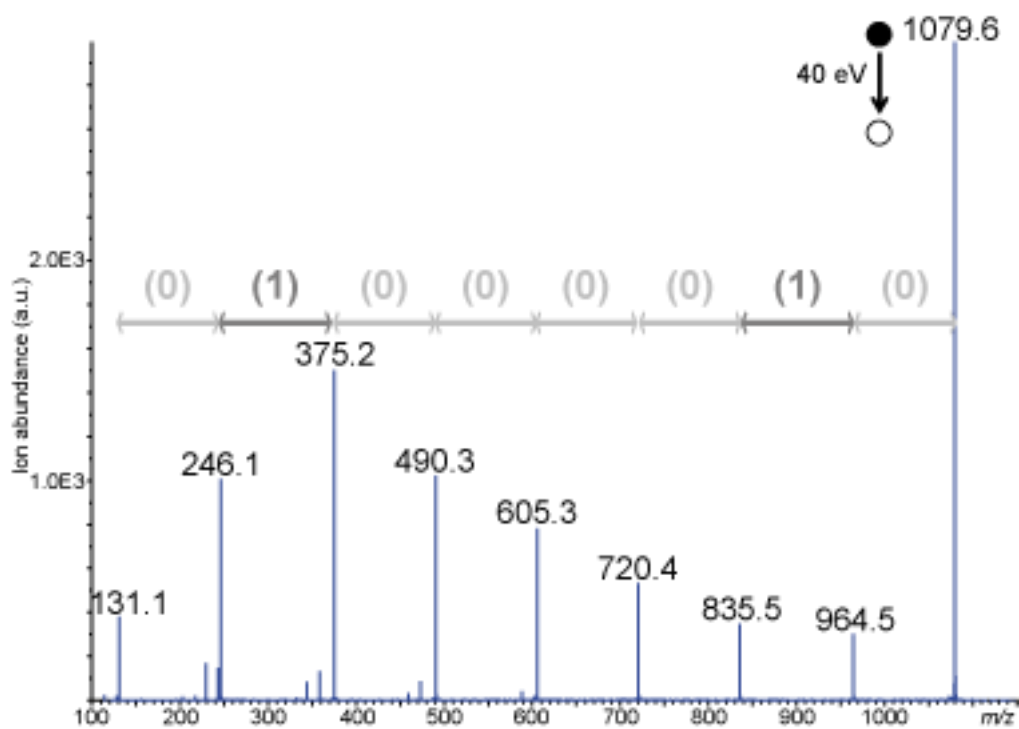
Figure S. 24 : MS/MS sequencing of [P6 − H]⁻ at *m/z* 1079.6 using a 40 eV collision energy, allowing the 01000010 sequence expected for P6 to be validated.
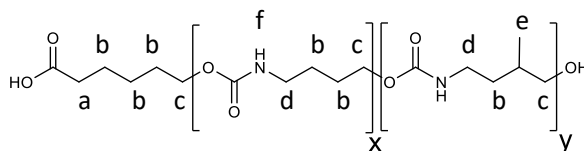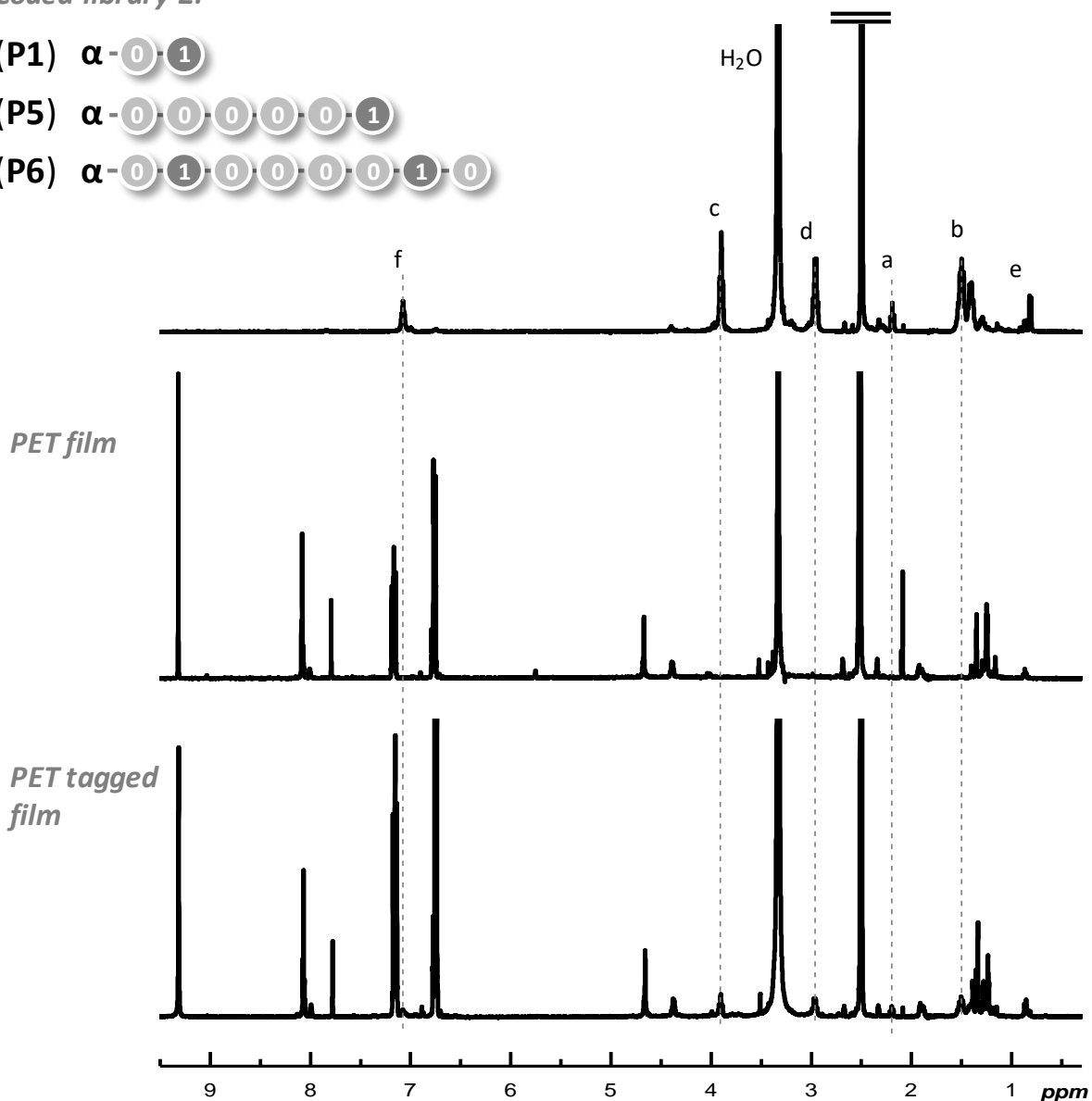
Figure S. 25: ¹H NMR spectra recorded in DMSO-*d6* for the coded oligourethane library 2 (top), a pristine PET film (middle) and a portion of a PET film labelled with coded oligourethane library 2 (bottom). The latter measurement was performed on several different film portions in order to evidence the homogeneous distribution of the oligourethanes in the PET matrix. However, for clarity, only a single example is shown in this figure. All other measurements were comparable
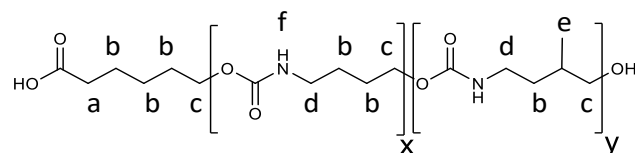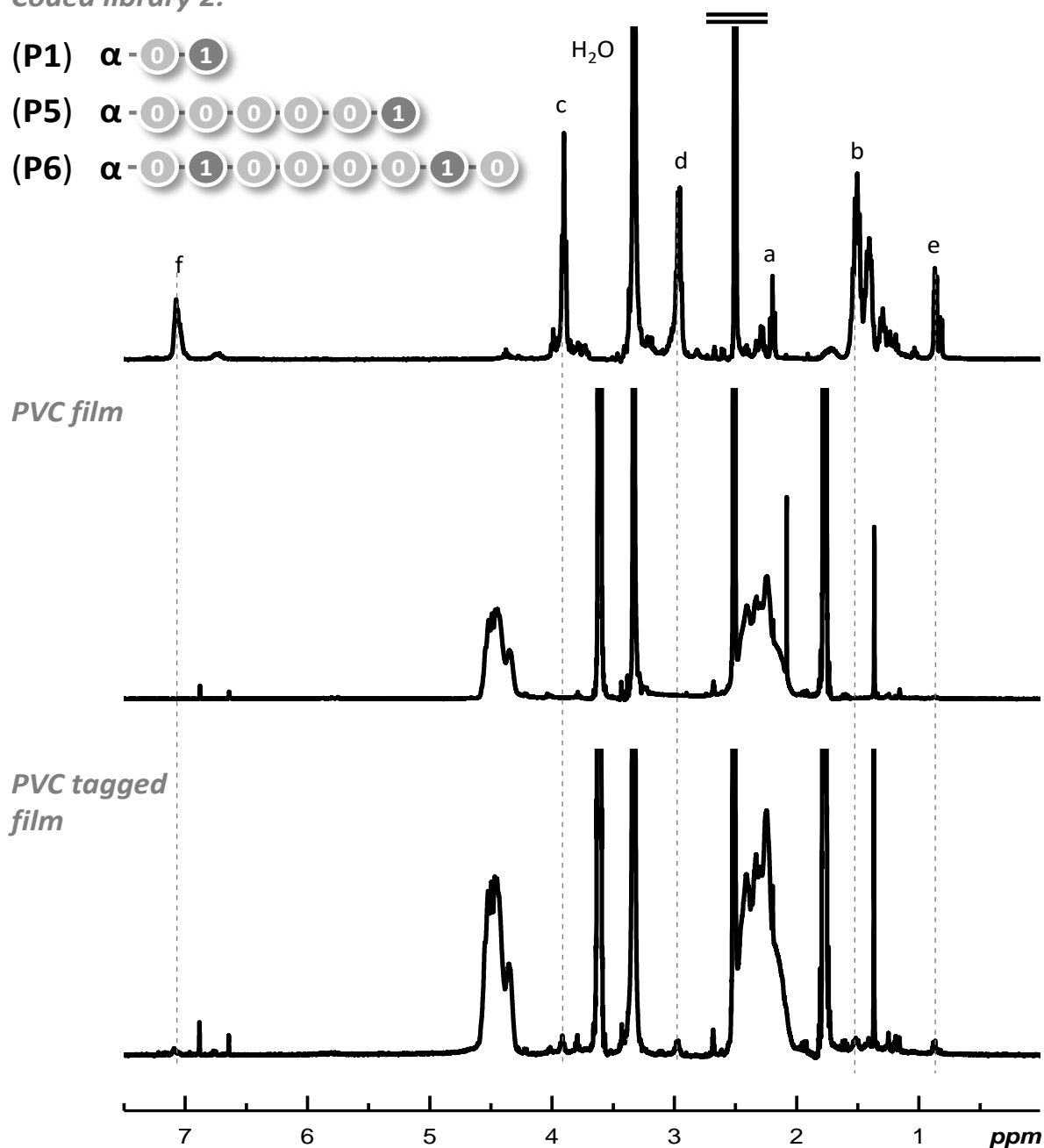
Figure S. 26: ¹H NMR spectra recorded in DMSO-*d6* for the coded oligourethane library 2 (top), a pristine PVC film (middle) and a portion of a PVC film labelled with coded oligourethane library 2 (bottom). The latter measurement was performed on several different film portions in order to evidence the homogeneous distribution of the oligourethanes in the PVC matrix. However, for clarity, only a single example is shown in this figure. All other measurements were comparable.
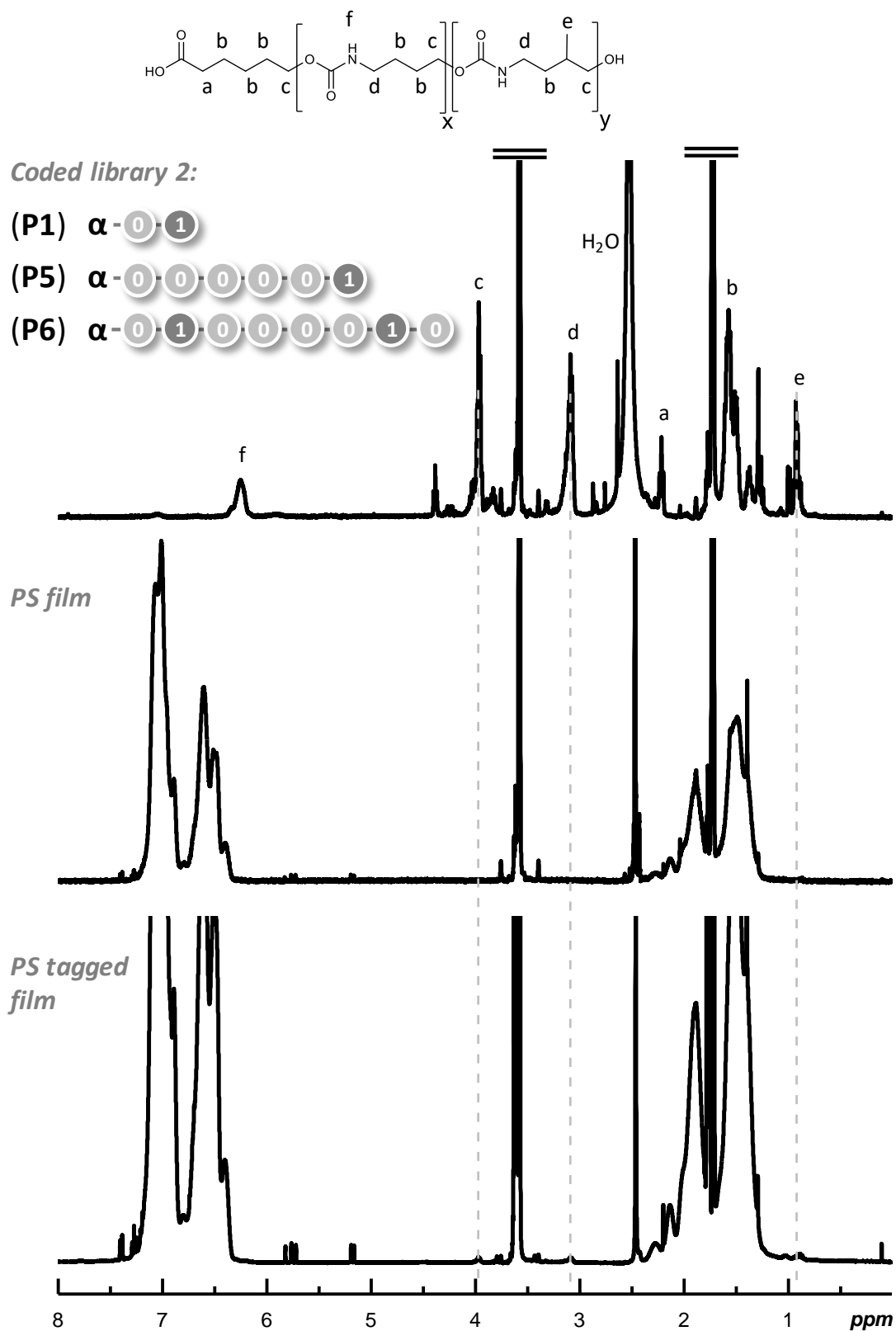
Figure S. 27: ¹H NMR spectra recorded in THF-*d6* for the coded oligourethane library 2 (top), a pristine PS film (middle) and a portion of a PS film labelled with coded oligourethane library 2 (bottom). The latter measurement was performed on several different film portions in order to evidence the homogeneous distribution of the oligourethanes in the PS matrix. However, for clarity, only a single example is shown in this figure. All other measurements were comparable.

CHAPTER VI: COVALENT INCORPORATION OF SEQUENCE-DEFINED POLYURETHANES ANTI-COUNTERFEIT TAGS IN CROSS-LINKED POLYMER NETWORKS

A. MATERIALS

Compounds	Suppliers	Purity (%)
4-Amino-1-butanol	TCI	98
4-amino-2-methyl-1-butanol	TCI	98
N,N'-disuccinimidyl carbonate	TCI	>98
anhydrous acetonitrile	Sigma-Aldrich	99.8%
dichloromethane (DCM)	Fisher Scientific	≥99.9% with amylene
	Carlo Erba	-
trifluoroacetic acid (TFA)	Alfa Aesar	99
diethyl ether	Carlo Erba	
anhydrous N,N-dimethylformamide(dry DMF)	Sigma-Aldrich	99.8
N,N-dimethylformamide(DMF)	Sigma-Aldrich	≥99.0 %
Tetrahydrofuran, inhibitor-free (THF)	Honeywell/Riedel de Haen	≥99.9 %
Dimethylsulfoxideanhydrous(dry DMSO)	Sigma-Aldrich	≥99.9%
anhydrous pyridine	Sigma-Aldrich	99.8 %, (in Sure/ Seal™),
Triethylamine (TEA)	Merck	>97
N-Isopropylacrylamide (NIPAM)	Acros Organics	99%, stabilized 500ppm MEHQ
N,N'-Methylenebis(acrylamide) (Bis-A)	Sigma-Aldrich	99%
2,2'-Azobis(2-methylpropionitrile), (AIBN)	Fluka	≥98.0%
KOH pellets	VWR	99%

Cystaminedihydrochloride	TCI	>97%
Methanol (MeOH)	Carlo Erba	99.9%
Di-tert-butyl Dicarbonate, (DiBoc)	TCI	>95.0%
Potassium phosphate monobasique KH_2PO_4	VWR	99.9%
NaOH pellets	Fisher Scientific	99%
Ethylacetate (AcOEt)	Carlo Erba	
Sodium sulfate anhydrous, (Na_2SO_4)	Fisher Scientific	99,6%
N,N-diisopropymethylamine (DIPEA)	TCI	>99%
Methacryloyl chloride	Sigma-Aldrich	97% contains ~0.02% 2,6-ditert-butyl-4-methylphenol as stabilizer
Hexane	Carlo Erba	

NIPAM, Bis-A and AIBN were recrystallized in hexane, methanol and methanol respectively before used and tried under vacuum. Triethylamine (TEA, Merck, >97%) was stored on KOH pellets in dark.

B. MEASUREMENTS

B.1 REACTIVE DESI-MS DESI-MS/MS

DESI-MS analyses were performed on a Synapt-G2 (Waters, UK) equipped with a 2D DESI ion source (Prosolia, USA) operated in the negative ion mode using the following parameters: Sprayed solution: H_2O + 0.1% NH_4OH with 4 mM DTT. The flow rate was 2 µL/min under a desolvation gas (N_2). Nebulizing gas pressure: 10 bars; DESI probe angle: 60°, distance: 4 mm; DESI voltage: –3.5 kV; Source temperature: 100°C.DESI geometry was optimized as follow: tip-to-plate angle 60°, tip-to-MS inlet distance 4mm, tip to plate distance 2mm. A piece of each sample was fixed onto the DESI plate using double-sided adhesive tape. In each case, four spectra were then recorded in the negative ion mode :DESI-MS (H_2O + NH_4OH) of the double-sided tape as a blank analysis, DESI-MS (H_2O + NH_4OH) of the sample to check for any residual unbounded oligourethane, reactive DESI-MS (H_2O + NH_4OH + DTT) of the gel sample and reactive DESI-MS/MS of the released PU in its deprotonated form.

C. EXPERIMENTAL PROCEDURES

C.1 SYNTHESIS OF N-METHACRYLOYL CYSTAMINE

The synthesis of the S-S DESI cleavable linker was described before in literature[258]. Briefly, in the first step (i) cystamine dihydrochloride (10.0 mmol) and trimethylamine (30.0 mmol) were dissolved in methanol (30mL) and added the di-t-butyl dicarbonate (5.00 mmol) dissolved in MeOH (20mL) The reaction lasted for 6 hours at -5oC to +5oC, after which the solvent was evaporated and the residue was rinsed with 1M KH_2PO_4 and extracted with diethyl ether for the removal of non-reacted di-t-butyl dicarbonate. The pH of the aqueous phase was adjusted to 9 by NaOH solution and then extracted with AcOEt. The organic phase was collected, dried under Na_2SO_4, filtrated and evaporate the solvent to afford a yellow oil.
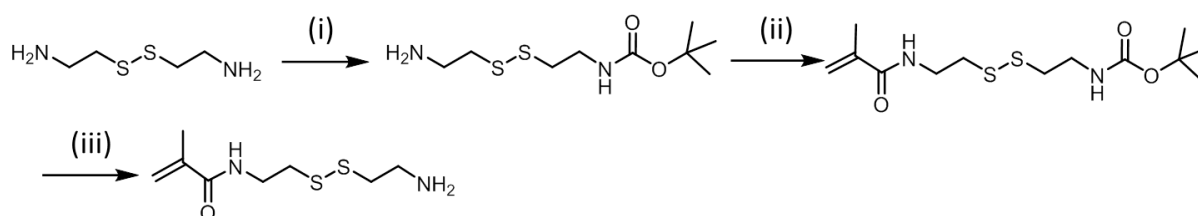
Figure S.28 :Synthesis of N-Methacryloyl cystamine. (i) protection with di-BoC the cystamine dihydrochloride, trimethylamine, di-BoC, MeOH, (ii) methacryloyl chloride, DIPEA, DCM (iii) TFA, DCM

Following, the second reaction(ii) took place to convert the free amine group in methacrylamide, leading to the synthesis the N-tert-Butoxycarbonylmethacryloyl cystamine. The N-tert-Butoxycarbonyl cystamine (2,28mmol, 0.576 g) with N,N-diisopropylethylamine (4,56 mmol, 0.79 mL)was dissolved in DCM (20mL) and added to methacryloyl chloride (2.96 mmol, 0.29 mL). After 24 hours of reaction, at 0^OC for the first two hours and then room temperature, the reaction mixture was washed with brine solution. The organic layer was evaporated and purified through silica column chromatography with eluents AcOEt/cyclohexane: 1/1. The compound after the purification dried as yellow solid. Via the reaction (iii) the N-tert-BoC-methacryloyl cystamine was deprotected with a solution of TFA in DCM 30% v/v for 6 hours at room temperature. The solution was evaporated to give the crude product as a yellow oil.

C.2 SYNTHESIS OF THE MODIFIED OLIGO(URETHANE)

The oligo(urethane)s were prepared as discussed previously multiple times and in the recent publication[299]. As far the oligo(urethane)s with monomer sequence α-0-1-0-1-0were anchored on the solid support, the reaction step of activation the oligo(carbamate) took place. As a result DSC (6 eq.) first solubilized with gentle heating in dry acetonitrile and the dry pyridine (12eq.) was added to the mixture. The reaction took place for 1 hour in the microwaves reactor (60ºC, 8W). Then, the resin was

transferred in the plastic SPE tube, rinsed with N,N DMF (5 times) and then let it react with the N-Methacryloyl cystamine. A solution of trimethylamine (30 eq.), DMF anhydrous and N-methacryloyl cystamine (10 eq.) was poured into the resin. The reaction lasted 1 hour and then the resin was rinsed with DMF several times. Pyridine (30 eq) was also used as base to catalyze the reaction of the activated carbonate of the oligomer with the N-methacryloyl cystamine. But the reaction didn't seem to work successfully. But when pyridine was replaced by triethylamine (30 eq) the reaction was successful leading to the desired modified oligomer with methacrylamide terminus. In the end, the modified oligo(urethane)s were cleaved under acidic conditions from the resin. Solution of TFA in DCM 10% v/v added to the resin for two hours for the completion of the reaction.

Modified oligourethane-macromonomer
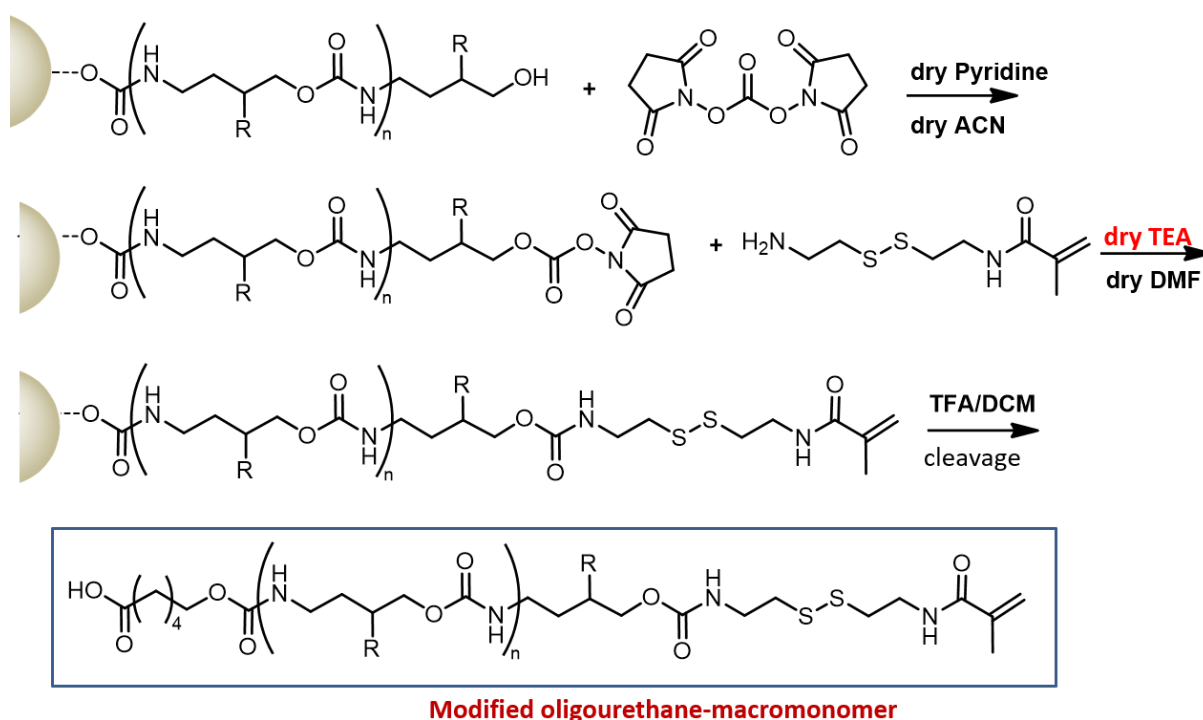
Figure S. 29 : Scheme of the modification of sequence-defined oligo(urethane). In the first step the anchored oligo(urethane) is activated once again by reacting with DSC, in dry ACN with dry pyridine and in the second step the activated adduct reacts with the amine of the methacryloyl cystamine. In the final step the modified oligomer is cleaved from the resin in TFA/DCM solution

C.3 SYNTHESIS OF NEAT P-NIPAM GELS

In order to find the best polymerization conditions for the polymerization of NIPAM and the formation of cross-linked P-NIPAM gels several parameters were tested as for example the amount of cross-linker and the solvent.

Regarding the needed amount of cross-linker, it was varying from 5% up to 10%When 5 eq. of N, N' Methylenebis(acrylamide)was used for the formation of the gels for the neat gels the cross-linking was successful but in the case of the gels including the poly(urethane) sequences the gels were dissolving during their rinsing. So the final quantity for the cross-linking was 10eq of N,N'-Methylenebis(acrylamide).

Regarding the solvents, an organic solvent was needed for this system because of the solubility of the oligo(urethane)s in organic solvents and not aqueous. Tetrahydrofuran, dry DMSO and dry DMF were tested. THF proved not ideal when 10 eq. of Bis-A were used. Dry DMS0 or dry DMF proved ideal for the P-NIPAM gels. Moreover, the amount of solvent played a crucial role. Concentrations of solids into solvent from 25% wt to 35%wt worked perfectly.

Poly(N-isopropylacrylamide) cross-linked networks were prepared through controlled radical polymerization. NIPAM (0.4g) and Bis-A (0.0605g) were weighed and placed in the flask. Four cycles of Ar-Vacuum were performed to assure oxygen-free reaction. Degassed anhydrous DMF (0.8mL) was added to dissolve the monomers. Cycles of Ar-Vacuum were again applied. The initiator AIBN was degassed and dissolved in 0.5 mL of dry DMF and then added to the reaction mixture. Reaction temperature set at 60°C. After two hours already it started solidifying. After 18 hours it was completely cross-linked. The reaction was stopped. The gel was washed with DMF and let dry under vacuum.

C.4 SYNTHESIS OF TAGGED P-NIPAM GELS

The P-NIPAM gels tagged with the sequence-defined oligo(urethane)s were prepared followed the optimized conditions from the section C.3. So, N-isopropylacrylamide (1.212mmol, 137mg) N,N'-Methylenebis(acrylamide) (0.142mmol, 22mg) and the modified oligo(urethane) tag (0.0713 mmol, 70mg) were added to the 10mL round flask. The flask was degassed by 4- cycles Argon-vacuum. Then 0.5mL of dry DMF degassed was added to solubilize the solids. Again 4-cycles Ar-vacuum were applied to the flask to add later the initiator AIBN (0.01427mmol, 2.4mg) dissolved in dry DMF. The reaction temperature was set to 60°C and after 18 hours of reaction the mixture was jellified. The gel was washed by DMF by changing the solvent 3-5 times. Then it was let dry under vacuum.

References

1   OCDE & Office, E. U. I. P. *Trade in Counterfeit and Pirated Goods*. (2016).
2   Mackey, T. K. & Nayyar, G. *Expert Opin. Saf.***16**, 587-602, (2017).
3   Paunescu, D., Stark, W. J. & Grass, R. N. *Powder Technol.***291**, 344-350, (2016).
4   Arppe, R. & Sørensen, T. J. *Nat. Rev. Chem.***1**, 0031, (2017).
5   J. Egner, B. *et al.Chem. Commun.*, 735-736, (1997).
6   Medintz, I. L., Uyeda, H. T., Goldman, E. R. & Mattoussi, H. *Nat. Mater.***4**, 435, (2005).
7   Beaurepaire, E. *et al.Nano Lett.***4**, 2079-2083, (2004).
8   Simons, R. *Google Patents*, (2014).
9   Keating, C. D. & Natan, M. J. *Adv. Mater.***15**, 451-454, (2003).
10   Ohlmeyer, M. H. *et al.PNAS***90**, 10922-10926, (1993).
11   Andres, J., Hersch Roger, D., Moser, J. E. & Chauvin, A. S. *Adv. Funct. Mater.***24**, 5029-5036, (2014).
12   Lutz, J.-F., Ouchi, M., Liu, D. R. & Sawamoto, M. *Science***341**, 1238149, (2013).
13   Mutlu, H. & Lutz, J.-F. *Angew. Chem., Int. Ed.***53**, 13010-13019, (2014).
14   Kydd, P. H. *Google Patents*, (1982).
15   Nikolaiev, V. *et al.Pept. Res.***6**, 161-170, (1993).
16   Jung, L., Hayward, J. A. & Liang, M. B. *Google Patents*, (2014).
17   Puddu, M., Paunescu, D., Stark, W. J. & Grass, R. N. *ACS Nano***8**, 2677-2685, (2014).
18   Bloch, M. S. *et al.J. Agric. Food. Chem.***62**, 10615-10620, (2014).
19   Daniela, P., Roland, F. & N., G. R. *Angew. Chem. Int. Ed.***52**, 4269-4272, (2013).
20   Lindahl, T. *Nature***362**, 709, (1993).
21   Lindahl, T. & Nyberg, B. *Biochemistry***11**, 3610-3618, (1972).
22   Lutz, J.-F. in *Sequence-Controlled Polymers: Synthesis, Self-Assembly, and Properties* Vol. 1170 *ACS Symposium Series* Ch. 1, 1-11 (American Chemical Society, 2014).
23   Colquhoun, H. & Lutz, J.-F. *Nat. Chem.***6**, 455-456, (2014).
24   Vandenbergh, J., Reekmans, G., Adriaensens, P. & Junkers, T. *Chem. Sci.***6**, 5753-5761, (2015).
25   Oh, D., Ouchi, M., Nakanishi, T., Ono, H. & Sawamoto, M. *ACS Macro Lett.***5**, 745-749, (2016).
26   Seitz, M. E. *et al.J.Am. Chem.Soc.***132**, 8165-8174, (2010).
27   Sworen, J. C., Smith, J. A., Berg, J. M. & Wagener, K. B. *J.Am. Chem.Soc.***126**, 11238-11246, (2004).
28   Driessen, F., Du Prez, F. E. & Espeel, P. *ACS Macro Lett.***4**, 616-619, (2015).
29   Amalian, J.-A., Trinh, T. T., Lutz, J.-F. & Charles, L. *Anal. Chem.***88**, 3715-3722, (2016).
30   Trinh, T. T., Oswald, L., Chan-Seng, D. & Lutz, J.-F. *Macromol. Rapid Commun.***35**, 141-145, (2014).
31   Al Ouahabi, A., Kotera, M., Charles, L. & Lutz, J.-F. *ACS Macro Lett.*, 1077-1080, (2015).
32   Roy, R. K. *et al.Nat. Commun.***6**, 7237, (2015).
33   Martens, S., Van den Begin, J., Madder, A., Du Prez, F. E. & Espeel, P. *J. Am. Chem. Soc.***138**, 14182-14185, (2016).
34   Espeel, P. *et al.Angew. Chem. Int. Ed.***52**, 13261-13264, (2013).
35   Cavallo, G., Al Ouahabi, A., Oswald, L., Charles, L. & Lutz, J.-F. *J. Am. Chem. Soc.***138**, 9417-9420, (2016).
36   Boukis, A. C. & Meier, M. A. R. *Eur. Polym. J.***104**, 32-38, (2018).
37   Zydziak, N. *et al.Nat. Commun.***7**, 13672, (2016).
38   Pinchuk, L. *J. Biomater. Sci., Polym. Ed.*   **6**, 225-267, (1995).
39   Gunay, U. S. *et al.Chem***1**, 114-126, (2016).
40   Amalian, J.-A. *et al.Int. J Mass Spectrom.***421**, 271-278, (2017).
41   Lutz, J. F. *Macromol. Rapid Commun.***38**, 1700582, (2017).
42   McNaught, A. D. & Wilkinson, A. *IUPAC Compendium of Chemical Terminology-the Gold Book*. 2nd ed. edn, 450 (Blackwell Science 1997, 1997).

43   Niaounakis, M. in *Biopolymers: Applications and Trends*   1-90 (William Andrew Publishing, 2015).

44   Berg, J. M., Tymoczko, J. L., Gatto, G. J. & Stryer, L. *Biochemistry*. (2015).

45   Altuntaş, E. & Schubert, U. S. *Anal. Chim. Acta* **808**, 56-69, (2014).

46   Ruijtenbeek, R., Versluis, C., Heck, A.J.R., Redegeld, F.A.M., Nijkamp, F.P., Liskamp, R.M.J. . *J. Mass Spectrom.* **37**, 47-55, (2002).

47   Cobb, M. *Current Biology* **24**, R55-R60, (2014).

48   Avery, O. T., MacLeod, C. M. & McCarty, M. *J. Exp. Med.* **79**, 137-158, (1944).

49   Watson, J. D., Crick, F. H. C. . *Nature* **171**, 737-738, (1953).

50   Lehman, I. R. *et al.* *PNAS* **44**, 1191-1196, (1958).

51   Haynie, D. T. *Biological Thermodynamics*. 2 edn, (Cambridge University Press, 2008).

52   Pauling, L., Corey, R. B. & Branson, H. R. *PNAS* **37**, 205-211, (1951).

53   Berg, J. M., Tymoczko, J. L. & Stryer, L. *Biochemistry*. 5th edn, (2002).

54   Anfinsen, C. B. *Science* **181**, 223-230, (1973).

55   Nelson, D. L. & Cox, M. M. *Principles of Biochemistry*. 5th edn, (W. H. Freeman, 2008).

56   Varki, A. *Glycobiology* **3**, 97-130, (1993).

57   Dwek, R. A. *Chem. Rev.* **96**, 683-720, (1996).

58   Linhardt, R. J. & Toida, T. *Acc. Chem. Res.* **37**, 431-438, (2004).

59   Pikulski, M., Hargrove, A., Shabbir, S. H., Anslyn, E. V. & Brodbelt, J. S. *J. Am. Soc. Mass. Spectrom.* **18**, 2094-2106, (2007).

60   Lewandowski, B. *et al.* *Science* **339**, 189-193, (2013).

61   De Bo, G. *et al.* *J. Am. Chem. Soc.* **136**, 5811-5814, (2014).

62   Lutz, J.-F., Lehn, J.-M., Meijer, E. W. & Matyjaszewski, K. *Nat. Rev. Mater.* **1**, 16024, (2016).

63   Satoh, K., Ozawa, S., Mizutani, M., Nagai, K. & Kamigaito, M. *Nat. Commun.* **1**, 6, (2010).

64   Zhang, C., Ling, J. & Wang, Q. *Macromolecules* **44**, 8739-8743, (2011).

65   Matyjaszewski, K. & Xia, J. *Chem. Rev.* **101**, 2921-2990, (2001).

66   Ouchi, M., Terashima, T. & Sawamoto, M. *Chem. Rev.* **109**, 4963-5050, (2009).

67   Hawker, C. J., Bosman, A. W. & Harth, E. *Chem. Rev.* **101**, 3661-3688, (2001).

68   Moad, G., Rizzardo, E. & Thang, S. H. *Polymer* **49**, 1079-1131, (2008).

69   Matyjaszewski, K. & Tsarevsky, N. V. *J.Am. Chem.Soc.* **136**, 6513-6533, (2014).

70   Benoit, D., Hawker, C. J., Huang, E. E., Lin, Z. & Russell, T. P. *Macromolecules* **33**, 1505-1507, (2000).

71   Pfeifer, S., Zarafshani, Z., Badi, N. & Lutz, J.-F. *J. Am. Chem. Soc.* **131**, 9195-9196, (2009).

72   Al Ouahabi, A., Charles, L. & Lutz, J.-F. *J. Am. Chem. Soc.* **137**, 5629-5635, (2015).

73   Edwardson, T. G. W., Carneiro, K. M. M., Serpell, C. J. & Sleiman, H. F. *Angew. Chem., Int. Ed.* **53**, 4567-4571, (2014).

74   R. N. Zuckermann, J. M. Kerr, S. B. H. Kent & Moost, W. H. *J.Am. Chem.Soc.* **114**, 10646-10647, (1992).

75   Roy, R. K., Laure, C., Fischer-Krauser, D., Charles, L. & Lutz, J.-F. *Chem. Commun.* **51**, 15677-15680, (2015).

76   Solleder, S. C. & Meier, M. A. R. *Angew. Chem. Int. Ed.* **53**, 711-714, (2014).

77   Merrifield, R. B. *Science* **150**, 178, (1965).

78   Merrifield, R. B. *Angew. Chem. Int. Ed.* **24**, 799-810, (1985).

79   R. L. Letsinger & Mahadevan, V. *J.Am. Chem.Soc.* **87**, (1965).

80   Schuerch, C. & Frechet, J. M. *J.Am. Chem.Soc.* **93**, 492-496, (1971).

81   Kunz, H. & Sager, W. *Angew. Chem. Int. Ed.* **26**, 557-559, (2003).

82   Gellman, S. H. *Acc. Chem. Res.* **31**, 173-180, (1998).

83   Rose, K. & Vizzavona, J. *J.Am. Chem.Soc.* **121**, 7034-7038, (1999).

84   Espeel, P. & Du Prez, F. E. *Eur. Polym. J.* **62**, 247-272, (2015).

85   Vaino, A. R. & Janda, K. D. *J. Comb. Chem.* **2**, 579-596, (2000).

86   Backes, B. J. & Ellman, J. A. *Curr. Opin. Chem. Biol.* **1**, 86-93, (1997).

87   Moss, J. A. in *Curr. Protoc. Protein Sci.* (John Wiley & Sons, Inc., 2001).

88   James, I. W. *Tetrahedron* **55**, 4855-4946, (1999).

89   Palomo, J. M. *RSC Advances* **4**, 32658-32672, (2014).

90   Shelton, P. T. & Jensen, K. J. in *Peptide Synthesis and Applications* (eds Knud J. Jensen, Pernille Tofteng Shelton, & Søren L. Pedersen) 23-41 (Humana Press, 2013).

91   Merrifield, R. B., Stewart, J. M. & Jernberg, N. *Anal. Chem.***38**, 1905-1914, (1966).

92   Beaucage, S. L. & Iyer, R. P. *Tetrahedron***48**, 2223-2311, (1992).

93   Knight, A. S., Zhou, E. Y., Francis, M. B. & Zuckermann, R. N. *Adv. Mater.***27**, 5665-5691, (2015).

94   Leibfarth, F. A., Johnson, J. A. & Jamison, T. F. *PNAS***112**, 10617-10622, (2015).

95   Hartmann, L., Krause, E., Antonietti, M. & Börner, H. G. *Biomacromolecules***7**, 1239-1244, (2006).

96   Martens, S., Van den Begin, J., Madder, A., Du Prez, F. E. & Espeel, P. *Journal of the American Chemical Society***138**, 14182-14185, (2016).

97   Fischer, E. & Fourneau, E. *Ber. Dtsch. Chem. Ges.***34**, 2868-2877, (1901).

98   Goodman, M., Cai, W. & Smith, N. D. *Journal of Peptide Science***9**, 594-603, (2003).

99   Merrifield, B. *J.Am. Chem.Soc.***85**, 2149–2154, (1963).

100   Hartmann, L. & Börner, H. G. *Advanced Materials***21**, 3425-3431, (2009).

101   Hartmann, L. *Macromol. Chem. Phys.***212**, 8-13, (2011).

102   Grate, J. W., Mo, K.-F. & Daily, M. D. *Angewandte Chemie International Edition***55**, 3925-3930, (2016).

103   Solleder, S. C., Schneider, R. V., Wetzel, K. S., Boukis, A. C. & Meier, M. A. R. *Macromol. Rapid Commun.***38**, 1600711, (2017).

104   Pfeifer, S., Zarafshani, Z., Badi, N. & Lutz, J.-F. *Journal of the American Chemical Society***131**, 9195-9197, (2009).

105   Porel, M. & Alabi, C. A. *J. Am. Chem. Soc.***136**, 13162-13165, (2014).

106   Kanasty, R. L. *et al.Angew. Chem. Int. Ed.***128**, 9681-9685, (2016).

107   Matsugi, M. & Curran, D. P. *Org. Lett.***6**, 2717-2720, (2004).

108   Edman, P. **4**, 283-293, (1950).

109   Edman, P. & Begg, G. *Eur. J. Biochem.***1**, 80-91, (2005).

110   Niall, H. D. in *Methods Enzymol.* Vol. 27   942-1010 (Academic Press, 1973).

111   Sanger, F. & Coulson, A. R. *J. Mol. Biol.***94**, 441-448, (1975).

112   Sanger, F., Nicklen, S. & Coulson, A. R. *PNAS***74**, 5463, (1977).

113   Sanger, F., Donelson, J. E., Coulson, A. R., Kössel, H. & Fischer, D. *PNAS***70**, 1209-1213, (1973).

114   Maxam, A. M. & Gilbert, W. *PNAS***74**, 560-564, (1977).

115   Saiki, R. K. *et al.Science***239**, 487, (1988).

116   Metzker, M. L. *Nat. Rev. Genet.***11**, 31, (2009).

117   Koboldt, Daniel C., Steinberg, Karyn M., Larson, David E., Wilson, Richard K. & Mardis, E. R. *Cell***155**, 27-38, (2013).

118   Edwards, J. R., Ruparel, H. & Ju, J. *Mutat. Res. Fundam. Mol. Mech. Mutagen.***573**, 3-12, (2005).

119   Smith, L. M. *et al.Nature***321**, 674, (1986).

120   Fenn, J. B., Mann, M., Meng, C. K., Wong, S. F. & Whitehouse, C. M. *Science***246**, 64, (1989).

121   Beavis, R. C., Chait, B. T. & Standing, K. G. *Rapid Commun. Mass Spectrom.***3**, 436-439, (1989).

122   Venter, J. C. *et al.Science***291**, 1304, (2001).

123   Consortium, I. H. G. S. *Nature***409**, 860, (2001).

124   The, E. P. C. *Nature***489**, 57, (2012).

125   Mutlu, H. & Lutz, J.-F. *Angewandte Chemie International Edition***53**, 13010-13019, (2014).

126   Colquhoun, H. M. & Zhu, Z. *Angew. Chem. Int. Ed.***43**, 5040-5045, (2004).

127   Zhang, L.-J., Deng, X.-X., Du, F.-S. & Li, Z.-C. *Macromolecules***46**, 9554-9562, (2013).

128   Boukhet, M. *et al.Biophys. J.***114**, 182a, (2018).

129   Charles, L. in *Sequence-Controlled Polymers* (ed Jean-François Lutz) (2017).

130   Charles, L., Laure, C., Lutz, J.-F. & Roy, R. K. *Macromolecules***48**, 4319-4328, (2015).

131   Burel, A., Carapito, C., Lutz, J.-F. & Charles, L. *Macromolecules***50**, 8290-8296, (2017).

132   Zhirnov, V., Zadegan, R. M., Sandhu, G. S., Church, G. M. & Hughes, W. L. *Nat. Mater.***15**, 366, (2016).
133   Church, G. M., Gao, Y. & Kosuri, S. *Science***337**, 1628-1628, (2012).
134   Shipman, S. L., Nivala, J., Macklis, J. D. & Church, G. M. *Nature***547**, 345, (2017).
135   Bornholt, J. *et al.SIGOPS Oper. Syst. Rev.***50**, 637-649, (2016).
136   Davis, J. *Art Journal***55**, 70-74, (1996).
137   Clelland, C. T., Risca, V. & Bancroft, C. *Nature***399**, 533, (1999).
138   Goldman, N. *et al.Nature***494**, 77, (2013).
139   Huffman, D. A. *Proc. IRE***40**, 1098-1101, (1952).
140   Paunescu, D., Puddu, M., Soellner, J. O. B., Stoessel, P. R. & Grass, R. N. *Nat. Protoc.***8**, 2440, (2013).
141   Paunescu, D., Fuhrer, R. & Grass, R. N. *Angew. Chem. Int. Ed.***52**, 4269-4272, (2013).
142   Blawat, M. *et al.Procedia Comput. Sci.***80**, 1011-1022, (2016).
143   Erlich, Y. & Zielinski, D. *Science***355**, 950, (2017).
144   Kosuri, S. & Church, G. M. *Nat. Methods***11**, 499, (2014).
145   Yazdi, S. M. H. T., Gabrys, R. & Milenkovic, O. *Sci. Rep.***7**, 5011, (2017).
146   Organick, L. *et al.Nat. Biotech.***36**, 242, (2018).
147   Cox, J. P. L. *Trends Biotechnol.***19**, 247-250.
148   Trinh, T. T., Oswald, L., Chan-Seng, D. & Lutz, J.-F. *Macromolecular Rapid Communications***35**, 141-145, (2014).
149   Trinh, T. T., Oswald, L., Chan-Seng, D., Charles, L. & Lutz, J.-F. *Chemistry – A European Journal***21**, 11961-11965, (2015).
150   Amalian, J.-A., Trinh, T. T., Lutz, J.-F. & Charles, L. *Analytical Chemistry***88**, 3715-3722, (2016).
151   Charles, L. *et al.J. Am. Soc. Mass. Spectrom.***28**, 1149-1159, (2017).
152   Roy, R. K., Laure, C., Fischer-Krauser, D., Charles, L. & Lutz, J.-F. *Chemical Communications***51**, 15677-15680, (2015).
153   Roy, R. K. *et al.Nature Communications***6**, 7237, (2015).
154   Laure, C., Karamessini, D., Milenkovic, O., Charles, L. & Lutz, J. F. *Angew. Chem. Int. Ed.***55**, 10722-10725, (2016).
155   Al Ouahabi, A., Charles, L. & Lutz, J.-F. *Journal of the American Chemical Society***137**, 5629-5635, (2015).
156   Amalian, J. A. *et al.J. Mass Spectrom.***52**, 788-798, (2017).
157   Al Ouahabi, A., Amalian, J.-A., Charles, L. & Lutz, J.-F. *Nature Communications***8**, 967, (2017).
158   Chaudhry, P. & Zimmerman, A. in *Protecting Your Intellectual Property Rights: Understanding the Role of Management, Governments, Consumers and Pirates*   7-31 (Springer New York, 2013).
159   Lewis, K. *The Park Place Economist* **17**, 47-58, (2009).
160   Hopkins D., Kontnik L. & M., T. *Counterfeiting Exposed: Protecting Your Brand and Customers*. First edn, (Wiley, 2003).
161   BASCAP & INTA. *Frontier Economics*, (2017).
162   Paunescu, D., Stark, W. J. & Grass, R. N. *Powder Technology***291**, 344-350, (2016).
163   Woodland, N. J. & Silver, B. Classifying apparatus and method. US2612994 (A) (1952).
164   GmbH, S., (2014).
165   J. Kim *et al.Nanotechnology***25**, 155303 (2014).
166   Nicewarner-Peña, S. R. *et al.Science***294**, 137-141, (2001).
167   Braeckmans, K. *et al.Nat. Mater.***2**, 169, (2003).
168   Gabor, D. *Nature***161**, 777, (1948).
169   Shah, R. Y., Prajapati, P. N. & Agrawal, Y. K. *J. Adv. Pharm. Technol. Res.***1**, 368-373, (2010).
170   Johnson, D. P., Dobbs, R. & Ge, C. *Am. J. Eng. Educ.*, (2011).
171   Han, M., Gao, X., Su, J. Z. & Nie, S. *Nat. Biotechnol.***19**, 631, (2001).
172   Fulton, R. J., McDade, R. L., Smith, P. L., Kienker, L. J. & Kettman, J. R. *Clin. Chem.***43**, 1749-1756, (1997).

173   Grøndahl, L., Battersby, B. J., Bryant, D. & Trau, M. *Langmuir* **16**, 9709-9715, (2000).

174   Demchenko, A. P. *Introduction to Fluorescence Sensing*. (Springer, 2008).

175   Alivisatos, A. P. *Science* **271**, 933-937, (1996).

176   Nirmal, M. & Brus, L. *Acc. Chem. Res.* **32**, 407-414, (1999).

177   Rosenthal, S. J., Chang, J. C., Kovtun, O., McBride, J. R. & Tomlinson, I. D. *Chemistry & biology* **18**, 10-24, (2011).

178   Hu, S.-H. & Gao, X. *Adv. Funct. Mater.* **20**, 3721-3726, (2010).

179   Han, M., Gao, X., Su, J. Z. & Nie, S. *Nature Biotechnology* **19**, 631, (2001).

180   Mialon, G. *et al.J. Lumin.* **129**, 1706-1710, (2009).

181   Bouzigues, C., Gacoin, T. & Alexandrou, A. *ACS Nano* **5**, 8488-8505, (2011).

182   Dejneka, M. J. *et al.PNAS* **100**, 389, (2003).

183   Lee, J. *et al.Nat. Mater.* **13**, 524, (2014).

184   Lawson, L. S. & Rodriguez, J. D. *Anal. Chem.* **88**, 4706-4713, (2016).

185   Demirok, U. K., Burdick, J. & Wang, J. *J. Am. Chem. Soc.* **131**, 22-23, (2009).

186   Roberts, C. M. *Computers & Security* **25**, 18-26, (2006).

187   Wise, S. H. & Almirall, J. R. *Appl. Opt.* **47**, G15-G20, (2008).

188   Kydd, P. H. Polypeptides as chemical taggingmaterials. 4441943 (1984).

189   Arppe, R. & Sørensen, T. J. *Nature Reviews Chemistry* **1**, 0031, (2017).

190   Hood, L. & Galas, D. *Nature* **421**, 444, (2003).

191   Choy, J. H., Oh, J. M., Park, M., Sohn, K. M. & Kim, J. W. *Adv. Mater.* **16**, 1181-1184, (2004).

192   Glover, A., Aziz, N., Pillmoor, J., McCallien, D. W. J. & Croud, V. B. *Fuel* **90**, 2142-2146, (2011).

193   Breithaupt, H. *EMBO Reports* **4**, 232-234, (2003).

194   M. Nelson & Chang, D. *Trademark Rep.* **96**, 1068–1100, (2006).

195   Casey, M. G., Isolini, D., Amrein, R., Wechsler, D. & Berthoud, H. *Dairy Sci. Technol.* **88**, 457-466, (2008).

196   Mullard, A. *Nature* **530**, 367, (2016).

197   Jung, L., James A. Hayward & Liang, M. B. DNA Marking of previously undistinguished items for traceability (2014).

198   Berrada, A., Liang, M. B., Jung, L. & Jensen, K. Alkaline activation for immobilization of DNA taggants. (2017).

199   Tyagi, S. & Kramer, F. R. *Nat. Biotech.* **14**, 303, (1996).

200   Bansal, D., Malla, S., Gudala, K. & Tiwari, P. *Scientia Pharmaceutica* **81**, 1-13, (2013).

201   Reggi, V. Anti-counterfeit Technologies for the Protection of Medicines. (World Health Organization, 2007).

202   Aldhous, P. *Nature* **434**, 132-136, (2005).

203   Peters, D. H. & Bloom, G. *Nature* **487**, 163-165, (2012).

204   Fayazpour, F. *et al.Adv. Mater.* **19**, 3854-3858, (2007).

205   Huang, C. *et al.Adv. Mater.* **22**, 2657-2662, (2010).

206   Hall, C. *Pathog. Glob. Health.* **106**, 73-76, (2012).

207   Han, S. *et al.Adv. Mater.* **24**, 5924-5929, (2012).

208   Bansal, D., Malla, S., Gudala, K. & Tiwari, P. *Sci. Pharm.* **81**, 1-13, (2013).

209   Lutz, J.-F. *Macromolecules* **48**, 4759-4767, (2015).

210   Laure, C., Karamessini, D., Milenkovic, O., Charles, L. & Lutz, J.-F. *Angew. Chem., Int. Ed.* **55**, 10722-10725, (2016).

211   Hartmann, L. & Börner, H. G. *Adv. Mater.* **21**, 3425-3431, (2009).

212   McKee, M. L. *et al.Angew. Chem., Int. Ed.* **49**, 7948-7951, (2010).

213   Niu, J., Hili, R. & Liu, D. R. *Nat. Chem.* **5**, 282-292, (2013).

214   Proulx, C., Yoo, S., Connolly, M. D. & Zuckermann, R. N. *J. Org. Chem.* **80**, 10490-10497, (2015).

215   Grate, J. W., Mo, K.-F. & Daily, M. D. *Angew. Chem., Int. Ed.* **55**, 3925-3930, (2016).

216   de Rochambeau, D. *et al.Polym. Chem.* **7**, 4998-5003, (2016).

217   Börner, H. G. *Prog. Polym. Sci.* **34**, 811-851, (2009).

218   Sun, J. & Zuckermann, R. N. *ACS Nano* **7**, 4715-4732, (2013).

219   Serpell, C. J., Edwardson, T. G. W., Chidchob, P., Carneiro, K. M. M. & Sleiman, H. F. *J. Am. Chem. Soc.***136**, 15767-15774, (2014).
220   Mannige, R. V. *et al.Nature***526**, 415-420, (2015).
221   Porel, M., Thornlow, D. N., Phan, N. N. & Alabi, C. A. *Nat. Chem.***8**, 590-596, (2016).
222   Große, S., Wilke, P. & Börner, H. G. *Angew. Chem., Int. Ed.***55**, 11266-11270, (2016).
223   Trinh, T. T., Laure, C. & Lutz, J.-F. *Macromol. Chem. Phys.***216**, 1498-1506, (2015).
224   Roy, R. K. *et al.Nat. Commun.***6**, 7237, (2015).
225   Charles, L., Laure, C., Lutz, J.-F. & Roy, R. K. *Rapid Commun. Mass Spectrom.***30**, 22-28, (2016).
226   Randall, D. & Lee, S.   494 (John Wiley & Sons Ltd, Chichester, UK, 2003).
227   Zdrahala, R. J. & Zdrahala, I. J. *J. Biomater. Appl.***14**, 67-90, (1999).
228   Lamba, N. M. K., Woodhouse, K. A. & Cooper, S. L. *Polyurethanes in Biomedical Applications*. (Taylor & Francis, 1997).
229   Burke, A. & Hasirci, N. in *Biomaterials: From Molecules to Engineered Tissue* (eds Nesrin Hasirci & Vasif Hasirci) 83-101 (Springer US, 2004).
230   Bellucci, R. *Cataract***3**, 38–55, (2013).
231   Bozukova, D., Pagnoulle, C., Jérôme, R. & Jérôme, C. *Mater. Sci. Eng., R***69**, 63-83, (2010).
232   Brandrup, J., Immergut, E. H. & A., G. E.,*Polymer Handbook* (John Wiley & Sons, 1999).
233   Werner, L. *J. Cataract Refract. Surg.***36**, 1398-1420, (2010).
234   van der Mooren, M., Franssen, L. & Piers, P. *Biomed. Opt. Express***4**, 1294-1304, (2013).
235   Dégardin, K., Roggo, Y. & Margot, P. *J. Pharm. Biomed. Anal.***87**, 167-175, (2014).
236   Shikha, S., Salafi, T., Cheng, J. & Zhang, Y. *Chem. Soc. Rev.***46**, 7054-7093, (2017).
237   Shendure, J. & Ji, H. *Nat. Biotech.***26**, 1135-1145, (2008).
238   Karni, M., Zidon, D., Polak, P., Zalevsky, Z. & Shefi, O. *DNA Cell Biol.***32**, 298-301, (2013).
239   Paunescu, D., Fuhrer, R. & Grass, R. N. *Angew. Chem., Int. Ed.***52**, 4269-4272, (2013).
240   Mora, C. A., Paunescu, D., Grass, R. N. & Stark, W. J. *Mol. Ecol. Resour.***15**, 231-241, (2015).
241   Karamessini, D., Petit, B. E., Bouquey, M., Charles, L. & Lutz, J.-F. *Adv. Funct. Mater.***27**, 1604595, (2017).
242   Karamessini, D., Poyer, S., Charles, L. & Lutz, J.-F. *Macromol. Rapid Commun.***38**, 1700426, (2017).
243   König, N. F., Al Ouahabi, A., Poyer, S., Charles, L. & Lutz, J.-F. *Angew. Chem., Int. Ed.***56**, 7297-7301, (2017).
244   Al Ouahabi, A., Amalian, J.-A., Charles, L. & Lutz, J.-F. *Nat. Commun.***8**, 967, (2017).
245   Solleder, S. C., Martens, S., Espeel, P., Du Prez, F. & Meier, M. A. R. *Chem. Eur. J.***23**, 13906-13909, (2017).
246   Cho, C. *et al.Science***261**, 1303-1305, (1993).
247   Warrass, R., Walden, P., Wiesmüller, K.-H. & Jung, G. *Lett. Pept. Sci.***5**, 125-128, (1998).
248   Kanasty, R. L. *et al.Angew. Chem., Int. Ed.***55**, 9529-9533, (2016).
249   Kobayashi, M., Toguchida, J. & Oka, M. *Biomaterials***24**, 639-647, (2003).
250   Chaouat, M. *et al.Adv. Funct. Mater.***18**, 2855-2861, (2008).
251   Baker Maribel, I., Walsh Steven, P., Schwartz, Z. & Boyan Barbara, D. *J. Biomed. Mater. Res. Part B***100B**, 1451-1457, (2012).
252   Ino, J. M. *et al.J. Biomed. Mater. Res. Part B***101**, 1549-1559, (2013).
253   Yusong, P., Jie, D., Yan, C. & Qianqian, S. *Mater. Technol.***31**, 266-273, (2016).
254   Chang, T. J. *Clin. Podiatr. Med. Surg.***35**, 133-143, (2018).
255   Lutz, J.-F., Gunay, U. S., Charles, L. & Gigmes, D. Uniform sequence-defined polyurethanes and uses thereof as molecular labels. (2017).
256   Hoogenboom, R., Meier, M. A. R. & Schubert, U. S. *Macromol. Rapid Commun.***24**, 15-32, (2003).
257   Chan-Seng, D., Zamfir, M. & Lutz, J. F. *Angew. Chem., Int. Ed.***51**, 12254-12257, (2012).
258   Suga, Y., Sunayama, H., Ooya, T. & Takeuchi, T. *Chem. Commun.***49**, 8450-8452, (2013).
259   Humphreys, E. S. *Mater. Today***5**, 32-37, (2002).
260   Bevilacqua, M., Ciarapica, F. E., Crosta, A., Mazzuto, G. & Paciarotti, C. *I. J. RF Technol.: Res. and Appl.***6**, 99-119, (2015).

261   Swedberg, C. *RFID Journal*, (2015).
262   Dykstram, D. P. *et al.World Bank / WWF Alliance for Forest Conservation and Sustainable Use* (2002).
263   Tzoulis, I. K., Andreopoulou, Z. S. & Voulgaridis, E. *J. Agric. Inform.***5**, 9-17, (2014).
264   Mtibaa, F. & Chaabane, A. *Proceedings of the 2014 Industrial and Systems Engineering Research Conference*, 1562-1571, (2014).
265   Häkli, J., Jaakkola, K., Pursula, P., Huusko, M. & Nummila, K. in *2010 IEEE International Conference on RFID (IEEE RFID 2010).* 245-251.
266   Dykstra, D. P., Kuru, G. & Nussbaum, R. *The International Forestry Review***5**, 262-267, (2003).
267   Takáts, Z., Wiseman, J. M., Gologan, B. & Cooks, R. G. *Science***306**, 471, (2004).
268   Mantanis George, I., Young Raymond, A. & Rowell Roger, M. in *hfsg* Vol. 48   480 (1994).
269   Edward C., P. *Forest Products Journal***7**, 235-244, (1957).
270   Mantanis George, I., Young Raymond, A. & Rowell Roger, M. *hfsg***49**, 239, (1995).
271   Ashton, H. E. *Wood Science***6**, 159-166, (1973).
272   Roger, R. M. *Forest Products Abstracts***6**, 363-382, (1983).
273   *Handbook of wood chemistry and wood composites*. Second edn, (CRC Press, 2013).
274   Moliński, W., Kuczyński, J., Puszyński, J. & Roszyk, E. *Forestry and Wood Technology***88**, 157-161, (2014).
275   Lutz, J.-F.
276   Grass, R. N., Heckel, R., Puddu, M., Paunescu, D. & Stark, W. J. *Angew. Chem., Int. Ed.***54**, 2552-2555, (2015).
277   Al Ouahabi, A., Kotera, M., Charles, L. & Lutz, J.-F. *ACS Macro Lett.***4**, 1077-1080, (2015).
278   Solleder, S. C., Zengel, D., Wetzel, K. S. & Meier, M. A. R. *Angew. Chem., Int. Ed.***55**, 1204-1207, (2016).
279   Wender, P. A., Rothbard, J. B., Jessop, T. C., Kreider, E. L. & Wylie, B. L. *J. Am. Chem. Soc.***124**, 13382-13383, (2002).
280   *Polymer Gels, Copyright, Foreword*. Vol. 833 (American Chemical Society, 2002).
281   Ahmed, E. M. *J. Adv. Res.***6**, 105-121, (2015).
282   Heskins, M. & Guillet, J. E. *J. Macromol. Sci., Chem.***2**, 1441-1455, (1968).
283   Islam, M. R. & Serpe, M. J. *Anal. Bioanal.Chem.***406**, 4777-4783, (2014).
284   Hendrickson, G. R. & Andrew Lyon, L. *Soft Matter***5**, 29-35, (2009).
285   Gao, Y., Zago, G. P., Jia, Z. & Serpe, M. J. *ACS Appl. Mater. Interfaces***5**, 9803-9808, (2013).
286   Gao, Y., Ahiabu, A. & Serpe, M. J. *ACS Appl. Mater. Interfaces***6**, 13749-13756, (2014).
287   Mura, S., Nicolas, J. & Couvreur, P. *Nat. Mater.***12**, 991, (2013).
288   Lee, K. Y. & Mooney, D. J. *Chem. Rev.***101**, 1869-1880, (2001).
289   Stuart, M. A. C. *et al.Nat. Mater.***9**, 101, (2010).
290   Ahiabu, A. & Serpe, M. J. *ACS Omega***2**, 1769-1777, (2017).
291   Sinz, A. *Anal. Bioanal.Chem.***409**, 33-44, (2017).
292   Zhang, Y., Dewald, H. D. & Chen, H. *J. Proteome Res.***10**, 1293-1304, (2011).
293   Zheng, Q., Zhang, H., Tong, L., Wu, S. & Chen, H. *Anal. Chem.***86**, 8983-8991, (2014).
294   Ifa, D. R., Wu, C., Ouyang, Z. & Cooks, R. G. *Analyst***135**, 669-681, (2010).
295   Tsarevsky, N. V. & Matyjaszewski, K. *Macromolecules***35**, 9009-9014, (2002).
296   Tsarevsky, N. V. & Matyjaszewski, K. *Macromolecules***38**, 3087-3092, (2005).
297   Konigsberg, W. in *Methods in Enzymology* Vol. 25   185-188 (Academic Press, 1972).
298   Singh, R. & Whitesides, G. M. in *Techniques in Protein Chemistry* Vol. 6 (ed John W. Crabb) 259-266 (Academic Press, 1995).
299   Gunay, U.-S. *et al.Chem***1**, 114-126, (2016).

Dionysia-Nteniz SARANTI-KARAMESINI

Synthèse et utilisation de polyuréthanes codés pour des applications anti-contrefaçon

Abstract

This PhD thesis deals with the development of a new anti-counterfeiting strategy. Sequence-defined oligourethane taggants were studied herein as a novel option for anti-counterfeit and traceability applications. These oligomers were prepared by iterative solid-phase chemistry. Their synthesis is based on the use of two successive chemoselective steps; the formation of an activated carbonate and its selective reaction with the primary amine function of an amino alcohol. The use of different amino alcohol building-blocks with different side-groups allows synthesis of sequence-coded polymers. Therefore, each oligourethane has a unique monomer sequence, which constitutes an exclusive product identity. In this work, oligourethane taggants were included in different types of host materials such as model commodity plastic films, biomedical implants and wood. The extraction and detection of the taggants by tandem mass spectrometry (MS/MS) was studied in a collaboration with a mass spectrometry laboratory. In all cases, the coded oligourethanes were efficiently extracted from the host materials and their sequences were deciphered by MS/MS, thus evidencing the robustness and versatility of the taggant strategy. For instance, it was even demonstrated in this thesis that the taggants can be successfully stored and used *in vivo*. Based on these successful results, more complex (thus more secure) tagging strategies were also studied in this work. For instance, the development of 2D-sequence-coded taggants and the covalent attachment of the taggants to polymer networks are also described in this thesis.

Keywords: anti-counterfeiting technologies, sequence-defined polymers, information-containing macromolecules, sequencing

Résumé

Ce travail s'inscrit dans le cadre du développement de nouvelles stratégies d'anti-contrefaçon. Des marqueurs oligouréthanes à séquences définies ont été étudiés comme nouvelles stratégies dans la traçabilité et la lutte contre la contrefaçon. Ces oligouréthanes à séquence définie ont été préparés par chimie itérative en phase solide. Leur synthèse est basée sur l'utilisation de deux étapes chimiosélectives successives; la formation d'un carbonate activé et sa réaction sélective avec la fonction amine primaire d'un aminoalcool. L'utilisation de différents blocs constitutifs d'aminoalcools avec différents groupes latéraux comme de monomères de base permet la synthèse de polymères codés en séquence. Par conséquent, chaque oligouréthane a une séquence de monomère unique qui constitue une identité exclusive du produit. Dans ce travail, les marqueurs oligouréthanes ont étéincorporés dans différents types de matériaux hôtes, tels que des films plastiques, des implants biomédicaux et du bois. L'extraction des marqueurs, par spectrométrie de masse en tandem (MS / MS) ont été étudiées en collaboration avec un laboratoire de spectrométrie de masse. Pour tous les matériaux étudiés, les différents marqueurs ont été extraits efficacement et leurs séquences ont été décryptées par MS/MS, démontrant ainsi la robustesse et la polyvalence de la stratégie de marquage basée sur l'utilisation de oligouréthanes à séquence-définie. Dans ce travail, il a été également démontré que ces marqueurs peuvent être stockés avec succès et utilisés *in vivo*. Sur la base de ces résultats forts prometteurs, des stratégies de marquage plus perfectionnées (donc plus sécurisées) ont

également été étudiées dans ce travail. Par exemple, le développement de marqueurs codés en séquence 2D et l'intégration de manière covalente des marqueurs aux réseaux de polymères sont également décrits dans cette thèse.